Non-Viral Gene Therapy: Design and Characterisation of Novel Non-Viral Vectors for Improved Cellular Transfection

Kimberly L. Douglas

Biomedical Engineering Department
McGill University
Montréal, Canada

Submitted May 2006

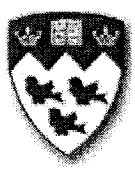

A thesis submitted to McGill University, Faculty of Graduate and Postdoctoral Studies, in partial fulfilment of the requirements of the degree of doctor of philosophy.

Your file Votre référence
ISBN: 978-0-494-27772-0
Our file Notre référence
ISBN: 978-0-494-27772-0

ABSTRACT

The promise of gene therapy, once hailed as the medical treatment of the future, has yet to be achieved. Problems related to the safety and efficacy of gene therapies have checked the enthusiasm once surrounding this field. The future of gene therapy relies on the development of safe and effective non-viral vectors for gene delivery.

This doctoral thesis describes the development and evaluation of a novel nanoparticle system that demonstrates characteristics suitable for gene delivery purposes. The work presented in this thesis is divided into three main phases: (1) *Development of a novel delivery system.* The development of a novel carrier was undertaken with the goal of producing a system that is biocompatible, biodegradable and non-toxic. The alginate-chitosan polyelectrolyte system, chosen for development due to its desirable characteristics at the macro- and micro-scales, was successfully used to prepare nanoparticles of appropriate size for delivery purposes. (2) *Evaluation of the delivery system as a gene carrier.* Alginate-chitosan nanoparticles were shown to complex DNA and effectively protect it from degradation. The inclusion of alginate in the system was confirmed to reduce the strength of binding between chitosan and DNA, thereby facilitating its release intracellularly. Cell viability studies confirm the non-toxicity of the system, while *in vitro* studies confirm the ability of alginate-chitosan nanoparticles to mediate efficient transfection. (3) *Investigation of the transfection process.* The cell line-dependent transfection ability of these nanoparticles, as observed with many non-viral vectors, led to the investigation of the processes involved in successful transfection. The intracellular trafficking of the non-viral vectors to the endosomal-lysosomal pathway, determined to be critical for efficient transfection, was found to be directly dependent on the internalisation mechanisms of the complexes.

The development and evaluation of the alginate-chitosan nanoparticle system confirms their suitability for gene delivery applications. The additional information provided by the thorough investigation of the cellular internalisation and intracellular trafficking pathways of the alginate-chitosan nanoparticles can

be exploited to further develop the system to allow tailoring to improve transfection.

RÉSUMÉ

L'idée de la thérapie génique, autrefois considerée comme le traitement médical de l'avenir, n'a toujours pas éte réalisée. Les problèmes reliés à la sécurité et l'efficacité des thérapies géniques ont reduit l'enthousiasme entourant ce domaine. Le futur de la thérapie génique nécessite le développement de vecteurs non-viraux efficaces et sécuritaires pour la livraison de gènes.

Cette thèse doctorale décrit le développement et l'évaluation d'un système original de nanoparticules qui presentent des caractéristiques convenant à la livraison de gènes. Le travail présenté dans cette thèse est divisé en trois phases principales : (1) *Développement d'un système de livraison original.* Le développement d'un transporteur original a été entrepris dans le but de produire un système biocompatible, biodégradable et non-toxique. Le système de polyélectrolyte d'alginate-chitosan, choisi pour le développement en raison de ses caractéristiques recherchées dans les systèmes de taille macro et micro, a été employé avec succès pour la préparation des nanoparticules de taille appropriée pour la livraison. (2) *Evaluation du système de livraison comme un transporteur de gènes.* Les nanoparticules d'alginate-chitosan démontrent la capacité d'associer avec l'ADN et le protègent efficacement de la dégradation. L'inclusion de l'alginate dans le système permet de réduire la force de liason entre le chitosan et l'ADN, facilitant de cette façon leur séparation intracellulaire. Les études de viabilité cellulaire confirment la non-toxicité du système et confirment la capacité des nanoparticules d'alginate-chitosan à agir comme médiateur efficace de transfection *in vitro*. (3) *Investigation des processus de transfection.* Étant donné que la capacité de transfection de ces nanoparticules depend de la lignée cellulaire, une investigation a été menée sur les procédés impliqués dans une transfection réussie. Le traffique intracellulaire des vecteurs non-viraux par la voie endosomale-lysosomale a été établi comme essentiel pour une transfection efficace. L'orientation des vecteurs vers ce chemin est directement dépendent sur les mécanismes d'internalisation des complexes.

Le développement et l'évaluation du système de nanoparticules d'alginate-chitosan confirment leur convenance aux applications de livraison des gènes.

L'information supplémentaire fournie par l'investigation de l'internalisation cellulaire et le transport intracellulaire des nanoparticules d'alginate-chitosan peut être exploitée dans le développement futur du système pour l'adaptation à une transfection améliorée.

ACKNOWLEDGEMENTS

I would like to begin by thanking my family for their support. Their love and encouragement helped give me the courage to change career paths and begin graduate studies. Their continued support was essential in helping me reach this goal. I will always be grateful for their unwavering love and encouragement.

I would also like to thank Shawn Carrigan for being a friend and valued co-worker. In difficult times he was the calm voice of reason that enabled me to keep working and helped me to see the value of my work. Not only did he provide expert editing for each of my manuscripts and acted occasionally as a "helping hand" in the lab, he was also the greatest champion of my work.

My supervisors, Dr. Maryam Tabrizian and Dr. Ciriaco Piccirillo, are also deserving of my sincere appreciation. The guidance and insight they provided during my studies are invaluable. With their support, I was able to complete this work, of which I am very proud. Under their supervision, I have been fortunate to gain experience with numerous methods of analysis and on several highly technical pieces of equipment. I have also benefited greatly from the opportunities provided by Dr. Tabrizian to attend numerous national and international conferences, where I was able to present and share my work with the biomaterials community.

I would like to acknowledge several other professors, who always had an open door, advice, and support for me. Dr. Christopher J. Barrett (Department of Chemistry), Dr. Hojatollah Vali (Department of Anatomy and Cell Biology), Dr. Henrietta Galiana (Department of Biomedical Engineering), and Dr. Jean-Luc Guerquin-Kern (Institut Curie, Orsay France) all demonstrated an interest in me and my success. Without their input, my experience would have been considerably less complete.

Several other individuals are deserving of my thanks for making grad school more enjoyable. Pina Sorrini, Patricia Cap, and Lina Vuch provided expert administrative assistance and ready smiles. Dr. Ross Wagner's steady supply of laughs, advice and assistance were particularly enjoyed and appreciated. Dr. S. Kelly Sears and Jeannie Mui, who prepared samples for TEM analysis, were always a source of invaluable information and assistance.

I would also like to thank my co-workers in Dr. Tabrizian's and Dr. Piccirillo's lab groups, in particular Annie Sénéchal and Valérie Hay. I am particularly indebted to the "409" group for their support and patience in showing a non-microbiologist the secrets of cell culturing and other assays.

I am fortunate to have several mentors, who open new doors to me, encourage me to pursue my interests, and remind me of what is really important in life. I am grateful to Brian and Carol Carrigan, Sue and Augie Auer, Robin Howard, Cheryl Woods, and Loi Lam for being such positive influences in my life.

Finally, I would like to acknowledge the funding sources that made this work possible. I am sincerely appreciative of the scholarships I received through the Natural Sciences and Research Council of Canada (NSERC) for allowing me to pursue graduate studies without financial difficulty. The following agencies provided funding for equipment, supplies and travel expenses: Québec Ministère de la Recherche de la Science et de la Téchnologie (MRST), Canadian Institutes of Health Research (CIHR), Fonds Québécois de Recherche sur la Nature et les Technologies (FQRNT), Ministère du développement économique, de l'innovation et de l'exportation (MDEIE), Ministère du Développement Économique et Régional et de la Recherche (MDERR), Ministère des Relations Internationales-Coopération France-Québec, Centre for Biorecognition and Biosensors (CBB), Canadian Biomaterials Society (CBS), and the McGill University Alumni Association.

TABLE OF CONTENTS

LIST OF FIGURES

LIST OF TABLES

GLOSSARY OF TERMS

293T	Human embryonic kidney cells
AFM	Atomic force microscopy
AIDS	Acquired immune deficiency syndrome
Alg	Alginate
Alg-Chi	Alginate-chitosan polyelectrolyte system
ATR-FTIR	Attenuated total reflectance Fourier transform infrared spectroscopy
Chi	Chitosan
CHO	Chinese hamster ovary cells
COS7	African green monkey kidney cells
DLS	Dynamic laser light scattering
DMEM	Dulbecco's modified Eagle medium
DNA	Deoxyribonucleic acid
EDTA	Ethylenediaminetetraacetic acid
EtBr	Ethidium bromide
FBS	Foetal bovine serum
FDA	Food and drug administration (USA)
GFP	Green fluorescent protein
HIV	Human immuno-deficiency virus
HMW/LMW	High or low molecular weight
HV/MV/LV	High, medium or low viscosity
MPS	Mononuclear phagocytic system
MTT	3-(4,5-dimethylthiazol-2-yl)-2,5-diphenyltetrazolium bromide
N:P	Ratio of cationic amino groups to anionic phosphate groups
NanoSIMS	Nano-scale secondary ion mass spectrometry
ON	Oligonucleotide
PBS	Phosphate buffered saline
pDNA	Plasmid DNA
PEG	Poly(ethylene glycol)
PEI	Poly(ethylene imine)
PLA	Poly(lactic acid)

PLGA	Poly(lactide-co-glycolide)
PLL	Poly-$_L$-lysine
RES	Reticulo-endothelial system
RNA	Ribonucleic acid
SCID	Severe combined immunodeficiencies
TEM	Transmission electron microscope
αMEM	Alpha modified Eagle medium

CONTRIBUTIONS OF AUTHORS

This thesis is presented as a collection of manuscripts written by the candidate under the supervision of the co-authors. The manuscripts are based on experimental data generated from experiments designed and executed by the candidate, who was also responsible for data collection and analysis. The first manuscript was generated from experiments performed prior to the establishment of Dr. Ciriaco Piccirillo as a co-supervisor; as such, Dr. Maryam Tabrizian appears as the sole co-author of this manuscript. Both supervisors appear as co-authors on manuscripts two and three to reflect their supervisory role during the execution of the work and their involvement in manuscript preparation.

Chapter 1
Introduction

Gene therapy has been defined as the introduction of genetic material into cells to elicit a therapeutic effect in order to prevent, control or cure disease[1]. Although first discussed in 1966[2], it was not until advances in cellular and molecular biology techniques, increased understanding of the genetic nature of disease, and the completion of the human genome project that gene therapy became a realistic goal. The ideal achievement of gene therapy is to replace a disease gene mutation with a healthy gene. In the short term, the goal is to deliver and express genes at therapeutically effective levels[3]. Since 1989 there have been over 1,100 clinical trials involving gene therapy worldwide for treatment of diseases ranging from arthritis and heart failure, to haemophilia, muscular dystrophy, and cancer[4,5]. However, no gene therapy treatment has been approved for use by the FDA and the promise of gene therapy has not yet been realised. Progress has been hampered by an inability to efficiently and safely deliver genes to cells due to the fragility of genetic material and difficulties introducing it into cells.

To achieve the promise of gene therapy, safe and efficient delivery systems must be designed to protect and stabilise the gene extracellularly and intracellularly, as well as aid its entry into cells. The ideal gene delivery vehicle, or vector, would improve the bioavailability of the gene and be non-immunogenic and non-toxic. At a minimum, the vector must be able to protect the gene and enable its entry into cells. Although viruses demonstrate a natural ability to transport genetic material into cells, issues related to their immunogenicity, oncogenicity, potential reinfectivity, manufacture, targeting and loading abilities have dampened enthusiasm for their development and use, encouraging many researchers to search for alternative non-viral gene delivery systems[6].

The focus of research into non-viral vectors has been on the development of gene carriers which can offer protection and assist cellular penetration. Non-viral vectors offer numerous advantages compared to their viral counterparts, particularly in the areas of safety, targeting and production. However, non-viral

vectors also present some significant disadvantages and remain inferior to viruses for effective gene delivery. Some of the materials used in non-viral vectors demonstrate toxicity to cells *in vitro* and consequent mild immune responses, as well as a range of toxic responses *in vivo*[7]. Furthermore, these carriers have not all exhibited the expected or desired prolonged stability of associated genes, due in part to the surface localisation of the nuclear material[8,9]. The major drawback of non-viral vectors is that they have not yet matched the efficiency of cell transfection exhibited by viral vectors[10]. None of the carriers used to date has been able to transfect cells resulting in expression comparable to viruses, regardless of the gene or the cell type.

Despite the sub-standard transfection efficiencies exhibited by non-viral vectors, the disadvantages are minor compared to the safety concerns surrounding the use of viral vectors. Because of this, and the numerous potential advantages of non-viral delivery systems, more laboratories are entering the field of gene delivery and aggressively pursuing the development of new systems. Their relative low cost, ease of production, safety and flexibility continues to make them attractive[11].

1.1 Thesis Outline

The research outlined in this thesis aims to develop a novel non-viral vector system to provide a solution to problems currently hindering the practical application of gene therapy. A review of published literature was undertaken to determine the current state of gene delivery and establish the criteria required for designing a safe and effective non-viral vector. Chapter 3 introduces the concept of gene therapy, highlighting the need for novel gene delivery systems. The assessment of non-viral vectors is discussed in Chapter 4. During this review, chitosan was identified as a non-toxic, biocompatible, biodegradable alternative for gene delivery systems.

Despite numerous attempts to improve the poor transfection of chitosan nanoparticles through modification, most of these resulted in systems with

increased toxicity and reduced biocompatibility. In addressing the need to create a modified chitosan system that would not alter the toxicity or biocompatibility of the system, we considered the incorporation of other biopolymers as a possible solution. This led to the identification of the alginate-chitosan system as being promising for gene delivery applications. Alginate and chitosan are both biocompatible natural polymers that together form a stable polyionic complex. The inclusion of alginate would be expected to reduce the strength of interaction between chitosan and DNA, and thereby improve transfection. The alginate-chitosan system has been used extensively in the pharmaceutical field and demonstrates a number of favourable characteristics for *in vivo* use as a gene carrier, including biocompatibility, biodegradability and stability. However, development of this system has been limited to the micro scale (~200 μm)[12].

It is well-established that natural polymers are less toxic than synthetic polymers, and can effectively carry and protect DNA more stably than liposomes. The development of alginate-chitosan nanoparticles offers a novel biocompatible, biodegradable non-viral vector alternative to synthetic polymeric nanoparticles and liposomes. Nano scale development would provide the ability to carry and deliver genes into cells for therapeutic purposes. Thus, attaining the goals outlined in this project will lead to biopolymeric nanoparticles that provide safe, stable, effective, gene carriers that could fulfill the promise of gene therapy.

The initial challenge of this research was to develop the alginate-chitosan system at the nano scale. Following the early development of alginate-chitosan nanoparticles, the process was optimised through a parametric study to minimise particle size. The optimised procedure allowed the formation of particles under mild conditions in water, in contrast to the harsh conditions and organic solvents used for many other non-viral vectors. Furthermore, alginate-chitosan nanoparticles, approximately 300 nm in diameter, demonstrated the ability to adsorb and release DNA. The development of the alginate-chitosan system at the nano scale was published in the Journal of Biomaterials Science – Polymer Edition (Douglas et al., 2005, 16(1):43-56), and is presented in Chapter 5.

Although the system was successfully developed at the nano scale and demonstrated desirable DNA adsorption characteristics, smaller nanoparticles were deemed necessary to facilitate cellular internalisation. The initial development was followed by work to improve the system characteristics, with subsequent analysis regarding its interaction with DNA and with cells. Through modification of the materials and the protocol, considerably smaller particles were obtained. The effect of alginate on the binding between DNA and chitosan, which has been thoroughly investigated as a gene delivery system, was also investigated. Alginate-chitosan nanoparticles were found to be non-toxic, yet transfected 293T cells with high efficiency. This work has been submitted to the Journal of Controlled Release and is presented in Chapter 6.

Following the successful transfection of the 293T cell line, alginate-chitosan nanoparticles were used to transfect COS7 and CHO cell lines. As with other viral and non-viral systems, cell line-dependent transfection was observed. To understand the observed differences between cell lines, the internalisation and intracellular trafficking of the nanoparticles were investigated. This was first attempted using NanoSIMS, a novel approach that required the development of corresponding protocols and analysis methods. A proof of principle was established for the method, and is summarised in Chapter 7. Confocal microscopy and flow cytometry were used to complete these studies, revealing that intracellular trafficking of the nanoparticles is directly linked to their transfection success or failure. Trafficking is related to the internalisation pathway, which in turn is determined by the cell line. These results, submitted for publication to Molecular Therapy, represent the first study to establish cell physiology as a determining factor in non-viral vector internalisation and trafficking, and are summarised in Chapter 8.

The remaining chapter includes a discussion of the conclusions to be drawn from this research as well as directions for future research stemming directly from this work. Appendix A contains a brief description of analysis techniques and conventions used in the field of gene delivery. Appendix B includes the experimental procedures for supplementary information provided in

Chapters 5 and 6. The NanoSIMS analysis method is briefly described in Appendix C.

Chapter 2
Rationale, Hypothesis and Objectives

2.1 Rationale

Chitosan-DNA nanoparticles are among the most biocompatible non-viral vectors developed to date. Their non-toxicity and biodegradability make them particularly attractive, but they demonstrate relatively poor transfection owing to the high strength of interaction between the two components. Several chitosan-based systems have incorporated modifications to improve transfection; however, most of these demonstrate increased toxicity. The development of a modified chitosan system with improved transfection capability, while maintaining biocompatibility, non-toxicity, and biodegradability would offer an attractive alternative to liposomal and synthetic polymeric systems.

2.2 Hypothesis

The inclusion of alginate in a chitosan-based nanoparticle system for gene delivery will reduce the strength of interaction between the vector and DNA, thereby improving transfection, while demonstrating favourable interactions with cells, being biocompatible, biodegradable, and non-toxic.

2.3 Thesis Objectives

After identifying the alginate-chitosan system as a promising candidate for a gene delivery system, the following objectives were established for this project:

1. Develop the alginate-chitosan system at the nano-scale. The following system characteristics were desired:
    a. Discrete, well-defined nanoparticles
    b. Small size, uniform distribution
    c. Reliable, repeatable results
    d. Preparation suitable for fragile biomolecules and *in vivo* delivery.

2. Characterise alginate-chitosan nanoparticles as efficient gene delivery vectors. In particular, the following features were required:
    a. Ability to interact with DNA to form complexes
    b. Ability to protect DNA from degradation by nucleases
    c. Ability to be taken up by cells effectively
    d. Non-toxic.

3. Investigate the role alginate plays in the formation of nanoparticle-DNA complexes.

4. Assess alginate-chitosan nanoparticles as transfection vectors *in vitro*. Transfection ability was gauged in comparison to a commercially available non-viral vector and unmodified chitosan nanoparticles.

5. Characterise the internalisation mechanism and intracellular fate of complexes. In particular, there was interest in investigating the relationship between intracellular trafficking of alginate-chitosan nanoparticle complexes and transfection efficiency. As part of this objective, a novel technique involving transmission electron microscopy (TEM) and correlational NanoSIMS analysis was developed.

2.4 Summary of Original Contributions

This thesis contains one published manuscript and two manuscripts presently under peer review. The first publication, printed in the peer-reviewed Journal of Biomaterials Science – Polymer Edition, presents the development of novel alginate-chitosan nanoparticles through a parametric study designed to optimise preparation conditions. The second manuscript, submitted to the Journal of Controlled Release, characterises the system as a gene delivery vehicle through evaluation of its ability to complex and protect DNA and to transfect cells. The role of alginate in the system is also evaluated. The third manuscript, submitted to

Molecular Therapy, details the internalisation and intracellular trafficking of alginate-chitosan nanoparticle complexes in three cell lines, and relates this to the observed cell line-dependent transfection. This represents the first study conclusively identifying cell physiology as the determining factor in the transfection efficiency of non-viral vectors.

Chapter 3
Gene Therapy – Promises and Problems

3.1 Gene Therapy

Gene therapy has been defined as the introduction of genetic material into cells to elicit a therapeutic effect in order to prevent, control or cure disease[1]. In contrast to the traditional approach of treating genetic disorders through management of disease symptoms, gene therapy aims to remedy the source of the problem by replacing the corresponding defective gene(s). Advances in cellular and molecular biology, including the ability to prepare, manipulate and control the production of recombinant genes, have contributed greatly to the development of this field[13]. With the recent completion of the human genome project and the resulting increased understanding of the genetic basis of disease, gene therapy has become a promising approach to the treatment of many diseases.

3.1.1 Therapeutic Applications of Gene Therapy

The ideal achievement of gene therapy would be to replace a disease gene mutation with a healthy gene; in the shorter term, the goal is to be able to deliver and express appropriate genes at the site of interest and at therapeutically effective levels[3]. The possibility of changing and controlling gene expression has enormous potential for the treatment of numerous pathological conditions.

3.1.1.1 Cancer

By far the greatest interest in gene therapy applications has been in the treatment and cure of cancer, being the focus of two-thirds of all clinical trials involving gene therapy[5]. The most basic approach to gene therapy treatment of cancer is through the replacement of mutated copies of the tumour suppressor gene[14]. Gene p53, which is involved in DNA repair and apoptosis mediation, is the most frequently mutated gene in human cancers[15]. Delivery of a healthy p53 gene to tumour cells could induce apoptosis, enhance chemosensitivity and restrict tumour growth through the prevention of angiogenesis[16]. A separate approach includes the delivery of genes encoding for an enzyme that activates an

anti-tumour pro-drug, which would allow delivery of an innocuous inactive drug systemically that would be converted to its active toxic form only in the tumour. Another approach involves the delivery of genes encoding for surface antigens that provoke an anti-tumour immune response[17]. A different tactic, called antisense therapy, involves the silencing rather than the promotion of gene expression and is promising for treatment of cancers. In this technique RNA that blocks the expression of specific genes is delivered to the cells. This technique can be used to silence oncogenes, oncogenic viral proteins, cell cycle-regulatory genes and anti-apoptotic genes[16].

3.1.1.2 Vaccination

An interesting application of gene therapy is the development of DNA vaccines that are able to stimulate immune responses and confer immune protection without the safety concerns associated with the use of attenuated or inactivated virulent organisms. In DNA vaccination, a gene encoding for a specific protein of the infectious agent (e.g. viral coat protein) is introduced into a cell where it is expressed, stimulating an immune response. DNA vaccines have been successfully administered intramuscularly, transdermally, intranasally, orally and epidermally[15]. This approach has been tested for vaccination against HIV in asymptomatic patients, bovine herpesvirus-1, mycobacterium avium, and peanut allergies[15,18].

3.1.1.3 Autoimmune Diseases

Diseases such as Crohn's, colitis, diabetes mellitus and arthritis are autoimmune diseases described by the inappropriate activity of the immune system against the patient's own tissues. For most of these diseases, no treatment exists and management is the only approach. Gene therapy offers a promising alternative through the ability to reduce immune reaction or induce immune tolerance of the specific tissue. This can be achieved through modulation of the immune response with expression of anti-inflammatory cytokines or by inducing tolerance in target cells through the expression of protective enzymes. In the case

of diabetes, an additional approach is to induce islet cell neogenesis in other tissues[15,19].

3.1.1.4 Organ Transplantation

Over 20,000 organ transplants are performed annually in the United States. Although organ transplantation incontrovertibly improves the quality of life of the recipient, the requirement of systemic immunosuppression to prevent organ rejection is associated with a decreased resistance to infection and an increased risk of malignancy[20]. Gene therapy has been explored to overcome the requirement of systemic immunosuppression by inducing the production of immunomodulatory proteins to be expressed in the donor organ, resulting in local immunosuppression[20].

3.1.1.5 Other Diseases

There are several other diseases for which gene therapy may be useful for treatment or cure. Many of these, including cystic fibrosis, haemophilia, severe combined immunodeficiencies (SCID), and the range of lysosomal storage disorders, are caused by single gene defects. In these cases, replacement of the defective gene is sufficient to improve patient health. Although some of these conditions, such as cystic fibrosis and SCID, require gene delivery and expression in specific organs and tissues[21,22], others, like lysosomal storage disorders and haemophilia, are treatable through gene expression and protein production in any tissue[23,24].

Diseases and conditions that do not have a clear genetic basis can also benefit from gene therapy. Treatment approaches for Parkinson's disease, a progressive disorder caused by the loss of dopamine-producing neurons, have included inhibition of apoptosis, stimulation of neurotrophic factor and inhibitory neurotransmitter expression, as well as the over-expression of enzymes involved in dopamine synthesis[25]. Ischemia caused by cardiac infarct and peripheral vascular disorders can be remedied through the delivery of genes that induce growth of new vessels in the area[26]. Gene therapy has also been investigated for

application in the fight against AIDS in asymptomatic HIV patients, through the delivery of suicide genes and antisense therapy to inhibit viral replication[27].

3.1.2 Limitations and Perspectives

Since 1989 there have been over 1,100 clinical trials involving gene therapy worldwide[5,28]. However, no gene therapy treatment has been approved for use by the FDA and the promise of gene therapy has not yet been realised. Progress has been hampered by an inability to efficiently and safely deliver genes to cells due to the fragility of genetic material and difficulties introducing it into target cells. The ability to induce greater gene delivery and protein expression while limiting the use of immunogenic agents is vital to the success of gene therapy.

Inducing gene expression in all cells of the target tissue is ideal, although it is not always necessary to elicit a therapeutic effect. In many diseases, including several mentioned previously, the expression of low levels of the missing enzyme or protein is sufficient to provide a therapeutic benefit to the patient. For example, expression of a specific enzyme in 25% of blood mononuclear cells is adequate to improve SCID patient health[22], while expression of factors VIII and IX in treatment of haemophilia at levels as low as 2% of normal is enough to improve patient welfare[23]. Furthermore, in many of these cases, such as with cancer, a significant bystander effect can be observed wherein neighbouring cells that do not express the transgene are impacted by its effect[16]. These observations emphasize that even a small increase in gene transfer efficiency can have a significant effect in disease treatment.

3.2 The Mechanics of Gene Therapy

Gene therapy is an elaborate process, involving several phases. The introduction of the gene 'drug' to the body is the first and easiest stage. This is followed by transfection (Figure 3.1): the gene must find and enter the target cell, followed by its transcription and translation into a functional protein. The

resulting protein ultimately produces the therapeutic effect and may act on the cell where it was produced, on neighbouring cells, or at distant sites following transportation by the circulatory system[3]. Unfortunately, the processes involved in many of these stages are only beginning to be investigated in detail, and as yet they are not easily inducible or controllable.

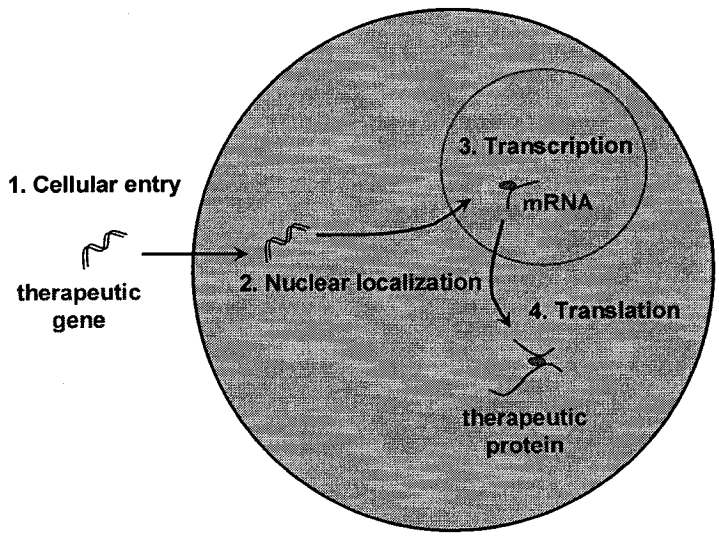

Figure 3.1. The main stages involved in transfection. **The therapeutic gene must gain entry to the cell and then into the cell nucleus. Once in the nucleus, the cellular machinery transcribes the DNA into mRNA. This is then shuttled outside the nucleus where it is used to make the protein.**

Since the protein is the biologically active agent and administration of the protein would preclude some of the steps involved in gene therapy, it is reasonable to speculate on the possibility of protein therapy rather than gene therapy. However, compared to DNA, proteins are generally more expensive to produce, less stable, demonstrate very short circulation life-times, require more stabilisation in transit, and post-translational modifications that are difficult to induce[6]. For these reasons, the delivery of genetic material to cells has been preferentially pursued.

Although the synthesis of recombinant genes can now be done relatively easily, there are several difficulties encountered in the transfection process. Targeting the gene to specific cells is desirable, although not always essential for transfection. Conversely, transport of the gene into the cell and its subsequent

transcription while avoiding degradation is vital for effective gene therapy. The achievement of these last steps is the primary focus of the field of gene delivery[7].

3.3 The Need for Gene Delivery Systems

The promise of gene therapy has not yet been realised; it has been hampered by the inability to efficiently and safely deliver genes to target cells *in vivo*[29]. Early attempts at *in vivo* gene therapy consisted of the injection of DNA without any carrier ("naked" DNA), usually into skeletal muscle[13]. This resulted in low transfection and transient expression, which was attributed to degradation and poor cellular penetration. Naked DNA is highly susceptible to and rapidly degraded *in vivo*[30]. The ability to remain active for a prolonged time in the body, and particularly in the plasma, is essential to allow the gene to reach target cells[31]. Any DNA that evades degradation and reaches a target cell encounters a further problem: genetic material, whether DNA, RNA or oligonucleotides, is anionic, which hinders its ability to approach and cross the negatively-charged cell membrane. Furthermore, the large size of plasmid DNA that is frequently used for gene therapy restricts entry into most cells[30].

Genes that manage to cross the cell membrane encounter an additional threat of degradation. Most material enters cells through the process of endocytosis. This process involves the infolding and pinching off of the cellular membrane to form small vesicles called endosomes (Figure 3.2). Endosomes then fuse to other small vesicles called lysosomes, which contain degradative enzymes (lysozyme) in an acidic environment. Most nuclear material is unable to withstand the harsh conditions in lysosomes and is rapidly degraded[32]. The degradation of naked genes extracellularly and intracellularly, combined with its poor cellular penetration, leads to low levels of transfection and transient gene expression.

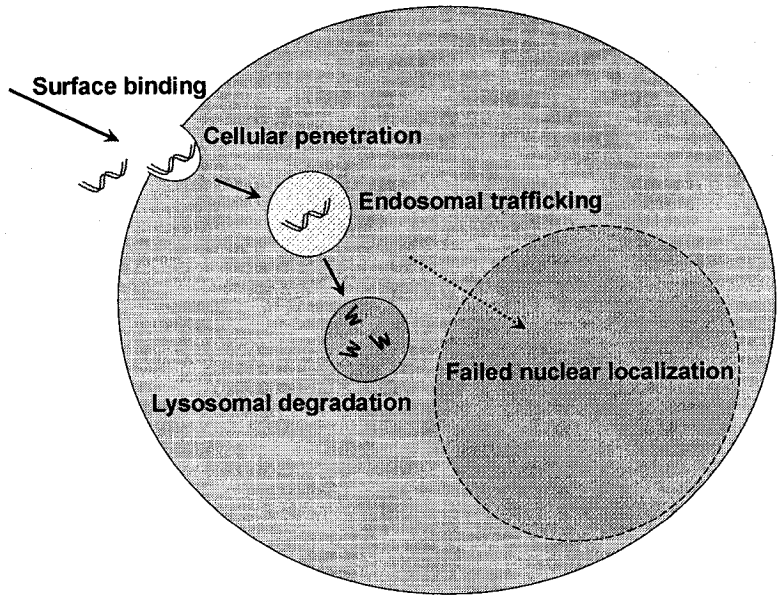

Figure 3.2. Schematic representation of the obstacles to effective transfection. **The therapeutic gene approaches the surface of the cell and, if it overcomes the electrostatic repulsion, enters the cell through endocytosis. Once endocytosed, the gene is trafficked to lysosomes where it is rapidly degraded, resulting in failed nuclear localisation.**

To realise the promise of gene therapy, a method must be developed to overcome these obstacles. The development of safe and efficient delivery systems, designed to protect and stabilise the gene extracellularly and in lysosomal compartments, as well as aid its entry into cells, is paramount to the success of gene therapy. The ideal gene delivery vehicle, or vector, would improve the bioavailability of the gene, be non-immunogenic and non-toxic, be able to conjugate targeting ligands, permit co-encapsulation of other bioactive agents if necessary, and be amenable to large-scale synthesis[33]. At a minimum, the vector must protect the gene and enable its entry into the target cell. This goal has been the focus of extensive research throughout the world. Despite this, the ideal gene delivery system has not yet been discovered[34]. It is likely that the development of one ideal system that works for all applications will not occur; rather, each therapy will demand the optimisation of its own delivery system, having specific requirements as to targeting and release. The two main approaches to gene delivery that are widely studied involve the use of viral vectors and non-viral vectors.

3.3.1 Viral Vectors

There are currently several types of viruses that have been used and are being studied for use as gene delivery systems, including adenovirus, adeno-associated virus, retrovirus, vaccinia virus, pox viruses, herpes virus and influenza virus[35]. Each of these has its own unique properties and is able to transfect a different variety of cells. The advantage they all share is their highly efficient ability, acquired through evolution, to transfect cells[36]. This ability had initially generated much interest in their development: viral vectors are the most commonly used delivery system for *in vivo* gene therapy and have been used in nearly 70% of all clinical gene therapy trials since 1989[5].

Viruses have the natural ability to transfer their genetic material into cells (Figure 3.3). They are well adapted to protect their genetic material from degradation in the body, can rapidly and easily penetrate cells, and escape lysosomal degradation. Furthermore, their nuclear material invariably enters the nucleus of the cell, leading to efficient translation and transcription. It was thought that the capacity of viruses to transfect cells could be exploited for gene therapy applications. By replacing the viral DNA with the gene of choice, the viral machinery could be manipulated to insert it into a host cell where it would be expressed. With a viral insertion, there is also the possibility that the gene could be integrated into the host genome and expressed indefinitely[37].

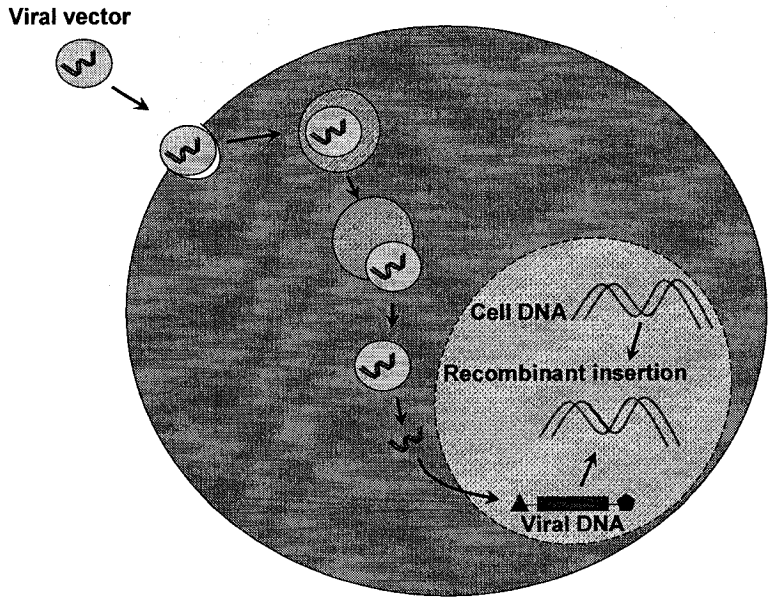

Figure 3.3. Schematic representation of viral-mediated gene delivery. The virus enters the cell through endocytosis and subsequently escapes the endosome to the cytoplasm. The gene is released and enters the nucleus, where it can be inserted into the host genome.

Despite the highly efficient nature of viral vectors, there are many disadvantages related to their use. Issues relating to their immunogenicity, oncogenicity, potential reinfectivity, and manufacture, targeting and loading abilities have dampened enthusiasm for their development[6].

While viruses remain highly evolved and adapted gene delivery vehicles, the body has also evolved and adapted to the threat they pose. Accordingly, the introduction of viruses into the body leads to an immune response. This reaction is initiated following the first administration of the virus and therefore does not usually hinder the activity of the first dose. However, if repeated dosing is required for cases where transient gene expression is observed, all subsequent administrations will elicit more severe immune responses, resulting in loss of the gene, reduction in therapeutic benefit, and discomfort to the patient. In some cases, immune responses can lead to severe reactions, including death. Two fatalities of patients undergoing human gene therapy in clinical trials involving viral vectors have been attributed to immune reactions[3]. Their immunogenic nature poses the single biggest threat of using viral vectors.

Viruses that do successfully reach their target cell and insert their genetic cargo have the possibility of creating more health problems for the host. The

genetic material delivered by viruses often has the ability to insert into the host genome. Integration into the host genome usually happens randomly, which leads to the possibility that a normally unexpressed gene may begin to be expressed, or a normal, healthy gene may become deficient. Either of these cases, termed insertional mutagenesis, can result in the development of mutagenic cells, leading to cancer in some instances[13]. This is believed to have happened in two cases involving clinical trials of human gene therapy using viral vectors. The genetic disease was cured by the therapy but resulted in the development of a rare and particularly virulent form of cancer[38].

An additional health threat posed by the use of viral vectors is related to their natural propensity to reproduce and infect. In the development of viral vectors for gene therapy, much of the viral genetic material is removed, leaving only those genes that are required for the virus to retain the capacity to insert the genetic material into a host cell and have it translated and transcribed. This modification is necessary to eliminate the infectivity of the virus. However, through genetic recombination with other viral genes, it is possible for viruses to regain their infectivity[35]. The threat of reinfectivity is serious for all patients but particularly so for individuals whose disease condition leads to an immunodeficiency.

Even if there were no safety concerns surrounding the use of viral vectors, preparation disadvantages inhibit widespread use. Viruses in their native state have the ability to reproduce at alarming rates; contrarily, the high numbers of viruses required for efficient gene therapy applications are difficult to achieve and control through the large scale manufacture of modified viruses[8]. Additionally, the naturally small amount of genetic material contained in viruses limits their capacity for genetic cargo; viruses usually carry up to 7.5 kb[6]. This presents a problem when larger amounts of genetic material are required for particular gene therapy applications. Additionally, although viruses have a tremendous ability to transfect certain cells, it is exceedingly difficult to target them to cells they do not normally infect (Table 3.1)[29]. The manufacturing difficulties of viral vectors,

combined with the considerable safety concerns regarding their use have led many researchers to search for alternative non-viral delivery systems for gene therapy.

Table 3.1. Common viruses and the cells they transfect.

Type of Virus	Cells/Tissues Infected
Adenovirus	Epithelium of respiratory, gastrointestinal and urinary tracts, conjunctiva (eye)
Adeno-associated virus (AAV)	Rapidly dividing cells, particularly intestinal epithelium and haematopoetic system; independently transduction incompetent
Herpes viruses	Neurons of the central nervous system
Hepatitis	Hepatocytes of the liver
Retrovirus	Dividing cells only

3.3.2 Non-Viral Vectors

Non-viral delivery systems for gene therapy have increasingly become the focus of much work in the field of gene delivery. All available methods for inserting a gene into a cell without the use of a virus form part of this class of vectors, including some physical methods that are usually performed *ex vivo*. In *ex vivo* methods, cells are removed from the organism, genes are inserted into the cells *in vitro*, and the cells are reintroduced to the body[13]. This method generally yields higher numbers of transfected cells, but is restricted to cells that can be easily biopsied and cultured *in vitro*, and is more invasive and time-consuming than is practical.

Unfortunately, the methods that have proven effective for *in vitro* transfection often cannot be applied *in vivo*. Some physical methods of gene delivery *in vivo* exist, including direct injection of DNA, and jet injection or particle bombardment[39,40]. However, these generally lead to transient expression and low levels of transfection, and can only be used for certain cell types (skeletal muscle, in particular). Although these physical methods are useful in certain cases, the ultimate goal of gene therapy is to develop methods that can be applied easily and effectively *in vivo*, can target specific cells, and elicit efficient transfection. The focus, therefore, of research into non-viral vectors has been on the development of gene carriers, usually either cationic lipids or polymers, that

offer protection for the therapeutic agent and assist cellular penetration. In effect, researchers are attempting to develop carriers that work like viral vectors without imparting the features that make them hazardous.

The early development of non-viral vectors was largely based on research in the field of drug delivery systems. This field has been highlighted as one of the most hopeful research fields in the realms of medicine and biotechnology[41,42], due in part to its applicability for the delivery of novel biomolecular therapeutic agents, including genes. Drug delivery systems exhibit a variety of shapes and sizes, ranging from nano- and micro- scale to macroscopic sizes, though the advantageous capacity of nanoparticles to penetrate cells and deliver their cargo intracellularly makes them particularly attractive for gene delivery applications.

Non-viral vectors offer numerous advantages compared to their viral counterparts, specifically in the areas of safety, targeting, and production. The materials used as carriers in these systems are usually non- or mildly immunogenic. This permits repeat administration where transient gene expression is observed[43]. The genes they carry do not integrate into the host genome, thereby eliminating the risk of insertional mutagenesis. Additionally, there is no way for the carriers themselves to become transformed into a unit that poses a threat of infectivity.

Non-viral vectors in their basic forms do not target any particular cell type; in this manner they may be taken up and the gene expressed by virtually any cell in the body[36]. Alternatively, targeting moieties or ligands can be incorporated, allowing specific tissues and cells to be targeted[10]. Plasmid DNA, which is the genetic material most often used in non-viral applications, can be generated relatively easily and in large quantities[6]. Generally, the materials used in non-viral carriers can also be produced relatively easily, making large-scale synthesis of these vectors a practical endeavour. A final advantage non-viral vectors have over viral vectors is their ability to incorporate genes of unlimited size; plasmids as large as 2.3Mb have successfully been delivered to cells using non-viral carriers[7]. This allows the delivery of any gene, or of several genes simultaneously should

disease management necessitate the production or inhibition of more than one protein.

The advantages non-viral vectors have compared to their viral counterparts, particularly with respect to safety, are significant. However, they do present their own disadvantages and remain inferior to viruses for effective gene delivery. While the materials used in non-viral vectors are generally non-immunogenic, the same cannot be said about their toxicity. Some systems have demonstrated toxicity to cells *in vitro* and mild immune and toxic responses *in vivo*[7]. Though not characteristic of all non-viral vectors, it does serve to remind researchers that the introduction of foreign matter into the body always involves some risk.

These carriers also present some disadvantages unrelated to their toxicity and safety. Though most non-viral carriers offer protection from degradation to genes *in vivo*, not all have demonstrated the prolonged stability expected or desired[8]. This is due, in part, to the way in which genetic material is associated with the carriers. Often, the genes are located not only within the carrier but on the surface as well. Surface-bound nuclear material has been found to be more susceptible to degradation, where interactions with the carrier at the surface are unable to sufficiently protect the genes[9]. This is a problem not exhibited by viral vectors, where all genetic material is located inside the protein coat. Although degradation of surface-bound material is problematic, the major drawback of non-viral vectors is that they have not yet matched the efficiency of cell transfection exhibited by viral vectors[10]. None of the carriers used to date has been able to transfect cells resulting in expression as high as demonstrated by viruses, regardless of the gene or the cell type.

Despite the sub-optimal transfection efficiencies exhibited by non-viral vectors, the disadvantages are minor compared to the safety concerns surrounding viral vectors. Considering these drawbacks and the numerous potential advantages of non-viral delivery systems, more laboratories are entering the field of gene delivery to aggressively pursue the development of new systems. Their relative

low cost, ease of production, safety and flexibility as compared to viral vectors continues to make them attractive[11].

Research into the development of non-viral vectors has focused mainly on the use of two types of systems: liposomal and polymeric. The properties of each of these groups of materials lead to vectors with certain shared characteristics, presenting their own advantages and disadvantages for use as gene vectors, as summarised in Table 3.2.

Table 3.2. Comparison of the characteristics of non-viral vectors.

	Non-Viral Vectors			
	Liposomes	**Biodegradable polymer nanoparticles**		
		Synthetic hydrophobic polymer	**Synthetic hydrophilic polymer**	**Natural polymer**
Examples	Lipofectamine™, DOPE, DOTAP	PLGA, PLA	PLL, PEI, PEG	Chitosan, dextran, gelatin
Biocompatibility	• *In vitro* and *in vivo* toxicity[44]	• Can be toxic, particularly at high concentrations • Toxicity depends on polymer, molecular weight, form (branched or linear), size and charge of particles [45] • Generally less toxic when complexed with DNA		• Generally non-toxic[46,47]
***In vivo* lifetimes**	• Rapid removal (in first capillary bed) unless "masked"[31,48]	• Longer than liposomes, shorter than desired • Hydrophilic particles display longer lifetimes[49]		
Stability	• Unstable in physiological fluid[43] • Sensitive to membrane disruption[50]	• Stable in physiological fluid and *in vivo*[50]		
Protective ability	• Dissociation of DNA in physiological conditions[50] • Degradation of surface-bound DNA[43] • Sustained release not possible[6,50] • Encapsulation difficult[13]	• Association causes DNA to condense [46] • Encapsulation possible, easier than for liposomes[43] • Difficult to associate hydrophilic DNA; causes conformational changes	• Association causes DNA to condense, offering protection[46] • Encapsulation possible, easier than for liposomes[43]	

Loading capacity and manufacture	• High compared to viruses. • Little control over release. • Quality control issues.	• Higher than liposomes[51] • Sustained release possible[52] • Genes may undergo conformational changes in hydrophobic nanoparticles[10] • Easy encapsulation of hydrophilic therapeutic agents in hydrophilic nanoparticles. Easy to manufacture		
Targeting	• Incorporation of targeting ligands possible[53,54]	• Incorporation of targeting ligands possible • Incorporation easier than with liposomes[43]		
Transfection ability	• Considerable *in vitro* efficiency (Lipofectamine ™); limited success *in vivo*[29]	• Generally not as high as liposomes • Evidence of higher transfection than liposomes *in vitro* and *in vivo*[55]	• Generally not as high as liposomes, • Evidence of higher transfection than liposomes *in vitro* and *in vivo* particularly with PEI-based nanoparticles[7]	• Generally not as high as liposomes. • Comparable to most synthetic polymeric nanoparticles

3.3.2.1 Liposomes

Until recently, liposomes had been the most studied delivery system[50]. Liposomes are spherical vesicles with a lipid bi-layer membrane, formed through the spontaneous organisation of lipids in aqueous medium (Figure 3.4)[13]. Any lipid or combination of lipids may be used in the preparation of liposomes, provided that there is a net ionic charge. Cationic liposomes have been widely studied since they are considered to have characteristics favourable for gene vectors. The positive charge is thought to facilitate electrostatic interactions between liposomes and genes, which have net negative charges, and between the liposomes and cells, the membranes of which are also negatively charged. It was thought that these non-toxic complexes would be able to provide non-targeted gene delivery throughout the body. However, widespread use has been hindered by factors relating to production and application. Notwithstanding the satisfactory transfection efficiencies demonstrated with liposomal vectors, the problems associated with cytotoxicity and stability have turned attention towards the use of polymeric nanoparticles for gene delivery.

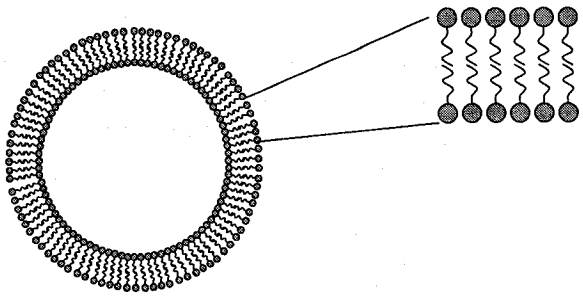

Figure 3.4. Schematic representation of liposome structure, showing organisation of lipids in the bilayer membrane.

3.3.2.2 Polymeric Nanoparticles

Nanoparticles prepared using polymers offer an interesting alternative to liposomes, and have been increasingly studied as the delivery vehicle of choice[50]. These particles can take various forms, including solid particles, capsules, and matrices. Solid particles are generally spheres where the core and surface are continuous. References to this form are not common in delivery systems, since the solid core prevents or limits the encapsulation of therapeutic agents. Capsules, on the other hand, comprise a polymeric outer membrane surrounding a hollow core, with a basic structure similar to liposomes. Matrix systems are generally formed by the interaction between several polymer chains, resulting in the formation of a "net-like" system with inter-chain spaces and pores. An analogy between these systems and sponges, which contain many small cavities within a distinct solid structure, has led to the use of the term *nanosponges* to label these structures. These structures remain the most popular for delivery systems, as they possess the physical characteristics favourable for gradual and sustained release of their cargo.

Nanoparticle preparation is dependent on the polymer used, of which there is an abundance to choose from. Nanoparticles made with non-biodegradable polymers were introduced in 1976, followed by the use of biodegradable polymers in 1979[56]. The use of non-biodegradable polymers has been nearly abandoned since biodegradation of the carriers allows their elimination from the body, preventing accumulation and any ensuing problems[57]. The preparative conditions of nanoparticles are a crucial aspect in the design of delivery systems since the incorporation of therapeutic agents necessitates their presence during

particle formation. As previously discussed, there is a need to stabilize and protect the activity of the DNA. Nanoparticle preparation ideally should be achieved using mild conditions, such as aqueous media, low temperature and near-neutral pH in order to preserve the structure and activity of the active molecules[58].

There are four main methods used to prepare nanoparticles: emulsification polymerisation (EP), emulsification–diffusion–solvent evaporation (EDSE), emulsification droplet coalescence (EDC) and ionic gelation (IG). Ionic gelation is sometimes referred to as complex coacervation (IG). Generally speaking, the processes used to prepare nanoparticles are more amenable to large-scale manufacture than liposome production methods[50]. Emulsification polymerisation forms particles by a polymerisation reaction occurring within micelles of an emulsion. Although this method can result in well-defined, uniform nanoparticles, there is a problem associated with any residual monomers, initiators or co-reactants, which may be highly toxic. The second and third methods, EDSE and EDC, also require the formation of an emulsion with the polymer of interest located in micelles. This is followed in EDSE by diffusion of the polymeric solvent outside of the micelles followed by its evaporation, causing the particle to precipitate. With EDC, two emulsions containing different polymers or a polymer and another agent are mixed together, allowing the micelles to unite. The mixture of the contents of the two emulsions causes a precipitation of the polymer leading to formed nanoparticles. Since these latter two methods require emulsions, they are generally easier to use for organic-soluble rather than water-soluble polymers. This is because organic-in-water (O/W) emulsions are generally easier to prepare and are more stable than water-in-organic emulsions. Furthermore, most suitable organic liquids have lower boiling points than water, making the EDSE method very difficult to use with water-soluble polymers.

Conversely, ionic gelation is a method particularly suited to water-soluble polymers. It involves the spontaneous interaction between two oppositely charged molecules, of which at least one is a polymer, and does not require the formation of an emulsification, nor any additional reagents (e.g. surfactants) that could lead to toxicity. The interaction between the soluble polymer and its ionic pair, or

between two oppositely-charged soluble polymers, leads to the formation of an insoluble gel. This is similar to the mechanisms involved in the EDC method, but eliminates the use of surfactants and organic solvents. Control of the size and characteristics of the resulting insoluble particles is the greatest difficulty associated with this method, and can be achieved by adjusting the concentrations and introduction of the starting materials.

Nanoparticle preparation through spontaneous ionic gelation is preferable for several reasons. Preparation does not involve the high temperatures required to evaporate the solvent in EDSE. All steps can be performed in an aqueous environment for water-soluble polymers, negating the possibility of residual organic solvents or surfactants used in emulsions. Both organic solvents and surfactants can be toxic to cells, as well as the environment, with residual traces often being enough to produce a cytotoxic effect[49]. Additionally, the spontaneous gelation of a pre-formed polymer also removes the threat posed by residual monomers, initiators, other reactants and any possible by-products, which can be encountered as a result of polymerisation reactions. For polymers that are suitable for its use, this preparation process offers many advantages over other available methods. However, owing to the electrostatic nature of the interactions involved, nanoparticle preparation via ionic gelation can be affected by various parameters, including ionic strength and pH. Generally, increasing ionic strength hinders ionic gelation, due to charge shielding by the presence of ions in solution[59]. Changing pH can also affect nanoparticle formation, by reducing or even reversing the charge of the polyion as the pK_a of the polyion is approached and crossed[60]. While it is important to be mindful of the effects of these parameters on particle formation, they can generally be easily controlled. Despite these concerns, the advantage of nanoparticle preparation under mild conditions has made it the standard method. The majority of nanoparticles made with hydrophilic polymers are prepared using spontaneous ionic gelation[33,43,44,60-63].

3.3.2.2.1 Synthetic Biodegradable Polymeric Nanoparticles

Most of the early work in polymeric non-viral vectors involved the use of synthetic biodegradable polymers, with the following polymers commonly used in the formulation of nanoparticles: polycaprolactones, poly(lactic acid) (PLA), poly(lactide-co-glycolide) (PLGA), polyacrylates and their copolymers. Of these, PLA and PLGA have been the most intensely studied[64]. All of these polymers are biodegradable and can provide sustained release of encapsulated materials for periods ranging to several weeks[65,66]. Unfortunately, many of them exhibit toxicity that can be detrimental to the therapeutic agent and the cells to which they are administered due to preparations involving organic solvents and relatively harsh conditions.

Additionally, many of these polymers are strongly hydrophobic, effectively preventing efficient encapsulation of hydrophilic biomolecules, including several drugs, proteins, peptides and genes. As well, incorporation often results in increased particle size and can cause the drug to undergo conformational changes that impair its activity[10]. *In vivo* distribution is also hampered by this hydrophobicity, which makes the particles susceptible to protein adsorption in the blood and clearance from the body. In order to overcome these difficulties, hydrophilic modification of these particles has been the focus of much research.

Several methods have been attempted to render hydrophobic nanoparticles more hydrophilic. The most popular method, and the one that has demonstrated the most promising results, involves the use of poly(ethylene glycol) (PEG) (Figure 3.5). PEG-grafted particles have demonstrated reduced adsorption of blood proteins, long circulation life-times and reduced uptake by the mononuclear phagocytic system (MPS), caused primarily by steric repulsion[49,67]. The molecular weight of the PEG used and its density on the surface of the nanoparticle affects the extent to which these benefits are manifest[49].

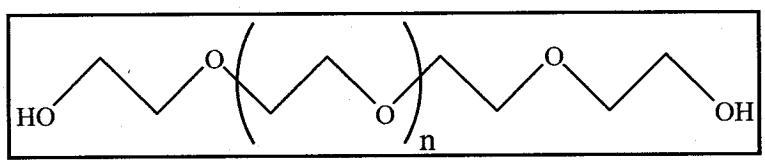

Figure 3.5. Structure of poly(ethylene glycol) (PEG).

The incorporation of hydrophilic components also facilitates the encapsulation of hydrophilic therapeutic agents, including genes[8]. The hydrophilic modification of synthetic polymeric nanoparticles circumvents the problems associated with hydrophobic particles. However, the preparation of these hydrophobic-hydrophilic nanoparticles still requires the use of organic solvents and surfactants, as well as homogenisation and sonication, which has been shown to affect the structure and activity of DNA[65]. There is also the additional possibility that grafted PEG chains may slowly desorb *in vivo*, reducing the efficacy of the particles[48]. Nonetheless, the incorporation of hydrophilic polymers in nanoparticles has shown improved characteristics for delivery systems.

3.3.2.2.2 "Stealth" Hydrophilic Polymeric Nanoparticles

The successful outcome obtained by coating hydrophobic particles inspired researchers to pursue the development of "stealth" particles. These particles were to be prepared using only hydrophilic polymers, providing all the benefits of these materials while reducing the problems associated with harsh preparative conditions and the possible desorption of the coating layer[48]. The term "stealth" refers to the expectation that these particles would travel through the bloodstream virtually unnoticed by the immune system, avoiding adsorption of blood proteins, uptake by the MPS, and clearance by the reticulo-endothelial system (RES).

Nanoparticles prepared with hydrophilic polymers demonstrate longer circulation times than their hydrophobic counterparts, and to facilitate the encapsulation of hydrophilic therapeutic agents. These materials offer the additional advantage of being water-soluble, thereby eliminating the risks posed by organic solvents and surfactants. There are a number of synthetic hydrophilic polymers used in the formulation of nanoparticles, including the commonly used poly-$_L$-lysine (PLL), and poly(ethylene imine) (PEI).

PEI demonstrates significant *in vitro* and *in vivo* transfection ability, and is generally considered to be the most effective cationic polymer among non-viral vectors[68]. The toxicity of PEI polymers varies depending on molecular weight,

form (branched vs. linear), and dose, with low molecular weight polymers demonstrating very little toxicity[61,69]. However, the lowest molecular weight PEIs do not generally mediate efficient transfection, and a positive correlation has been observed between the effectiveness of PEI transfection and its toxicity[70]. PLL, while also demonstrating cytotoxicity, does not mediate transfection efficiently[71]. Furthermore, PLL-DNA complexes are prone to aggregation in solution, creating problems for delivery and cellular internalisation[72].

Although the hydrophilic nature of these polymers increases *in vivo* stability and lifetimes, both are detrimentally affected by their positive charge. The highly charged nature of these particles seems to enhance their clearance from the bloodstream following intravenous administration[73]. The incorporation of uncharged hydrophilic polymers, such as PEG, has been investigated in an attempt to shield the particle charge. While this results in improved circulation lifetimes, it was not as prolonged as was observed with stealth liposomes[73].

3.3.2.2.3 Natural Polymeric Nanoparticles

Perhaps of greater interest for biological application are natural polymers. These polymers exhibit numerous characteristics suitable for delivery systems. A variety of natural polymers, such as albumin, chitosan, collagen, dextran, and gelatin, have been used in the formulation of delivery systems[66]. Although there are relatively few polymers found in nature compared to the abundance of synthetic polymers, their desirable characteristics make them particularly appealing for use in delivery systems[46]. These polymers, also called biopolymers, are biocompatible and display low immunogenicity and minimal cytotoxicity[46]; systemic toxicity is not observed following administration[47]. Moreover, many of these polymers are hydrogels, which are materials that have the ability to swell in and retain water[74]. This ability, mediated by the presence of hydrophilic groups, can be exploited for swelling-controlled devices. Additionally, hydrogels are generally biodegradable and biocompatible[75]. The interest of medical and pharmaceutical industries has turned increasingly towards the use of biopolymers in an attempt to exploit their desirable characteristics[76].

3.4 Designing Novel Non-Viral Vectors

Evidently, there are numerous options for the development of non-viral vectors. The basic requirements of protecting the gene and enabling its cellular internalisation are fairly easily met, considering the range of materials and forms available. With the availability of numerous vectors that fulfill these fundamental requirements, the focus in the design of novel gene delivery systems has expanded to include vector characteristics that improve delivery. In addition to protecting the gene and aiding its cellular penetration, the ideal vector would also be non-immunogenic, non-toxic, biocompatible and biodegradable. Furthermore, a hydrophilic character would benefit preparation and delivery aspects by avoiding the use of organic solvents and by reducing opsonisation and removal from circulation. Natural polymers offer numerous advantages compared to their synthetic counterparts and to liposomes, and are particularly well suited for use in gene delivery systems.

Within the field of drug delivery, the use of polysaccharides and other biodegradable polymers has commanded much interest due to the ability of the polymers to be degraded and reabsorbed by the body, and to their general biocompatibility[75,77]. It is well established that natural polymers are less toxic than synthetic polymers, more stable than liposomes, and can effectively carry and protect DNA. These biopolymers, which are naturally hydrophilic, have demonstrated protective capacities towards associated therapeutic biomolecules[78,79].

3.4.1 Chitosan-based Systems

Polysaccharides are the most abundant polymers in nature, and exhibit desirable characteristics for delivery systems: they are hydrophilic, biocompatible, biodegradable, can encapsulate therapeutic agents, and allow for the incorporation of targeting ligands[80]. They are also generally non-toxic and non-immunogenic. The polysaccharide chitosan has been extensively studied for drug delivery

applications, and is the most widely studied biopolymer for the purpose of gene delivery systems[81,82].

Chitosan, the second most abundant natural polymer, is a deacetylated derivative of chitin, a biopolymer found in the shells of crustaceans (Figure 3.6). Composed of *D*-glucosamine and *N*-acetyl-*D*-glucosamine units, chitosan is biocompatible, non-toxic, and non-immunogenic[46]. As well as having improved biocompatibility over synthetic polymers, chitosan demonstrates exceptional abilities in crossing mucosal barriers, passing through tight junctions in the intestinal epithelium, and binding to and traversing cellular membranes[83]. Chitosan-based delivery systems continue to command interest for delivery of drugs, proteins, DNA and oligonucleotides, with promising results[43,57,65,81,84-88].

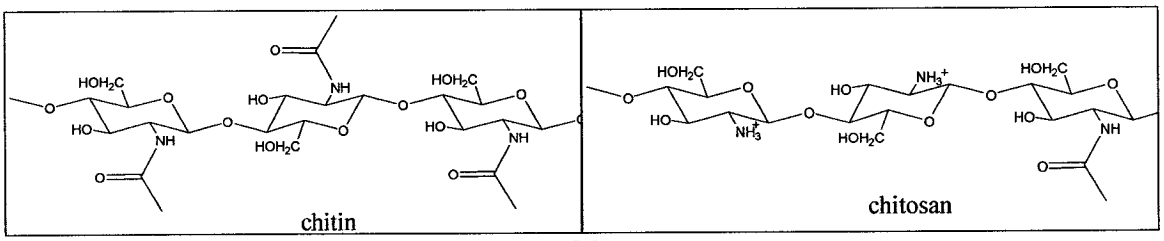

Figure 3.6. Structure of chitin and chitosan. **The ratio of *D*-glucosamine and *N*-acetyl-*D*-glucosamine units in chitosan is referred to as the *degree of deacetylation*.**

3.4.1.1 Chitosan Nanoparticles

The cationic nature of chitosan at acidic and neutral pH creates electrostatic interactions between it and DNA, leading to the formation of distinct nanoparticles. Chitosan nanoparticles can be prepared using several methods, including desolvation[44] and ionic gelation[89]. In the first method, sodium sulphate or sodium nitrate is used to desolvate the local water environment surrounding the polymer, increasing its interaction with DNA[43]. Ionic gelation involves the spontaneous interaction between two oppositely charged molecules, of which at least one is a polymer. The interaction between the soluble polymer and its ionic pair, or between two oppositely-charged soluble polymers, leads to the formation of an insoluble gel. Tripolyphosphate is the most commonly used reagent for the formation of chitosan-DNA nanoparticles through ionic gelation[90]. Control of the size and characteristics of the resulting insoluble particles is the greatest difficulty

associated with this method, and can be achieved by adjusting the concentrations and introduction of the starting materials.

Transfection studies with chitosan nanoparticles exhibit dependence on molecular weight, degree of deacetylation, pH, and chitosan:DNA charge ratio[91]. Regardless of these parameters, chitosan-DNA nanoparticles are not able to mediate transfection as desired; they generally transfect cells more efficiently than naked DNA but less than commercially available liposome formulations[86,89,89,90,92,93]. The reason for inefficient transfection is not well understood. Thorough studies of this system have shown that DNA is effectively protected in the particles, the particles are not disrupted by the presence of proteins or high salt concentrations, and that they are effectively taken up by cells[89,94-96].

Some studies have discovered that chitosan-DNA nanoparticles are particularly stable, remaining intact intracellularly several days following administration, suggesting that the strength of interaction between chitosan and DNA, and inadequate release of DNA, may be preventing efficient transfection[97,98]. It has been proposed that formulations enabling the release of DNA could improve the transfection efficiency of chitosan nanoparticles[83].

3.4.1.2 Modified Chitosan Nanoparticles

Numerous modifications have been made to chitosan in an attempt to exploit its favourable characteristics for gene delivery while improving its transfection ability. Many of these have incorporated targeting ligands in order to increase cellular internalisation[89,96,99]. While this approach generally increases transfection slightly, it does not address the problem of poor DNA release intracellularly.

To address this, hydrophobic molecules have been conjugated to chitosan, usually through the acetyl groups, to create polymers that will self-assemble and exhibit reduced strength of interaction with DNA. Moieties used to date include deoxycholic acid, alkyl groups and trimethyl groups[82,83,86], though none has resulted in satisfactory transfection efficiencies. Inclusion of synthetic polymers,

such as PEI and PEG, has also been attempted, with varying results[100,101]. Regardless of the transfection abilities of these modified chitosans, their significantly higher toxicity negates the initial motive for using chitosan.

3.4.1.3 Polyelectrolyte Systems with Chitosan

A different approach to adapting the chitosan nanoparticle system consists of the formation of polyelectrolyte complexes. In a process similar to ionic gelation, spontaneous interactions occur between polymers of opposite charge, resulting in the formation of insoluble polyelectrolyte complexes[102]. The inclusion of a negatively charged polyanion could improve the transfection ability of chitosan-based systems by decreasing the strength of interaction between chitosan and DNA. Since the compaction of DNA by chitosan is driven mainly by electrostatic interactions, the amount of charges available is expected to play a role. The presence of a polyanion establishes a competition between electrostatic interactions of chitosan-DNA and chitosan-polyanion[103]. A portion of chitosan amino groups interacts with the anionic groups of the polyanion, thereby reducing the number available to interact with DNA and consequently reducing the strength of interaction between chitosan and DNA.

Some research has investigated polyelectrolyte complexes prepared using polysaccharides and a synthetic polymer, such as PLL or PEI, in an attempt to improve the release profile of the complex[102]. However, as mentioned previously, the use of synthetic polymers carries with it the increased toxicity demonstrated by these molecules. In contrast, the use of natural polyanions should not increase toxicity. More recently, the development of nanoparticles prepared by complex coacervation between chitosan and a derivative of konjac glucomannan, a natural polysaccharide derived from the *Konjac* plant, has been reported; however, the system has not been used with cells, and no toxicity data was reported[59].

Despite the range of anionic biopolymers available for use with chitosan, the polyelectrolyte system consisting of chitosan and alginate has been described as the most interesting for drug delivery purposes[104]. Alginate is a biodegradable and biocompatible anionic polysaccharide composed of linear copolymers of α-L-

guluronic acid and β-$_D$-mannuronic acid residues (Figure 3.7); its favourable properties make it one of the most widely used carriers in controlled release systems at the micro scale[105].

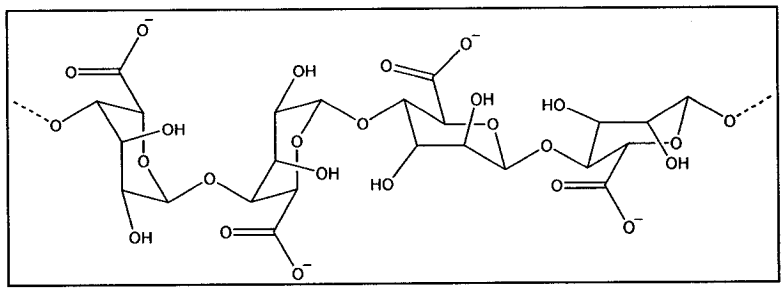

Figure 3.7. Structure of alginate.

Electrostatic interactions between the carboxyl groups of alginate and the amine groups of chitosan form the alginate-chitosan polyelectrolyte complex system (Figure 3.8). This polyelectrolyte complex fulfills the requirements for delivery systems, including being biocompatible, biodegradable and non-toxic, while effectively protecting associated biomolecules. Moreover, the alginate-chitosan system has been shown to protect and limit the release of associated materials more effectively than either biopolymer alone[106]; chitosan is thought to strengthen the alginate network and increase trans-membrane absorption[58].

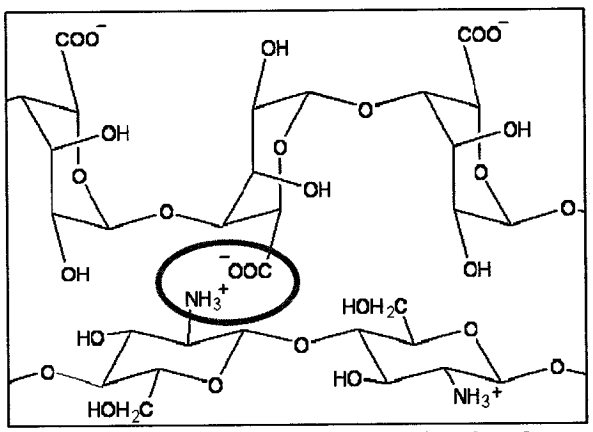

Figure 3.8. Electrostatic interactions involved in the formation of alginate-chitosan polyelectrolyte complexes.

The alginate-chitosan system has been widely studied at the macro- and micro-scales, in the development of microparticles, beads and scaffolds. This biopolymeric system is a polyionic hydrogel, which has demonstrated favourable

characteristics for drug entrapment and delivery[57]. Micro scale formulations have been used for the encapsulation of various drugs, proteins, genetic material, and even cells, with promising results[12,47,58,76,104,107-113]. Despite the favourable characteristics of this polyionic system, development has generally been limited to the micro scale. Prior to 2003, no information regarding the alginate-chitosan system in the nano scale had been published in peer-reviewed journals; since that time, fewer than 10 reports of the system have been published.

The creation of nano scale particles with the alginate-chitosan system is promising for use in delivery systems, and in particular for gene therapy. The desirable characteristics of the system, proven at the micro scale, could be exploited in numerous applications, including the ability to carry and deliver genes into cells for gene therapy purposes. The system demonstrates the required biocompatibility, biodegradability and non-toxicity, is hydrophilic, and exhibits protective capabilities. Both polymers are soluble in water, allowing preparation in mild conditions suitable for fragile biomolecules. Furthermore, the inclusion of anionic alginate should serve to reduce the strength of interaction between chitosan and DNA, thereby improving the release of DNA intracellularly and increasing transfection. Moreover, the presence of alginate could reduce the charge of the particles, improving their characteristics for *in vivo* use. Development of nanoparticles composed of the alginate-chitosan polyionic system could provide a safe and stable biopolymeric alternative to lipid- and synthetic polymer-based systems for effective non-viral gene delivery.

Chapter 4
Evaluating Non-Viral Vectors

The ideal gene delivery system should be biocompatible, biodegradable, non-immunogenic and non-toxic, be targetable to specific cells or tissues, permit encapsulation of multiple biomolecules, and demonstrate transfection efficiency at therapeutically effective levels. In contrast, the basic requirements of gene delivery systems include the ability to form complexes with and protect the gene, and to enable the entry of the gene into cells. While the biocompatibility, biodegradability, immunogenicity and toxicity of a system are largely determined by material choice, the remaining characteristics are dependent on the vector and must be independently assessed. In general, all non-viral vectors are characterised according to their physico-chemical characteristics, ability to form complexes with DNA, and transfection efficiency. Evaluation of toxicity is also common. (The common techniques associated with the evaluation of non-viral vectors are described briefly in Appendix A.)

4.1 Physico-chemical Characteristics

The two basic requirements of gene delivery systems are determined by its physical characteristics. Particle size and charge both play a significant role in the ability of the system to associate with DNA and to enter into cells.

4.1.1 Particle Size

Control of particle size and size distribution determines a number of important characteristics of the vectors[114]. Nano-sized particles demonstrate advantages compared to micro-sized particles, as summarised in Table 4.1. The most significant advantage of nanoparticles is their ability to be internalised by cells, which is generally restricted to microparticles. It is important to note that differences in cellular uptake are also observed between nanoparticles of different size: 150 nm particles have been shown to transfect cells with a 27-fold improvement over 300 nm particles. It is thought that this observed difference

may be attributable to the uptake of larger numbers of smaller particles, resulting in higher intracellular levels of the gene, and increased protein production[52]. The most common method used for measurement of particles is called dynamic light scattering (DLS) (see Appendix A 11.1).

Table 4.1. Comparison of microparticles and nanoparticles for gene delivery.

	MICROPARTICLES	NANOPARTICLES
Size	1 – 1000 μm Upper limit usually 500 μm	1 – 1000 nm Generally 10 – 700 nm
Administration	Intravascular[114] Trans-dermal[94]	Virtually any route Intravascular Trans-mucosal[30] Nasal[115] Pulmonary[116] Oral[18]
***In vivo* Distribution**	Risk of arterial occlusion[79]	Unrestricted[66] Able to cross blood-brain barrier[66]
Circulation times	Rapidly cleared by reticulo-endothelial system[56]	Generally longer life times[66,78]
Cellular Internalisation	Restricted to < 5 μm[52]	Dependent on particle size (2.5-fold increase in uptake of 100 nm particles compared to 1 μm particles) [66]
Loading	Encapsulation easier[114]	Encapsulation difficult
Stability	Less stable in storage Less stable in physiological conditions	More stable in storage More stable in physiological conditions[80]

4.1.2 Particle Charge

In the development of gene delivery systems, characterisation of particle surface charge is common. While size influences particle distribution in the body and cell penetration ability, the surface charge controls interactions with DNA, as well as with cells. A positive surface charge is generally required for successful complexation with DNA and to facilitate approach of the cell membrane. Moreover, surface charge affects opsonisation and clearance from the blood stream following *in vivo* delivery[29]. The importance of the charge of delivery systems is highlighted by the accepted protocol for describing complexes prepared with cationic carriers and anionic DNA, which references the relative charges of each component. Although this is occasionally done through the description of charge ratios (+/-), N:P ratios are more commonly seen in literature

(see Appendix A 11.2 for further explanation). Zeta potential measurements are the most common technique to evaluate the surface charge of particles (see Appendix A 11.3).

4.2 DNA-Vector Interactions

Gene delivery systems must demonstrate the ability to carry DNA while maintaining its structure and activity, as well as protect it from degradation. Owing to the importance of these characteristics, the evaluation of complex formation between the delivery system and DNA is categorically performed for all novel delivery systems. These studies investigate the N:P ratios at which all DNA is associated with the carrier, as well as assess the ability of the system to protect against enzymatic degradation of DNA. Agarose gel electrophoresis (Appendix A 11.4) and ethidium bromide assays (Appendix A 11.5) are commonly used to evaluate nanoparticle-DNA interactions.

4.3 Cell-Vector Interactions

In addition to a proven ability to interact favourably with DNA, vectors must also be able to interact with cells. In particular, they must demonstrate non-toxicity, the ability to bind to and penetrate cells, and ultimately, to transfect them. All non-viral vectors are assessed for their ability to transfect cells; many are also evaluated for toxicity

Non-toxicity and biocompatibility are important for gene delivery systems. The accepted definition of biocompatibility refers to "the ability of a material to perform with an appropriate host response in a specific application"[117]. This definition covers a broad range of materials, since it does not place limits on the appropriate host response. In most applications, and particularly for delivery systems, biocompatible materials are expected to be non-toxic and to interact with biological fluids, including blood, without adverse effects either to the system or the host[45]. In general, a distinct dividing line does not exist between biocompatible and non-biocompatible materials, or between toxic and non-toxic

materials. Rather, a broad spectrum of materials presents varying degrees of biocompatibility and toxicity. General practice makes use of the MTT assay to assess the viability of cells under exposure (Appendix A 11.6).

Achieving efficient transfection is unquestionably the focus of the development of non-viral vectors. Transfection assays involve the delivery of a transgene encoding for a specific protein to cells with the help of the vector. Evaluation of transfection is accomplished by measurement of transgene expression. Depending on the nature of the transgene, this can be accomplished through detection of fluorescence or luminescence, or quantification of enzymatic activity. Importantly, there are two ways to measure transfection efficiency. In the first, the fraction of cells expressing the transgene is quantified. In the second, the relative production of the transgene protein is quantified for a given population of cells. In general, an increase in either the number of cells transfected or the amount of protein produced is considered beneficial. (See Appendix A 11.7 for a description of the measurement techniques.)

4.4 Intracellular Fate of Vectors

Traditionally, non-viral vectors are assessed by the methods described above, evaluating transfection ability but providing little information as to why transfection is successful or unsuccessful. Specifically, these methods provide no information as to the ability of vectors to overcome specific barriers to transfection, particularly the cell, endosomal, lysosomal, and nuclear membranes[118,119]. Studies indicate that while non-viral vectors penetrate cells efficiently, they may fail to mediate a corresponding level of gene expression, suggesting that penetration is not the only critical barrier to transfection[118,120].

Initial studies into overcoming barriers to transfection have focused on the impact of the characteristics of the vectors themselves. Numerous studies report that the size, charge and nature of the vector affect its ability to transfect[121-126]. However, these findings have proven insufficient to explain or predict the observed differences in transfection efficiency between cell lines or between

similar vectors[89,127,128]. These factors make it evident that greater consideration of the uptake and trafficking mechanisms is required in designing vectors that maximise transfection.

Few studies of non-viral vectors have incorporated investigation of their internalisation and intracellular trafficking. However, studies into the intracellular mechanisms for transfection have been gaining importance[129], as indicated by recent studies in this area[61,130-133]. Confocal microscopy and flow cytometry are the most common methods used for these assays (Appendix A 11.7). New analysis methods, including techniques involving transmission electron microscopy and molecular imaging, would be valuable for use in this field. NanoSIMS (Nanoscale Secondary Ion Mass Spectrometry), in particular, offers considerable promise as a quantitative tool to monitor isotopic labels as they are trafficked throughout cells. However, this technology is presently in its infancy for tracking non-metallic elements in biological samples, and its application for tracking the intracellular fate of non-viral vectors has not been investigated. Studies investigating the internalisation and intracellular trafficking of vectors are imperative to increase the understanding of observed transfection. More importantly, they can also provide knowledge to benefit the design of new non-viral vectors.

Chapter 5
Novel Biopolymeric Nanoparticle Delivery System

Countless delivery systems have been introduced to meet the needs of novel therapeutic agents including peptides, proteins and genes. As highlighted in Chapter 3, such systems need to be non-immunogenic and biodegradable while simultaneously protecting their biomolecular cargo. The majority, which incorporate synthetic polymers or lipids, unfortunately demonstrate significant cytotoxicity. The use of natural products, such as biopolymers, in the development of nanoparticles is promising for the development of the "ideal" delivery system. These materials are generally biocompatible, non-toxic, biodegradable, and hydrophilic. However, many systems comprised of biopolymers often use cross-linking agents, are chemically modified, or include synthetic co-polymers, which negate the desirable characteristics of the biopolymer.

The main objective of this phase of the project was to develop a delivery system suitable for new therapeutic agents. The design of the system was directed by several requirements. As with all delivery systems, the chosen materials were to be non-immunogenic and biodegradable, and able to interact with and protect biomolecules. Non-toxicity and biocompatibility were also deemed essential. Finally, nano-scale design was considered necessary for intracellular delivery applications. These criteria led to the consideration of polyelectrolyte systems composed entirely of biopolymers.

Guided by these requirements, the alginate-chitosan system, which has been used extensively at the macro- and micro-scales, was identified as a promising candidate. Initial work involved the development of the polyelectrolyte system at the nano-scale. A method was developed to prepare alginate-chitosan nanoparticles based on ionic gelation. Through a parametric study designed to optimise conditions for nanoparticle formation, a reliable and repeatable procedure to consistently prepare particles as small as 314 nm was developed. Preliminary evaluation of the system's ability to carry and release DNA was also

performed. This work has been published in the *Journal of Biomaterials Science – Polymer Edition*, and is reprinted with permission.

Following publication of this manuscript, continuing development and characterisation of alginate-chitosan nanoparticles identified the nanoparticle preparation conditions that favour association with DNA and with cells. Further development of the procedure resulted in the formation of considerably smaller particles (~150 nm). These results are reported following presentation of the manuscript (Section 5.7).

Effect of Experimental Parameters on the Formation of Alginate-Chitosan Nanoparticles and Evaluation of their Potential Application as DNA Carriers

Kimberly L. Douglas, Maryam Tabrizian

McGill University, Biomedical Engineering Department

5.1 Abstract

This study introduces a new procedure to prepare alginate-chitosan nanoparticles and examines several experimental parameters in relation to their formation and characteristics. Using DLS and TEM analysis, nanoparticle formation was shown to be predominantly affected by the ratio of alginate to chitosan, the molecular weight of the biopolymers, and the solution pH. We report a method that results in spherical particles with mean diameters ranging from 314nm to 1.6μm depending on the preparation conditions. The smallest particles were formed using lower molecular weight polymers with pH between 5.0 and 5.6 and having an alginate:chitosan weight ratio of 1:1.5. We have shown that DNA can be loaded with 60% association efficiency. Our system demonstrates suitable size, loading, and release characteristics for application in drug and gene delivery systems.

Keywords: Alginate, chitosan, nanoparticles, DNA carrier, controlled release

5.2 Introduction

The main principles in drug and gene delivery therapies are to design systems that maintain the structure and activity of biomolecules, are non-immunogenic, release the therapeutic agent predictably over time, and degrade to metabolites that are either absorbed or excreted[6]. Recently, the development of delivery systems has focused on the creation of non-viral vectors for gene therapy applications. Within this field, there are three main types of systems: those prepared with synthetic polymers, natural compounds, and lipids[50]. Each type of system has its own characteristics with regard to circulation time, degradation, loading capabilities and release profiles.

The use of polysaccharides, and specifically natural biopolymers, has commanded particular interest due to their desirable biocompatible, biodegradable, hydrophilic and protective properties[75,77]. The interaction between biodegradable cationic and anionic biopolymers leads to the formation of polyionic hydrogels, which have demonstrated favourable characteristics for drug entrapment and delivery[57]. Chitosan and alginate are two biopolymers that have received much attention and been extensively studied for such use. Entrapment in biopolymers of therapeutic agents, including peptides, proteins and polynucleotides, has been shown to maintain their structure and activity and to protect them from enzymatic degradation[78,79]. Additionally, many of these polymers, hydrogels in particular, are naturally hydrophilic, which is advantageous since this property is thought to contribute to longer circulation times *in vivo* and allows encapsulation of water-soluble biomolecules.

Chitosan is a natural cationic polysaccharide obtained by the N-deacetylation of chitin, a product found in the shells of crustaceans. Its use as a gene carrier has been studied by several groups due to its ability to bind DNA and protect it from degradation[44,87,89,93,94,134]. To this end, chitosan-DNA (Chi-DNA) nanoparticles have been prepared using a variety of methods, including ionic gelation or complexation, cross-linking, preparation using reverse micellar systems, and chemical modification leading to self-assembly[89,134,135]. However, all studies with Chi-DNA nanoparticles have demonstrated significantly lower

transfection efficiencies than is attainable with commercial formulations[44,89,93,134]. Thorough studies of the system have shown that Chi-DNA nanoparticles are stable to challenge in salt and serum (but are pH sensitive), protect the nucleic acid from degradation by serum nucleases, and are effectively taken up by cells[89,94,95]; the reason for inefficient transfection is, therefore, not well understood.

The incorporation of secondary polymers has been one approach used to improve the characteristics of liposome and/or polycation non-viral systems[136,137]. There are numerous chitosan-polyanion complexes that have been investigated as delivery systems for drugs, proteins, DNA and other oligonucleotides, with encouraging results[43,57,84-86,88]. Among the chitosan-polyanion complexes investigated, the combination of chitosan and alginate is considered to be among the most interesting for delivery systems[104].

Alginate is an anionic polysaccharide consisting of linear copolymers of α-$_L$-guluronate and β-$_D$-mannuronate residues. Alginates are hemocompatible, have not been found to accumulate in any major organs, and show evidence of *in vivo* degradation[48]. In the presence of calcium ions, ionic interactions between the divalent calcium ions and the guluronic acid residues cause alginates to form gels. The properties of calcium-alginate gel beads make them one of the most widely used carriers for controlled release systems[105]. Coating of these beads with other polymers, including chitosan, has been shown to improve their stability during storage and in biological fluids.

Alginate-chitosan polyionic complexes form through ionic gelation via interactions between the carboxyl groups of alginate and the amine groups of chitosan. The complex protects the encapsulant, has biocompatible and biodegradable characteristics, and limits the release of encapsulated materials more effectively than either alginate or chitosan alone[106]. A further advantage of this delivery system is its non-toxicity, which permits repeat administration of therapeutic agents. Alginate-chitosan (Alg-Chi) microspheres, or beads, have been widely studied for the encapsulation of drugs, oligonucleotides, proteins and cells, with promising results[47,58,76,104,109,112]. Despite the attractive properties of this

system, its development and application in the submicron scale has scarcely been studied. Recently, De and Robinson have reported the only preparation of alginate-chitosan nanoparticles[138].

Due to the numerous desirable characteristics and demonstrated success of the Alg-Chi system, we decided to explore its development and use in the submicron scale and evaluate its potential use as a gene carrier. Through the formation of a stable polyionic system, we hoped to avoid the sensitivity to pH that is observed with Chi-DNA complexes. As well, by avoiding the use of cross-linking agents or chemically modified polymers, we aimed to develop a system that would demonstrate the biocompatibility and non-toxicity of the native polymers. Addressing the issue raised by McLaughlin et al., who proposed that poor transfection by Chi-DNA nanoparticles may result from a limited release in the cell due to the high affinity of chitosan for DNA[94], we hypothesized that the incorporation of negatively charged alginate in the system would reduce the strength of interaction between the DNA and the particles, facilitating its release and increasing transfection. Prior to thorough analysis of their applicability as gene carriers, we sought first to develop and optimise the particles.

In this paper we introduce a new method to prepare Alg-Chi nanoparticles based on the formation of a polyionic complex between the two biopolymers. The influence of various experimental parameters on the formation of nanoparticles, including the ratio of the biopolymers, solution pH, addition of calcium chloride and stirring time, has been investigated. The size of the nanoparticles was determined using dynamic laser light scattering (DLS) and transmission electron microscopy (TEM) imaging, while nanoparticle composition was assessed by ATR-FTIR. Spectroscopic methods were used to monitor the ability of the Alg-Chi nanoparticles to load and release DNA as a preliminary assessment of their suitability as gene carriers.

5.3 Materials and Methods

5.3.1 Preparation of Nanoparticles

Sodium alginate extracted from *Macrocystis pyrifera* was purchased from Sigma Chemical in three different molecular weights: high viscosity (HV), 120-190kDa; medium viscosity (MV), 80-120kDa; and low viscosity (LV), 12-80kDa. Calcium chloride was purchased from Aldrich Chemical. Chitosan, 85% deacetylated, having molecular weights of 1000kDa (HMW) and 50kDa (LMW) were obtained from Vanson HaloSource. Other chemicals were reagent grade. All chemicals were used as received without further purification or modification.

Both the sodium alginate and calcium chloride solutions were prepared by dissolving the chemicals in distilled water. The pH of the sodium alginate solution was adjusted using hydrochloric acid. The chitosan solution was prepared using a previously published method, adjusting the amount of chitosan used to yield the desired concentration[75]. Briefly, a known amount of chitosan was dissolved in a solution of 1.0M HCl, volume adjusted using distilled water, and pH modified to between 5.0 and 5.7 using NaOH.

The method used to prepare the nanoparticles is a two-step method adapted from Rajaonarivony's method of preparing alginate–poly-L-lysine nanoparticles[48]. The first step in the nanoparticle preparation is the formation of a calcium-alginate pre-gel. This was obtained by adding a calcium chloride solution (18mM) to an alginate solution (0.063% w/v) while stirring (Fisher Scientific Isotemp hotplate stirrer, 700rpm). Various concentrations of chitosan solutions were then added with continuous stirring.

The effect of individual experimental parameters on the preparation of the nanoparticles was assessed while all other variables were kept constant. The concentration of the chitosan solution was varied between 0.06% and 1.5% (w/v) to obtain different ratios of alginate to chitosan (w/w) in the final solution. Solutions of high molecular weight (HMW) and low molecular weight (LMW) chitosan were combined with solutions of low (LV), medium (MV), and high viscosity (HV) sodium alginate. The pH of the sodium alginate and chitosan solutions was adjusted using sodium hydroxide or hydrochloric acid. The amount

of calcium chloride added during the calcium-alginate pre-gel formation was also varied. Lastly, the final solutions were allowed to stir for 30 minutes, 1, 2, 5, 12 and 24 hours.

Prior to analysis, all samples were centrifuged at 1100g for 30 minutes to remove any large aggregates. Centrifugation under these conditions allowed aggregates to pellet, leaving nanoparticles suspended in the supernatant. Initially, particle suspensions were purified by means of dialysis using a Spectra/Por CE Float-A-Lyzer (Spectrum) with a molecular weight cut-off of 300kDa to remove free polymer from the solution. It was found that dialysis did not change the results of DLS, TEM or zeta potential particle characterisation.

5.3.2 Nanoparticle Analysis

Morphological analysis of the nanoparticles was performed using TEM (JEOL 2000FX). Samples of nanoparticle suspensions (5μL) were dropped onto Formvar-coated copper grids. After drying, samples were stained using phosphotungstic acid (2% w/v). DigitalMicrograph software (Gaetan v3.4) was used to perform image capture and analysis, including sizing. Particle composition was assessed using a Perkin Elmer Spectrum One FTIR fitted with a Universal ATR Sample Analyzer on samples that were frozen at -20°C, and subsequently lyophilised (ThermoSavant ModulyoD) prior to analysis. Zeta potential analysis was performed using a ZetaPlus (Brookhaven Instruments). The size and distribution of the particles were assessed by dynamic light scattering (DLS) using a low-angle laser light-scattering device (Malvern Instruments HPPS).

5.3.3 DNA Loading and Release Study

Preliminary tests were carried out in order to assess the feasibility of using the Alg-Chi nanoparticles as gene carriers. Deoxyribonucleic Acid from Herring Sperm (Sigma Chemicals), which consists of oligonucleotides, was used for these preliminary studies. The amount of DNA introduced to the system was varied and is reported as stoichiometric ratios of DNA phosphate groups (P) to chitosan

amine groups (N); the P:N ratios investigated for this study include 1:50, 1:25, 1:10 and 1:5.

Two methods, based on research examining oligonucleotide loading of alginate–poly-L-lysine nanoparticles[139], were used to load DNA in the nanoparticles. The first method (DNA+NP) consisted of mixing a certain amount of DNA (2mg/mL) with pre-formed Alg-Chi nanoparticles (1:1.5 w/w ratio). The second method (DNA+Chi) involved the preparation of nanoparticles using chitosan that had been allowed to complex with DNA (DNA+Chi). The DNA-Chitosan (DNA-Chi) complex solutions were prepared by adding the appropriate amount of DNA solution (2mg/mL) to the chitosan solution, and allowing them to mix for 24 hours. Nanoparticles were then prepared as above, with the addition of the DNA-Chi in place of the usual addition of chitosan. The DNA-loaded nanoparticles were characterised through DLS sizing and zeta potential analysis, as described for the unloaded nanoparticles.

For quantitative determination of DNA loading, samples were ultra-centrifuged for one hour at 220 000g (Beckman TL-100 Ultracentrifuge) to pellet the nanoparticles and associated DNA. Unadsorbed DNA remaining in the supernatant was quantified using a spectrophotometer at 260nm (μQuant, Bio-Tek Instruments, Inc.). Suitable controls were used for all analyses. The amount of DNA associated with the nanoparticles was calculated as the difference between the initial amount of DNA added to the suspensions and the amount measured in the supernatant. The following equations were used to determine association efficiency (AE) and mass adsorption (MA):

$$AE(\%) = \frac{DNA_{total} - DNA_{super}}{DNA_{total}} \qquad [5.1]$$

$$MA = \frac{DNA_{total} - DNA_{super}}{mass_{np}} \qquad [5.2]$$

where DNA_{total} is the initial amount of DNA added, DNA_{super} is the amount measured in the supernatant following centrifugation, and $mass_{np}$ is the mass of nanoparticles.

Following analysis of DNA-loading, nanoparticles prepared using P:N ratios of 1:25 and 1:10 were resuspended in phosphate buffered saline (PBS) and

stored at room temperature for periods of 2, 4, 8, 12, 24 and 48 hours. Samples were then ultra-centrifuged as above and the supernatant was analysed spectrophotometrically to determine DNA release.

5.3.4 Statistical Analysis

For all results, triplicate readings were obtained for a minimum of three separate samples. Values reported are the mean ± standard error of the mean, unless otherwise noted. Statistical analysis was accomplished using a two-sided Student's t-test for two samples assuming unequal variance.

5.4 Results and Discussion

5.4.1 Identification of Nanoparticle Constituents

Nanoparticles analysed using FTIR demonstrate absorption bands characteristic of both alginate and chitosan in addition to peaks indicative of their interaction (Figure 5.1). The peak at 1520cm^{-1} in both the chitosan and nanoparticle spectra is due to unreacted $-NH_2$ groups of chitosan. Similarly, peaks at 800cm^{-1} and 1260cm^{-1} seen in the alginate and nanoparticle spectra represent unreacted –COOH groups of alginate. The peak seen at 1420 cm^{-1} in the nanoparticle spectrum has been attributed to the ionic interaction between these two reactive groups[102]. This served to confirm that the spontaneous interaction between alginate and chitosan leads to the formation of nanoparticles.

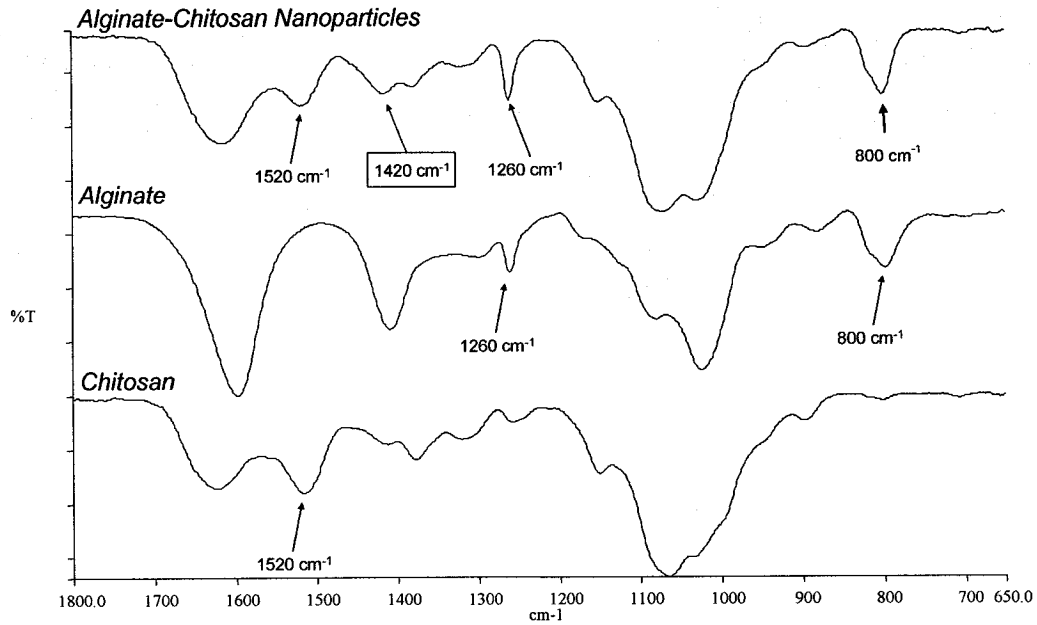

Figure 5.1. FT-IR spectra of alginate–chitosan nanoparticles compared to chitosan and alginate, demonstrating characteristic absorption bands of each. The peak at 1420 cm^{-1} has been attributed to the interaction between chitosan NH_3^+ and alginate COO^- groups.

5.4.2 Nanoparticle Size

5.4.2.1 Effect of Alginate to Chitosan Ratio and Polymer Molecular Weight

Nanoparticles were prepared with HV alginate and HMW chitosan and with LV alginate and LMW chitosan at seven different Alg:Chi ratios. The resulting mean particle sizes as determined by DLS are shown in Figure 5.2. The same trend can be observed for both molecular weight combinations, with the smallest sizes obtained when the Alg:Chi ratio is in the range between 1:1.5 and 1.5:1. These results confirm that smaller particles result when the availability of the functional groups are in stoichiometric proportion. Increasing the relative amount of alginate or chitosan causes an increase in DLS measured particle size up to 1.6μm for the ratios tested. Larger sizes for these particles are attributable to the presence of larger single particles and to aggregate formation, as confirmed by TEM analysis. The trend of sizes related to Alg:Chi ratio is observed regardless of the polymer molecular weights used, though the difference is more pronounced when using higher molecular weight polymers.

Also evident in the figure is the effect of polymer molecular weight on particle size. Generally, use of the low molecular weight polymers resulted in smaller particles for most ratios of Alg:Chi. We further studied this effect by preparing and assessing nanoparticles using Alg:Chi ratios of 1.5:1, 1:1 and 1:1.5 for all possible combinations of the different molecular weight polymers (HMW Chi with HV, MV and LV Alg; LMW Chi with HV, MV and LV Alg). Results from these permutations indicate that chitosan molecular weight has a greater influence on particle size than alginate molecular weight; generally particles prepared with LMW Chi are smaller than those prepared with HMW Chi (data not shown). Furthermore, formulations using LV alginate and LMW chitosan solutions result in the formation of fewer aggregates. This may stem from the ability of LMW chitosan to diffuse more readily in the alginate gel matrix to form smaller, more homogeneous particles. Conversely, higher molecular weight polymers may bind to the surface of such matrices, forming an outer membrane and increasing particle size[140].

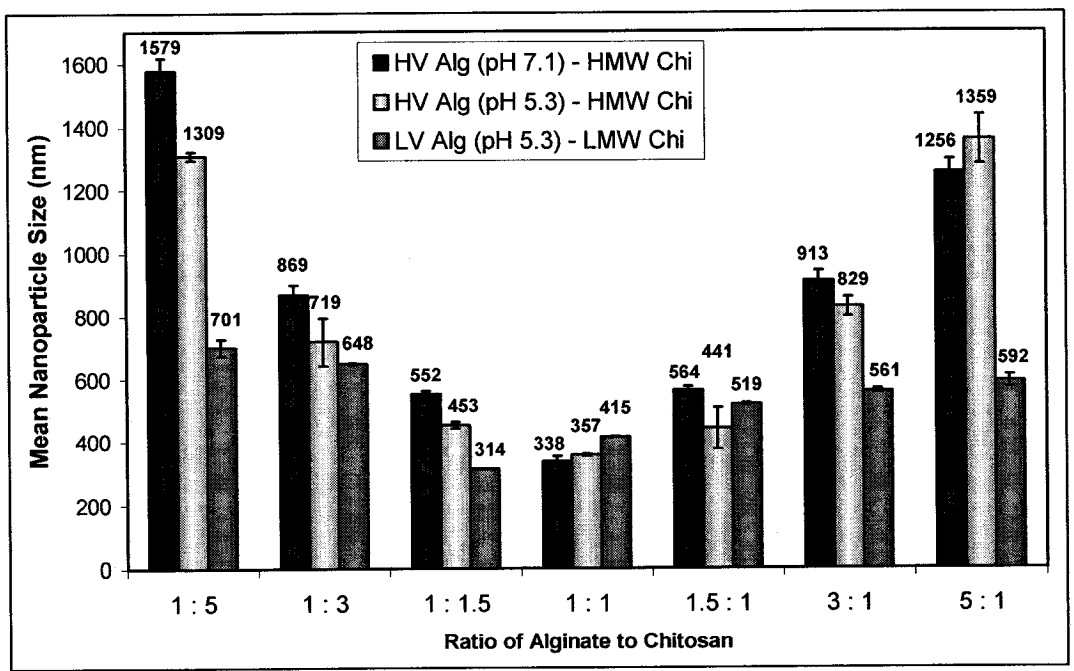

Figure 5.2. Effect of the ratio of alginate to chitosan on particle size ($n \geq 9$). **For all samples the calcium/alginate ratio was kept constant at 0.22 and the pH of the chitosan solution was kept constant at 5.5. The first two series illustrate the effect of alginate pH on particle size; the last two series show the effect of molecular weight on particle size.**

Recently, De and Robinson reported the development of chitosan-alginate nanoparticles[138]. Investigating Alg:Chi ratios between 30:1 and 7:1, they found that the smallest nanoparticles resulted from a ratio of Alg:Chi of 30:1, yielding particles with a diameter of 506 ± 26 nm. As they decreased the Alg:Chi ratio, they found that nanoparticle size increased, with aggregation occurring when ratios less than 7:1 were used. These results contrast our DLS and TEM results, which show that increasing either the alginate or chitosan in proportion to the other increases nanoparticle size. We did notice that the large sizes observed for particles prepared with ratios of 1:5 or 5:1 result partially from the presence of aggregates, in accordance with observations by De and Robinson. Potential causes for this discrepancy are pH differences, which we found to affect particle formation and size, and the possibility that different driving forces control the spontaneous formation of nanoparticles as the ratio of Alg:Chi increases beyond a critical range.

5.4.2.2 *Effect of pH, Calcium Chloride and Stirring Time*

In order to assess the effect of pH on nanoparticle formation, particles were prepared using an alginate solution of pH 7.1 at all Alg:Chi ratios. Comparison with particles prepared using an alginate solution of pH 5.3 demonstrate generally smaller particle sizes when combined with HMW chitosan (pH 5.5) (Figure 5.2). Much of the chitosan, which is poorly water-soluble and thus prepared under acidic conditions, likely precipitates upon addition to an alginate solution with pH 7.1, so that less chitosan is available for particle formation. As well, since the pK_a of chitosan is known to be 6.5[89], addition to an alginate solution at pH 7.1 would result in the majority of amine groups being unprotonated, and therefore unable to participate in ionic interactions. The few protonated groups available for interaction would result in weaker electrostatic interactions with the alginate gel, leading to larger particle sizes. Using an alginate solution with a slightly lower pH resolves these problems by allowing a stronger interaction between chitosan and alginate, leading to the formation of more compact nanoparticles. Other groups investigating chitosan for the

preparation of nanoparticles, microparticles and polyionic systems report working within the same pH range (5.0-6.3)[57,75,141].

Additional pH studies in the more acidic range reveal that using acidified alginate (pH 2.2) or chitosan (pH 0.3) results in increased particle sizes, up to 200nm larger (Table 5.1). Smaller Alg-Chi nanoparticles are obtained when both the sodium alginate and chitosan solutions have a pH in the range of 5.1-5.7. Within this range the carboxyl group of the alginate is ionised and the amine group of the chitosan is protonated, a necessity for optimum interaction in the polyionic complex formation. Similar observations have been reported in the formation of other polyionic complexes containing chitosan[141].

Table 5.1. Effect of calcium/alginate ratio and solution pH on nanoparticle size (Alg/Chi 1:1.5). The second row of each data set represents the 'standard' condition (italics). Values are reported as mean ± SEM (n ≥ 9). * indicates significance at p <0.05 compared to standard nanoparticles.

Alg pH (LV)	Chi pH (LMW)	Ca^{2+}:Alg Ratio	Size (nm)	Polydispersity Index
pH 5.3	*pH 5.5*	0.00	403 ± 1 *	0.31 ± 0.01
		0.22	*314 ± 1*	*0.22 ± 0.01*
		0.43	400 ± 62	0.23 ± 0.06
		0.87	344 ± 9 *	0.20 ± 0.01
pH 2.2	pH 5.5	*0.22*	428 ± 4 *	0.35 ± 0.01
pH 5.3	*pH 5.5*		*314 ± 1*	*0.22 ± 0.01*
pH 7.1	pH 5.5		528 ± 6 *	0.34 ± 0.01
pH 5.3	pH 0.3		547 ± 24 *	0.21 ± 0.04

In addition to the impact of pH on particle size, other groups investigating alginate-chitosan beads or microspheres suggest that the presence of calcium ions is important to maintain the alginate gel network during the reaction with chitosan[104]. In adjusting the ratio of calcium to alginate (Ca^{2+}:Alg) from 0.00 to 0.87, it was observed that an absence of calcium ions results in marginally larger particles with a wider distribution than those produced with the "standard" ratio of 0.22 (Table 5.1). Similarly, those prepared with a ratio of 0.43 have somewhat larger diameters. However, all particles display similar stability, demonstrated by consistent DLS measurements after several weeks of storage, indicating that aggregation does not occur.

It is known that gel formation between the calcium ions and the guluronate (G) residues in the alginate is a direct function of the length of homopolymer G blocks, with more homopolymer G blocks leading to greater cross-linking and a stronger gel. The alginate derived from *Macrocystis pyrifera* used in this study typically has a ratio of mannuronate to guluronate residues of approximately 1.5, with less than 20% consisting of homopolymer G blocks[142]. Given this low concentration, the first step of pre-gel formation likely does not result in a strong or well-defined gel with these materials, indicating that the addition of calcium is not essential to nanoparticle formation. We found that ratios ranging from 0.00 - 0.87 do not greatly affect nanoparticle formation or size (Table 5.1). In contrast, De and Robinson concluded that it was necessary to have a Ca^{2+}:Alg ratio <0.2 for nanoparticle formation to occur, with microparticles forming at higher ratios[138]. This incongruity may arise from different methods of analysis; De and Robinson used nephelometry to assess the interaction between calcium and alginate, whereas we evaluated the effect of calcium addition to alginate on nanoparticle formation and found that although particle size is affected by the Ca^{2+}:Alg ratio, higher ratios and complete omission do not prevent the formation of nanoparticles.

Lastly, the stirring time of the final solution was also found to have no effect on particle size. Solutions that were allowed to stir for just 30 minutes or as long as 24 hours contained nanoparticles whose mean sizes differed by no more than 20 nanometres (data not shown). This result suggests that nanoparticle formation is rapid and that reorganisation of the polymers is not occurring over time. Consistent particle size measurements following room temperature storage periods up to one month confirm particle stability.

5.4.3 Particle Analysis

Electron microscopy analysis confirmed the presence of nanoparticles and provided morphological information. With the TEM, particles were seen to be spherical and distinct (Figure 5.3). Nanoparticles were considerably smaller when viewed with TEM than when measured by DLS. TEM images show particle sizes

between 50nm and 150nm depending on the experimental parameters used to prepare them, whereas DLS sizing indicates that the smallest population has an average diameter of at least 300nm. This apparent discrepancy can be explained by the dehydration of the hydrogel particles during sample preparation for TEM imaging. Additionally, DLS measures the apparent size of a particle, including hydrodynamic layers that form around hydrophilic particles such as those composed of Alg:Chi, leading to an overestimation of particle size[52]. Our attempt to verify particle size in solution by AFM imaging in fluid was unsuccessful since the nanoparticles were displaced by the approaching tip.

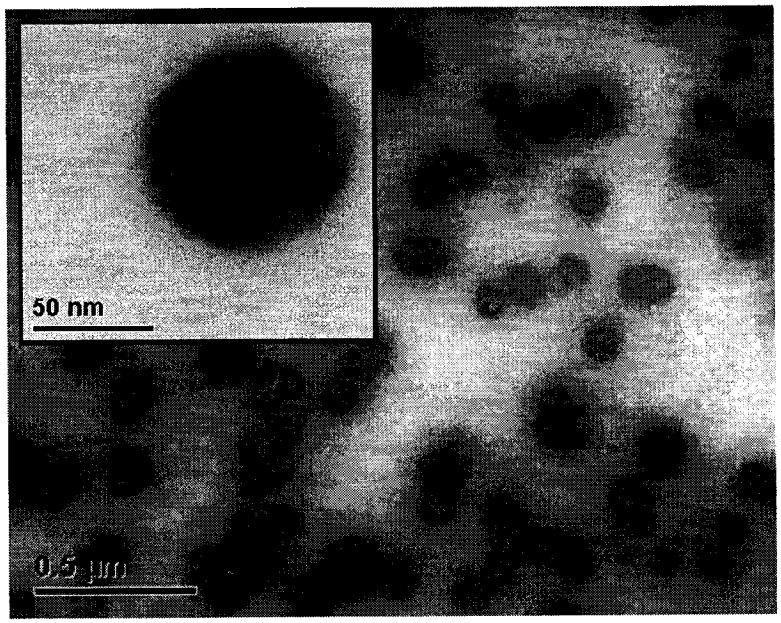

Figure 5.3. TEM micrograph (bar = 0.5 µm) **illustrating typical particle morphology and distribution. Nanoparticles were prepared with a 1:1.5 ratio of LV alginate (pH 5.3) to LMW chitosan (pH 5.5) using the standard calcium/alginate ratio of 0.22. Inset: detail of one nanoparticle (bar = 50 nm).**

5.4.4 DNA Loading and Release Study

A preliminary feasibility study analysing the potential application of Alg:Chi nanoparticles as gene carriers was conducted by evaluating the ability of the nanoparticles to load DNA and assessing the particle characteristics once loaded. We evaluated two methods of DNA loading analogous to a study involving alginate–poly-L-lysine (Alg-PLL) nanoparticles, where it was

hypothesized that oligonucleotides (ON) are shuttled into particles more rapidly when introduced with a polycation[139].

We found that DNA association in the Alg-Chi nanoparticles is affected by the method of introduction: with method 1 (DNA+NP), DNA association reaches a peak after two days, whereas for method 2 (DNA+Chi), adsorption was an average of 20% lower over the first two days of storage but continued to increase or remain steady beyond the first two days (data not shown). Generally, adsorption was higher when DNA associated with preformed nanoparticles, rather than being introduced as Chi-DNA complexes (Table 5.2). An adsorption efficiency of 60% (±14%) was achieved using a P:N ratio of 1:25, resulting in a mass adsorption of 27±6μg DNA/mg nanoparticle. The highest mass adsorption, 89±5μg DNA/mg nanoparticle, was observed with a P:N ratio of 1:5, using method 1. However, this system resulted in the formation of aggregates, rendering it ineffective for gene carrier applications. Comparing the results of DNA loading using both methods, we found that complexing DNA with chitosan prior to nanoparticle formation results in slower adsorption kinetics; it is evident that pre-complexing DNA with chitosan does not improve DNA-loading of the nanoparticles. The discrepancy between the improvement in ON loading of Alg-PLL by pre-complexing ON with the polycation may be due to the considerably shorter chain lengths used (PLL 3.9-7.9kDa vs. Chi 50kDa)[139].

Table 5.2. Influence of loading method and P/N ratio on efficiency of DNA incorporation and particle characteristics. All complexes were prepared based on the standard conditions (1:1.5 ratio of LV Alg (pH 5.3) and LMW Chi (pH 5.5) with Ca^{2+}/Alg ratio of 0.22). Values are reported as mean ± SEM (n ≥ 9). * Indicates significance at p <0.05 compared to blank nanoparticles.

DNA Loading Method	P:N Ratio	Size (nm)	Adsorption Efficiency (%)	Mass Adsorption (μg DNA/mg NP)	ζ Potential (mV)
DNA+NP (Method 1)	1:50	499 ± 3*	42 ± 9	10 ± 2	26 ± 1
	1:25	549 ± 2*	60 ± 14	27 ± 6	24 ± 2
	1:10	aggregates	54 ± 4	62 ± 4	15 ± 2*
	1:5	aggregates	39 ± 2	89 ± 5	10 ± 2*
DNA+Chi–NP (Method 2)	1:50	419 ± 6*	40 ± 5	9 ± 1	17 ± 2*
	1:25	407 ± 2*	45 ± 4	20 ± 2	22 ± 1*
	1:10	377 ± 3*	48 ± 8	57 ± 5	16 ± 4*
	1:5	299 ± 1*	26 ± 3	60 ± 7	16 ± 4*

Additional characterisation of the DNA-loaded nanoparticles included DLS sizing and zeta potential analysis (Table 5.2). With the exception of the particles prepared using the DNA+Chi method and a P:N ratio of 1:5, particles were significantly larger than their unloaded counterparts. Incorporation of DNA and the ensuing molecular reorganisation likely causes the size increase.

Results of the zeta potential analysis are perhaps more informative. Unloaded nanoparticles have a zeta potential of 27±1 mV, which was not seen to change significantly with the adsorption of up to 27μg DNA/mg nanoparticle when prepared using method 1 (Table 5.2). This suggests that method 1 actually leads to DNA absorption, since surface adsorption would be expected to result in a change in zeta potential. The introduction of increasing amounts of DNA to the system results in surface adsorption and a corresponding reduction of the zeta potential below the threshold necessary to prevent to particle aggregation.

In contrast, method 2 resulted in DNA-nanoparticle complexes with significantly lower zeta potentials than unloaded nanoparticles, regardless of the amount of DNA incorporated, suggesting that molecular reorganisation required for particle formation is different under these conditions. Interestingly, particles prepared using this method with P:N ratios of 1:10 and 1:5 exhibited

approximately equal mass adsorption and surface charges, suggesting that 60μg DNA/mg nanoparticle may represent the upper limit of DNA incorporation for particles of this type which do not aggregate. Most significantly, zeta potential analysis indicates that DNA-loaded Alg-Chi particles retain a positive charge without aggregation, which is important for transfection purposes since it allows particles to interact with negatively-charged cell membranes[99].

A preliminary test to evaluate DNA release from the nanoparticles was performed by re-suspending two formulations of pelleted particles in PBS for 48hrs. Results indicate that 6% and 3.5% of the adsorbed DNA is released from the P:N 1:10 and 1:25 formulations, respectively. Many groups working with biopolymeric nanoparticles report similar initial release rates, depending on the polymer[33,55,143]. The possibility of gene release, in combination with the noted loading characteristics, may be advantageous for gene therapy applications.

5.5 Conclusions

A method to prepare alginate-chitosan nanoparticles was developed and optimized to yield small, relatively monodisperse and uniform particles. The ratio of alginate:chitosan in the preparation was found to affect nanoparticle formation, as did polymer molecular weight and pH. The smallest nanoparticles have a mean diameter of 314nm as measured by DLS and are prepared using low viscosity alginate and low molecular weight chitosan in a ratio of 1:1.5. Nanoparticle formation is improved when the pH of both the sodium alginate and the chitosan solutions are between 5.1 and 5.7.

The ratio of alginate:chitosan in the preparation was found to affect particle size to a greater degree than any other parameter. Particle sizes were lowest in the range that permitted stoichiometric interaction between the functional groups of both polymers, and increased to 5 times the minimum size at the ratio extremes. The molecular weight of chitosan was found to be more important in determining particle formation and resulting size than alginate

molecular weight, which reinforces the hypothesized mechanism of particle formation.

DNA-loading of the nanoparticles was found to occur with high efficiency; maximum adsorption efficiency was 60%, while maximum mass loading was 60μg DNA/mg nanoparticles. Adsorption of DNA in formed nanoparticles occurred more rapidly than when a DNA-chitosan complex was used in the preparation of the particles, although the association was less stable. The high encapsulation of DNA from alginate-chitosan nanoparticles is encouraging for application in the field of gene therapy. Studies are in progress to evaluate cell-nanoparticle interactions and transfection ability.

5.6 Acknowledgments

The authors wish to thank our funding sources: the Natural Sciences and Engineering Research Council of Canada (NSERC) and the Quebec Ministère de la Recherche de la Science et de la Téchnologie (MRST) for making this research possible. We also wish to thank Dr. S.K. Sears and J.Mui for assistance with TEM analysis, Dr. S. Prakash and Dr. J. Bergeron for access to centrifugation equipment, and Shawn Carrigan and Dr. Christelle Catuogno for advice and assistance.

5.7 Further Development of Alginate-Chitosan Nanoparticles

Following the development of the alginate-chitosan system at the nano-scale, the system was further characterised with regards to its ability to associate with DNA and interact with cells. It was found that experimental parameters used in the preparation of nanoparticles affect both of these characteristics. Further development of the system also allowed the formation of significantly smaller nanoparticles. This section summarises the findings of this work, which led to the identification of optimal parameters for gene delivery purposes and guided the second phase of research, as described in Chapter 6.

5.7.1 *Effect of Preparation Parameters on Delivery System Capabilities*

As demonstrated in the work outlined above, nanoparticle size varies depending on the ratio of alginate:chitosan used to prepare them. While small particles are favourable for delivery of the new class of therapeutics due to their ability for cellular penetration, other factors must be considered in the design of optimal conditions. Specifically, the ability of the delivery system to complex the biomolecule, in this case DNA, and its ability to interact with cells are both affected by the physico-chemical characteristics of the nanoparticles which are, in turn, influenced by the conditions used to prepare them.

5.7.1.1 *DNA Complexation*

Owing to the highly anionic nature of DNA, it was presumed that DNA would interact with the nanoparticles through electrostatic interactions. In this case, the ratio of alginate:chitosan used in the preparation of nanoparticles could directly affect the DNA complexation ability of nanoparticles by altering their surface charge. To verify this hypothesis, alginate-chitosan nanoparticles were prepared at the ratios of 1:1.5 and 1.5:1 and characterised for size and charge (see Appendix B 12.1 for a description of the experimental methods for this assay). Nanoparticles were mixed with DNA in varying proportions to yield N:P ratios

between 1:1 and 1:7. The ability of nanoparticles to complex DNA was assessed by evaluating DNA migration with agarose gel electrophoresis.

Results indicate that the ability of the nanoparticles to complex DNA is affected by their preparation conditions (Figure 5.4). In all cases, the nanoparticles prepared at an Alg:Chi ratio of 1:1.5 complexed more plasmid than those prepared at a ratio of 1.5:1. This is particularly clear for the complexes prepared at an N:P ratio of 1:1. The 1:1.5 particles demonstrate smaller size (314 nm) and greater positive charge (+32 mV) compared to the 1.5:1 particles (370 nm, +27 mV). Since the larger size of the 1.5:1 particles should permit the complexation of greater amounts of DNA given the same charge, these results suggest that the charge of the particles plays a significant role in the complexation of DNA. Furthermore, these results prove that the interaction between the nanoparticles and plasmid DNA is driven primarily by electrostatics.

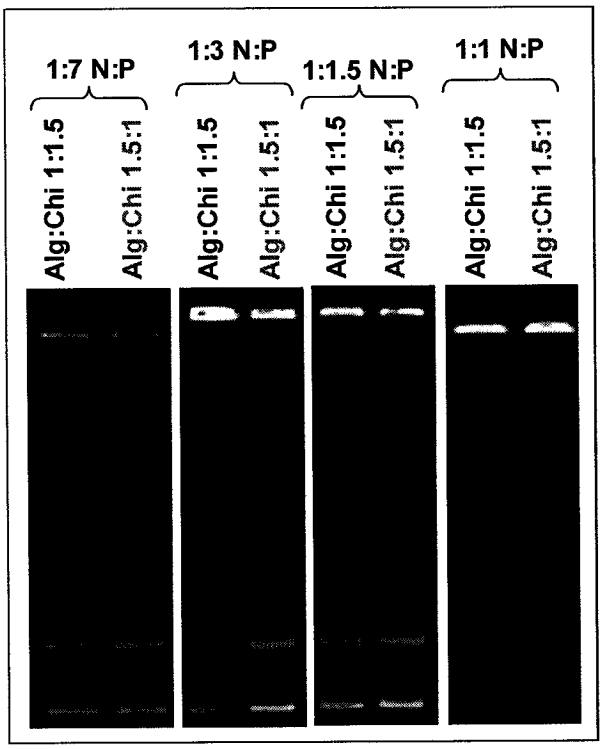

Figure 5.4. Effect of the ratio of alginate to chitosan on the ability of nanoparticles to complex DNA. **Note that particles prepared at a 1:1.5 ratio, containing relatively more chitosan, are able to prevent the migration of plasmid DNA better than particles prepared at a 1.5:1 ratio. This is particularly noticeable in the last column, where plasmid DNA was added in an amount to provide charge equivalence to the nanoparticles. DNA is prevented from migrating with particles prepared at a 1:1.5 Alg:Chi ratio, but not by those prepared at a 1.5:1 Alg:Chi ratio.**

5.7.1.2 Cellular Interactions

It is customary in the field of gene delivery to develop cationic carriers to improve interactions with DNA and to enhance its ability to approach the negatively-charged cell membrane. As indicated above, the ratio of alginate:chitosan influences not only the size of the resulting nanoparticles, but also the charge. Considering the role that charge plays in cellular interactions, the effect of preparation conditions was also evaluated in this respect.

To determine the extent of the effect of preparation conditions on cellular interactions, nanoparticles were prepared using fluorescein-labelled chitosan with Alg:Chi ratios of 1:1.5 and 1.5:1, as above. Cells were treated with these nanoparticles and at designated times flow cytometry was used to evaluate the percentage of cells with associated fluorescence. (For more details, see Appendix B 12.2.)

Results indicate a clear difference in the binding and uptake of particles prepared with varying ratios of alginate:chitosan (Figure 5.5). Nanoparticles prepared with an alginate:chitosan ratio of 1:1.5 demonstrate enhanced association with COS7 cells at all time points, as compared to the Alg:Chi 1.5:1 particles. At 24 h, the 1:1.5 particles showed a 40% increase in cell association. In the case of cellular interaction, the individual contributions of particle size and charge are difficult to determine, since both are known to have an effect. Despite this, it is clear that the presence of relatively more chitosan in the nanoparticles is favourable for cellular interactions, whether it is due to the smaller size of the particles or their higher charge.

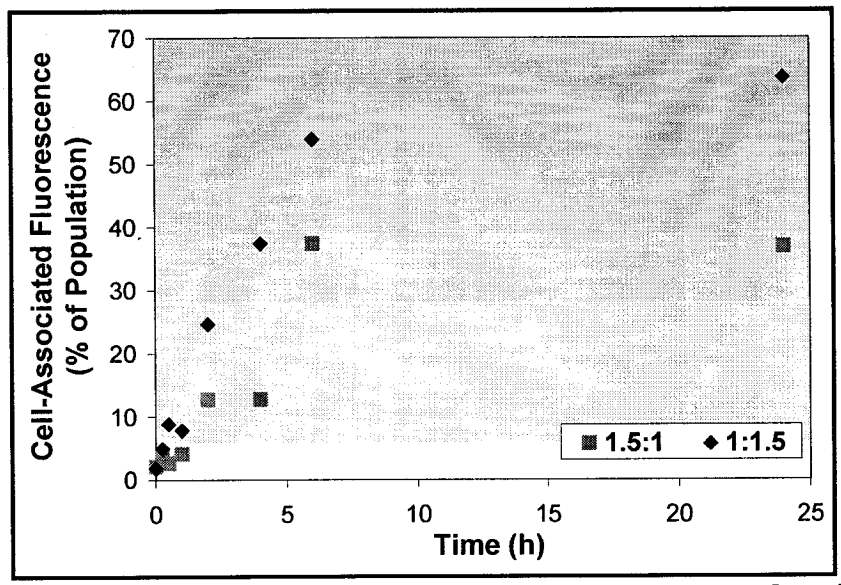

Figure 5.5. Effect of the ratio of alginate to chitosan on the ability of nanoparticles to bind to and enter into COS7 cells. **Note that particles prepared at a 1:1.5 ratio, containing more chitosan, demonstrate an enhanced ability to bind to and enter into cells.**

These results further demonstrate the importance of experimental parameters in the preparation of novel delivery systems. While size is an important consideration, the physico-chemical properties also contribute to the ability of the system to interact favourably with the therapeutic agent, and also with cells. As summarised in the published manuscript, size considerations led to the selection of experimental parameters including the use of alginate and chitosan in 1:1.5 ratio. These results further support that choice by demonstrating that size and charge characteristics are favourable, enhancing the complexation of DNA and cellular interactions. Accordingly, alginate-chitosan nanoparticles prepared at an alginate:chitosan ratio of 1:1.5 were used for all further work.

5.7.2 Modified Preparation of Alginate-Chitosan Nanoparticles

Initially, the development of the alginate-chitosan system at the nano-scale followed the common processes used to prepare it at the micro-scale. Specifically, the idea was to coat chitosan onto nano-sized pre-gels composed of alginate and calcium (Figure 5.6). The ability of alginate to form gels in the presence of divalent cations, particularly calcium ions, is well known. The interaction between

successive guluronic acid residues and the divalent cation induces parallel packing, in what is termed the *egg-box* structure[48]. Calcium-alginate gels, which are considered to be strong and stable, benefit from additional coating by polymers such as PLL or chitosan[140].

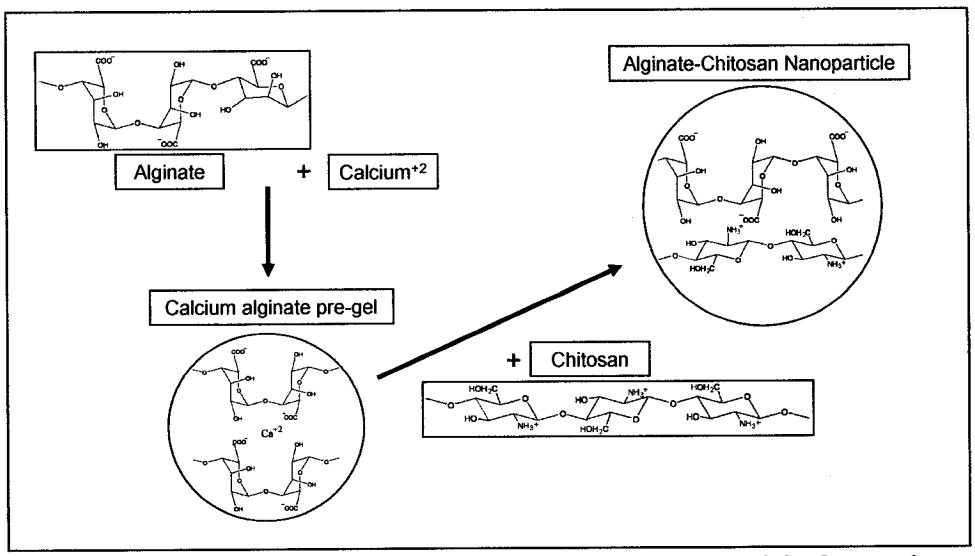

Figure 5.6. Proposed scheme of alginate-chitosan nanoparticle formation.

While initial studies, reported in the published manuscript, suggest the importance of calcium for the formation of small particles, further experimentation led to preparative conditions precluding the need of calcium, and resulting in significantly smaller particles. The major alteration to the preparation was the use of a 10 kDa chitosan. The decision to use a 10 kDa chitosan in this system was based on two principles which could improve its behaviour as a gene delivery system: formation of smaller particles with enhanced characteristics for intracellular penetration, and reduction of the strength of interaction with DNA over higher molecular weight chitosans. Previous work suggested that lower molecular weight chitosan allowed formation of smaller particles due to its ability to form more interpenetrating networks with alginate[144]. Furthermore, it has been repeatedly suggested that use of lower molecular weight polymers, and chitosan in particular, may reduce the strength of the polycation-DNA interaction, thereby increasing release of DNA to improve gene delivery and transfection[145]. The minimum polymer size, determined to be that required for forming stable complexes with DNA, has been suggested to be 10 kDa for chitosan[91].

As with all systems formed through ionic gelation, control of component concentrations is critical to allow formation of particles rather than continuous gels. A ten-fold reduction in the concentration of the alginate and chitosan solutions, together with the use of a lower molecular weight chitosan, resulted in the formation of particles approximately half the size of those originally reported (Figure 5.7). As previously reported in Chapter 4, size significantly affects the ability of particles to be taken up by cells. Therefore, this modification, and the resulting ability to prepare considerably smaller particles, represents a significant improvement in the characteristics of this system to be used as a gene delivery system.

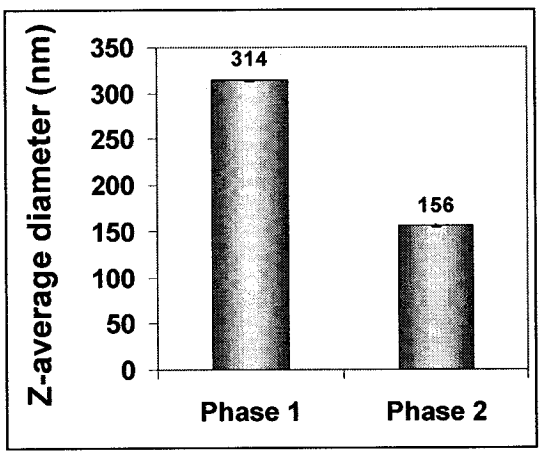

Figure 5.7. Comparison of nanoparticle sizes prepared using the method published in *Journal of Biomaterials Science – Polymer Edition*, and prepared using 10kDa chitosan and polymer solutions diluted ten-fold.

5.7.3 Summary

The alginate-chitosan system was successfully developed at the nano scale, suitable for gene delivery. Preparative conditions were critical to the formation of nanoparticles and to their resulting physico-chemical properties. Nanoparticles prepared with a 1:1.5 ratio (w/w) of alginate:chitosan have a mean diameter of 156 ± 1 nm, which is suitable for intracellular delivery, and demonstrate favourable charge characteristics for interaction with DNA and with cells. Based on these criteria, this system was chosen for further investigation and development. Details of the preparative conditions are included in Appendix B 12.3.

Chapter 6
Evaluation of Alginate-Chitosan Nanoparticles for Gene Delivery

Having developed a nano-scale system known to be non-immunogenic, non-toxic, biodegradabile, and biocompatible at the micro-scale, the first main objective of this phase of the project was to evaluate the nanoparticles as gene delivery vectors. Initial work involved a thorough evaluation of the ability of alginate-chitosan nanoparticles to interact favourably with DNA and to protect it from degradation. Although preliminary work suggested the ability to load DNA, this study involved a comprehensive investigation into the nature of interactions between nanoparticles and genetic material. In particular, the role of alginate in the system was investigated, since its inclusion was based in part on the premise of a non-toxic and biocompatible chitosan-based system with improved transfection efficiency through increased DNA release intracellularly.

A separate requirement for delivery systems is the ability to release the cargo in a predictable fashion. Although this is clearly important for many delivery systems, advances in the field of gene delivery suggest that DNA release from non-viral vectors does not use traditional processes. Rather, it is thought to involve displacement of the DNA from the vector by genomic DNA in the nucleus, or by anionic lipids or proteins in the cytoplasm[129,146]. For this reason, no further evaluation of DNA release from the nanoparticles was performed.

The second main objective of this work was the evaluation of the transfection ability of alginate-chitosan nanoparticles. Transfection is a term commonly used to describe the sum of all processes involved in the delivery of a gene to a cell and its subsequent transcription and translation into the corresponding protein. In this study a gene encoding for green fluorescent protein (GFP) was used; successfully transfected cells, which appear green under appropriate light, were identified through flow cytometry. The transfection ability of alginate-chitosan nanoparticles was compared to that of chitosan nanoparticles and of a commercially available liposome formulation. Results demonstrate that the alginate-chitosan system transfects the 293T cell line with high efficiency.

The work in this chapter has been described in a manuscript submitted to the *Journal of Controlled Release*. Additional information regarding the formation of nanoparticle-DNA complexes was not included in the manuscript due to length restrictions. These results are included at the end of the chapter (Section 6.7).

Manuscript submitted for publication to Journal of Controlled Release (May 17, 2006)

Effects of Alginate Inclusion on the Vector Properties of Chitosan-Based Nanoparticles

Kimberly L. Douglas[1], Ciriaco A. Piccirillo[2], Maryam Tabrizian[1]

1. **McGill University, Biomedical Engineering Department**
2. **Department of Microbiology and Immunology**

6.1 Abstract

Chitosan nanoparticles have shown considerable promise as gene vectors but do not mediate transfection with satisfactory efficiency. To improve upon the transfection efficiency of chitosan, we approached the development of alginate-chitosan nanoparticles with the goals of maintaining non-toxicity, biocompatibility, and biodegradability. Through spontaneous complex coacervation, particles were formed with a mean Z-average diameter of 157 nm and a zeta potential of +32 mV. Competition binding assays indicated that the presence of alginate reduces the strength of interaction between chitosan and DNA, contributing to improved transfection. Cell viability assays indicated that nanoparticles exhibit the same non-toxicity as chitosan, and significantly reduced toxicity compared to a commercial liposome formulation. As well, complexation with nanoparticles maintained DNA integrity and protected it from nuclease degradation better than chitosan alone. Alginate-chitosan nanoparticles were able to mediate transfection of 293T cells four times that achieved by chitosan nanoparticles; at 48 h, the transfection efficiency was as high as with Lipofectamine™, with significantly reduced cytotoxicity. Overall, alginate inclusion improved the vector properties of chitosan-based nanoparticles, demonstrating superior transfection ability while maintaining biocompatibility and non-toxicity.

Keywords: Chitosan, alginate, nanoparticles, cell viability, *in vitro* transfection

6.2 Introduction

On-going research suggests that an effective and safe method for delivering genes to cells remains a critical barrier, where the challenges of cellular internalisation, intracellular transport of genetic material, and translation into therapeutic proteins are compounded by the fragile nature of DNA and the physiologic responses designed to remove foreign matter from the body. To facilitate the delivery of genetic material, the use of appropriate carriers, or vectors, is necessary to protect DNA from degradation extra- and intra-cellularly, and to aid cellular penetration. Despite the high transfection efficiencies attainable using viral vectors, they are limited in the size of plasmid they can transport and are hampered by manufacturing difficulties, limited targeting ability, and safety concerns. These limitations have prompted considerable research into the development of non-viral vectors[6].

Among those reported in the literature, hydrophilic biodegradable polymers are commanding increased interest due to their demonstrated abilities to complex and protect DNA, and to mediate cellular penetration. These natural polymers also provide the added benefits of preparation under mild aqueous conditions and degradation to harmless by-products[118]. Of the available biodegradable polymers, the three most studied include poly(ethylene imine) (PEI), poly-L-lysine (PLL), and chitosan[82]. While polyplexes prepared with PEI and PLL demonstrate efficient transfection both *in vitro* and *in vivo*, they also show significant toxicity[72,147]. In contrast to these synthetic polymers, chitosan is biocompatible and displays low immunogenicity and minimal toxicity[46].

Chitosan is a natural linear polysaccharide composed of *D*-glucosamine and *N*-acetyl-*D*-glucosamine units and is cationic at acidic and neutral pH. Its cationic nature allows it to interact with and easily form complexes with negatively charged DNA. Chitosan-DNA nanoparticles generally transfect cells more efficiently than naked DNA but less than commercially available liposome formulations[86,92]. It has been suggested that the strength of the interaction between chitosan and DNA results in highly stable particles, thereby preventing dissociation within the cell and ultimately precluding translation of the DNA,

resulting in low transfection[98]. Studies of the intracellular fate of chitosan-DNA nanoparticles demonstrate that particles remain intact intracellularly after several days, lending support to this hypothesis[97]. Formulations facilitating the release of DNA, such as the inclusion of hydrophobic moieties, could improve chitosan-based vector transfection[83].

Modified chitosan formulations have incorporated the conjugation of targeting ligands such as galactose, lactose, and transferrin, in order to increase endocytosis through receptor-mediation[89,96,99]. Hydrophobic moieties have also been integrated through conjugation of deoxycholic acid to and trimethylation of the acetyl groups[82,86]. Systems incorporating graft co-polymers, including synthetic polymers such as PEG and PEI, have also been accomplished[100,101]. While targeting generally increases transfection, the incorporation of hydrophobic moieties and the formation of graft co-polymers has had mixed results, depending on the degree of substitution and the ratio of polymers. Furthermore, most modifications result in systems with greater toxicity than chitosan alone.

To improve the transfection efficiency of chitosan, we approached the development of a modified chitosan system with the goal of maintaining non-toxicity, biocompatibility, and biodegradability. This precluded the use of more toxic elements, such as PLL or PEI, and chemical modification of the chitosan itself. To reduce the strength of interaction between chitosan and DNA, we incorporated a secondary polymer, an approach previously used to improve liposome and other polycationic non-viral systems[136,137]. Alginate, an anionic biopolymer consisting of linear chains of α-$_L$-guluronic acid and β-$_D$-mannuronic acid residues, was selected as the secondary polymer. Like chitosan, alginate is biocompatible, biodegradable, and non-toxic. Through ionic gelation alginate and chitosan spontaneously form a polyionic complex that is biocompatible, biodegradable, non-toxic, and effectively protects associated biomolecules[106].

While the alginate-chitosan system has been widely studied at the micro and macro scales for drug delivery and wound healing purposes, its development at the nano scale has been limited, and it has not been used for gene delivery. We previously reported the development of alginate-chitosan nanoparticles through a

parametric study designed to optimise preparation conditions[144]. The present study investigates the suitability of alginate-chitosan nanoparticles as biocompatible, biodegradable, non-viral vectors. In addition to characterising the physico-chemical properties of nanoparticle-DNA complexes and the role alginate plays in nanoparticle formation, the system was evaluated for transfection efficiency and cytotoxicity using 293T cells.

6.3 Materials and Methods

6.3.1 Materials

Polymers for nanoparticle synthesis include low viscosity sodium alginate (M_W 12-80 kDa) (Sigma, Oakville ON, Canada) and chitosan (M_W 10kDa, ~90% deacetylated) (Carbomer, San Diego CA, USA). Nanoparticle-DNA complexes employed a plasmid encoding for green fluorescent protein (pEGFP-N1 plasmid, 4.7 kb) (Clontech, Mountain View CA, USA). Oligonucleotides (0.5-0.8 kb) from herring sperm were used for one set of experiments (Sigma). For cell culturing, Dulbecco's Modified Eagle Medium (DMEM) and penicillin/streptomycin were from Gibco (Invitrogen, Burlington ON, Canada). Foetal bovine serum (FBS) was from ATCC (Manassas VA, USA). The remaining reagents were supplied as follows: ethidium bromide, DNase I, and Lipofectamine (Invitrogen), chitosanase, lysozyme, sucrose, sodium sulphate, and ethylenediaminetetraacetic acid (EDTA, 0.6 mM in PBS) (Sigma), pH 5.5 acetate buffer (Biacore, Piscataway NJ, USA). Finally, 3-(4,5-dimethylthiazol-2-yl)-2,5-diphenyltetrazolium bromide (MTT, 12 mM in PBS) and sodium dodecyl (lauryl) sulphate-hydrochloride (SDS-HCl) were supplied in a Molecular Probes Vybrant MTT assay (Invitrogen). All other reagents were analytical grade.

6.3.2 Particle Preparation

Low viscosity sodium alginate was prepared by dissolving in MilliQ water. Chitosan was dissolved in 1.0 M HCl. Both solutions were pH adjusted to 5.6 – 5.8 and filtered (0.22 μm) prior to use. Nanoparticles were prepared under

sterile conditions by mixing appropriate volumes of 0.005% (w/w) sodium alginate and 1% (w/w) chitosan under stirring for 1 h at room temperature to give a final weight ratio of 1:1.5 alginate:chitosan. Subsequently, DNA was allowed to complex with alginate:chitosan nanoparticles by adding appropriate volumes to obtain specific N:P ratios and letting the solution incubate for 30 min. The charge ratio, or N:P ratio, is the ratio of theoretical free chitosan amines in the nanoparticles (N) to negative phosphates of DNA (P). Unless otherwise noted, nanoparticle suspensions were used directly without subsequent processing.

To ascertain suitability for long-term storage, unloaded alginate-chitosan nanoparticle suspensions were lyophilised in the presence of varying amounts of sucrose (50% w/v in MilliQ water), added subsequent to nanoparticle formation to obtain final concentrations ranging from 0 – 15% (w/v) and stirred for 5 min. After measuring the size and charge of the particles, the suspensions were frozen in a bath of acetone-dry ice and immediately transferred to a lyophiliser (Modulyo D, ThermoSavant, Waltham MA, USA). After 4 days, samples were removed, reconstituted with MilliQ water and vortexed for 30 s, followed immediately by particle size and charge measurements.

Chitosan-DNA nanoparticles were used in some experiments for comparative purposes. These were prepared by mixing solutions of 0.02% chitosan (100 μL) and 200 μg/mL DNA (100 μL in 4.3 mM sodium sulphate) pre-warmed to 55°C and vortexing immediately for 1 min. These particles have a mean size inferior to 100 nm and positive charge[44].

6.3.3 Plasmid DNA

The green fluorescent protein plasmid (pEGFP-N1, 4.7 kb) was used to prepare nanoparticle-DNA complexes and to monitor transgene expression. pEGFP-N1 was amplified and isolated using a Plasmid Maxi Kit (QIAGEN, Mississauga ON, Canada). Recovered plasmid was stored at -20°C in sterile water. Plasmid concentration was measured by UV absorption at 260 nm (μQuant, Bio-Tek Instruments, Winooski VT, USA) and the purity was determined using agarose gel electrophoresis.

6.3.4 Physical Characterisation of Particles

Particles were characterised for size and size distribution using low-angle dynamic laser light scattering (DLS) (HPPS, Malvern Instruments, Worcestershire, UK). Particle surface charge was determined through zeta potential measurements (ZetaPlus, Brookhaven Instruments, Holtsville NY, USA). Nanoparticles were visualised using transmission electron microscopy (TEM) (JEOL 2000FX, Peabody MA, USA). Samples of nanoparticle suspensions (5 μL) were dropped onto Formvar-coated copper grids and stained using phosphotungstic acid (2% w/v). DigitalMicrograph software (Gaetan v3.4) was used to perform image capture.

The effect of DNA complexation on the size and charge of nanoparticle complexes was investigated using DLS and zeta potential analysis. Oligonucleotides (ON) from herring sperm (0.5-0.8 kb) were used for these experiments since the quantities required were prohibitive for the use of plasmids.

6.3.5 Competition Binding Assay

Fluorescence was measured using a FluoroMax-2 fluorimeter (HORIBA Jobin Yvon, Edison NJ, USA) (excitation 516 nm, emission 605/10 nm). To an aqueous solution (3 mL) containing 15 μg plasmid DNA and 3 μg ethidium bromide, the following treatments were effected: (a) incremental addition of chitosan (0.06%, 3 μL); (b) incremental addition of nanoparticles (80 μL, as prepared); and (c) initial doping with alginate (0.7%, 1.2 μL) followed by incremental chitosan addition (0.06%, 3 μL). For these assays, each addition consisted of chitosan or nanoparticles in an amount to increase the charge ratio (+/-) of the solution by 0.2. A further experiment consisted of the incremental addition of alginate (0.7%, 2.5 μL) to a solution containing chitosan-DNA complexes at a charge ratio of 2.5:1 (37.5 μL 0.06% chitosan, 15 μg pDNA); this ratio was chosen based on results from assay (a) that indicated complete complexation of the DNA at this ratio. For all experiments, 3 min incubations

followed each addition prior to measurement. All solutions were prepared as indicated in section 2.2 above.

6.3.6 DNA Complexation – Agarose Gel Retardation Assays

Nanoparticles and plasmid DNA were mixed in varying amounts to yield charge ratios (+/-) between 10:1 and 1:10 and incubated at room temperature for 30 min. The theoretical charge of the unloaded nanoparticles is calculated as the number of chitosan amine groups minus the number of alginate carboxylate groups present in each polymer. Samples of DNA, unloaded nanoparticles, and the nanoparticle-DNA complexes were run on a 0.8% agarose gel at 100 V for 50 min and photographed using a gel imaging station (DNR, Montreal Biotech, Montreal QC, Canada). This experiment was repeated varying the incubation times of the nanoparticle-DNA solutions from 5 min to 90 min.

Plasmid integrity following complexation and release from the nanoparticles, and the ability of complexation to protect the plasmid from degradation were also evaluated. Naked plasmid, alginate-chitosan nanoparticle-DNA complexes, and chitosan-DNA nanoparticles were treated with 1U DNase I for 15 min at 37°C, followed by heat inactivation (60°C for 15 min) in the presence of 25 mM EDTA. Nanoparticles were then digested through incubation (4 h, 37°C) with 10 μL chitosanase (48 U/mL in 50 mM acetate buffer pH 5.5) and 8 μL lysozyme (0.5 U/mL in 50 mM acetate buffer pH 5.5)[89]. Samples were then run on a 0.8% agarose gel, as described above.

6.3.7 Cell Culture

293T cells, epithelial human embryonic kidney cells, were cultured in DMEM supplemented with 10% (v/v) FBS and 1% penicillin/streptomycin at 37°C in a humidified 5% CO_2 atmosphere. Cells were sub-cultured prior to confluence using trypsin-EDTA.

6.3.8 Cytotoxicity

Cells were seeded in 48-well plates at $4x10^4$ cells/well in phenol red-free DMEM with 10% FBS. Cells were treated the following day with 200 µL of medium containing 42, 84 or 126 µg/mL alginate-chitosan nanoparticles, both unloaded and complexed with 1 µg DNA. Lipofectamine™ (5 µg/mL) and chitosan nanoparticles (42 µg/mL), both unloaded and loaded with 1 µg DNA, were used as controls. Cells were incubated in treatment medium for 6 h and 24 h, after which time the MTT assay was performed. Briefly, treatment solutions were replaced with 300 µL culture medium to which 30 µL MTT was added. After a 4 h incubation at 37°C, 300 µL of SDS-HCl surfactant was added, followed by further incubation at 37°C (4 h). Samples were then read at 570 nm by a plate spectrophotometer (µQuant, Bio-Tek Instruments, Winooski VT, USA). As a blank, one empty well was treated with the nanoparticle suspension followed by the MTT assay to ensure that residual material would not interfere with the reading. The viability of cells incubated with DMEM alone was taken as 100%.

6.3.9 In vitro Transfection

Cells were seeded in 24-well plates at $4x10^4$ cells/well in DMEM/10% FBS 18 h prior to transfection. Each well was treated with 300 µL serum-free medium containing complexes prepared with varying charge ratios; regardless of the ratio, each well received 2 µg DNA. Lipofectamine™ was used as a positive control, with each well receiving 4 µL complexed with 2 µg DNA. Chitosan nanoparticles were used for comparison, with each well receiving the particles as prepared, in an amount to provide 2 µg DNA. Medium was increased to 500 µL with DMEM/10% FBS after 4 h, and was completely replaced with fresh complete medium after 24 h.

Transfection was assessed at 48 h and 96 h post-transfection using flow cytometry. Cells were removed from the wells using cold EDTA (0.6 mM in PBS), transferred to tubes and analysed directly (FACSCalibur, BD Biosciences, San Jose CA, USA). Appropriate controls and gates were used for analysis of the results.

6.3.10 Statistical Analysis

All experiments were repeated a minimum of three times and measured in triplicate. Results reported are the means and standard deviations, unless otherwise noted. Statistical significance was determined using Student's two-sided t-test with $p < 0.05$ deemed significant.

6.4 Results and Discussion

6.4.1 Nanoparticle Preparation and Characterisation

Alginate-chitosan nanoparticles were prepared in mild aqueous conditions through complex coacervation. Driven by electrostatic interactions, alginate and chitosan spontaneously interact under these conditions to yield nanoparticles with small size and narrow distribution. Particles had a mean Z-average diameter of 157 ± 1 nm and a number average size of 84 ± 8 nm, with a mean polydispersity index of 0.23 ± 0.02 (n = 30) indicating a narrow size distribution[148]. Transmission electron microscopy imaging revealed the presence of spherical particles and qualitatively confirmed particle size and size uniformity (Figure 6.1). Zeta potential measurements indicated a positive overall charge of 32.2 ± 0.8 mV (n = 30), suitable for complex formation with anionic DNA.

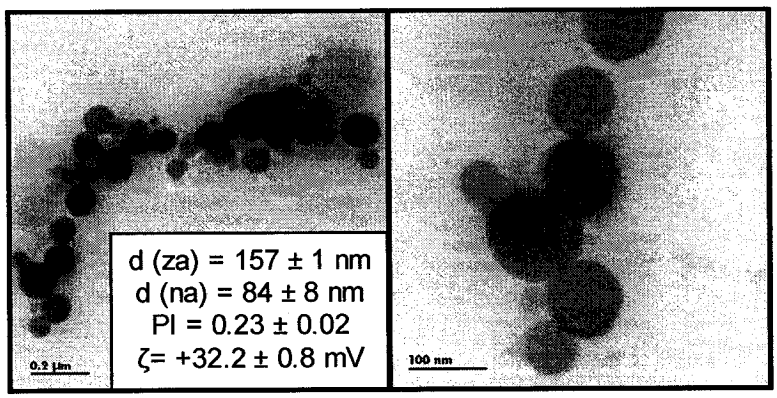

Figure 6.1. TEM micrograph showing alginate-chitosan nanoparticles. Particle characteristics described in inset: Z-average diameter – d (za), number average size – d (na), polydispersity index – PI, zeta potential – ζ.

Previous studies have shown that particle size significantly affects transfection efficiency: particles having a mean size of ~150 nm led to a 4-fold

transfection increase in 293 cells, and a 27-fold increase in COS7 cells, as compared to particles twice as large[52]. Although the precise reasons for size-dependent transfection efficiency have yet to be identified, it is suspected that cellular endocytosis of complexes is a size limited process[149]. Since previous work indicated that lower molecular weight chitosan allowed the formation of smaller particles due to its ability to form more interpenetrating networks with alginate, a 10 kDa chitosan was used for particle preparation in this study[144]. Particles prepared with the lower molecular weight chitosan demonstrated a 50% decrease in mean diameter compared to the original formulation, which is particularly beneficial for transfection applications.

To characterise the formation of alginate-chitosan nanoparticle-DNA complexes, size and charge measurements were executed for complexes over a range of ratios. Complexes showed more variability in size when DNA was present in excess (Figure 6.2). At an N:P ratio of 1:2 the surface charge is insufficient to prevent aggregation, explaining the observed large complex sizes. Complexes prepared with N:P ratios 1:1 or greater were larger than unloaded nanoparticles, having mean sizes an average of 24 nm larger. Zeta potentials of complexes followed a very distinctive trend: generally, increasingly excess amounts of DNA led to more negatively charged complexes, while increasing the N:P ratio led to more positively charged complexes.

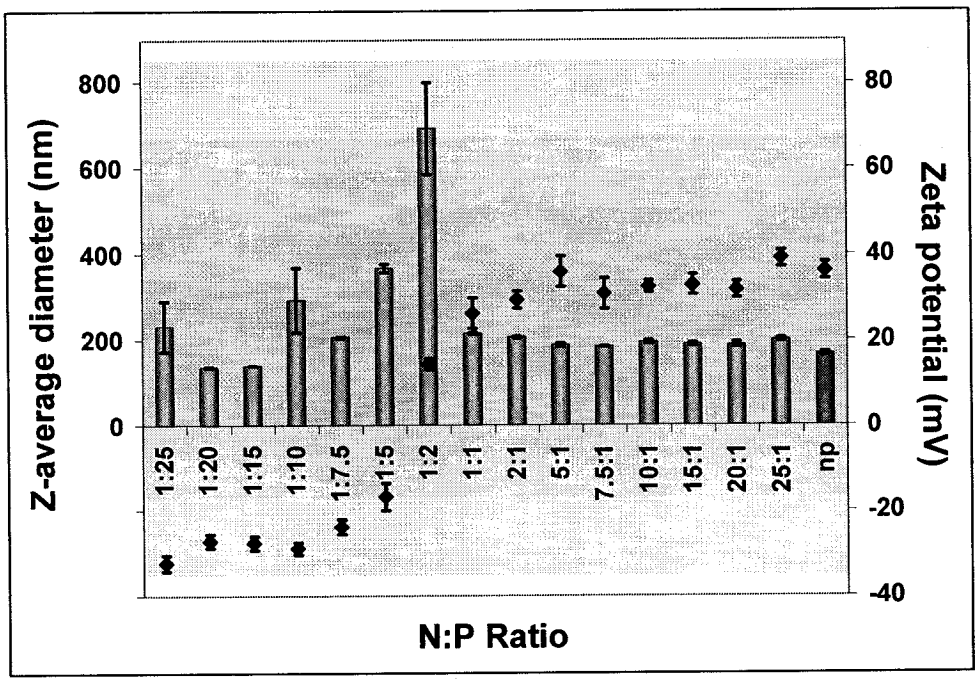

Figure 6.2. Effect of N:P ratio on the size and zeta potential of nanoparticle-DNA complexes. **All complexes show sizes significantly different from unloaded nanoparticles. Small, stable complexes are only formed at N:P ratios of 1:1 or greater. Values represent means ± standard deviation ($n \geq 3$). Note: "np" in the figures refers to unloaded alginate-chitosan nanoparticles.**

Based on these measurements, it is surmised that DNA is adsorbing at the surface of the nanoparticles during complex formation. Additional support for this model is provided by the observed differences in complex sizes, with adsorption of DNA on the surface resulting in increased particle size. It should be noted that the use of ON in these experiments cannot reproduce the exact complex charges and sizes that would result with the use of plasmid DNA. However, these experiments were conducted to better understand complex formation, which should occur similarly with DNA plasmids. In addition to suggesting complex formation, these experiments provide evidence suggesting that alginate increases the stability of the system as compared to chitosan-DNA nanoparticles. Size and zeta potential measurements have previously indicated that stable small chitosan-DNA nanoparticles can only be achieved at N:P ratios of 4:1 or greater[89]. The inclusion of alginate in this system allowed stable, small complexes to be formed at ratios as low as 1:1.

A practical challenge separate from improved transfection and low toxicity is the development of easily prepared systems that can be stored over prolonged periods. Freeze-drying is normally the preferred storage method, since most systems do not survive long-term storage in solution[150]. In the absence of sucrose, the alginate-chitosan nanoparticle suspension could not be reconstituted through resuspension. Addition of sucrose as a cryoprotectant prior to lyophilisation allowed the particles to be resuspended in water. Results indicate that sucrose in concentrations ranging from 0.5 to 2% (w/v) protected the system from critical aggregation during freeze-drying. Some reorganisation did occur during the lyophilisation process in the presence of sucrose, as evidenced by an increase in measured particle size following reconstitution; resuspended particles showed a mean increase in size of 57 ± 3 nm. This may be partially attributable to the hydrogel nature of the system, which undergoes variable swelling depending on pH[151]. Sucrose concentrations greater than 5% led to particle suspensions yielding sizes more than twice the original diameter, indicating significant aggregation. While the transfection ability of the lyophilised and reconstituted particles was not assessed, agarose gel retardation assays demonstrated that their ability to complex DNA at N:P ratios as low as 1:1 was not affected (data not shown).

6.4.2 Competition Binding Assays

Ethidium bromide exclusion assays were performed to better understand the role alginate plays in the interaction between chitosan and DNA, as well as to evaluate the interaction between alginate-chitosan nanoparticles and DNA. Gradual addition of chitosan to DNA in solution with ethidium bromide resulted in a sharp reduction in fluorescence until a 1:1 ratio was attained (Figure 6.3, curve a). Beyond this point, the decrease in fluorescence was more moderate, gradually reaching 4.4 ± 0.2% at an N:P ratio of 3:1. The effect of chitosan addition to a solution containing DNA and alginate with P=C (where C is the number of carboxylic groups present in alginate) was also investigated, producing a comparable curve that became asymptotic at an N:P ratio of 2:1, and had a minimum relative fluorescence of 16.0 ± 3.5% (Figure 6.3, curve c). The

increased relative fluorescence in the presence of alginate indicates a competition between DNA and alginate for binding to chitosan. This competition leads to decreased binding strength between DNA and chitosan in the presence of alginate, which should facilitate its eventual dissociation[103].

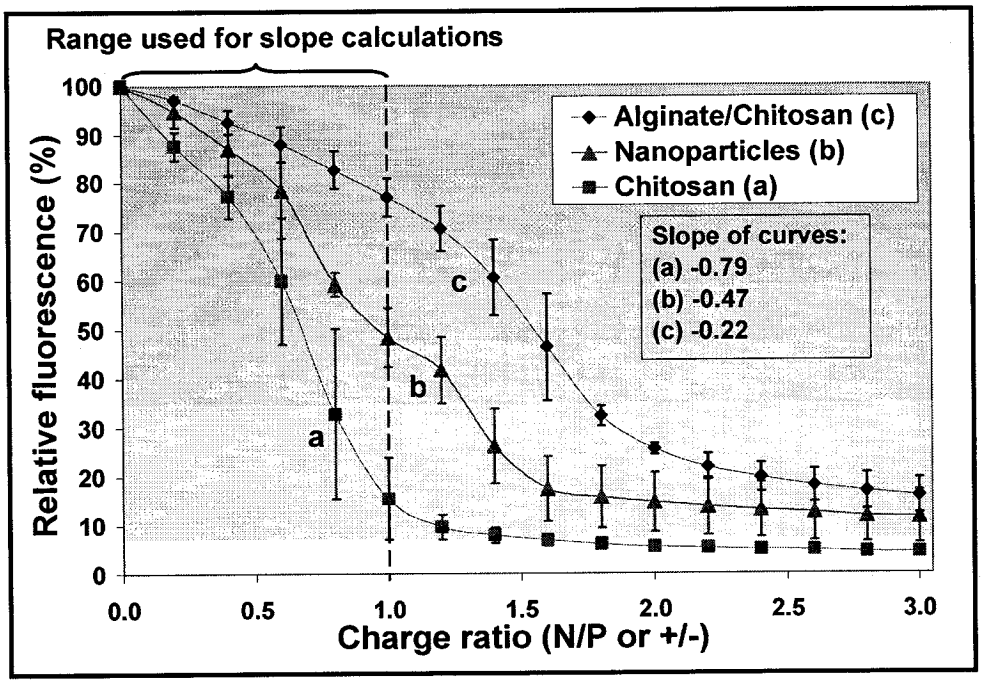

Figure 6.3. Inhibition of EtBr-DNA fluorescence through complexation of DNA. The three curves represent the loss of fluorescence caused by addition of chitosan (a), addition of nanoparticles (b), and addition of chitosan in the presence of alginate (c). The values plotted represent the measured intensities relative to the value obtained for EtBr-DNA alone. The amount of chitosan or nanoparticles added is specified in terms of the relative number of chitosan amino groups (N) to DNA phosphate groups (P). Points represent means ± standard deviation ($n \geq 3$). Comparisons of the absolute slope in the range indicated were used to infer the relationship of binding between chitosan-alginate and chitosan-DNA.

Following the method of Danielsen *et al.*, a comparison was made of the absolute values of the slopes of the curves generated between the beginning of the experiment and an N:P ratio of 1:1[103]. In the presence of alginate, the slope decreased to ~30% of that observed with chitosan alone, suggesting that chitosan preferentially binds alginate. Interestingly, titrating alginate to a solution containing chitosan and DNA did not result in 100% recovery of fluorescence, indicating that alginate is not capable of completely displacing DNA from chitosan (Figure 6.4). These results suggest that while the presence of alginate

reduces the strength of interaction between chitosan and DNA, it does not prevent efficient complexation when both polymers are present in solution.

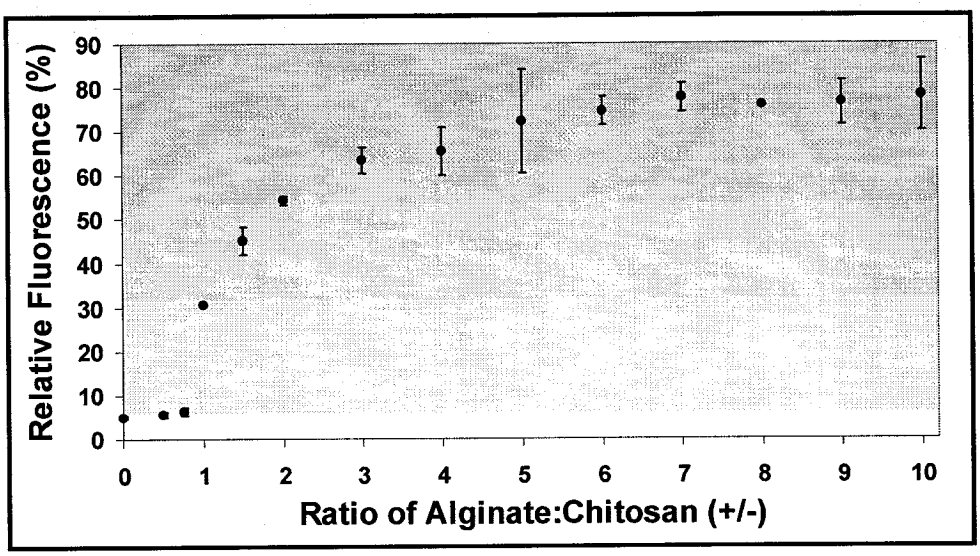

Figure 6.4. Recovery of EtBr-DNA fluorescence following the addition of alginate to chitosan-DNA complexes prepared at 2.5:1 N:P ratio. The values plotted represent the measured intensities relative to the value obtained for EtBr-DNA alone. Points represent mean ± standard deviation ($n \geq 3$).

In consideration that the interaction between alginate-chitosan nanoparticles and DNA may be different, the exclusion assay was repeated with the incremental addition of nanoparticles to a solution of DNA and ethidium bromide. This produced a similar curve, becoming asymptotic at an N:P ratio of 1.6:1, with a relative fluorescence that did not fall below 10% (Figure 6.3, curve b). Interestingly, the change to an asymptotic curve occurred where N=P+C, suggesting that the behaviour of alginate and chitosan in the nanoparticles is governed by the same stoichiometric relationship as observed with polymers in solution. The slope of this curve was reduced to ~60% as compared to that observed with chitosan alone, revealing that binding between alginate-chitosan nanoparticles and DNA is moderated compared to binding between DNA and chitosan alone. Overall, the competition binding assays indicated that the presence of alginate in this nanoparticle system effectively decreases the strength of interaction between DNA and chitosan, which should increase the transfection efficiency of the system by facilitating the release of DNA once the particles have been internalised by cells.

6.4.3 Nanoparticle-DNA Complex Formation

The ability of alginate-chitosan nanoparticles to complex DNA was further assessed by agarose gel retardation assays. Decreasing fluorescence of the bands as the N:P ratio increases indicated greater complexation of DNA (Figure 6.5). At a 1:1 ratio, plasmid DNA was completely complexed by nanoparticles and unable to migrate. Repeating the experiment with incubation times ranging from 5 to 90 min revealed that complex formation occurs almost immediately, with the same pattern of bands seen after 5 min (data not shown).

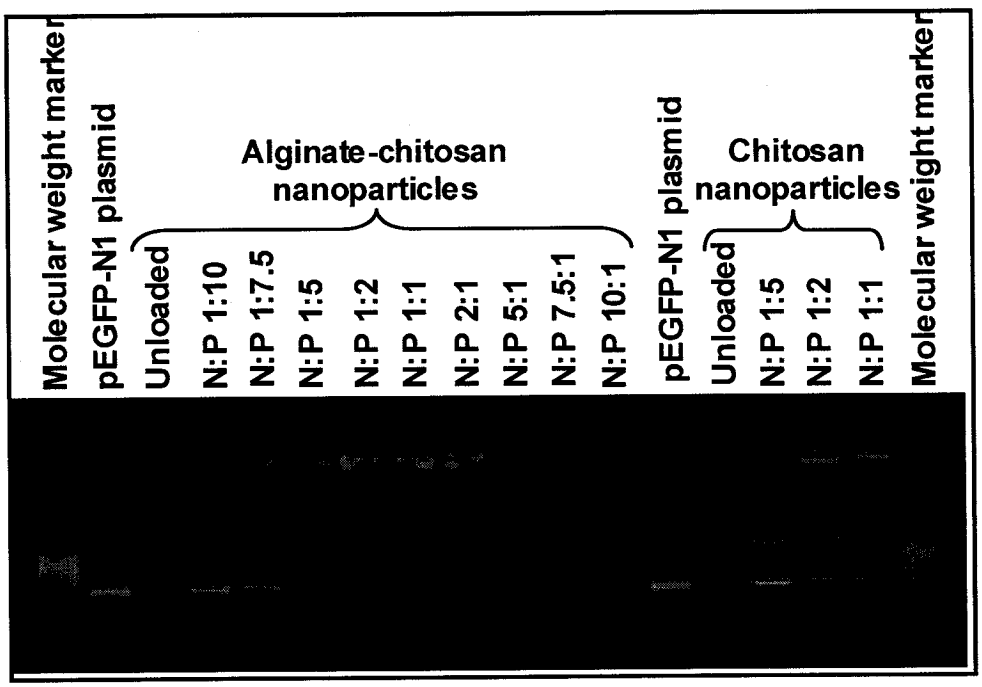

Figure 6.5. Agarose gel electrophoresis of alginate-chitosan nanoparticle-DNA complexes to determine degree of complexation. Samples were run on a 0.8% gel and stained using ethidium bromide. Note complete complexation of DNA at 1:1 ratio with alginate-chitosan nanoparticles.

Alginate-chitosan nanoparticles demonstrated greater capacity to prevent DNA migration compared to chitosan nanoparticles (Figure 6.5). This likely stems from nanoparticles having more chitosan amino groups available to complex the DNA than was calculated, resulting in a difference between the theoretical and true N:P ratios. The theoretical charge was calculated as the number of chitosan amino groups remaining after complexation with alginate carboxylate groups. Failing to interact in a 1:1 stoichiometric ratio would lead to

higher than calculated particle charge, explaining the increased binding of DNA over chitosan alone, which was not subjected to the same theoretical calculations.

Correlation of these results to those of the ethidium bromide exclusion assay further supports the notion that alginate reduces the strength, but does not prevent, binding between chitosan and DNA. While nanoparticles were able to completely complex plasmid at a theoretical N:P ratio of 1:1, the competition binding assay clearly showed that there were more available spaces for the ethidium bromide to intercalate with DNA than observed with chitosan alone at the same ratio, as indicated by the increased fluorescence (Figure 6.3). This indicates that the nanoparticles are able to complex the same amount of DNA (since none migrated), but with reduced overall binding.

Some reports question the ability of nanoparticle systems to protect DNA, since surface adsorption may allow exposure of DNA to environmental degradation and digestion. In order to assess the ability of our system to protect DNA, its integrity was assessed following complexation and release from nanoparticles, with and without exposure to nucleases. Plasmids complexed with alginate-chitosan nanoparticles at an N:P ratio of 2:1 were protected from enzymatic digestion, as indicated by the release of intact DNA following subsequent inactivation of DNase I and degradation of the nanoparticles (Figure 6.6, lane G). Conversely, naked DNA is completely digested by DNase I after 15 min incubation at 37°C (lane C). While DNA released from alginate-chitosan nanoparticles showed a slight shift to the open coiled form, the majority maintained the supercoiled structure of the naked plasmid. It is generally accepted that there is little difference between the activity of open coiled and supercoiled DNA, suggesting that complexation with the alginate-chitosan nanoparticles did not affect the integrity of DNA[52]. Furthermore, it afforded DNA protection from nuclease attack. Chitosan-DNA nanoparticles formed at the same N:P ratio did not offer the same degree of protection from nucleases (lane I). There was also some indication that complexation with chitosan affected the integrity of the DNA, as indicated by the trailing band. It has been reported that alginate-chitosan polyionic microparticles demonstrate greater stability and afford more protection

to biomolecules than either polymer alone[106]. Our results support this observation for alginate-chitosan nanoparticles.

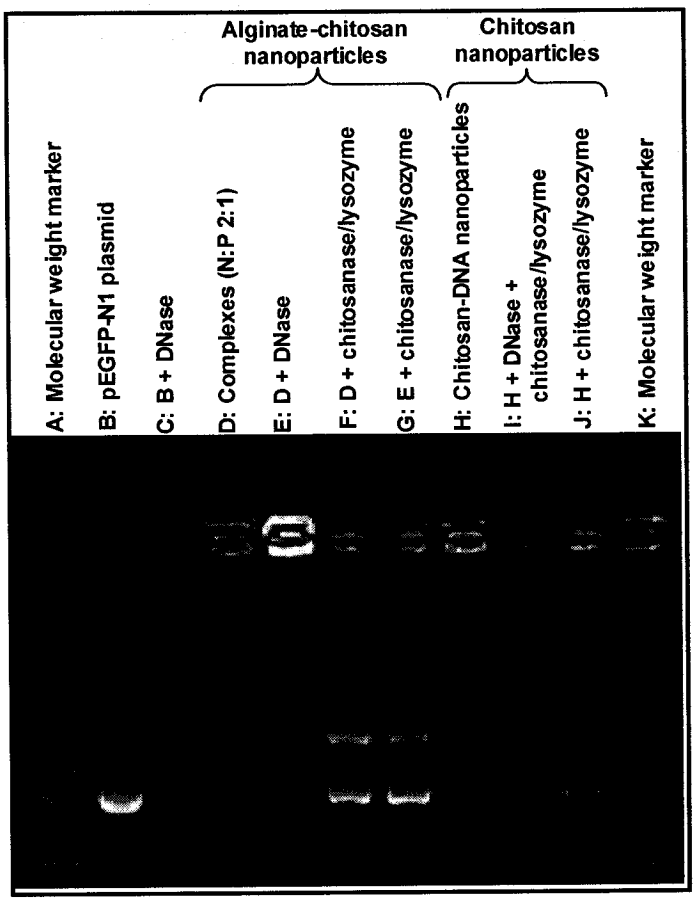

Figure 6.6. Agarose gel electrophoresis of alginate-chitosan nanoparticle-DNA complexes following DNase digestion and/or treatment with chitosanase/lysozyme to digest particles. Complexation with alginate-chitosan nanoparticles preserves activity of DNA (lane F), and protects it from DNase digestion (lane G).

6.4.4 Cytotoxicity of Alginate-Chitosan Nanoparticles

Prior to cell studies, the stability of nanoparticle-DNA complexes in cell culture medium was confirmed using DLS, zeta potential measurements and gel electrophoresis. Complex size and charge were invariable, indicating that complexes maintained their structure. Gel electrophoresis of complexes in medium confirmed that DNA remained complexed by the nanoparticles in medium (data not shown).

The effect of nanoparticle-DNA complexes on cell viability was determined using the MTT assay. As illustrated in Figure 6.7, alginate-chitosan

nanoparticles showed no toxicity to 293T cells when incubated at low concentrations. At the lowest concentration tested, neither nanoparticle-DNA complexes nor unloaded nanoparticles showed difference from controls at 6 h or 24h. However, increasing the concentration of nanoparticles resulted in decreased viability over 6 h and 24 h exposures, with the highest concentration demonstrating statistically reduced viability over the two lesser concentrations after 24 h. The cytotoxicity at the lower alginate-chitosan nanoparticle concentration was considerably reduced compared to the commercial liposome formulation despite an eight fold higher concentration.

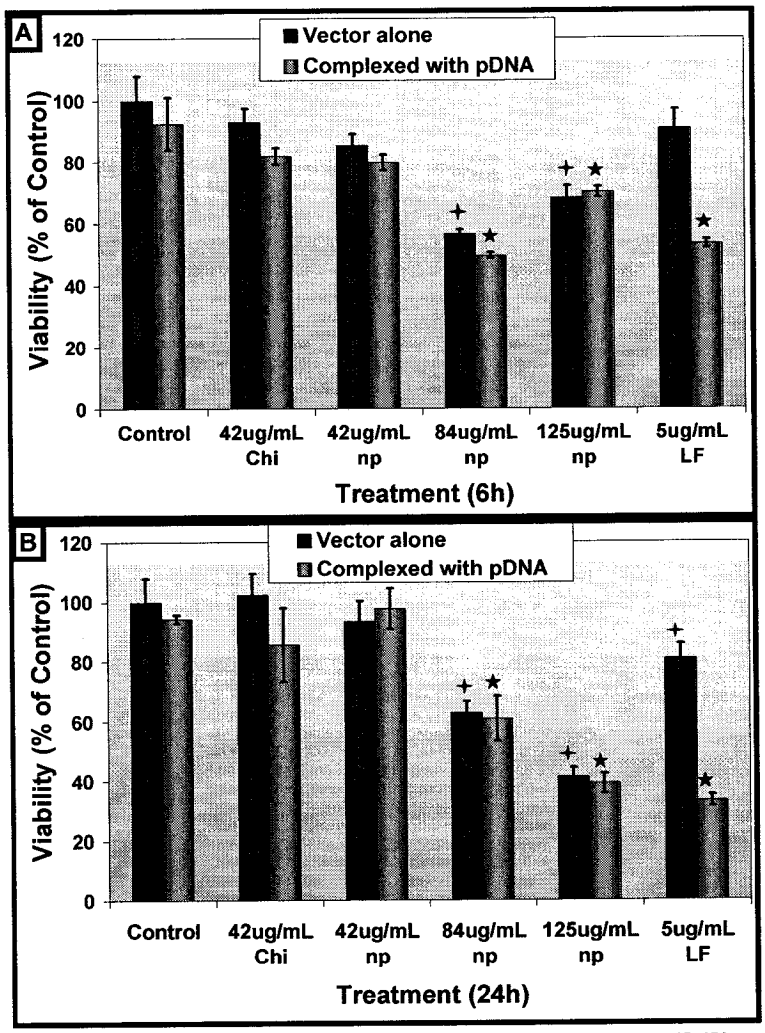

Figure 6.7. Results of MTT assay demonstrating biocompatibility of alginate-chitosan nanoparticles as suggested by lack of cellular toxicity. Alginate-chitosan nanoparticles have the same effect on cell viability as chitosan alone after 6 h (A) and 24 h (B). Values represent the mean ± standard deviation (n = 3). Stars indicate significant difference from control ($p < 0.05$). The following abbreviations are used in the figure: Chi – chitosan, np – alginate-chitosan nanoparticles, LF – Lipofectamine™.

Significantly, alginate-chitosan nanoparticles displayed the same non-toxicity as chitosan after 6 h and 24 h exposures. While most of the modifications that have been made to chitosan to improve transfection resulted in systems with higher toxicity[68,82], these results indicate that the presence of alginate does not increase the toxicity of the system, successfully achieving one of the primary goals of this project. Although cytotoxicity was not assessed beyond 24 h, cell viability was maintained for periods up to 8 days in cells treated with alginate-chitosan nanoparticle-DNA complexes. Surprisingly, cells seemed to proliferate more quickly when treated with the complexes. In contrast, cells treated with Lipofectamine™ were visibly affected, with evident decreased proliferation and altered morphology (data not shown).

An additional benefit of this system is the equivalent toxicity observed using nanoparticles that are unloaded or complexed to DNA. This is significant since many systems demonstrate higher toxicity in the absence of complexed DNA, indicating that they become toxic to cells that have internalised them and received their DNA cargo[152]. Furthermore, it has been shown that the presence of unloaded nanoparticles is often required for efficient transfection, although the reasons for this are not well understood[147]. Since the unloaded and complexed alginate-chitosan nanoparticles display the same non-toxicity, unloaded nanoparticles can be included to enhance transfection without reducing cell viability.

6.4.5 Transfection of 293T Cells in vitro

To investigate the ability of alginate-chitosan nanoparticles to transfect mammalian cells, transfection studies were performed on 293T cells using particles complexed with pEGFP-N1 plasmid, coding for green fluorescent protein (GFP). This cell line was used since it has previously been transfected with chitosan-DNA nanoparticles and modified chitosan-DNA complexes, and thus could be used to assess the transfection efficiency of alginate-chitosan nanoparticles[44,68,70,134]. Complexes were prepared at four N:P ratios and compared

to both Lipofectamine™ and chitosan-DNA nanoparticles. The ratios tested, in the range of 1:2 to 5:1, were specifically chosen to ascertain the effects that size, charge and stability have on transfection efficiency. Low ratios were deliberately selected to judge the transfection ability of complexes by limiting the amount of unloaded nanoparticles.

Results demonstrated a dependence of transfection efficiency on the charge ratio of the complex. At 48 h post-treatment, the transfection efficiency of complexes prepared at a 5:1 N:P ratio was marginally higher than with Lipofectamine™, though not significantly different (Figure 6.8). All other ratios exhibited transfection levels similar to that achieved with naked DNA. Complexes prepared at a 5:1 ratio demonstrated significantly smaller size ($p < 0.05$) and higher positive charge ($p < 0.1$) relative to the other ratios, suggesting that these factors play a role in efficient transfection with this system. The presence of unloaded nanoparticles may also have played a role and cannot be ruled out, suggesting that higher ratios could result in even greater transfection efficiencies.

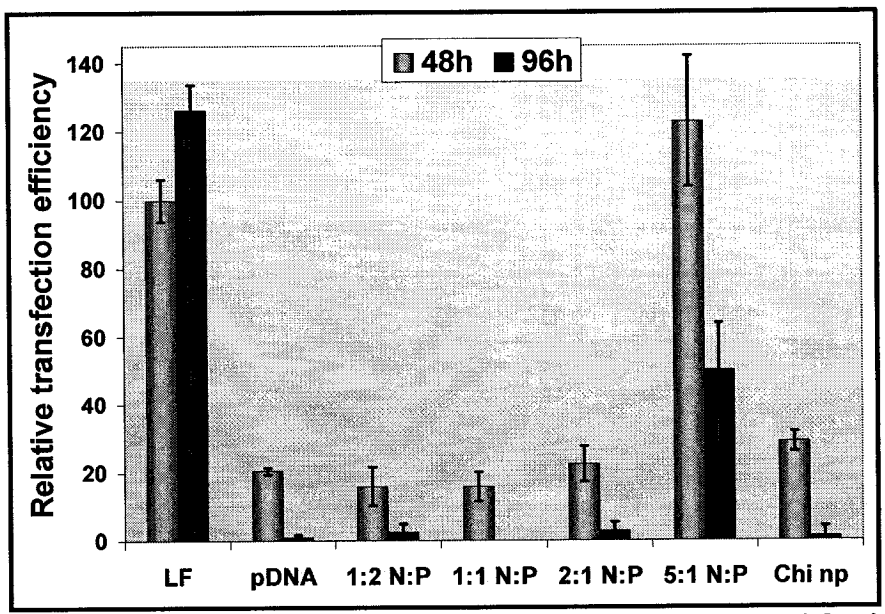

Figure 6.8. Transfection efficiency of alginate-chitosan nanoparticles in 293T cells. Transfection was assessed after 48h and 96h using flow cytometry. The efficiency of transfection by Lipofectamine™ (LF) after 48h was taken as 100%; all other values presented are relative. Values represent the mean ± standard deviation (n = 3). The following abbreviations are used in the figure: Chi np – chitosan nanoparticles, LF – Lipofectamine™, pDNA – naked pEGFP-N1 plasmid. All ratios represent alginate-chitosan nanoparticle-DNA complexes prepared at the indicated ratios.

The transfection efficiency of nanoparticle complexes decreased by 96 h, while it increased for Lipofectamine™. This is consistent with previous studies that showed maximum gene expression in 293 cells following transfection with chitosan-DNA nanoparticles between 48 h and 72 h depending on the molecular weight of the chitosan, and decreasing thereafter[153]. This decrease in the number of cells expressing GFP can be related to the effect of complexes on the cells. Cells transfected with Lipofectamine™ demonstrate decreased proliferation and increased cell death, and as a result the population may not have changed significantly between 48 h and 96 h. Conversely, alginate-chitosan nanoparticle complexes do not adversely affect cell viability or cycles. Accordingly, the population likely increased appreciably in the intervening 48 h, leading to decreased transfection readings since complexes were removed from the wells after the first 24 h, and thus were no longer available to transfect the newly divided cells. Nevertheless, transfection efficiency with nanoparticle complexes prepared at a 5:1 N:P ratio remained twice as high as achieved with naked DNA alone. Significantly, alginate-chitosan nanoparticles were observed to transfect with 4-fold greater efficiency than chitosan nanoparticles at both 48 h and 96 h. Considering that both systems displayed similar size, surface charge, and cytotoxicity, this indicates that the inclusion of alginate sufficiently affects the binding between chitosan and DNA to change its release behaviour, and thereby provide more efficient transfection than chitosan-DNA nanoparticles.

6.5 Conclusions

Alginate-chitosan nanoparticles were prepared through complex coacervation to yield particles with a mean Z-average diameter of 157 nm and a zeta potential of +32 mV, providing characteristics desirable for gene delivery. Alginate-chitosan nanoparticle-mediated transfection of 293T cells resulted in transfection levels as high as achieved with Lipofectamine™ after 48 h. Transfection efficiency of complexes prepared at a 5:1 N:P ratio was higher than with chitosan nanoparticles or naked plasmid. The improvement in transfection

efficiency may be explained by the presence of alginate. Exclusion assays indicated competitive binding with chitosan between alginate and DNA while gel electrophoresis revealed efficient retardation of DNA, supporting the hypothesis that alginate inclusion reduces the interaction strength between chitosan and DNA but does not prevent it. The improvement in transfection while maintaining the non-toxicity of chitosan nanoparticles makes alginate-chitosan nanoparticles a suitable candidate for gene delivery applications.

6.6 Acknowledgments

The authors would like to thank Valérie Hay for technical assistance and Shawn Carrigan for expert assistance with manuscript preparation. We would also like to acknowledge the Natural Sciences and Engineering Research Council of Canada (NSERC), the Québec Ministère de la Recherche de la Science et de la Technologie (MRST), and the Canadian Institutes of Health Research (CIHR) for funding this research.

6.7 Further Characterisation of Nanoparticle-DNA Complexes

Additional characterisation of the formation of alginate-chitosan nanoparticle-DNA complexes was executed by performing size and charge measurements of complexes formed using two protocols over a range of ratios. In protocol 1, the method presented in the preceding results, oligonucleotides (ON) were mixed with prepared nanoparticles at N:P ratios from 1:25 to 25:1. Protocol 2 involved mixing the chitosan and ON prior to the addition of alginate for nanoparticle formation (Figure 6.9) (see Appendix B2.3 for further details).

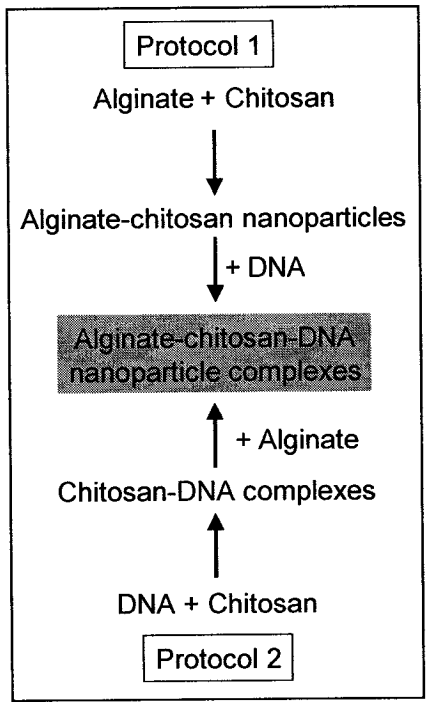

Figure 6.9. Two protocols to prepare DNA-loaded alginate-chitosan nanoparticles.

Regardless of the preparation method, complexes showed more variability in size when DNA was present in excess (Figure 6.10). Complexes prepared with N:P ratios greater than 1:1 using protocol 1 were larger than unloaded nanoparticles, having mean sizes an average of 24 nm larger. With protocol 2, the same N:P ratios led to complexes an average of 18 nm smaller than unloaded nanoparticles.

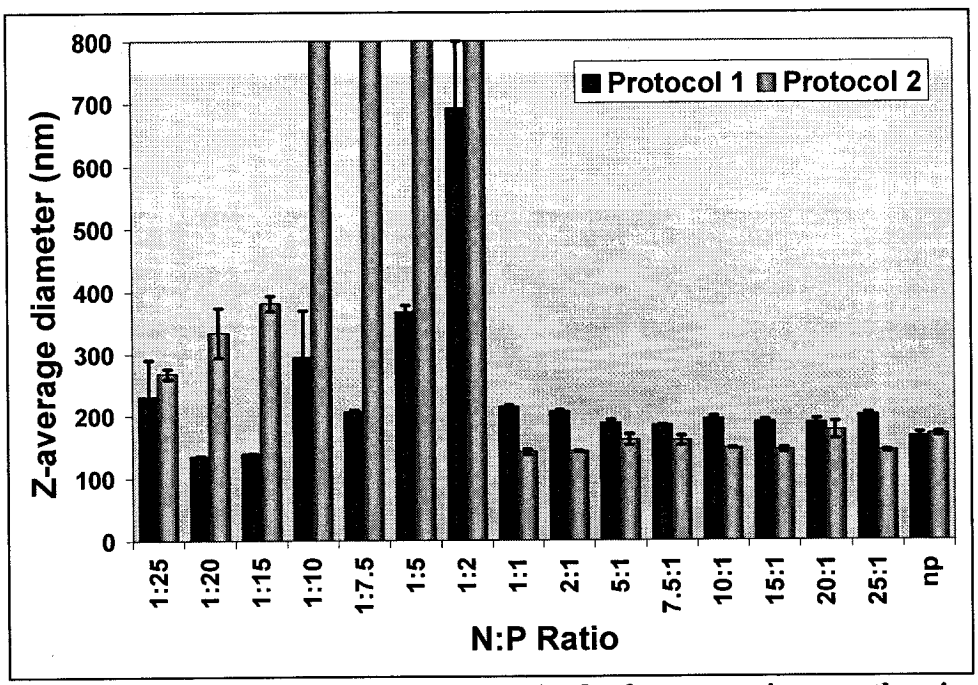

Figure 6.10. Effect of N:P ratio and method of preparation on the size of nanoparticle-DNA complexes. All complexes show sizes significantly different from the nanoparticles, except for ones prepared at 7.5:1 and 20:1 ratios using protocol 2. Small, stable complexes are only formed in the presence of an excess of nanoparticles. Values represent means ± standard deviation ($n \geq 9$).

The overall charge of the complexes was similarly found to change with N:P ratio, and depended on the method of preparation. Zeta potentials of complexes prepared using protocol 1 followed a very distinctive trend (Figure 6.11A). Generally, increasingly excess amounts of DNA led to more negatively charged complexes, while increasing the N:P ratio led to more positively charged complexes. Similarly, protocol 2 produced complexes with negative charges overall at N:P ratios less than 1:2, and positive charges above this ratio (Figure 6.11B). Surprisingly, complexes prepared using this method at N:P ratios of 1:5, 1:7.5 and 1:10 had the highest negative charges, usually indicative of stable systems, though they suffered critical aggregation (Figures 6.10, 6.11B). At present there is no satisfactory explanation for this phenomenon, although similar observations with other polymer systems led to the hypothesis that it results from the cross-linking of ONs by the polymer[154].

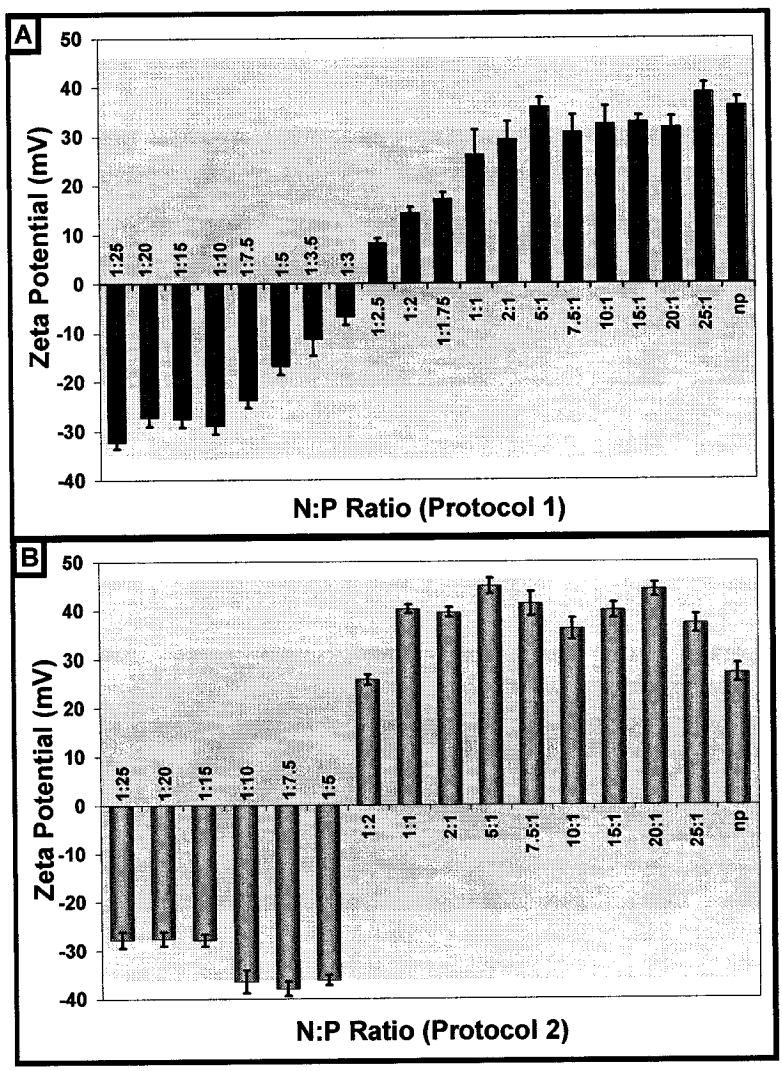

Figure 6.11. Effect of N:P ratio and method of preparation on the zeta potential of nanoparticle-DNA complexes. **(A) Zeta potential of complexes prepared through the addition of DNA to formed nanoparticles (protocol 1). (B) Zeta potential of complexes prepared through the addition of DNA to chitosan followed by addition of alginate for nanoparticle formation (protocol 2). Values represent means ± standard deviation (n ≥ 9). Note: "np" in the figures refers to unloaded alginate-chitosan nanoparticles.**

Based on size and charge measurements, the suggested scheme of complex formation under both protocols is summarised in Figure 6.12. The gradual change in the charge of complexes prepared using protocol 1 can be described by a system of charged spheres being coated by DNA strands of opposite charge, which explains the occurrence of intermediate surface charges. Complex formation using protocol 2 is a different process, exhibiting no intermediate states. This suggests that the complexes formed in this method undergo reorganisation

upon addition of alginate, with the formation of a more uniform network of all three components. This is further supported by the observation that complexes with ratios where N>P demonstrate higher overall positive charge than unloaded nanoparticles. Similar effects have been reported in the preparation of ON-loaded alginate-PLL nanoparticles[139]. Additional support for this model is provided by the observed differences in complex sizes, with adsorption of DNA on the surface resulting in increased particle size, whereas the formation of an interpenetrating network results in more compact particles. It should be noted that the use of ON in these experiments cannot reproduce the exact complex charges and sizes that would result with the use of plasmid DNA. However, these experiments were conducted to better understand complex formation, which should occur similarly with DNA plasmids.

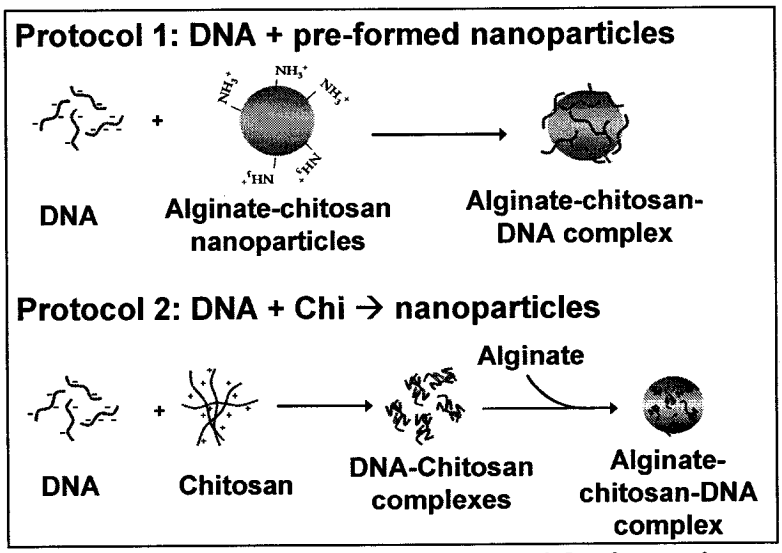

Figure 6.12. Proposed mechanism of nanoparticle formation depending on preparation method. Zeta potential analysis suggests that DNA is adsorbed on the surface of formed nanoparticles (protocol 1), whereas pre-mixing with chitosan results in nanoparticles with the DNA intertwined throughout the particle (protocol 2).

In addition to suggesting complex formation, these experiments provided further insight into the role of alginate in the system. While competition binding assays demonstrated that alginate did not prevent binding between chitosan and DNA, as explained in Section 6.4.3, it was important to verify that alginate was not excluded during complex formation, since chitosan and DNA alone can form nanoparticles. The role of alginate in the formation of particles was confirmed

with interim size and zeta potential measurements acquired prior to the addition of alginate to the ON-chitosan mixture (protocol 2), indicating that its presence is necessary for the formation of discrete populations of small particles (data not shown). Further evidence suggested that alginate increases the stability of the system as compared to chitosan-DNA nanoparticles. Size and zeta potential measurements have previously indicated that stable small chitosan-DNA nanoparticles can only be achieved at N:P ratios of 4:1 or greater[89]. The inclusion of alginate in this system allowed stable, small complexes to be formed at ratios as low as 1:1, regardless of the method of preparation.

Based on these results, protocol 1 was deemed to be preferential for gene delivery applications. Although there is a slight size disadvantage to complexes prepared this way, it is proposed that the surface adsorption of DNA is more likely to allow its release intracellularly, whereas its release from a complex interpenetrating network might require degradation of the system. Recent work has shown that protein release from chitosan nanoparticles was significantly reduced and delayed following addition of alginate, in a preparation method similar to protocol 2[155]. Furthermore, these studies indicated that complexes prepared at N:P ratios of 2:1 and above were more stable, even though electrophoretic analysis revealed complexation at a 1:1 ratio. Finally, since nanoparticles demonstrated the ability to be stored through lyophilisation, and given that complex formation is a rapid process, protocol 1 allows for complex preparation immediately prior to use so that DNA can be stored under optimum conditions until needed.

Chapter 7
Development of a Novel Technique to Detect and Image Nanoparticles Intracellularly

Having established the suitability of alginate-chitosan nanoparticles as gene delivery vectors, it became desirable to understand their fate following cellular internalisation. Traditionally, gene delivery vectors are evaluated solely on their ability to mediate transfection. Although this is suitable as an end-point measure of success, it cannot impart information as to processes involved in transfection or where transfection fails. For example, it is unknown whether the entire vector enters the nucleus to mediate transfection or if DNA is released in the cytosol and enters the nucleus independently. Although uncommon in the field of gene delivery, knowledge of the intracellular fate of vectors is imperative to understanding and improving transfection processes.

The main objective of this phase of the project was to characterise the intracellular fate of alginate-chitosan nanoparticle complexes by developing a novel technique incorporating transmission electron microscopy (TEM) imaging and nano-scale secondary ion mass spectrometry (NanoSIMS). Although development of the so-called correlative imaging technique did not provide the desired information regarding the intracellular fate of complexes, the work did establish a "proof of principle" for the future application of this technique. This work was presented at a conference of the *Canadian Biomaterials Society* (Waterloo, ON, Canada, 2005), and is summarised in Chapter 7. A brief description of the NanoSIMS technique is provided in Appendix C.

Tracking Endocytosed Alginate-Chitosan Nanoparticles using Combined NanoSIMS and Electron Microscopy

7.1 Introduction

The methods currently used to evaluate intracellular transport of complexes include flow cytometry[130,156,157], confocal microscopy[133,157,158], and transmission electron microscopy[61,159]. Although confocal microscopy is an invaluable tool that can provide sufficient detail to surmise the intracellular trafficking of the complexes, it is insufficient to define their precise sub-cellular localisation. The limits of detection inherent to optical microscopy of any kind prevent the visualisation of non-viral vectors passing through the nuclear pore complex, or capturing their escape from endosomes, for example. Furthermore, this method requires the conjugation of fluorophores, generally bulky molecules, to the non-viral vectors, which can alter their behaviour or trafficking.

Conversely, the resolution of transmission electron microscopy (TEM) is significantly enhanced over optical microscopy, so as to enable visualisation of individual non-viral vectors as they traffic through cells. Transmission electron microscopy tracking of polymeric or liposomal non-viral vectors located intracellularly has been undertaken in only a few studies, despite its ability to provide high resolution images of cellular ultra-structure[61,160]. The principle reason for this is that most non-viral vectors are not sufficiently dense to be easily distinguishable from cellular features.

Where other techniques fail, NanoSIMS (Nano-scale Secondary Ion Mass Spectroscopy) analysis may provide the means to further elucidate and visualise the mechanism of intracellular trafficking of nanoparticle complexes. NanoSIMS analysis provides the ability to construct compositional 2D images based on the

molecular and isotopic constituents of the sample. While the resolution of this method does not compare to electron microscopy, using both techniques may allow precise sub-cellular identification and localisation of nanoparticle complexes. Through NanoSIMS analysis, the presence of nanoparticles can be confirmed and situated, and correlated to the information from TEM analysis.

The goals of this research phase were (a): to assess the suitability of NanoSIMS for monitoring the intracellular trafficking of alginate-chitosan nanoparticles in an effort to better understand the transfection process by correlating NanoSIMS and TEM images to identify specific cellular organelles or structures involved in nanoparticle trafficking, and (b) to contribute to the developing knowledge base surrounding NanoSIMS application in biological analyses. The NanoSIMS technique is relatively new and has not yet been validated as a standard analysis method. The development of a method to prepare samples for analysis by TEM and NanoSIMS would help to validate the analysis method, creating possibilities for numerous other applications.

7.2 NanoSIMS Theory

NanoSIMS is the name given to the technique of ultra fine feature analysis using secondary ion emission. The technique is based on the same theory behind SIMS: bombarding a sample under ultra-high vacuum with an ion beam to impart high energy collisions, resulting in a cascade of atomic collisions. If the cascade returns to the surface, it can sputter or eject ionised atoms or molecules from the surface of the sample (Figure 7.1). The ejected ions are collected and directed by magnetic fields to an analyser that separates and counts the quantity of specific ions based on mass and charge. By using a raster pattern, this technique produces an image mapping the composition of specific elements in the sample, which is destroyed during the analysis.

The SIMS technique has been used successfully for surface analysis in many disciplines. The features of this technique include elemental, molecular and isotopic analysis, high sensitivity, and good resolution. Improvements in SIMS instruments have made ultra fine feature analysis possible. In order to acquire

information about ultra fine features, analysis must be performed on a limited spatial area. SIMS analysis had to be improved to enhance spatial resolution by enhancing secondary ion emission and maximised secondary ion detection. These improvements allow ultra-fine feature analysis that was not previously possible given the limitations of commercially available SIMS microscopes[161]. (For a description and brief discussion of the improvements offered by NanoSIMS over previous methods, see Appendix C.)

An additional improvement in the NanoSIMS design relates to the detection of multiple species. In SIMS techniques, secondary ions are separated according to their mass prior to detection. This is necessary to ensure identification and accurate quantisation of the secondary ions. Often, it is desirable to analyse samples to acquire information about multiple species. In conventional SIMS instruments, this detection is done sequentially. NanoSIMS instruments make use of a Mattauch-Herzog double focusing mass spectrometer that offers high mass resolution and parallel detection of up to 5 species. This system maximises the resolution and detection of the secondary ions while minimising acquisition time.

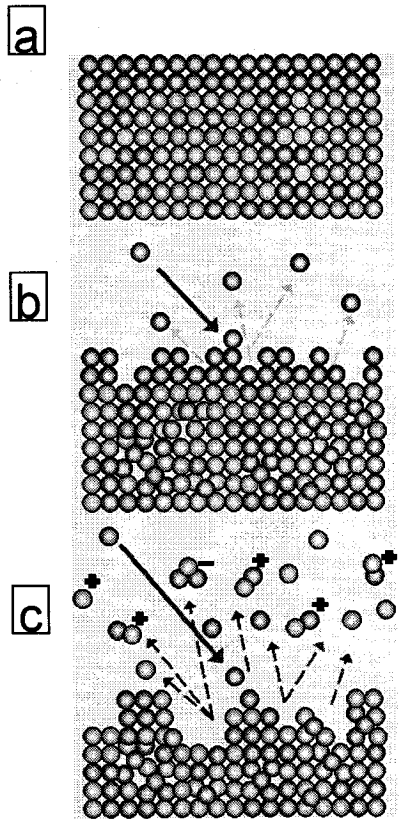

Figure 7.1. NanoSIMS Theory **(a) Sample prior to bombardment containing two atomic species and a layer of contamination on the upper surface. (b) The sample is bombarded with an ion beam, causing sputtering of surface contamination. This also allows the primary ions to build up in the sample. (c) After removal of the surface contamination, bombardment continues sputtering the sample. As atoms and molecules are ejected from the surface, they may ionise. Degradation of the sample is not uniform and depends on the species present.**

7.3 Experimental Procedures for NanoSIMS Analysis

7.3.1 Chemical Synthesis to Label Nanoparticles

Owing to their biopolymeric nature, alginate-chitosan nanoparticles are composed solely of carbon, nitrogen, oxygen and hydrogen. As such, they would be virtually invisible through NanoSIMS analysis against the background of the cell, which is composed primarily of the same atomic species. For this reason, nanoparticles had to be modified to incorporate an easily identifiable element that is not native to cells. Since a source of chitosan or alginate containing stable isotopes (^{13}C or ^{15}N) could not be located, the decision was made to use iodine as a label because it is readily detected through NanoSIMS analysis.

Chitosan was chemically modified with Bolton-Hunter reagent, which contains iodine and is a standard method used to stably label proteins. Bolton-Hunter reagent was prepared according to the method published by Bolton and Hunter (Figure 7.2)[162]. Briefly, sodium iodide (50 μg/mL in 0.25 mM phosphate buffer, pH 7.5) was added to N-succinimidyl 3-(4-hydroxphenyl) propionate in the presence of chloramine-T, followed by addition of potassium iodide (20 mg/mL in 0.05 M phosphate buffer pH 7.5) in the presence of sodium metabisulfite (12 mg/mL in 0.05 M phosphate buffer pH 7.5). Following the addition of dimethylformamide, Bolton-Hunter reagent was extracted with benzene.

Chitosan was then chemically modified with the Bolton-Hunter reagent, according to published methods, yielding an iodinated chitosan derivative (Figure 7.3)[163]. In brief, Bolton-Hunter reagent was added to a pre-chilled solution of chitosan mixed with triethylamine and stirred on ice for 15 min. The solution was then transferred to dialysis tubing (Spectra/Por MWCO 2000) and dialysed against 1% HCl for 48 h. This method resulted in the labelling of approximately 1/15,000 chitosan monomers. Although this low level of substitution reduces the signal for NanoSIMS, another study found it to be sufficient for radiometric analysis using a radio-isotope of iodine[163]. Furthermore, it was imperative to keep substitution low enough to prevent altered distribution or intracellular trafficking due to the modification.

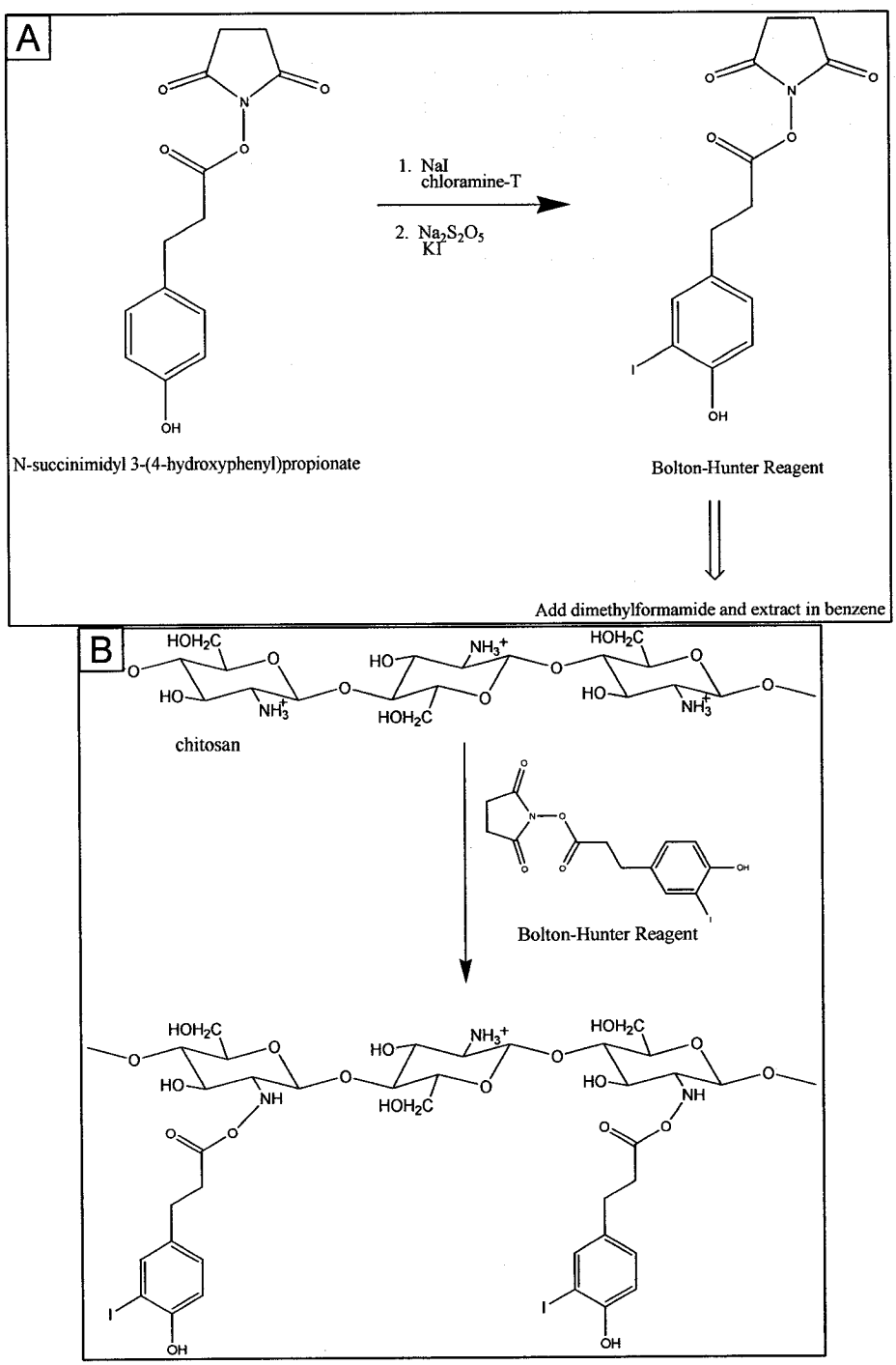

Figure 7.2. Preparation of iodine-labelled chitosan (A) Preparation of Bolton Hunter reagent through iodination of N-succinimidyl 3-(4-hydroxypheynyl)propionate. (B) Preparation of iodinated chitosan through reductive amination of amino groups of chitosan with Bolton-Hunter reagent.

Nanoparticles were prepared as usual, using the Bolton-Hunter labelled chitosan (1%) in place of the non-modified chitosan. As usual, the nanoparticle suspensions were analysed for size and distribution, using dynamic light

scattering (Malvern Instruments HPPS) and zeta potential (Brookhaven Instruments Corporation ZetaPlus).

7.3.2 Cell Culture and Sample Preparation

Nanoparticle uptake assays were performed using COS-7 cells (ATCC) cultured in 12-well plates in Dulbecco's Modified Eagle Medium (DMEM, Invitrogen) supplemented with 10% Foetal Bovine Serum (FBS, ATCC). One day after initial seeding, cells were treated with 500 µL of serum-free medium containing Bolton-Hunter labelled nanoparticles (200 µL as prepared/well). At pre-defined time intervals, cells were fixed in 2.5% glutaraldehyde for 24 h. Following fixation, samples were stained with osmium tetraoxide, dehydrated in an ascending series of ethanol:water washes, and embedded in epon, which was allowed to polymerise at 60°C for 48 h. Samples were then cut in 150 nm-thick sections and mounted on carbon- and formvar-coated copper grids. Selected samples were post-stained with uranyl acetate and lead citrate to improve contrast for TEM imaging, and to ascertain the effects of staining on NanoSIMS analysis.

7.3.3 NanoSIMS and Transmission Electron Microscopy Analysis

Samples were analysed using the NanoSIMS (Cameca Inc., France). After bombarding the surface to remove the layer of contamination, the samples were analysed using Cs^+ as a primary ion source and detecting the following five molecular ion species: CN^-, S^-, P^-, O^- and I^-. The first four species were used to establish cell morphological information, while the last was used to detect the presence of the labelled nanoparticles.

Selected samples were imaged using TEM prior to NanoSIMS analysis. Maps of selected cells were created by thorough, grid-patterned imaging of samples using the transmission electron microscope at 80 kV (JEOL 2000FX). A minimum of four adjacent squares were imaged for each sample at 10,000x magnification, yielding high resolution images of 8 – 16 cells per sample. These samples were then subject to NanoSIMS analysis.

7.4 Results

7.4.1 *NanoSIMS Analysis*

Early attempts to visualise alginate-chitosan nanoparticle complexes following internalisation in COS7 cells by TEM confirmed that they do not provide sufficient density to be discernible from the cell. Standard staining procedures did not render them more noticeable. TEM images of treated samples demonstrated no distinct features that could be definitively recognised as nanoparticle complexes (Figure 7.3). Several features were noticeably different from control samples, but could not be conclusively identified. With the categorical identification of sub-cellular features being difficult even for experts, a different high resolution technique is clearly required for definitive identification of intracellular nanoparticles.

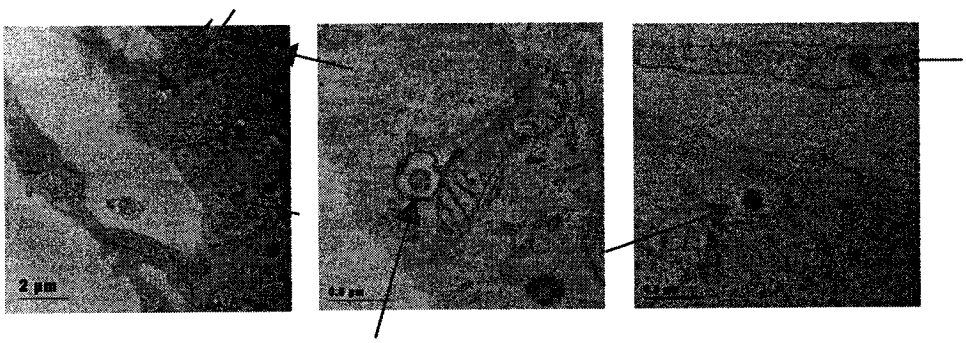

Figure 7.3. TEM images of COS-7 cells, 2hrs after exposure to nanoparticles. Structures identified as possible nanoparticles indicated by arrows.

Whereas TEM imaging could not confirm the presence of nanoparticle complexes intracellularly, NanoSIMS analysis provided distinct localisation of I^- labelled particles, with clear evidence of nuclear penetration (Figures 7.4-7.6).

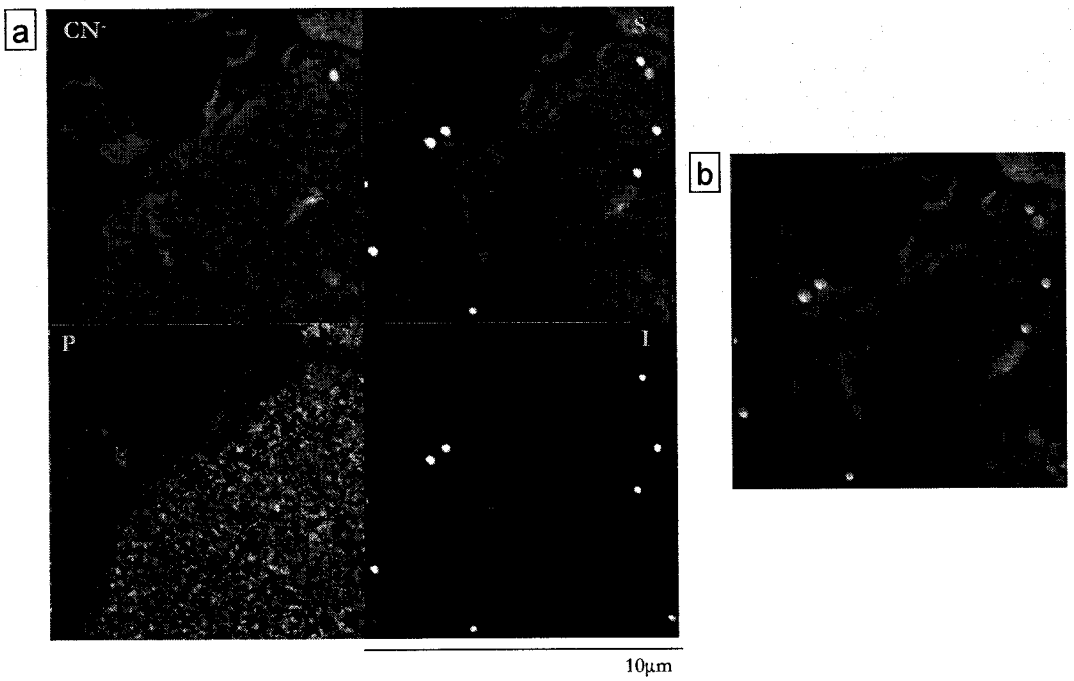

Figure 7.4. NanoSIMS images of COS-7 cells, 4hrs after treatment with nanoparticles. CN gives cell structural details, I^- denotes presence of nanoparticles. (a) Image dimensions 10μm. (b) Super-imposed image of CN^- (blue), S^- (green) and I^- (red).

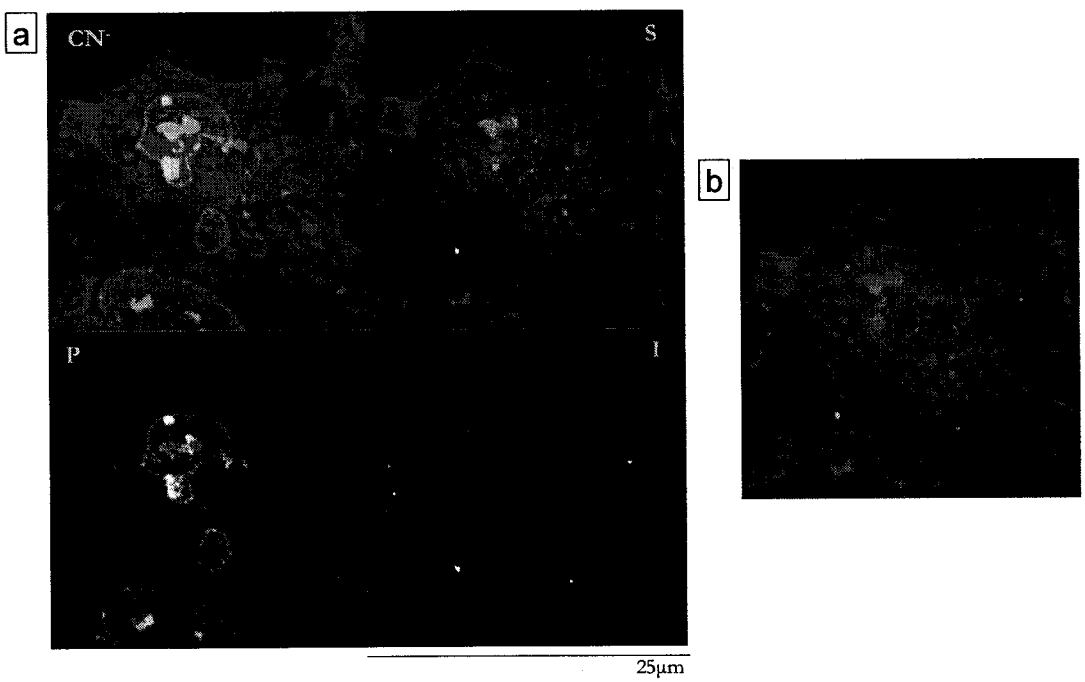

Figure 7.5. NanoSIMS images of COS-7 cells, 4hrs after treatment with nanoparticles clearly showing presence of nanoparticle complexes intracellularly. CN^- gives cell structural details, I^- denotes presence of nanoparticles. (a) Image dimensions 25μm. (b) Super-imposed image of CN^- (blue), S^- (green) and I^- (red).

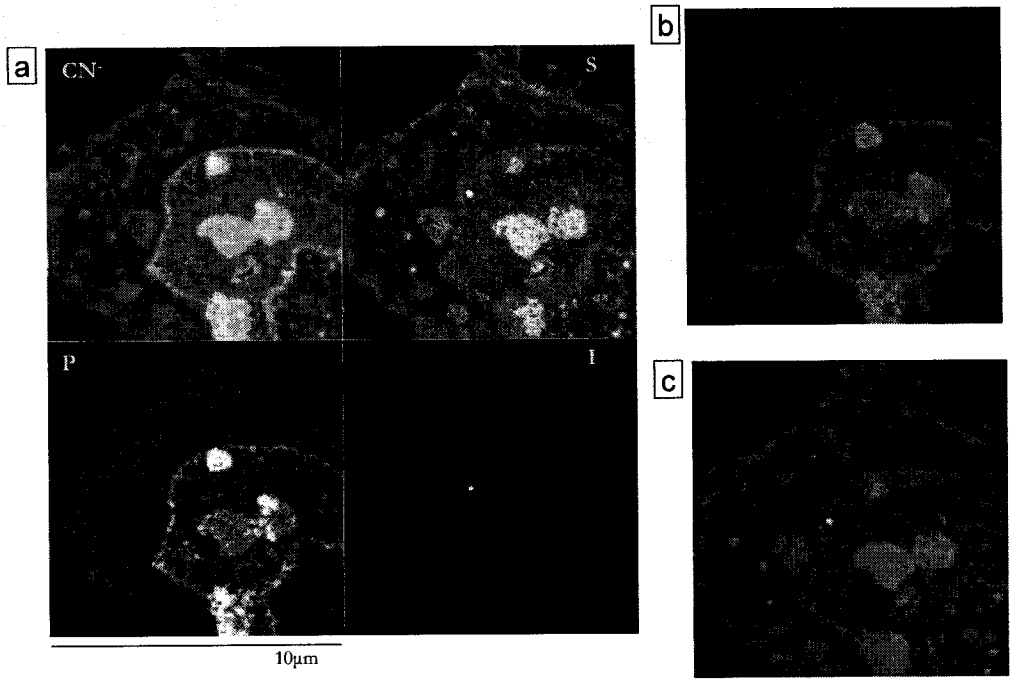

Figure 7.6. Detail of Figure 7.5. NanoSIMS images of COS-7 cells, 4hrs after treatment with nanoparticles clearly showing presence of nanoparticle complexes in the nucleus. CN^- gives cell structural details, I^- denotes presence of nanoparticles. (a) Image dimensions 10μm. (b) Super-imposed image of CN^- (blue), P- (green), and I^- (red). (c) Super-imposed image of CN^- (blue), S^- (green) and I^- (red).

Although iodine was found in several cells, it was only found in samples of cells that were fixed 4 h following treatment with the labelled nanoparticle complexes. No iodine was detectable in the 30 min, 1 h, or 6 h samples. Based on the restrictions of the analysis technique, it was hypothesised that the low level of iodination in the nanoparticles was limiting their detection intracellularly. Although the nanoparticles were likely present intracellularly at all time points, they individually did not contain enough iodine to produce a detectable signal. We surmised that aggregation of nanoparticles was required to provide a sufficiently concentrated pool of iodine for detection and hypothesised that intracellular trafficking led to aggregation by 4 h post-treatment and that aggregates were subsequently dissembled and/or removed (Figure 7.7).

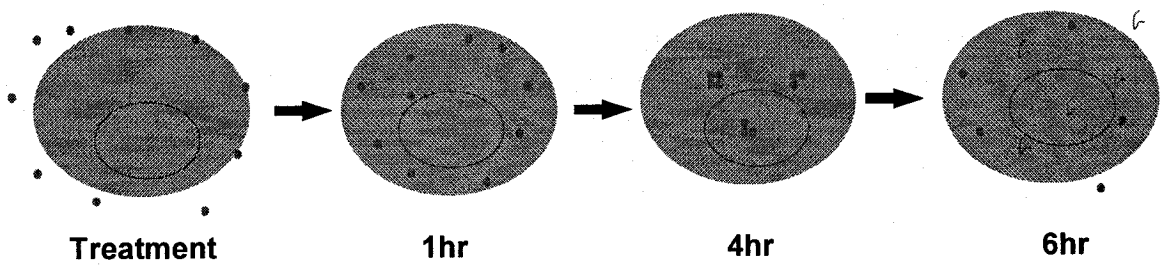

Figure 7.7. Proposed trafficking of alginate-chitosan nanoparticle complexes. **NanoSIMS analysis suggests that complexes are internalised and form aggregates by 4 h post-treatment, allowing the iodine to be detected. Aggregates then dissemble and/or are degraded so that iodine is no longer sufficiently concentrated to be detectable.**

7.4.2 *Correlational TEM Imaging and NanoSIMS Analysis*

Based on these promising proof-of-principle results, we imaged separate samples with TEM prior to analysis by NanoSIMS. The intention was to correlate NanoSIMS images with the TEM images, so meticulous imaging was performed at 10,000x magnification of a selected area of each sample (Figure 7.8). Any structure of interest was imaged at higher magnification. Unfortunately, during NanoSIMS analysis, iodine was only found inside cells which had not been imaged using TEM.

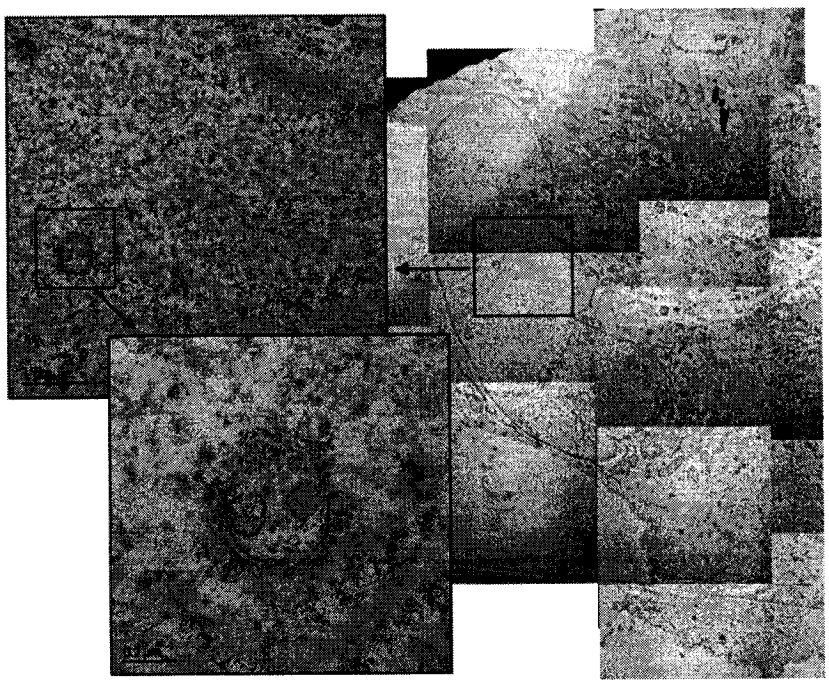

Figure 7.8. Example of TEM image mapping performed to correlate to NanoSIMS analysis. TEM images of COS-7 cells, 4hrs after treatment with nanoparticles. Insets are sequential magnifications of an area of interest within the nucleus.

7.5 Discussion

NanoSIMS analysis has been used for the investigation of biological samples only during the past several years, with a few applications published recently[164-166]. However, previous to this undertaking, the use of TEM as a correlating imaging technique had never been attempted. Although correlation of structural details with ionic information was not achieved as hoped, the analysis led to conclusions regarding sample preparation and analysis for correlational TEM-NanoSIMS imaging. The following summarises the conclusions drawn from these analyses:

1. Samples prepared for TEM analysis can be subsequently analysed using NanoSIMS.

   Prior to this attempt at correlational imaging, samples prepared for TEM and NanoSIMS analysis were both prepared by fixation, dehydration, embedding and thin-sectioning. However, while samples prepared for TEM analysis were generally cut in sections ranging from 90-110 nm, samples for NanoSIMS analysis were cut in ~500 nm thick sections and mounted on solid steel blocks. Due to the destructive nature of the analysis, thicker samples were used. To our knowledge, this study represented the first time that samples cut thin enough for TEM analysis (150 nm) were also analysed by NanoSIMS. These samples are sufficiently thick for NanoSIMS analysis. It is important to note that samples had to be mounted on carbon-coated formvar-coated sample grids. The carbon-coating is important to prevent charge build-up with ion bombardment during NanoSIMS analysis.

2. Staining with osmium tetraoxide is possible. Post-staining can be problematic.

   For TEM imaging of biological samples, staining with osmium tetraoxide is required to create contrast between biological tissue and epon. The use of osmium tetraoxide was not found to alter the results of NanoSIMS analysis in any way.

Although post-staining with uranyl acetate and lead citrate, which is common for preparation of biological samples, is not required for TEM imaging, it can improve contrast and facilitate the identification of features of interest within the cell. Select samples were stained and subsequently analysed by NanoSIMS. Although initial analysis did not yield any evident effects of staining on anionic emissions, further analysis revealed spots highly concentrated in O^- that were not observed in unstained samples. Thus, it was inferred to arise due to the staining process. This effect was particularly surprising since staining should generally be confined to the upper surface of the sample, which should have been removed during the bombardment stage to remove contamination. The results of this preliminary work suggest that staining can be used if necessary, but researchers should use caution upon interpretation of the results since the effects of staining are still unknown.

3. TEM imaging causes changes in sample.

While mounting the sample in the NanoSIMS, an internal CCD camera is used to locate the sample and pinpoint an area of interest. With the CCD camera, changes in the sample were evident that clearly located the areas which had been imaged using transmission electron microscopy. Generally, these areas were textured compared to the very smooth nature of the non-imaged areas, and there was a noticeable colour difference. Although the nature of this change is presently unknown, it is worth noting. The changes could be purely physical and macro-scale or limited to the surface. However, there is also a chance that the samples are undergoing some reorganisation that can introduce artefacts.

Further analysis revealed that environmental conditions following TEM analysis affect sample stability. Samples analysed by TEM during cool conditions (March) provided better NanoSIMS images than ones prepared during warmer, more humid conditions (May/June). The latter samples demonstrated decreased contrast compared to the former samples,

and to samples not imaged by TEM. Moreover, the bars of the grid were particularly evident in the samples prepared during hot/humid conditions. This phenomenon is one that merits further investigation by researchers in the field, due to its potential to alter not only subsequent NanoSIMS analysis, but also subsequent TEM imaging. This effect may be avoided by preserving samples in temperature controlled conditions under vacuum.

4. Bombardment in the NanoSIMS changes the sample.

   Due to the limited thickness of these samples compared to conventional samples, the initial bombardment to remove surface contamination was monitored through NanoSIMS analysis and visualised by CCD camera. It was noted that bombardment caused the sample to flatten at first, removing the texture created through TEM analysis. Further bombardment caused the sample to ripple and bubble. Since this effect was not desirable, leading to possible rupture of the sample, ways to reduce changes in the sample were sought. It was found that sequential bombardment for short times with a rest in between was best for preserving sample structure.

7.6 Conclusions

NanoSIMS offers the capacity for intracellular monitoring of the trafficking mechanisms to which delivery systems are subjected. Whereas analysis by transmission electron microscopy is non-definitive since biopolymeric-based nanoparticles have similar density to cell structures, NanoSIMS analysis allows definitive localisation of I-labelled nanoparticles intracellularly, with evidence of nuclear localisation of the complexes. However, owing to the protracted nature of sample preparation, the possibility of artefacts during fixation and sample preparation, and the time-consuming nature of the analysis, correlational TEM-NanoSIMS imaging will likely be reserved for more detailed investigations. In contrast, the relative ease of use of confocal

microscopy, and the ability to use live cells will likely preserve its status as the foremost tool for analysis of the intracellular trafficking of non-viral vectors.

Although this attempt to develop a correlational NanoSIMS-TEM imaging technique did not provide the desired detailed information regarding the intracellular fate of alginate-chitosan nanoparticle complexes, it did establish a "proof of principle" for the application of correlational NanoSIMS-TEM imaging for future investigations of this nature. Clearly, further work is required to fully develop correlational NanoSIMS-TEM imaging, following the guidelines established by this work. Due to the intensive work required to optimise sample preparation and analysis protocols, the decision was made to continue with the intracellular tracking of nanoparticles through more conventional means.

7.7 Acknowledgements

The idea of a correlational NanoSIMS-TEM imaging technique was first proposed by Jean-Luc Guerquin-Kern (Institut Curie, Orsay France) and Hojatollah Vali (McGill University). Analysis of samples with the NanoSIMS was performed by Ting-Di Wu. Samples for TEM and NanoSIMS analysis were cut by Jeannie Mui. Funding was provided by the Ministère des Relations Internationales-Coopération France-Québec.

Chapter 8
Tracking the Internalization and Intracellular Fate of Alginate-Chitosan Nanoparticles

Following the inability of the correlational NanoSIMS-TEM technique to provide information regarding the intracellular fate of nanoparticle complexes, established methods were employed to further characterise the system as gene delivery vectors. Assessment of their transfection ability in multiple cell lines revealed a strong cell-line dependency. This finding guided the direction of the fourth phase of the project, which involved the investigation of the intracellular fate of the nanoparticles, in an effort to better understand transfection capabilities.

As previously mentioned, non-viral vectors are usually evaluated solely on their ability to mediate transfection. Although a good end-point measure of success, it does not provide information regarding the capacity of complexes to overcome the many physical hurdles to successful transfection[118], nor does it explain observed differences in transfection efficiency between cell lines or between similar vectors[89,127,128]. It was once believed that cellular internalisation was the greatest barrier to transfection; however, studies have demonstrated that many non-viral vectors penetrate cells efficiently but fail to mediate a corresponding level of gene expression. Further investigation has revealed four main obstacles to cell transfection: internalisation, intracellular trafficking, escape into the cytosol, and translocation to the nucleus. To understand and predict the performance of non-viral vectors as gene delivery agents, and to be able to incorporate modifications to improve transfection, knowledge of the intracellular trafficking is imperative.

The main objective of this phase of the project was to characterise the internalisation mechanisms and intracellular fate of alginate-chitosan nanoparticle complexes. This required evaluation of the cellular interactions of the nanoparticles as well as their transfection ability in additional cell lines.

Flow cytometry and confocal microscopy were used to continue studying the intracellular fate of nanoparticle complexes. These established methods provided the means to identify the endocytosis pathways and intracellular

trafficking that lead to successful transfection. This work revealed that intracellular trafficking, which is determined by the specific endocytosis pathway used for internalisation, is directly related to transfection. Moreover, this information provided crucial explanations for observed cell-line dependent transfection. This work is described in a manuscript submitted to *Molecular Therapy*, and is presented in Chapter 8.

Manuscript submitted for publication to Molecular Therapy (May 24, 2006)

Cell-Line Dependent Internalization Pathways and Intracellular Trafficking Determine Transfection Efficiency of Nanoparticle Vectors

Kimberly L. Douglas[1], Ciriaco A. Piccirillo[2], Maryam Tabrizian[1,3]

1. **McGill University, Biomedical Engineering Department**
2. **Department of Microbiology and Immunology**
3. **Faculty of Dentistry, Centre for Biorecognition and Biosensors**

8.1 Abstract

It has been suggested that cell membrane composition and physiology may affect the internalization pathways of non-viral vectors, leading to cell-line dependent transfection efficiency. To verify this hypothesis, fluorescently-labelled alginate-chitosan nanoparticle complexes were used as non-viral vectors to transfect 293T, COS7, and CHO cells and to observe the cellular interactions and internalization mechanisms of the complexes in each cell line. 293T cells, which demonstrate the highest transfection efficiency, internalize complexes primarily through clathrin- and cholesterol-mediated processes. COS7 cells also demonstrate some internalization of complexes through the clathrin-dependent pathway, explaining the moderate transfection exhibited. In contrast, CHO cells internalize complexes predominantly through caveolin-mediated pathways and are not transfected. Results suggest that following clathrin-mediated endocytosis, complexes are trafficked to the endosomal/lysosomal pathway, where the proton-sponge effect leads to their release into the cytosol. Contrarily, the absence of trafficking to this pathway following caveolin-mediated endocytosis results in vesicle-entrapped complexes that become transfection-incompetent. These results

demonstrate that cell physiology is a critical factor in efficient transfection, and that trafficking to the endosomal/lysosomal pathway through specific internalization mechanisms is essential for transfection with alginate-chitosan nanoparticle complexes.

Keywords: Nanoparticles, non-viral vectors, cell physiology, internalization, intracellular trafficking, clathrin, caveolin, transfection.

8.2 Introduction

The frequency of reports on the development of new non-viral vectors suggests that gene delivery to cells in a safe and efficient manner remains an elusive goal. Cationic lipids and polymers have been used extensively in the production of non-viral vectors due to their ability to associate with DNA through charge interactions to form compact complexes, which facilitates cellular entry and protects DNA from nuclease attack and degradation[167].

Although non-viral vectors lead to significant improvements in cellular penetration, protection, and transfection over naked DNA, they have not yet achieved consistent transfection suitable for practical application[10]. The inability to explain or predict transfection efficiencies may result from the general lack of consideration as to how internalization mechanisms impact transfection. Non-viral vectors are evaluated predominantly through gene expression, a method that evaluates transfection but provides no insight into the capacity of complexes to evade specific barriers[118]. The following processes represent the greatest obstacles to vector-mediated transfection: internalization, avoidance of lysosomal degradation, escape to the cytoplasm, and trafficking to the nucleus.

As the first step in effective transfection, elucidating the mechanism of vector uptake is a prerequisite to understanding and improving transfection. Non-viral vectors enter cells via endocytosis, of which mammalian cells demonstrate a number of distinct processes. Some of these processes include clathrin- and caveolin-mediated endocytosis, macropinocytosis, and phagocytosis, as well as via cholesterol-mediated lipid rafts[132,168,169]. Intracellular trafficking of material is influenced by the pathway used to traverse the cell membrane, and thus has a direct effect on transfection[131]. However, recent studies have failed to demonstrate the dominance of any particular uptake pathway leading to transfection. Further confounding this issue are the effects of size, charge, nature and stability of the complexes on their cellular internalization and trafficking[7,52,62,131,170,171]. These factors make it evident that greater consideration of uptake and trafficking mechanisms is required in designing vectors that maximize transfection.

We recently reported the application of newly developed alginate-chitosan nanoparticles for gene delivery[172]. To improve upon the efficiency of chitosan nanoparticles while maintaining non-toxicity, biocompatibility and biodegradability, alginate-chitosan nanoparticles were prepared through spontaneous complex coacervation forming particles with an average size of 157 nm and a zeta potential of +32 mV. Nanoparticles mediated transfection of 293T cells four times that achieved by chitosan nanoparticles, with the increased transfection attributed to reduced strength of interaction between chitosan and DNA due to the presence of alginate.

Since cell line-dependent transfection has been reported for numerous vectors[89,127,128], the purpose of this study was to examine the transfection efficiency of alginate-chitosan nanoparticles in multiple cell lines and to correlate this to the internalization mechanisms and intracellular trafficking of the vectors. The three cell lines used in this study, 293T (human kidney epithelial), COS7 (African green monkey kidney fibroblast) and CHO (Chinese hamster ovary epithelial) cells, were chosen to represent different cell types, distinct mammals, and organs.

8.3 Results

8.3.1 Cell Line-Dependent Transfection

Cells were transfected with the pEGFP-N1 plasmid coding for the green fluorescent protein and analyzed using flow cytometry after 48 h. Results, expressed as percentage of cells transfected or change in mean fluorescence intensity demonstrated a clear dependence of transfection efficiency on the cell line, as well as on the charge ratio of the alginate-chitosan nanoparticle complexes (Figure 8.1). Among the ratios tested, transfection was greatest with 293T cells using complexes prepared at an N:P ratio of 5:1, demonstrating equivalent efficiency to Lipofectamine™ though with comparably reduced protein production. Similarly, COS7 cells were transfected most efficiently with complexes prepared at a ratio of 5:1, showing 4-fold greater efficiency than naked

DNA. However, transfection efficiency in this cell line remained significantly lower than was achieved with Lipofectamine™. In contrast, alginate-chitosan nanoparticle complexes did not mediate transfection in CHO cells, where the efficiency was on par with naked DNA.

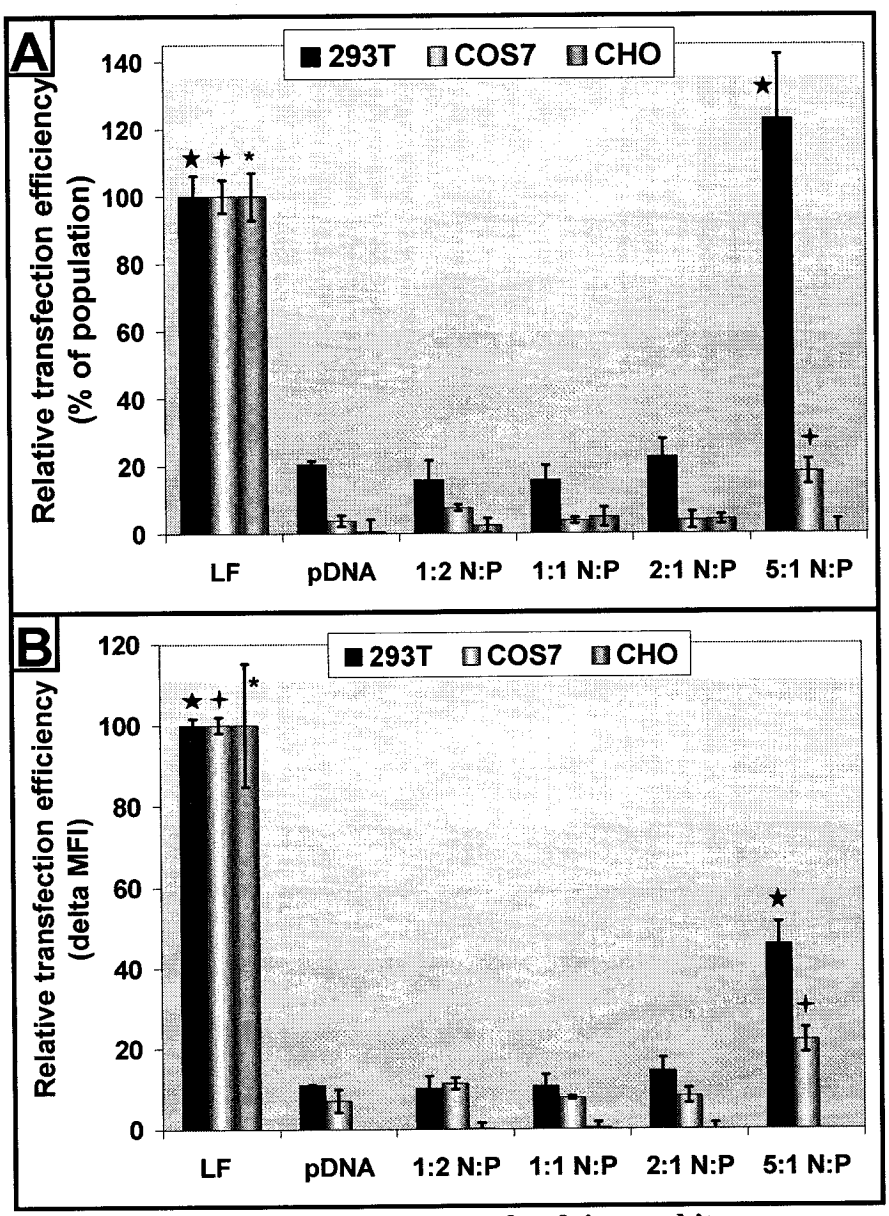

Figure 8.1. Transfection efficiency of alginate-chitosan nanoparticle complexes as determined by flow cytometry at 48h, measuring (A) proportion of cells expressing GFP, and (B) change in mean fluorescence intensity. The efficiency of Lipofectamine™ (LF) transfection was taken as 100%, all other values being relative. Transfection was evident only in 293T and COS7 cells using complexes prepared at a 5:1 N:P ratio. 293T cells are transfected with 6-fold greater efficiency than COS7 cells in terms of cell population (A), but with only twice the ΔMFI (B). Values represent the mean ± standard deviation (n = 3). Stars represent significant difference from cells transfected with naked pDNA, with $p < 0.05$. LF – Lipofectamine™, pDNA – naked pEGFP-N1 plasmid.

8.3.2 Binding, Internalization and Intracellular Trafficking of Nanoparticle-DNA Complexes

Confocal microscopy was used to investigate complex uptake in each cell line and to examine subsequent internal trafficking. Cells were incubated with complexes prepared using fluorescein-labelled chitosan and treated with LysoTracker Red, a pH sensitive dye that fluoresces in the acidic environment of lysosomes, and with DAPI to label nuclei.

In 293T cells, complexes were observed bound to the cell membrane at 30 min (Figure 8.2). The fluorescence appeared spotted on the cell surface rather than in a homogeneous covering, suggesting that the complexes were binding to distinct areas on the cell surface through specific interactions. This is further rationalized by the noted complex aggregation in some areas, as indicated by larger and brighter regions than would be expected from singular complexes. By 1 h post-treatment, complexes were visible as discrete points and in distinct compartments within the cells, suggesting that numerous complexes may have been entrapped within single endosomes. Some co-localization of fluorescein and LysoTracker Red was observed, indicating that a few complexes were trafficked to lysosomes. After 2 h, fluorescein fluorescence was no longer confined to distinct patches; diffuse, homogeneous, intracellular fluorescence was observable for the first time. At this time, fluorescence was evident in peri-nuclear locations and also co-localized with the nucleus. Diffuse fluorescence throughout the cell, including the nucleus, remained evident 4 h post-treatment.

Initial binding of complexes to COS7 cells occurred in a similar fashion to 293T cells, with distinct surface localization apparent 30 min following treatment. Some larger and brighter areas were also evident (Figure 8.2). Internalized complexes were visible as early as 30 min, present as discrete points indicative of single complexes. Nuclear co-localization was also observable as early as 30 min post-treatment, suggesting that internalization and internal trafficking processes may be more rapid in this cell line. After 2 h, intracellular fluorescence began to appear in larger, brighter compartments, suggestive of vesicles containing numerous complexes. The size of these patches increased by 4 h post-treatment,

with a corresponding decrease in the number of singular points. Co-localization of fluorescence with DAPI-stained nuclei was observable at all time points, though only as distinct points or in patches. Fluorescence was never dispersed homogenously throughout the cell.

In CHO cells, membrane-bound complexes appeared predominantly as distinct spots 30 min post-treatment, though to a considerably reduced degree relative to COS7 and 293T cells (Figure 8.2). Some co-localization with LysoTracker Red was also apparent as early as 30 min post-treatment, indicating trafficking to lysosomes. After 1 h, fluorescence was visible in distinct compartments intracellularly that varied in size but were generally larger than single complexes, suggesting vesicular confinement of numerous complexes. As with COS7 cells, the number and size of these vesicles continued to grow through 4 h post-treatment with a coincident reduction in the number of singular complex points. Nuclear co-localization of these vesicles was evident between 2 h and 4 h post-treatment. By 4 h post-treatment, all fluorescence remained confined to distinct compartments, though the brightness and quantity had diminished. This may have resulted from trafficking leading to expulsion of the particles from the cells, or from dilution following cell division, as suggested by the altered cellular morphology.

In all three cell lines, binding of alginate-chitosan nanoparticle complexes occurred at distinct areas on the cell surface, with subsequent internalization and trafficking clearly differing between cell lines.

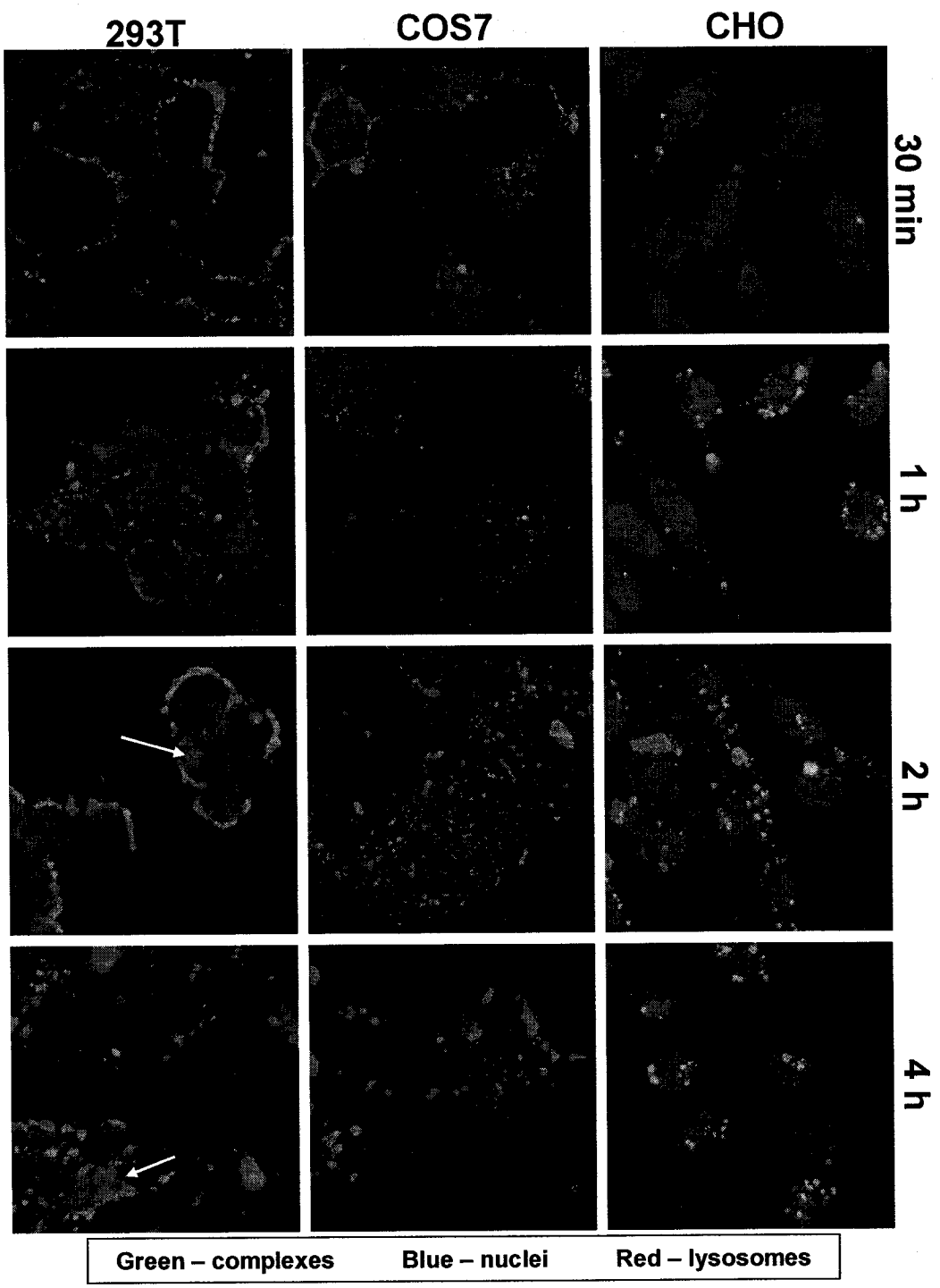

Figure 8.2. Tracking fluorescein-labelled complex internalization in 293T, COS7 and CHO cells, with additional staining of nuclei (DAPI-blue) and lysosomes (LysoTracker Red). 30 min post-treatment, complexes are bound to the cell membrane and have begun entering cells. The spotted appearance of complexes on membranes suggests a specific interaction with surface features. After 1 h, complexes were internalized; some were located in distinct compartments suggestive of vesicles. With time, the number and size of vesicle entrapped complexes increased in CHO and COS7 cells, as seen at 2 h and 4 h. By 4 h, complexes were co-localized with the nucleus in all cell lines, though in patches in CHO and COS7 cells. Diffuse homogenous fluorescence was only seen in 293T cells (arrows).

8.3.3 Binding and Internalization of Nanoparticle-DNA Complexes: Flow Cytometry Analysis

Having qualitatively analyzed complex uptake in the various cell lines, flow cytometry was used to obtain more quantitative information regarding the interaction between complexes and cells. The dose and N:P ratio of complexes affected binding and uptake in all three cell lines, with increased uptake resulting from increasing doses and increasing N:P ratios; the highest fraction of cell-associated fluorescence resulted from N:P ratios between 3:1 and 6:1 (data not shown).

In all three cell lines, binding and internalization of complexes was rapid and effective (Figure 8.3). The interaction between cells and complexes occurred almost immediately, with significant fluorescence detected within 15 min. Notably, COS7 cells exhibited an extremely rapid association with complexes; 57% demonstrated associated fluorescence following exposure of less than 1 minute. The fraction of cells exhibiting fluorescence increased sharply over the first hour, reaching a plateau by 2 h post-treatment in all cell lines. At this time, the fractions of cells with bound or internalized complexes in 293T, COS7, and CHO cell lines were 79%, 91%, and 97%, respectively. The considerable difference between 293T and CHO cell populations may in part be attributed to greater numbers of complexes binding to individual 293T cells as compared to CHO cells (Figure 8.2), leading to an insufficient supply of complexes. This may have been compounded further by the smaller size of 293T cells, which led to higher seeding densities in the uptake assays.

To measure fluorescence only from internalized complexes, cells were treated with trypan blue to quench external fluorescence prior to analysis. This produced similar curves for each cell line with a 30 min delay. As shown for CHO cells in Figure 8.3, a steep signal increase was apparent after 30 min, ultimately reaching the same plateau as without quenching. Thus, fluorescence measured at 2 h post-treatment with and without trypan blue quenching are equivalent, indicating that they are largely attributable to internalized rather than surface-bound complexes. It is evident that external binding occurs immediately with

sufficient attraction to withstand washing, followed by the slower process of complex internalization. These results confirm that internalization of the complexes is efficient in each cell line, and is therefore not the cause of the discrepant transfection efficiencies.

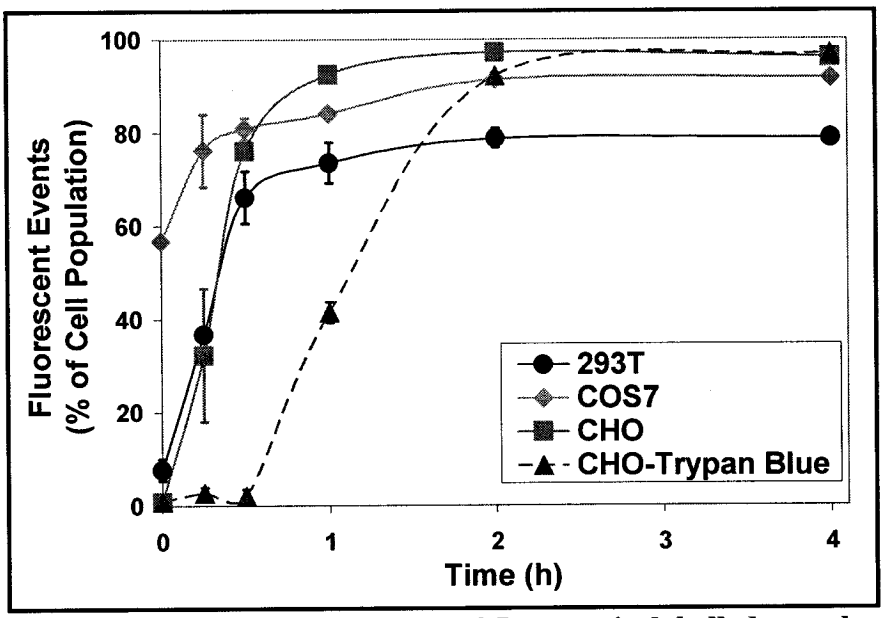

Figure 8.3. Binding and internalization of fluorescein-labelled complexes. **Note the immediate high association with COS7 cells. Treatment with trypan blue to allow assessment of internalization resulted in similar curves with a ~30 min delay (CHO-Trypan Blue shown as an example); curves for the other cell lines were analogously delayed but reached the same plateau as without quenching. Values represent the mean ± standard deviation of the fraction of the cell population showing fluorescence ($n \geq 3$).**

8.3.4 *Protein-Mediated Surface Interactions: Trypsinization and Competition Binding Assay*

To further elucidate differences in the uptake mechanisms, the nature of complex interactions with cell membranes was investigated by treating cells with trypsin-EDTA prior to analysis to cleave surface proteins. Trypsinization resulted in decreased cell-associated fluorescence at 30 min, at which time fluorescence can be considered to be predominantly membrane-bound (Table 8.1). The 293T and COS7 cell lines demonstrated a substantial decrease (75-85%) in cell-associated fluorescence following trypsinization, indicating that complexes were attached to cells through proteins that are cleaved by trypsin. In contrast, CHO cells demonstrated a considerably smaller reduction (15%), signifying that the

majority of complexes were not bound to the surface through trypsin-sensitive proteins.

Table 8.1. Involvement of surface proteins on binding (30 min) and uptake (2 h) of complexes in three cell lines. Results are expressed as the measured cell-associated fluorescence relative to untreated cells and are all statistically significant. Values represent mean ± standard deviation (n = 3).

		293T	*COS7*	*CHO*
Trypsinization	30 min	24 ± 3%	15 ± 1%	85 ± 4%
Excess chitosan	30 min	49 ± 7 %	40 ± 6 %	109 ± 3 %
	2 h	50 ± 2 %	42 ± 1 %	89 ± 0 %

To further investigate the involvement of surface proteins, the uptake assay was repeated in the presence of excess chitosan. Since the alginate-chitosan nanoparticle complexes display chitosan amino groups at the surface[172], this would reduce binding mediated by a specific ligand-receptor interaction. Unlabeled chitosan was added to the treatment medium in an amount equivalent to that present in the complexes. In 293T and COS7 cells, both binding and internalization were affected by excess chitosan, as indicated by decreased readings (50-60%) at 30 min and 2 h post-treatment (Table 8.1). These results support the hypothesis that specific interactions may be involved in cell binding of complexes. Conversely, cell-associated fluorescence of CHO populations were somewhat increased at 30 min (9%), and slightly decreased (11%) at 2 h. Given these findings, cell membrane physiology obviously affects the binding of alginate-chitosan nanoparticle complexes.

8.3.5 Evaluation of Intracellular Trafficking to Lysosomes

Although internalization was effective in each cell line, differences in uptake pathways could affect the intracellular fate of complexes, potentially contributing to the noted differences in transfection. Cells were assessed to evaluate the trafficking of complexes to lysosomes, where transfection could be prevented by degradation or digestion. Since fluorescein reversibly loses fluorescence below pH 5.5, transfer of complexes to lysosomes would quench

fluorescence; co-incubation with an endosomolytic agent can prevent transfer to or acidification of lysosomes to counter quenching. Thus, increased fluorescence resulting from treatment with an endosomolytic agent would suggest that complexes were being trafficked to lysosomes.

Treatment with chloroquine, which causes endosome rupture and content release to the cytosol, did not increase measured fluorescence in any of the cell lines, suggesting that complexes were not trapped in lysosomes (Figure 8.4). For additional verification, a separate assay was conducted whereby cells were treated with monensin, which re-establishes neutral pH in lysosomes, following detachment and prior to analysis. Treatment with monensin failed to reveal any significant changes in cell-associated fluorescence, as would be expected if complexes were trapped in an acidic environment. It can therefore be concluded that complexes are either not trafficked to or are able to escape from lysosomes in all three cell lines.

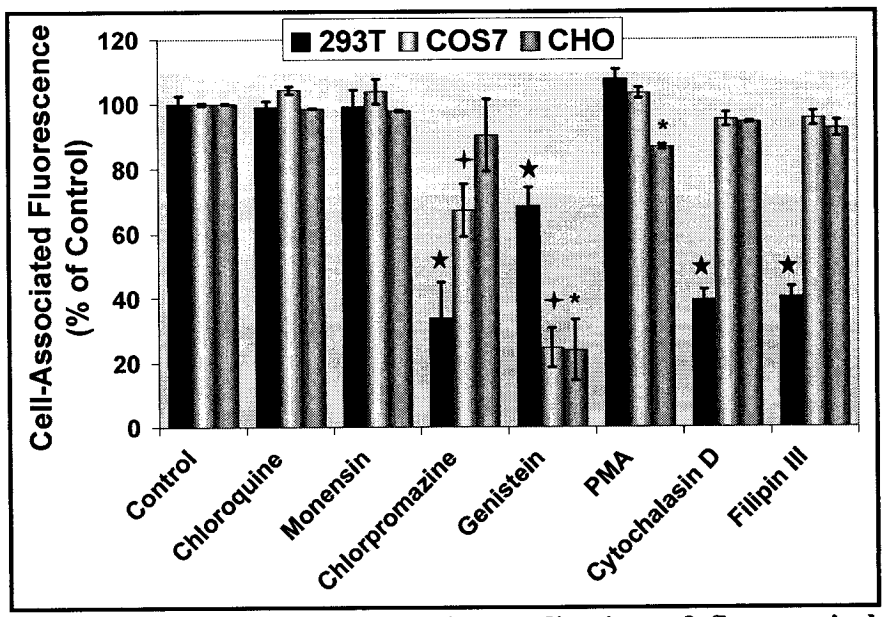

Figure 8.4. Effects of inhibitors on internalization of fluorescein-labelled alginate-chitosan nanoparticle complexes. **Monensin treatment was done prior to analysis, while chloroquine was applied with complexes. For the remaining treatments, cells were pre-treated 30 min prior to treatment with complexes. After 2 h, cells were analyzed by flow cytometry. Values indicate means ± standard deviations (n = 3). Stars indicate significant difference from the respective controls, with $p < 0.05$.**

8.3.6 Mechanisms of Nanoparticle-DNA Complex Endocytosis

The endocytic pathways used for complex internalization in each cell line was then investigated. Flow cytometry analysis of complex internalization was repeated under conditions known to affect specific endocytosis pathways.

Treatment with chlorpromazine, an inhibitor of clathrin-dependent endocytosis, had significant effects on 293T and COS7 cell lines (Figure 8.4). The reduction in internalization was greatest in 293T cells, where cell-associated fluorescence was reduced by 66%, as compared to the more moderate reduction in COS7 cells (33%) and no significant effect in CHO cells (10%). In contrast, genistein, an inhibitor of caveolin-dependent endocytosis, resulted in greater reductions in complex internalization in both COS7 (75%) and CHO (76%) cells, with a lesser effect in 293T cells (32%). Phorbol myristate acetate (PMA), a macropinocytosis stimulator, did not increase complex internalization in any cell line, and rather induced a slight decrease in CHO cells, indicating that macropinocytosis was not involved in complex uptake. In contrast, interruption of actin microfilament polymerization and depolymerization processes by cytochalasin D led to reduced internalization in 293T cells (60%) but had no significant effect on COS7 (5%) and CHO cells (7%). Similar results were obtained with filipin III treatment, which binds to membrane cholesterol. These data suggest that both clathrin- and caveolin-dependent routes were involved in the internalization of complexes in 293T and COS7 cells, while CHO cells exclusively used clathrin-independent routes. Furthermore, a separate mechanism involving actin microfilaments and membrane cholesterol, which was not macropinocytosis, was active in 293T cells but not in the other cell lines.

8.3.7 Effect of Endocytosis Inhibitors on Transfection

The relationship between internalization pathways and transfection was investigated through transfection studies in the presence of the three chemical inhibitors found to have the greatest effect on internalization processes. Using expression of the luciferase plasmid, results showed no difference in luciferase

protein production between 293T and COS7 cells at 48 h, but virtually no transfection of CHO cells (Figure 8.5). Treatment with chlorpromazine and filipin III significantly reduced transfection in both 293T and COS7 cells, whereas treatment with genistein had no effect in either line. This suggests that the clathrin- and the cholesterol-mediated pathways led to transfection with these complexes, whereas the caveolin-mediated pathway did not.

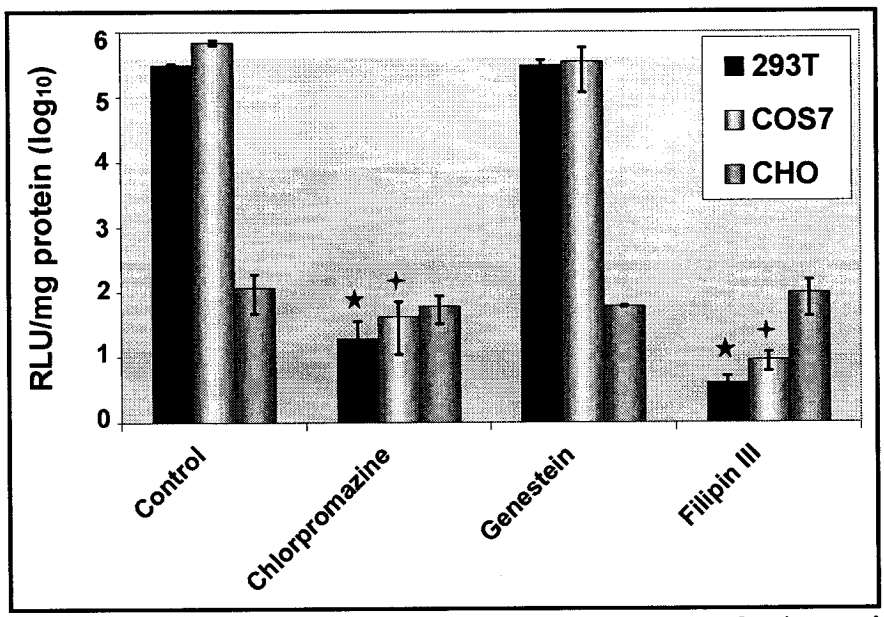

Figure 8.5. Effects of endocytosis inhibitors on transfection with the luciferase plasmid. **Cells were pre-treated with chlorpromazine, genistein or filipin III for 30 min prior to treatment with alginate-chitosan nanoparticle-DNA complexes. Note that chlorpromazine and filipin III treatment led to reduced transfection in 293T and COS7 cell lines, whereas genistein had no effect. No effect was observed by any chemical inhibitors in CHO cells, which did not show efficient transfection. Values indicate means ± standard deviations (n = 3). Stars indicate significant difference from controls ($p < 0.05$).**

8.4 Discussion

Several studies have noted cell-line dependent transfection efficiency with a variety of non-viral vectors. While some have investigated the role that vector size and nature have on transfection, we chose to examine cell physiology. The goal of the present work was to determine the cause of cell-line dependency by investigating the relationships between transfection and cellular binding and internalization mechanisms in three cell lines. Alginate-chitosan nanoparticle

complexes, whose development we recently reported[172], were used to transfect 293T, COS7 and CHO cells, with results indicating strong cell line dependence.

Transfection is considerably higher in 293T cells than COS7 cells, as measured by the percentage of cells expressing GFP, whereas there is virtually no transfection in CHO cells (Figure 8.1); GFP production is greater in 293T cells than COS7 cells, though the difference is more moderate. In contrast, luciferase protein production was similar in 293T and COS7 cells, and three to four orders of magnitude greater than observed in CHO cells (Figure 8.5). The comparable levels of luciferase production in 293T and COS7 cells may be due to a difference in plasmid size between pEGFP-N1 and pCMV-Luc; it could also reflect the use of complexes prepared at a different N:P ratio, chosen for optimum binding and internalization behaviour. Though the reasons for cell line dependence remain unconfirmed, these results support the suggestion that the mechanism of complex internalization may be affected by cell membrane composition and physiology[128,159].

Flow cytometry and confocal microscopy studies confirm that the initial stage of transfection, complex binding and uptake, is a rapid and efficient process in all three cell lines, substantiating the notion that poor transfection results do not necessarily correlate with inadequate internalization of the complexes (Figures 8.2, 8.3)[118]. COS7 cells demonstrated a remarkable ability to bind complexes immediately upon exposure, with 57% of cells showing associated fluorescence following contact of less than 1 minute. However, this rapid binding did not correlate with increased internalization or transfection.

Confocal microscopy demonstrates that complexes bind to specific sites on cell membranes, as illustrated by spotted patterns of fluorescence on the membranes (Figure 8.2). Further supporting the hypothesis that surface-bound complexes are associated with membrane proteins is the considerably reduced binding upon treatment with trypsin, where a 75-85% decrease in cell-associated fluorescence occurred at 30 min in 293T and COS7 cells (Table 8.1). Moreover, supplementing the treatment medium with chitosan led to a considerable decrease in surface-bound complexes in the same cell lines, typical of competition assays

for receptor-mediated endocytosis, further suggesting the involvement of specific interactions in complex binding. In contrast, neither trypsinization nor the presence of chitosan had a substantial effect on the measured binding of complexes to CHO cells. Complex binding to these cells may not involve proteins, or may involve membrane features that are insensitive to trypsin. Since confocal microscopy reveals non-homogeneous membrane binding in this cell line, the latter case is considered more likely (Figure 8.2). A recent study suggests that the mannose receptor may be involved in oligochitosan binding and uptake in macrophages[173]. The results of this study endorse the involvement of this receptor, given that 293T and COS7 cells express the mannose receptor, and that CHO cells, which do not express this receptor, were unaffected by trypsinization and excess chitosan[174]. Clearly, cell membrane physiology is a determining factor in complex binding.

Given that binding and internalization is successful in each cell line, chemical inhibitors of specific endocytic processes were employed to determine if specific pathways lead to transfection. Results of uptake assays under inhibition in 293T cells indicate that clathrin-dependent endocytosis plays a significant role in complex internalization, with a 66% reduction observed under chlorpromazine treatment. A cholesterol-mediated pathway involving actin microfilaments also contributes significantly, as demonstrated by a 60% reduction with filipin III or cytochalasin D treatment. Caveolin inhibition with genistein had a significantly smaller impact on internalization in 293T cells (33% reduction). In COS7 cells, clathrin inhibition had a comparatively reduced impact (33% reduction), while caveolin inhibition induced a substantial reduction in internalization (75%). Treatment with cytochalasin D or filipin III did not reduce uptake significantly (5%), indicating that internalization via the cholesterol- or actin-mediated pathways is not significant in COS7 cells. Finally, CHO cells demonstrate a strong dependence on caveolin for internalization of complexes, with a 76% reduction observed with genistein treatment. While no effects were observed with inhibition of clathrin, actin or cholesterol, it is evident that other internalization

pathway(s) are involved since obstruction of caveolin-mediated pathways did not eliminate complex uptake.

The similar responses observed within each cell line with cytochalasin D and filipin III treatment are indicative of a singular pathway utilizing both actin microfilaments and membrane cholesterol (Figure 8.4). Ostensibly, this is suggestive of macropinocytosis, though treatment with PMA did not increase uptake as would have been expected. Our results suggest that a lipid raft pathway requiring cholesterol and actin microfilaments, as suggested by Huang *et al.*[168], contributes to complex uptake in 293T cells but not significantly in COS7 or CHO cells.

Since all three cell lines express both clathrin and caveolin proteins, the reasons for alternative uptake pathways is not immediately evident. It has previously been reported that complex size can affect the mechanism of internalization, with clathrin-mediated processes limited to particles under 200 nm, and caveolin-dependent uptake prevailing for particles between 200-500 nm[131]. However, pathway dependencies cannot be explained by size since all cells were treated with the same preparations of complexes. Nor can these results be explained by the nature of the complexes[132], since the same complexes were clearly shown to be internalized via different pathways. Rather, these findings support other studies that collectively infer that cell physiology is critical in complex internalization[32,175,176]. The combined effects of complex size, nature, and cell physiology on internalization pathways requires additional investigation as knowledge of these interactions is essential for designing effective transfection vectors.

The disparate endocytic pathways of the complexes attain increased significance upon consideration of the effect of internalization mechanisms on transfection efficiency. Transfection studies performed with luciferase plasmid in the presence of clathrin-, caveolin- or cholesterol-mediated endocytosis inhibitors confirm the importance of specific internalization mechanisms for successful transfection. In 293T cells, transfection was inhibited by clathrin and cholesterol inhibitors, in accordance with the internalization studies (Figures 8.4, 8.5).

Surprisingly, similar results were obtained with transfection of COS7 cells, though they showed a greater dependence on caveolin-mediated endocytosis and negligible cholesterol-mediated internalization. CHO cells, which depended only on clathrin- and cholesterol-independent uptake pathways, were not transfected. These results suggest that clathrin- and cholesterol-mediated internalization leads to efficient transfection using alginate-chitosan nanoparticle complexes.

Since complex internalization is effective in all cells regardless of the pathway, the observed cell line-dependent transfection must be determined by the fate of complexes post-internalization. Transfer of internalized material to lysosomes, where it is degraded by the acidic environment and/or various enzymes, is believed to be the greatest barrier to effective transfection[132]. However, internalization assays with chloroquine or monensin treatment did not change measured fluorescence in any cell line, indicating that complexes are not entrapped in highly acidic environments (Figure 8.4). Moreover, confocal microscopy failed to show significant co-localization of complexes with LysoTracker Red (Figure 8.2), suggesting that acidic or enzymatic degradation in lysosomes is not a reasonable explanation for the observed internalization pathway-dependent transfection discrepancies.

Pathways leading to efficient transfection, and the requisite subsequent internal trafficking, can be intimated from investigation of the confocal microscopy images. Fluorescence in COS7 and CHO cells occurs in distinct patches that grow in size and number following internalization. Fluorescence co-localizes with the nucleus in these cells, appearing as distinct spots. The manifestation of fluorescence in distinct compartments in CHO and COS7 cells suggests that complexes remain trapped within vesicles. In contrast, the homogeneous, diffuse fluorescence observed in 293T cells after 2 h indicates that complexes escape from vesicles, ultimately leading to transfection[177]. A recent study reports similar findings: PEI complexes that escape endosomes in 293T cells are transfection competent, whereas PLL complexes that remain entrapped in vesicles do not mediate transfection[129]. Thus, the ability to escape vesicles, which

is affected by the internalization mechanism, is a critical barrier to efficient transfection.

Several hypotheses have been proposed to explain the escape of complexes from endosomes. It has been suggested that chitosan nanoparticles are able to escape the endosomal/lysosomal pathway through the proton-sponge effect, due to their abundance of amine groups[70]. The sequestration of protons during acidification of secondary endosomes leads to segregation between the protons and their counter-ions, resulting in increased osmotic pressure, osmotic swelling, and ultimate rupture of the vesicles[178]. The complexes used in this study, composed of alginate and an excess of chitosan, are capable of mediating this effect. However, the results of this study suggest that the mechanism of endosomal escape is dependent on the internalization mechanism, and thus cell line. While the proton-sponge mechanism also explains the lack of complex co-localization with and trafficking to lysosomes, its failure to mediate vesicle escape in CHO and COS7 cells requires an alternate explanation.

Studies with polyplexes in A549 and HeLa cells have shown that the clathrin-mediated pathway leads to trafficking to the endosomal/lysosomal pathway, whereas the caveolin-mediated pathway does not, due to the absence in caveosomes of signal molecules required for interaction with other cellular compartments[132]. This avoidance of transfer to the endosomal/lysosomal pathway can explain the entrapment of complexes in vesicles in CHO and COS7 cells, as has been observed with PLL-based vectors in HepG2 cells[130].

Correlation between intracellular fate and transfection

Based on the results of this study, the following binding and internalization mechanisms of the complexes in each cell line are proposed (Figure 8.6):

1. In 293T cells, complexes bind to the surface by means of specific interactions and are subsequently internalized through a variety of endocytic pathways, dominated by clathrin- and cholesterol- mediated processes. Following internalization, complexes are trafficked to late endosomes and/or lysosomes, where acidification is countered by the

proton-sponge pH buffering capacity of chitosan within the complexes. This effect results in endosomal rupture, escape of the complexes, and ultimately leads to transfection.

2. While complexes also bind to COS7 cells through interactions with specific surface features, they are predominantly internalized via caveolin-mediated endocytosis. Complexes entering through the clathrin-dependent process are presumed to be trafficked similarly as in 293T cells, leading to transfection. In contrast, complexes internalized by caveolin-mediated endocytosis are entrapped in caveosomes but are not trafficked to the endosomal/lysosomal pathway. Since these vesicles do not undergo acidification, there remains no mechanism for the complexes to escape; they consequently remain entrapped in vesicles where they cannot mediate transfection.
3. Trypsin and competition binding assays indicate no evidence for the involvement of proteins in complex binding to CHO cells. Inhibition assays demonstrate that the internalization mechanism of complexes is primarily through caveolin-mediated endocytosis. As with COS7 cells, this pathway is transfection incompetent, resulting in the entrapment of complexes within vesicles.

Although it remains unclear why the internalization mechanisms of the complexes differed between cell lines, successful transfection is evidently dependent on the internalization pathway. For these complexes, transfection requires trafficking to the endosomal/lysosomal pathway, where the proton-sponge effect allows them to escape and mediate transfection. In these cell lines, this seems to occur via clathrin- and cholesterol-dependent endocytosis, but not through caveolin-mediated internalization. The inclusion of design elements to direct these complexes to late endosomes of the clathrin-dependent endocytic pathway could further improve the transfection efficiency of these complexes in multiple cell lines.

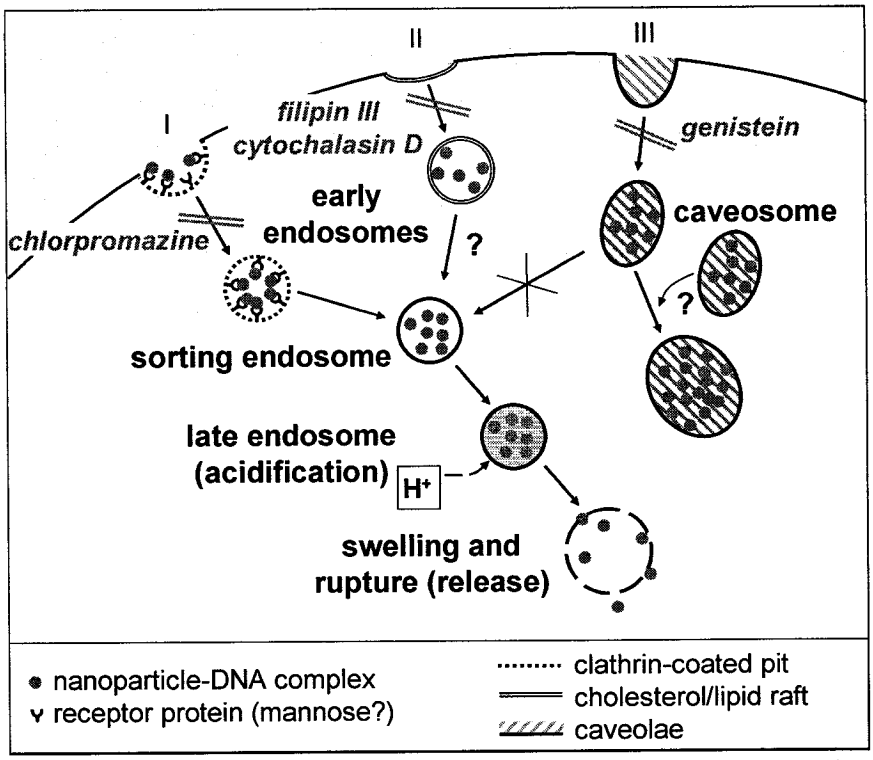

Figure 8.6. Proposed uptake pathways and intracellular trafficking of alginate-chitosan nanoparticle-DNA complexes.
(I) In 293T and COS7 cells, complexes are internalized via clathrin-dependent endocytosis following protein-mediated binding, where they are transferred to sorting endosomes. Complexes are transferred to late endosomes where acidification begins, leading to rupture and release due to the proton sponge effect.
(II) Some complexes enter cells via a cholesterol- and actin-dependent pathway in 293T cells. Through this pathway, complexes are also likely transferred to sorting endosomes where they join the pathway outlined in (I).
(III) In CHO and COS7 cells, complexes are internalized through caveolin-dependent endocytosis. Following uptake, complexes remain trapped in caveosomes, which lack signal molecules for trafficking, where they become transfection incompetent. Caveosomes may fuse leading to large vesicles of entrapped complexes.

8.5 Conclusions

The results of this study suggest that cell-line dependent transfection efficiency is related to internalization mechanisms and subsequent internal trafficking of the vectors. Alginate-chitosan nanoparticle complexes were shown to mediate transfection in 293T and COS7 cells, but did not lead to transfection in CHO cells. Internalization studies indicate that effective transfection follows clathrin- or cholesterol-mediated endocytosis of the complexes. Clathrin-dependent endocytosis accounted for the majority of internalized complexes in 293T cells, and a fraction of those that penetrated COS7 cells. Conversely,

complexes were found to enter CHO cells predominantly through caveolin-dependent endocytosis, which did not lead to transfection. Transfection studies in the presence of inhibitors confirm these pathway dependencies.

Transfection efficiency was found to be affected by the internalization pathway as it relates to intracellular trafficking. Complexes that entered cells through transfection-competent pathways were trafficked to the endosomal/lysosomal pathway where they were able to escape, presumably due to the proton-sponge effect. Complexes were then able to enter the nucleus and mediate transfection. In contrast, complexes that entered cells through caveolin-mediated processes were not trafficked to the endosomal/lysosomal pathway and thus were unable to escape from the vesicles, remaining trapped and ineffective for transfection.

This study demonstrates that different internalization mechanisms lead to disparate transfection efficiencies in diverse cell lines. While both the nature and size of complexes have been proposed as influencing internalization mechanisms, this study clearly indicates that cell physiology is a dominant factor, since the same complexes were internalized and trafficked differently in three cell lines. Although the reasons for the different uptake mechanisms remain unclear, this study underscores the importance of understanding the cellular interaction and internalization mechanisms of non-viral vectors. Knowledge of these mechanisms is critical for the development of efficient vectors that can exploit transfection-effective pathways in diverse cell lines through designs that favour endosomal escape and delivery to the cytoplasm and nucleus.

8.6 Materials and Methods

8.6.1 Cell Cultures

Three cell lines were used in this study: CHO, 293T and COS7. CHO cells were grown in Alpha Minimum Essential Medium (αMEM), while 293T and COS7 cells were cultured in Dulbecco's Modified Eagle Medium (DMEM). Medium was supplemented with 10% (v/v) foetal bovine serum (FBS, ATCC,

USA) and 1% penicillin/streptomycin. Cells were cultured at 37°C in a humidified 5% CO_2 atmosphere and sub-cultured prior to confluence using trypsin-EDTA. Cell culture media, penicillin/streptomycin and trypsin-EDTA were obtained from Gibco (Invitrogen, Burlington ON, Canada).

8.6.2 Plasmid DNA

Two plasmids, encoding for green fluorescent protein (pEGFP-N1, Clontech, Mountain View CA, USA) and firefly luciferase (pCMV-Luc), were used to prepare nanoparticle-DNA complexes and to monitor gene transfer and transgene expression after transfection. Plasmids were amplified and isolated using a Plasmid Maxi Kit (QIAGEN, Mississauga ON, Canada) or PureLink HiPure Plasmid Maxiprep Kit (Invitrogen, Burlington ON, Canada). Plasmid concentration was measured by UV absorption at 260 nm and the purity was determined using agarose gel electrophoresis.

8.6.3 Complex Preparation

Alginate-chitosan nanoparticles were prepared as previously described[172]. Briefly, nanoparticles were prepared by mixing 0.005% (w/v) sodium alginate (Sigma, Oakville ON, Canada) and 1% (w/v) chitosan (Carbomer, San Diego CA, USA), each dissolved in MilliQ water and pH adjusted to 5.6-5.8 using 1M HCl, to give a final weight ratio of 1:1.5 alginate:chitosan and stirred for 1 h at room temperature. Labelled nanoparticles, prepared using fluorescein-labelled chitosan (Carbomer, San Diego CA, USA), were used for confocal microscopy and internalization studies. Non-labelled nanoparticles were used for transfection assays. Complexes were prepared by adding DNA to the nanoparticle suspension to give the desired N:P ratio and incubated at room temperature for 30 min prior to use. (N:P ratio is ratio of the available amino groups in the alginate-chitosan nanoparticles to the DNA phosphate groups.)

For all uptake studies, complexes of fluorescein-labelled nanoparticles and pEGFP-N1 were used. Based on the optimization of complex parameters for uptake, the treatment solutions contained complexes of labelled nanoparticles and DNA prepared at an N:P ratio of 3.7:1 for CHO and COS7 cells, and 5.6:1 for

293T cells (Table 8.2) due to higher cell seeding densities. Note that the amount of DNA (2 μg) remained constant for all assays.

Table 8.2: Preparation conditions of alginate-chitosan nanoparticle-DNA complexes for transfection.

Treatment	Amount of Vector (as provided or prepared)	Amount of pDNA
pDNA	---	2 μg
Lipofectamine	4 μL	2 μg
N:P 1:2	27 μL	2 μg
N:P 1:1	54 μL	2 μg
N:P 2:1	109 μL	2 μg
N:P 3.7:1	200 μL	2 μg
N:P 5:1	271 μL	2 μg
N:P 5.6:1	300 μL	2 μg

8.6.4 Confocal Microscopy

Cells were seeded 24 h prior to treatment in 12-well plates containing glass cover slips at $8x10^4$ (CHO), $1x10^5$ (293T), and $6x10^4$ (COS7) cells/well in medium containing 10% (v/v) FBS. For treatment, the medium was removed and cells were washed once with phosphate buffer solution (PBS, Sigma, Oakville ON, Canada) prior to the addition of 600 μL of the treatment solution, which consisted of LysoTracker Red™ (75 nM) (Molecular Probes, Eugene OR, USA) in serum-free medium with complexes containing 4 μg of pEGFP-N1. At specified intervals (30 min, 1 h, 2 h, and 4 h), the treatment medium was removed, cells were washed twice in cold PBS, and fixed with paraformaldehyde (4%, 20 min) (Sigma, Oakville ON, Canada). Cover slips were washed twice with PBS, then incubated with DAPI (300 nM 4',6-diamidino-2-phenylindole dihydrochloride in PBS) (Molecular Probes, Eugene OR, USA) for 3 min to stain nuclei. Following two additional washes with PBS, cover slips were mounted on slides using GelTol mounting medium (Thermo Electron Corporation, Waltham MA, USA). Slides were analyzed using a confocal microscope (LSM510 META, Carl Zeiss, Germany) with the following excitation and emission wavelengths: fluorescein excitation 488 nm, emission band pass 505-530 nm; DAPI excitation 405 nm, emission band pass 420-480 nm; LysoTracker Red excitation 543 nm,

emission band pass 560-615 nm. Settings were determined using appropriate controls and were maintained for all image capture and analysis. Images were obtained of 3 randomly selected areas of 2 separate slides for each treatment. All areas were analyzed using Z-sectioning.

8.6.5 Flow Cytometry Analysis

One day prior to treatment with nanoparticle complexes, CHO, 293T and COS7 cells were seeded in 24-well plates at $4x10^4$, $8x10^4$, and $3x10^4$ cells/well, respectively. The medium was removed and cells were washed once with PBS prior to addition of 300 μL of treatment solution, containing 2 μg of pEGFP-N1 within the fluorescein-labelled complexes. At specified intervals (0 min, 15 min, 30 min, 1 h, 2 h and 4 h), the medium was removed and the cells were washed with cold PBS. (Note that for the 0 min treatment, medium containing complexes was added to wells, the well was rocked once, and the medium was subsequently removed. Total exposure time was less than 1 minute.) Except where noted, cells were treated with trypan blue (0.04% in PBS) for 1 min to quench external fluorescence and washed again with PBS before being detached using cold EDTA (0.6 mM in PBS). In all cases, cells were removed to tubes, centrifuged and resuspended in PBS, and analyzed directly (FACSCalibur, BD Biosciences, Mississauga ON, Canada). Five to ten thousand events were measured for each sample; appropriate controls and gates were used for analysis.

The uptake study was repeated under various conditions designed to directly affect binding and to ascertain trafficking to lysosomes. Treatment in the presence of excess chitosan, equivalent to the amount in the nanoparticle complexes (0.05 μg/μL), was done to detect saturable or receptor-mediated processes. In one set of experiments, cells were detached using trypsin-EDTA (ethylenediaminetetraacetic acid) to remove nanoparticles associated with surface proteins; in this case trypan blue quenching was not performed. In a separate set of experiments, cells were incubated with monensin (25 μM in PBS) (Sigma, Oakville ON, Canada) following detachment for 30 min at 4°C to neutralize late endosomal and lysosomal pH and thereby reverse quenching of fluorescein

fluorescence, which is inhibited at acidic pH. To promote endosomal escape, cells were treated with complexes in the presence of chloroquine (100 μM) (Sigma, Oakville ON, Canada), with no pre-treatment.

The identification of specific endocytic processes involved in complex internalization was done through uptake assays in the presence of chemicals known to inhibit specific pathways. In all cases, optimization studies were performed to maximize the effects of the chemicals while minimizing their inherent toxicity. Cytoskeleton reorganization was prevented by incubating the cells with cytochalasin D (10 μg/mL) (Sigma, Oakville ON, Canada) for 30 min followed by application of nanoparticle complexes. Macropinocytosis was promoted through treatment with phorbol myristate acetate (PMA, 1 μM) (Sigma, Oakville ON, Canada) for 30 min prior to addition of the complexes. Clathrin-dependent endocytosis was disturbed by co-treatment with chlorpromazine (10 μg/mL) (Sigma, Oakville ON, Canada), following a 30 min pre-incubation at the same concentration. To perturb caveolin-mediated pathways, cells were pre-treated with genistein (200 μg/mL) (Sigma, Oakville ON, Canada) for 30 min. Membrane cholesterol was depleted through incubation in serum-free medium for 2 h prior to 30 min pre-treatment with filipin III (5 μg/mL) (Sigma, Oakville ON, Canada). In all cases, treatment of the cells with nanoparticle-DNA complexes was done in the presence of the respective drug at the same concentration as used for the pre-treatment. Following treatment under these various conditions, cells were harvested at specific intervals (15 min, 30 min, 1 h, 2 h, and 4 h), prepared and analyzed as described above.

8.6.6 *In vitro Transfection*

In 24-well plates, CHO, 293T and COS7 cells were seeded at $4x10^4$, $5x10^4$, and $3x10^4$ cells/well, respectively, the day prior to transfection. For transfection, the culture medium was replaced with 300 μL serum-free medium containing unlabeled nanoparticle-DNA complexes of varying charge ratios (Table 8.2), with each well receiving 2 μg DNA. As a positive control, cells were treated with 4 μL Lipofectamine™ (Invitrogen, Mississauga ON, Canada) complexed with 2 μg DNA. After 4 h, the medium was increased to 500 μL with

medium supplemented with 10% (v/v) FBS; the medium was replaced with fresh complete medium (containing FBS and penicillin/streptomycin) after 24 h.

For pEGFP-N1 transfected cells N:P ratios of 1:2, 1:1, 2:1 and 5:1 were used. Transfection was assessed 48 h post-transfection using flow cytometry. Cells were removed using cold EDTA (0.6 mM in PBS), transferred to tubes, washed with PBS, and analyzed directly (FACSCalibur). Ten thousand events were measured in each sample, using appropriate controls and gates for analysis.

Cells transfected with pCMV-Luc (N:P ratio 3.7:1 for CHO and COS7 cells; N:P ratio 5.6:1 for 293T cells) were also analyzed after 48 h. Cells were removed using cold EDTA (0.6mM in PBS), transferred to micro-centrifuge tubes, and resuspended in cell culture lysis reagent (Luciferase Assay Kit, Promega BioSciences, Madison WI, USA). Following centrifugation at 12,000 g for 1 min, 20 μL aliquots of the supernatant were removed, added to 100 μL luciferase assay reagent, and analyzed using a luminometer (MiniLumat LB 9506, Berthold Technologies, Germany) over 30 sec. Appropriate controls were used for analysis. Results are reported as relative light units per mg of protein, with protein content determined using a standard BCA assay (Bicinchoninic acid, Pierce Biotechnology, Rockford IL, USA).

8.6.7 Statistical Analysis

All experiments were repeated three times and analyzed in triplicate. Results reported are the means and standard deviations, unless otherwise noted. Statistical significance was determined using Student's two-sided t-test with $p < 0.05$ deemed significant.

8.7 Acknowledgements

The authors would like to thank Shawn Carrigan for expert assistance with manuscript preparation. We would also like to acknowledge the Natural Sciences and Engineering Research Council of Canada (NSERC), the Fonds québécois de la recherche sur la nature et les technologies (FQRNT), and the Canadian Institutes of Health Research (CIHR) for funding this research.

Chapter 9
Conclusions and Future Perspectives

9.1 Summary of Accomplishments as Related to Objectives

Objective 1: Develop the alginate-chitosan system at the nano-scale.

A method was developed to prepare novel alginate-chitosan nanoparticles. The procedure is reliable and reproducible, producing well-defined, uniform nanoparticles with a mean diameter of 157 nm, which is appropriate for intracellular delivery. Preparation of the nanoparticles occurs in water under mild conditions, which is beneficial for the inclusion of fragile biomolecules, and also eliminates toxic effects often observed in other systems due to the presence of by-products or remnants of harsh organic solvents. The hydrophilic nature of the system is also beneficial for the incorporation of hydrophilic drugs or biomolecules, and for future *in vivo* applications.

Objective 2: Characterise nanoparticles as efficient gene delivery vectors.

Alginate-chitosan nanoparticles interact with DNA rapidly and effectively, forming compact complexes. Characterisation of DNA loading provided evidence that it adsorbs to the surface of nanoparticles, forming suitable complexes for intracellular delivery. Complexation with nanoparticles does not alter the DNA, maintaining its integrity for transcription in the cell. Complexed DNA is also protected from enzymatic degradation by nucleases. Alginate-chitosan nanoparticle-DNA complexes are taken up by cells rapidly and efficiently, and are relatively non-toxic.

Objective 3: Investigate the role alginate plays in the formation of nanoparticle-DNA complexes.

Tests indicate that alginate reduces the strength of interaction between chitosan and DNA, but does not prevent it. Furthermore, while the strength of

interaction between chitosan and DNA is reduced, the amount of DNA the nanoparticles can complex is unchanged.

Objective 4: Assess alginate-chitosan nanoparticles as transfection vectors *in vitro*.

Transfection was assessed in three cell lines. Transfection efficiency was found to depend on the preparation of the nanoparticle-DNA complexes and on the cell line. Alginate-chitosan nanoparticles were found to transfect cells with greater efficiency than chitosan nanoparticles in two cell lines; transfection was ineffective in the third cell line. In one cell line, the efficiency was equivalent to a commercially available non-viral vector.

Objective 5: Characterise the internalisation mechanism and intracellular fate of complexes.

The reasons for cell line-dependent transfection were examined with regard to the internalisation and intracellular trafficking of the alginate-chitosan nanoparticle-DNA complexes. It was determined that effective transfection depends on trafficking of the nanoparticles to the endosomal/lysosomal pathway, which follows clathrin-mediated endocytosis. Complexes were found to avoid lysosomes in all three cell lines, but trafficking to late endosomes is required for their release into the cytoplasm and eventual transfer to the nucleus, where transcription occurs.

As a separate endeavour to meet this objective, a novel analysis method was attempted. Correlational NanoSIMS-TEM imaging was investigated as a feasible alternative to confocal microscopy and flow cytometry analysis. NanoSIMS analysis confirmed the presence of nanoparticles in the nucleus of cells, although it was not possible to correlate NanoSIMS analysis with TEM images as planned. Though a proof of principle has been established and suggests that this analysis method will be effective, this correlational analysis technique requires further development.

9.2 Conclusions

The development of safe and effective methods of gene delivery to cells has been aggressively pursued for nearly 30 years as the next generation of disease treatment. Despite considerable effort, a safe and efficient means to introduce genes into target cells remains elusive. Continued research in this field is required to allow the use of novel therapeutics for treatment and management of numerous medical conditions. The inspiration for this project was the development of a biopolymeric-based non-viral vector which maintains biocompatibility and non-toxicity while providing superior transfection.

The initial goal of this project was to develop a novel gene delivery system composed entirely of biopolymers. The decision to use the biopolymers alginate and chitosan was based on their demonstrated biocompatibility and non-toxicity, the favourable characteristics of the polyelectrolyte system at the micro scale, and the hypothesis that the inclusion of alginate would improve transfection by enabling DNA release intracellularly. A protocol to prepare alginate-chitosan nanoparticles was developed and optimised through parametric studies designed to minimise particle size. The initial work revealed that polymer molecular weight, solution pH, and most critically, the ratio of the two polymers affect particle formation. Optimised conditions resulted in the preparation of particles with a mean size of 314 nm. Further development, including the use of a low molecular weight chitosan (10 kDa), resulted in particles with a mean size of 157 nm. Since size is known to directly affect the internalisation and transfection capabilities of non-viral vectors, the ability to prepare smaller particles represents a considerable improvement. In addition to the biocompatibility and biodegradability of this system, a further advantage is that preparation occurs in water under mild conditions, making it suitable as a delivery system for fragile biomolecules.

The suitability of alginate-chitosan nanoparticles for gene delivery was confirmed through investigations of their interactions with DNA and with cells. Studies suggest that DNA is primarily adsorbed to prepared nanoparticles, which exhibit a positive surface charge. The system was shown to maintain the integrity

of DNA and to protect it from enzymatic degradation. The specific role of alginate in complexing DNA was also investigated. Using two different analysis methods, it was established that the presence of alginate does not affect the amount of complexed DNA, but effectively reduces the strength of interaction with DNA compared to chitosan alone. This significant finding supports the hypothesis that the poor transfection observed with chitosan nanoparticles results from the elevated strength of interaction between chitosan and DNA; therefore, a reduction in this interaction should improve transfection. This was validated by transfection results that indicated a 4-fold greater improvement in transfection by alginate-chitosan nanoparticle complexes as compared to chitosan nanoparticle complexes.

The transfection efficiency of the system was found to depend on the charge ratio between nanoparticles and DNA (N:P ratio) during complex preparation, and on the cell line. Studies of the interaction between alginate-chitosan nanoparticle complexes and cells revealed that complexes are relatively non-toxic. They readily associate with cells and are rapidly and efficiently internalised, regardless of cell line. However, an observed correlation between N:P ratio of the complexes and cellular internalisation revealed that complexes prepared at N:P ratios less than 2.5:1 demonstrated a 50% reduction in internalisation, which explains the observed transfection dependence on N:P ratio. Under optimal conditions, transfection efficiency continued to vary depending on the cell line despite demonstrated efficient internalisation in all cell lines. It was concluded that transfection efficiency must be determined by the fate of the complexes following cell entry.

Investigation of the internalisation and intracellular trafficking of alginate-chitosan nanoparticle complexes revealed that these processes are strongly interdependent and that they directly affect transfection. Studies revealed that trafficking of complexes to the endosomal/lysosomal pathway is critical for transfection, and that acidification in late endosomes is likely required for escape of the complexes to the cytosol. Internalisation through clathrin-dependent endocytosis allowed particles to reach the endosomal/lysosomal pathway while

caveolin-mediated endocytosis did not, resulting in failed transfection. The observed cell-line dependent transfection efficiency was directly related to the endocytosis processes used to internalise the complexes. Although the reasons for varied internalisation mechanisms between cell lines are not known, this study was the first to provide a direct correlation between cell physiology and transfection efficiency.

A novel technique involving transmission electron microscopy imaging and nano-scale secondary ion mass spectroscopy analysis was also developed and investigated for use in tracking the intracellular fate of non-viral vectors. Preliminary development of the technique was completed and a proof of principle has established that this analysis method will be effective following further development. Furthermore, while the technique did not allow the tracking of alginate-chitosan nanoparticle complexes over time, as was hoped, it did provide evidence for the nuclear localisation of complexes.

This thesis presents the development and evaluation of novel biopolymeric nanoparticles for gene delivery applications. The ability of this system to transfect cells as efficiently as a commercial liposome formulation at least in one cell line is particularly promising, since liposomes are known to be more toxic and less stable than polymeric systems. Alginate-chitosan nanoparticles are exceptional in their ability to offer equivalent transfection to liposomes with considerably reduced toxicity and increased stability. This system demonstrates considerable promise for further development and investigation for *in vitro* and *in vivo* gene delivery applications, and provides the potential for intracellular delivery of other therapeutic agents, owing to its demonstrated ability to penetrate cells. Moreover, given that alginate-chitosan nanoparticles display chitosan amino groups at the surface, the muco-adhesive properties of chitosan could be exploited for delivery across mucosal membranes, via the gastric, nasal, or pulmonary routes.

The studies investigating the intracellular fate of nanoparticles were particularly informative. These findings, which were critical to understanding and explaining the transfection efficiency of this system, can also be used to explain

observed transfection efficiencies with other systems. Furthermore, the results are invaluable for the future development of systems for improved transfection. In addition to these benefits, these studies also established a relationship between cell line, internalisation, and intracellular trafficking, identifying a clear role of physiology in cellular functioning. Given the demonstrated utility of this system, the alginate-chitosan nanoparticle system could be used as a tool in further studies investigating cellular mechanisms.

9.3 Future Perspectives

As previously stated, the ideal gene delivery system should be biocompatible, biodegradable, non-immunogenic and non-toxic, be targetable to specific cells or tissues, permit encapsulation of multiple biomolecules, and demonstrate transfection efficiency at therapeutically effective levels. In contrast, the basic requirements of vectors are the ability to carry and protect a gene while enabling its entry into cells. While alginate-chitosan nanoparticles have been shown to fulfill the basic requirements for gene delivery systems, they can not yet be labelled as "ideal". Although their relative non-toxicity was validated through experimentation, the maintenance of biocompatibility, biodegradability and non-immunogenicity of the system, as demonstrated at the micro-scale, remains to be confirmed. The nanoparticles as prepared do not target specific cell lines or tissues, although results suggest the involvement of mannose receptors in their binding and internalization, suggesting that passive targeting to cells expressing these receptors may exist. However, the abundance of functional groups in the particles makes them amenable to the incorporation of targeting ligands. The ability of the nanoparticles to incorporate multiple biomolecules has not been assessed, though their manufacturing conditions make them amenable for incorporation of various fragile molecules. Nanoparticle systems involving alginate and chitosan have been studied for the delivery of various biomolecules or simulated drugs[138,155,179,180], suggesting that the inclusion of other biomolecules should be possible. With respect to the ability of the system to mediate

transfection at therapeutically effective levels, the system demonstrates improved transfection efficiency over chitosan nanoparticles, but *in vivo* studies will be required to determine if the system can mediate transfection sufficiently to have an effect. The alginate-chitosan nanoparticles developed do not represent an ideal gene delivery system; however, they exhibit promise for further development into effective non-viral vectors.

Despite the benefits of a non-toxic, biocompatible, biopolymeric system with improved transfection efficiency, as demonstrated by alginate-chitosan nanoparticles, several issues must be addressed prior to their application for *in vivo* gene therapy. Though the system demonstrated very respectable transfection compared to non-viral vectors, the level achieved remained significantly below that normally attained using viral vectors. Continued development of the system to encourage clathrin-mediated endocytosis could further improve transfection and benefit application, since slight increases in transfection can provide a therapeutic effect in the treatment of some diseases, as mentioned in Chapter 3. Nevertheless, their *in vivo* application will also require the evaluation of toxicity, immunogenicity, circulation life-times, and fate in the body. Although the hydrophilic nature of the alginate-chitosan system is beneficial with respect to circulation life-times, opsonisation and clearance through the reticulo-endothelial system is still a possibility that will have to be addressed, if observed. Moreover, evaluation of transfection efficiency and the sustainability of transfection *in vitro* and *in vivo* will be required.

The proposed strategies for further development of this system are suggested below.

9.3.1 Targeting

Investigation of the transfection ability of alginate-chitosan nanoparticles in multiple cell lines demonstrated a strong cell line-dependence. Although this may be useful as a "passive" approach to targeting particular cell lines, more specific targeting may be required for some applications.

In an attempt to improve transfection efficiencies by non-viral vectors, several researchers have incorporated cell-specific targeting ligands on their surfaces. The use of ligands in this capacity allows the vector to be taken up into the cell via normal ligand/receptor internalisation pathways (Figure 9.1b), while limiting their uptake by cells not expressing the appropriate receptor (Figure 9.1c). In general, this increases the specificity and uptake of the particles. This type of targeting has been shown to increase *in vitro* transfection efficiency up to 1000-fold and to result in successful organ-specific transfection *in vivo*[71,181]. An additional benefit of targeted particles is that receptor-mediated endocytosis generally occurs via the clathrin-dependent route, which traffics particles to the endosomal/lysosomal pathway. As discussed in Chapter 8, this is critical for efficient transfection by alginate-chitosan nanoparticle complexes. Table 9.1 lists some of the ligands that have been used and the cells for which they are specific[182]. The choice of ligand will be largely determined by the intended application of the vector. The incorporation of folate may be a suitable primary target, owing to its smaller size, compared to many other ligands.

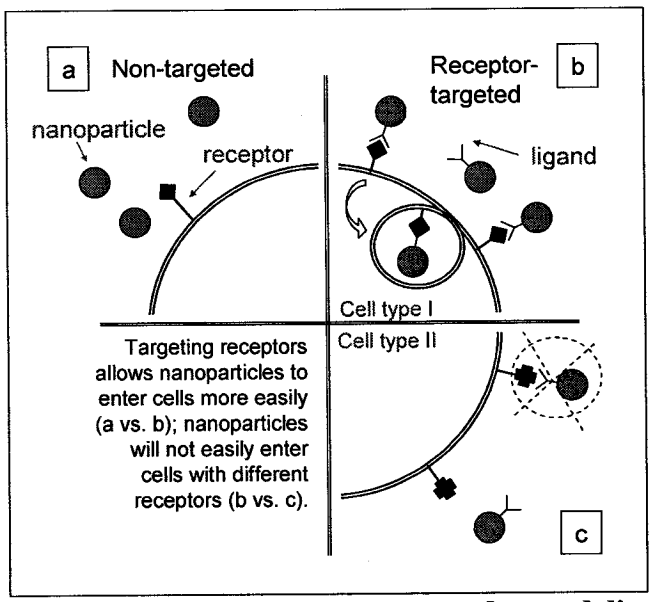

Figure 9.1: Schematic explaining receptor-targeted gene delivery.

Table 9.1: Ligands for Cell-Specific Receptors

Ligand	Target Cell/Organ
Asialoglycoprotein; galactose[183]	Hepatocyte/liver
Transferrin[184]	Liver, lung, and many others (not ideal for selective targeting)
Folate[182]	Cancer cells; KB, HeLa
Adenovirus fibre[182]	Lung, liver, many others
Epidermal growth factor (EGF) [182]	Lung, brain, and pancreatic cancer cells, other types of cancer cells
Human papilloma virus capsid[182]	Epithelial cells/cervix
Fibroblast growth factor[182]	Brain
Various antibodies[184-186]	Various
Synthetic peptides[187-189]	Various

The challenge of incorporating targeting ligands will be to control the binding of ligands to the biopolymer so that subsequent formation of the nanoparticles is unaffected while ensuring ligands remain active and accessible. The carboxylic groups of alginate and the amino groups of chitosan can be used as reactive points for bonding to targeting ligands. Depending on the chosen ligand, either polymer may be used for functionalisation. Most ligands considered will contain at least one amino group ($-NH_2$) or one carboxylic group (-COOH), which will allow straightforward bonding between the polymers and the ligand through standard amine coupling, which leads to an amide linkage between a carboxylic group and an amine group. The reaction proceeds via functionalisation of the amine group with a reagent such as *N*-hydroxysuccinimide (Figure 9.2).

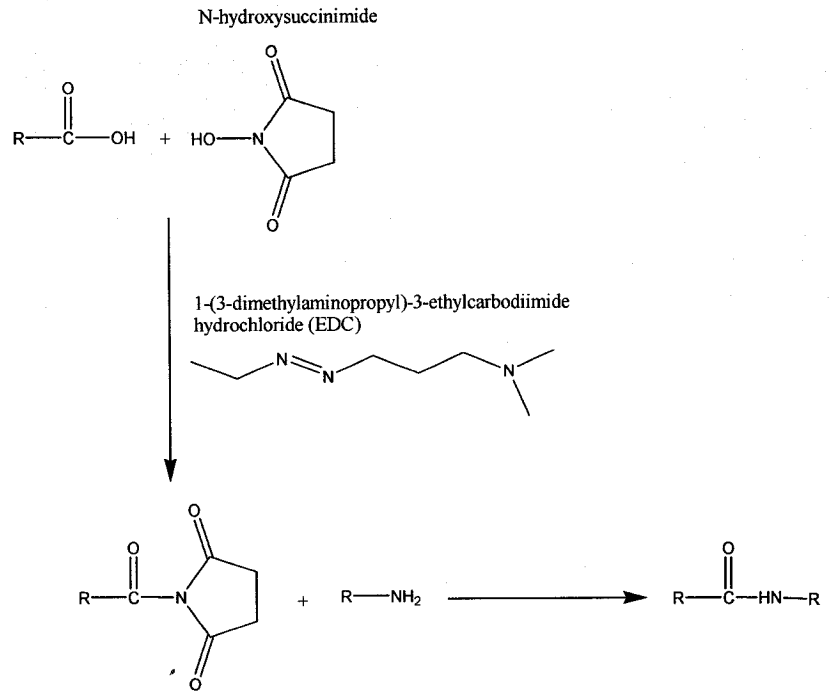

Figure 9.2: General reaction of amine coupling and amide bond formation

9.3.2 Internalisation and Intracellular Tracking of Non-Viral Vectors

The work described in Chapter 8 clearly establishes differing internalisation mechanisms and intracellular trafficking of complexes between cell lines. Repeating this work in related cell lines would be interesting to establish a relationship between cell physiology and internalisation mechanisms (for example, to determine if all kidney epithelial cells, regardless of species, internalise non-viral vectors through the same pathways). (Note: the two kidney cell lines used in this study include one epithelial cell line (293T) and one fibroblast cell line (COS7).) Comparison of the fate of alginate-chitosan nanoparticles to a different vector would also provide valuable information. Furthermore, the use of molecular markers could be used to confirm the endocytic mechanisms used for the internalisation of the complexes. Live-cell imaging would also prove interesting.

9.3.3 Drug Delivery

Numerous drugs, including the new classes of therapeutics encompassing peptides, proteins, and DNA, must penetrate cells to have an effect, yet are often excluded. Owing to the proven ability of alginate-chitosan nanoparticles to penetrate cells, it may be of interest to examine their potential as carriers for other drugs. This would require characterisation of the drug loading and release properties of the system with respect to the drug of interest. Results of these studies may identify a further advantage of this system in the ability to offer sustained release profiles.

9.3.4 Correlational NanoSIMS-TEM Analysis

The work described in Chapter 7 constitutes the early developmental stages and offers proof of principle for a novel correlational TEM imaging – NanoSIMS analysis technique. This technique warrants further development and investigation, as it has numerous potential applications.

9.3.5 In vivo Work

Since the ultimate gene delivery application is gene therapy, evaluation of the transfection efficiency of the alginate-chitosan nanoparticle system *in vivo* is of interest. Transfection efficiency *in vitro* and *in vivo* do not often correlate[15,190], which emphasises the need to assess it independently, regardless of the success of the system *in vitro*. *In vivo* studies are also valuable to assess the toxicity and immunogenicity of the system, as well as its circulatory lifetime. Assuming toxicity and immunogenicity are not issues, poor circulation lifetimes can be enhanced through attachment of PEG groups at the surface, masking the charge and reducing opsonisation and clearance by the RES.

Chapter 10
Cumulative Reference Listing

1. BioDelivery Sciences International . Gene Therapy. *http://www.biodeliverysciences.com/Applications/Gene_Therapy/gene_therapy.html* 02/28/2003.

2. American Society of Gene Therapy, *http://www.asgt.org/history.shtml* 02/28/2003.

3. Rubanyi, G. M. The future of human gene therapy. *Mol. Aspects Med.* **2001,** *22* (3), 113-142.

4. U.S.National Institutes of Health, *www.clinicaltrials.gov* 02/28/2003.

5. Journal of Gene Medicine, *http://www.wiley.co.uk/genetherapy/clinical* 02/28/2003.

6. Richardson, T. P.; Murphy, W. L.; Mooney, D. J. Polymeric delivery of proteins and plasmid DNA for tissue engineering and gene therapy. *Critical Reviews in Eukaryotic Gene Expression* **2001,** *11* (1-3), 47-58.

7. Godbey, W. T.; Mikos, A. G. Recent progress in gene delivery using non-viral transfer complexes. *J. Control Release* **2001,** *72* (1-3), 115-125.

8. Rungsardthong, U.; Deshpande, M.; Bailey, L.; Vamvakaki, M.; Armes, S. P.; Garnett, M. C.; Stolnik, S. Copolymers of amine methacrylate with poly(ethylene glycol) as vectors for gene therapy. *J. Control Release* **2001,** *73* (2-3), 359-380.

9. Lambert, G.; Fattal, E.; Couvreur, P. Nanoparticulate systems for the delivery of antisense oligonucleotides. *Adv. Drug Deliv. Rev.* **2001,** *47* (1), 99-112.

10. Hirosue, S.; Muller, B. G.; Mulligan, R. C.; Langer, R. Plasmid DNA encapsulation and release from solvent diffusion nanospheres. *J. Control Release* **2001,** *70* (1-2), 231-242.

11. Wightman, L.; Kircheis, R.; Rossler, V.; Carotta, S.; Ruzicka, R.; Kursa, M.; Wagner, E. Different behavior of branched and linear polyethylenimine for gene delivery in vitro and in vivo. *J. Gene Med.* **2001,** *3* (4), 362-372.

12. Alexakis, T.; Boadi, D. K.; Quong, D.; Groboillot, A.; O'Neill, I.; Poncelet, D.; Neufeld, R. J. Microencapsulation of DNA within alginate microspheres and crosslinked chitosan membranes for in vivo application. *Appl. Biochem. Biotechnol.* **1995,** *50* (1), 93-106.

13. Reimer, D. L.; Bally, M. B.; Singh, S. M. Human gene therapy: principles and modern advances. [3], 59-108. 1997.

14. Habib, N. A.; Ding, S. F.; el-Masry, R.; Mitry, R. R.; Honda, K.; Michail, N. E.; Dalla, S. G.; Izzi, G.; Greco, L.; Bassyouni, M.; el-Toukhy, M.; bdel-Gaffar, Y. Preliminary report: the short-term effects of direct p53 DNA injection in primary hepatocellular carcinomas. *Cancer Detect. Prev.* **1996,** *20* (2), 103-107.

15. Brown, M. D.; Schatzlein, A. G.; Uchegbu, I. F. Gene delivery with synthetic (non viral) carriers. *Int. J. Pharm.* **2001,** *229* (1-2), 1-21.

16. Palmer, D. H.; Young, L. S.; Mautner, V. Cancer gene-therapy: clinical trials. *Trends Biotechnol.* **2006,** *24* (2), 76-82.

17. Stopeck, A. T.; Hersh, E. M.; Brailey, J. L.; Clark, P. R.; Norman, J.; Parker, S. E. Transfection of primary tumor cells and tumor cell lines with plasmid DNA/lipid complexes. *Cancer Gene Ther.* **1998,** *5* (2), 119-126.

18. Roy, K.; Mao, H. Q.; Huang, S. K.; Leong, K. W. Oral gene delivery with chitosan--DNA nanoparticles generates immunologic protection in a murine model of peanut allergy. *Nat. Med.* **1999,** *5* (4), 387-391.

19. Yechoor, V.; Chan, L. Gene therapy progress and prospects: gene therapy for diabetes mellitus. *Gene Ther.* **2005,** *12* (2), 101-107.

20. Bagley, J.; Iacomini, J. Gene therapy progress and prospects: gene therapy in organ transplantation. *Gene Ther.* **2003,** *10* (8), 605-611.

21. Griesenbach, U.; Ferrari, S.; Geddes, D. M.; Alton, E. W. Gene therapy progress and prospects: cystic fibrosis. *Gene Ther.* **2002,** *9* (20), 1344-1350.

22. Gaspar, H. B.; Howe, S.; Thrasher, A. J. Gene therapy progress and prospects: gene therapy for severe combined immunodeficiency. *Gene Ther.* **2003,** *10* (24), 1999-2004.

23. Walsh, C. E. Gene therapy progress and prospects: gene therapy for the hemophilias. *Gene Ther.* **2003,** *10* (12), 999-1003.

24. Cheng, S. H.; Smith, A. E. Gene therapy progress and prospects: gene therapy of lysosomal storage disorders. *Gene Ther.* **2003,** *10* (16), 1275-1281.

25. Burton, E. A.; Glorioso, J. C.; Fink, D. J. Gene therapy progress and prospects: Parkinson's disease. *Gene Ther.* **2003,** *10* (20), 1721-1727.

26. Khan, T. A.; Sellke, F. W.; Laham, R. J. Gene therapy progress and prospects: therapeutic angiogenesis for limb and myocardial ischemia. *Gene Ther.* **2003,** *10* (4), 285-291.

27. Wolkowicz, R.; Nolan, G. P. Gene therapy progress and prospects: novel gene therapy approaches for AIDS. *Gene Ther.* **2005,** *12* (6), 467-476.

28. U.S.National Institutes of Health,*www.clinicaltrials.gov* 02/28/2003.

29. Wolfert, M. A.; Seymour, L. W. Atomic force microscopic analysis of the influence of the molecular weight of poly(L)lysine on the size of polyelectrolyte complexes formed with DNA. *Gene Ther.* **1996,** *3* (3), 269-273.

30. Perez, C.; Sanchez, A.; Putnam, D.; Ting, D.; Langer, R.; Alonso, M. J. Poly(lactic acid)-poly(ethylene glycol) nanoparticles as new carriers for the delivery of plasmid DNA. *J. Controlled Release* **2001,** *75* (1-2), 211-224.

31. Dash, P. R.; Read, M. L.; Barrett, L. B.; Wolfert, M. A.; Seymour, L. W. Factors affecting blood clearance and in vivo distribution of polyelectrolyte complexes for gene delivery. *Gene Ther.* **1999,** *6* (4), 643-650.

32. Panyam, J.; Zhou, W. Z.; Prabha, S.; Sahoo, S. K.; Labhasetwar, V. Rapid endo-lysosomal escape of poly(DL-lactide-co-glycolide) nanoparticles: implications for drug and gene delivery. *FASEB J.* **2002,** *16* (10), 1217-1226.

33. Truong, L.; August, J. T.; Leong, K. W. Controlled gene delivery by DNA-gelatin nanospheres. *Hum. Gene Ther.* **1998,** *9* (12), 1709-1717.

34. Tiera, M. J.; Winnik, F. O.; Fernandes, J. C. Synthetic and natural polycations for gene therapy: state of the art and new perspectives. *Curr. Gene Ther.* **2006,** *6* (1), 59-71.

35. Orson, F. M.; Song, L.; Gautam, A.; Densmore, C. L.; Bhogal, B. S.; Kinsey, B. M. Gene delivery to the lung using protein/polyethylenimine/plasmid complexes. *Gene Ther.* **2002,** *9* (7), 463-471.

36. Abdallah, B.; Sachs, L.; Demeneix, B. A. Non-viral gene transfer: applications in developmental biology and gene therapy. *Biol. Cell* **1995,** *85* (1), 1-7.

37. Larrick, J. W.; Burck, K. L. *Gene Therapy: Applications of Molecular Biology;* Elsevier: New York, 1991.

38. Hacein-Bey-Abina, S.; Von, K. C.; Schmidt, M.; Le, D. F.; Wulffraat, N.; McIntyre, E.; Radford, I.; Villeval, J. L.; Fraser, C. C.; Cavazzana-Calvo, M.; Fischer, A. A serious adverse event after successful gene therapy for X-linked severe combined immunodeficiency. *N. Engl. J. Med.* **2003,** *348* (3), 255-256.

39. Vahlsing, H. L.; Yankauckas, M. A.; Sawdey, M.; Gromkowski, S. H.; Manthorpe, M. Immunization with plasmid DNA using a pneumatic gun. *J. Immunol. Methods* **1994,** *175* (1), 11-22.

40. Williams, R. S.; Johnston, S. A.; Riedy, M.; DeVit, M. J.; McElligott, S. G.; Sanford, J. C. Introduction of Foreign Genes into Tissues of Living Mice by DNA-Coated Microprojectiles. *PNAS* **1991,** *88* (7), 2726-2730.

41. Ravi Kumar, M. N. Nano and microparticles as controlled drug delivery devices. *J. Pharm. Pharm. Sci.* **2000,** *3* (2), 234-258.

42. Ochiya, T.; Nagahara, S.; Sano, A.; Itoh, H.; Terada, M. Biomaterials for gene delivery: atelocollagen-mediated controlled release of molecular medicines. *Curr. Gene Ther.* **2001,** *1* (1), 31-52.

43. Leong, K. W.; Mao, H. Q.; Truong, L.; Roy, K.; Walsh, S. M.; August, J. T. DNA-polycation nanospheres as non-viral gene delivery vehicles. *J. Controlled Release* **1998,** *53* (1-3), 183-193.

44. Corsi, K.; Chellat, F.; Yahia, L.; Fernandes, J. C. Mesenchymal stem cells, MG63 and HEK 293 transfection using chitosan-DNA nanoparticles. Biomaterials 24, 1255-1264. 2003.

45. Fischer, D.; Li, Y.; Ahlemeyer, B.; Krieglstein, J.; Kissel, T. In vitro cytotoxicity testing of polycation: influence of polymer structure on cell viability and hemolysis. Biomaterials 24, 1121-1131. 2003.

46. Wilson, G. L.; Dean, B. S.; Wang, G.; Dean, D. A. Nuclear import of plasmid DNA in digitonin-permeabilized cells requires both cytoplasmic factors and specific DNA sequences. *J. Biol. Chem.* **1999,** *274* (31), 22025-22032.

47. Takka, S.; Acarturk, F. Calcium alginate microparticles for oral administration: I: Effect of sodium alginate type on drug release and drug entrapment efficiency. *J. Microencapsul.* **1999,** *16* (3), 275-290.

48. Rajaonarivony, M.; Vauthier, C.; Couarraze, G.; Puisieux, F.; Couvreur, P. Development of a new drug carrier made from alginate. *J. Pharm. Sci.* **1993,** *82* (9), 912-917.

49. Soppimath, K. S.; Aminabhavi, T. M.; Kulkarni, A. R.; Rudzinski, W. E. Biodegradable polymeric nanoparticles as drug delivery devices. *J. Control Release* **2001,** *70* (1-2), 1-20.

50. Quintanar-Guerrero, D.; Allemann, E.; Fessi, H.; Doelker, E. Preparation techniques and mechanisms of formation of biodegradable nanoparticles from preformed polymers. *Drug Dev. Ind. Pharm.* **1998,** *24* (12), 1113-1128.

51. Yi, Y. M.; Yang, T. Y.; Pan, W. M. Preparation and distribution of 5-fluorouracil (125)I sodium alginate-bovine serum albumin nanoparticles. *World J. Gastroenterol.* **1999,** *5* (1), 57-60.

52. Prabha, S.; Zhou, W. Z.; Panyam, J.; Labhasetwar, V. Size-dependency of nanoparticle-mediated gene transfection: studies with fractionated nanoparticles. *Int. J. Pharm.* **2002,** *244* (1-2), 105-115.

53. de Lima, M. C.; Simoes, S.; Pires, P.; Gaspar, R.; Slepushkin, V.; Duzgunes, N. Gene delivery mediated by cationic liposomes: from biophysical aspects to enhancement of transfection. *Mol. Membr. Biol.* **1999,** *16* (1), 103-109.

54. Zauner, W.; Brunner, S.; Buschle, M.; Ogris, M.; Wagner, E. Differential behaviour of lipid based and polycation based gene transfer systems in transfecting primary human fibroblasts: a potential role of polylysine in nuclear transport. *Biochim. Biophys. Acta* **1999,** *1428* (1), 57-67.

55. Cohen, H.; Levy, R. J.; Gao, J.; Fishbein, I.; Kousaev, V.; Sosnowski, S.; Slomkowski, S.; Golomb, G. Sustained delivery and expression of DNA encapsulated in polymeric nanoparticles. *Gene Ther.* **2000,** *7* (22), 1896-1905.

56. Couvreur, P.; Dubernet, C.; Puisieux, F. Controlled Drug Delivery with Nanoparticles: Current Possibilities and Future Trends. *Eur. J. Pharm. Biopharm.* **1995,** *41* (1), 2-13.

57. Chellat, F.; Tabrizian, M.; Dumitriu, S.; Chornet, E.; Rivard, C. H.; Yahia, L. Study of biodegradation behavior of chitosan-xanthan microspheres in simulated physiological media. *J. Biomed. Mater. Res.* **2000,** *53* (5), 592-599.

58. Coppi, G.; Iannuccelli, V.; Leo, E.; Bernabei, M. T.; Cameroni, R. Protein immobilization in crosslinked alginate microparticles. *J. Microencapsulation* **2002,** *19* (1), 37-44.

59. Du, J.; Zhang, S.; Sun, R.; Zhang, L. F.; Xiong, C. D.; Peng, Y. X. Novel polyelectrolyte carboxymethyl konjac glucomannan-chitosan nanoparticles for drug delivery. II. Release of albumin in vitro. *J. Biomed. Mater. Res. B Appl. Biomater.* **2005,** *72* (2), 299-304.

60. Arnedo, A.; Espuelas, S.; Irache, J. M. Albumin nanoparticles as carriers for a phosphodiester oligonucleotide. *Int. J. Pharm.* **2002,** *244* (1-2), 59-72.

61. Bieber, T.; Meissner, W.; Kostin, S.; Niemann, A.; Elsasser, H. P. Intracellular route and transcriptional competence of polyethylenimine-DNA complexes. *J. Control Release* **2002,** *82* (2-3), 441-454.

62. Laurent, N.; Wattiaux-De, C. S.; Mihaylova, E.; Leontieva, E.; Warnier-Pirotte, M. T.; Wattiaux, R.; Jadot, M. Uptake by rat liver and intracellular fate of plasmid DNA complexed with poly-L-lysine or poly-D-lysine. *FEBS Lett.* **1999,** *443* (1), 61-65.

63. Du, J.; Sun, R.; Zhang, S.; Zhang, L. F.; Xiong, C. D.; Peng, Y. X. Novel polyelectrolyte carboxymethyl konjac glucomannan-chitosan nanoparticles for drug delivery. I. Physicochemical characterization of the carboxymethyl konjac glucomannan-chitosan nanoparticles. *Biopolymers* **2005,** *78* (1), 1-8.

64. Leroueil-Le Verger, M.; Fluckiger, L.; Kim, Y. I.; Hoffman, M.; Maincent, P. Preparation and characterization of nanoparticles containing an antihypertensive agent. *Eur. J. Pharm. Biopharm.* **1998,** *46* (2), 137-143.

65. Hu, Y.; Jiang, X.; Ding, Y.; Ge, H.; Yuan, Y.; Yang, C. Synthesis and characterization of chitosan-poly(acrylic acid) nanoparticles. *Biomaterials* **2002,** *23* (15), 3193-3201.

66. Panyam, J.; Labhasetwar, V. Biodegradable nanoparticles for drug and gene delivery to cells and tissue. *Adv. Drug Deliv. Rev.* **2003,** *55* (3), 329-347.

67. Leroux, J.-C.; Allemann, E.; De Jaeghere, F.; Doelker, E.; Gurny, R. Biodegradable nanoparticles -- From sustained release formulations to improved site specific drug delivery. *J. Control Release* **1996,** *39*, 339-350.

68. Kim, T. H.; Kim, S. I.; Akaike, T.; Cho, C. S. Synergistic effect of poly(ethylenimine) on the transfection efficiency of galactosylated chitosan/DNA complexes. *J. Control Release* **2005,** *105* (3), 354-366.

69. Ahn, C. H.; Chae, S. Y.; Bae, Y. H.; Kim, S. W. Biodegradable poly(ethylenimine) for plasmid DNA delivery. *J. Control Release* **2002,** *80* (1-3), 273-282.

70. Koping-Hoggard, M.; Varum, K. M.; Issa, M.; Danielsen, S.; Christensen, B. E.; Stokke, B. T.; Artursson, P. Improved chitosan-mediated gene delivery based on easily dissociated chitosan polyplexes of highly defined chitosan oligomers. *Gene Ther.* **2004,** *11* (19), 1441-1452.

71. Lee, H.; Kim, T. H.; Park, T. G. A receptor-mediated gene delivery system using streptavidin and biotin-derivatized, pegylated epidermal growth factor. *J. Control Release* **2002,** *83* (1), 109-119.

72. Han, S.; Mahato, R. I.; Sung, Y. K.; Kim, S. W. Development of biomaterials for gene therapy. *Mol. Ther.* **2000,** *2* (4), 302-317.

73. Read, M. L.; Etrych, T.; Ulbrich, K.; Seymour, L. W. Characterisation of the binding interaction between poly(L-lysine) and DNA using the fluorescamine assay in the preparation of non-viral gene delivery vectors. *FEBS Lett.* **1999,** *461* (1-2), 96-100.

74. Peppas, N. A.; Khare, A. R. Preparation, structure and diffusional behavior of hydrogels in controlled release. *Adv. Drug Deliv. Rev.* **1993,** *11*, 1-35.

75. Chellat, F.; Tabrizian, M.; Dumitriu, S.; Chornet, E.; Magny, P.; Rivard, C. H.; Yahia, L. In vitro and in vivo biocompatibility of chitosan-xanthan polyionic complex. *J. Biomed. Mater. Res.* **2000,** *51* (1), 107-116.

76. Skaugrud, O. Drug Delivery Systems with Alginate and Chitosan. Special Publications of the Royal Society of Chemistry 161, 96-107. 1995.

77. Barichello, J. M.; Morishita, M.; Takayama, K.; Nagai, T. Encapsulation of hydrophilic and lipophilic drugs in PLGA nanoparticles by the nanoprecipitation method. *Drug Dev. Ind. Pharm.* **1999,** *25* (4), 471-476.

78. Madan, T.; Munshi, N.; De, T. K.; Maitra, A.; Sarma, P. U.; Aggarwal, S. S. Biodegradable nanoparticles as a sustained release system for the antigens/allergens of *Aspergillus fumigatus*: preparation and characterisation. *Int. J. Pharm.* **1997,** *159*, 135-147.

79. Davda, J.; Labhasetwar, V. Characterization of nanoparticle uptake by endothelial cells. *Int. J. Pharm.* **2002,** *233* (1-2), 51-59.

80. Nakache, E.; Poulain, N.; Candau, F.; Orecchioni, A.-M.; Irache, J. M. Biopolymer and Polymer Nanoparticles and their Biomedical Applications. [Volume 5: Organics, Polymers, and Biological Materials], Chapter 11: 577-635. 2000.

81. Tokumitsu, H.; Ichikawa, H.; Fukumori, Y. Chitosan-gadopentetic acid complex nanoparticles for gadolinium neutron-capture therapy of cancer: preparation by novel emulsion-droplet coalescence technique and characterization. *Pharm. Res.* **1999,** *16* (12), 1830-1835.

82. Kean, T.; Roth, S.; Thanou, M. Trimethylated chitosans as non-viral gene delivery vectors: cytotoxicity and transfection efficiency. *J. Control Release* **2005,** *103* (3), 643-653.

83. Liu, W. G.; Zhang, X.; Sun, S. J.; Sun, G. J.; Yao, K. D.; Liang, D. C.; Guo, G.; Zhang, J. Y. N-alkylated chitosan as a potential nonviral vector for gene transfection. *Bioconjug. Chem.* **2003,** *14* (4), 782-789.

84. Janes, K. A.; Fresneau, M. P.; Marazuela, A.; Fabra, A.; Alonso, M. J. Chitosan nanoparticles as delivery systems for doxorubicin. *J. Controlled Release* **2001,** *73* (2-3), 255-267.

85. Yin, Y.; Xu, M.; Chen, X.; Yao, K. Drug release behavior of chitosan/gelatin network polymer microsphere. *Chinese Science Bulletin* **1996,** *41* (15), 1266-1270.

86. Lee, K. Y.; Kwon, I. C.; Kim, Y. H.; Jo, W. H.; Jeong, S. Y. Preparation of chitosan self-aggregates as a gene delivery system. *J. Controlled Release* **1998,** *51* (2-3), 213-220.

87. Sato, T.; Ishii, T.; Okahata, Y. In vitro gene delivery mediated by chitosan. effect of pH, serum, and molecular mass of chitosan on the transfection efficiency. *Biomaterials* **2001,** *22* (15), 2075-2080.

88. Borchard, G. Chitosans for gene delivery. *Adv. Drug Deliv. Rev.* **2001,** *52* (2), 145-150.

89. Mao, H. Q.; Roy, K.; Troung, L.; Janes, K. A.; Lin, K. Y.; Wang, Y.; August, J. T.; Leong, K. W. Chitosan-DNA nanoparticles as gene carriers: synthesis, characterization and transfection efficiency. *J. Control Release* **2001,** *70* (3), 399-421.

90. Li, X. W.; Lee, D. K.; Chan, A. S.; Alpar, H. O. Sustained expression in mammalian cells with DNA complexed with chitosan nanoparticles. *Biochim. Biophys. Acta* **2003,** *1630* (1), 7-18.

91. Guang, L. W.; De, Y. K. Chitosan and its derivatives--a promising non-viral vector for gene transfection. *J. Control Release* **2002,** *83* (1), 1-11.

92. Agnihotri, S. A.; Mallikarjuna, N. N.; Aminabhavi, T. M. Recent advances on chitosan-based micro- and nanoparticles in drug delivery. *J. Control Release* **2004,** *100* (1), 5-28.

93. Mansouri, S.; Lavigne, P.; Corsi, K.; Benderdour, M.; Beaumont, E.; Fernandes, J. C. Chitosan-DNA nanoparticles as non-viral vectors in gene therapy: strategies to improve transfection efficacy. *Eur. J. Pharm. Biopharm.* **2004,** *57* (1), 1-8.

94. Cui, Z.; Mumper, R. J. Chitosan-based nanoparticles for topical genetic immunization. *J. Control Release* **2001,** *75* (3), 409-419.

95. Ma, Z.; Lim, L. Y. Uptake of chitosan and associated insulin in Caco-2 cell monolayers: a comparison between chitosan molecules and chitosan nanoparticles. *Pharm. Res.* **2003,** *20* (11), 1812-1819.

96. Gao, S.; Chen, J.; Xu, X.; Ding, Z.; Yang, Y. H.; Hua, Z.; Zhang, J. Galactosylated low molecular weight chitosan as DNA carrier for hepatocyte-targeting. *Int. J. Pharm.* **2003,** *255* (1-2), 57-68.

97. Kiang, T.; Wen, J.; Lim, H. W.; Leong, K. W. The effect of the degree of chitosan deacetylation on the efficiency of gene transfection. *Biomaterials* **2004,** *25* (22), 5293-5301.

98. MacLaughlin, F. C.; Mumper, R. J.; Wang, J.; Tagliaferri, J. M.; Gill, I.; Hinchcliffe, M.; Rolland, A. P. Chitosan and depolymerized chitosan oligomers as condensing carriers for in vivo plasmid delivery. *J. Control Release* **1998,** *56* (1-3), 259-272.

99. Erbacher, P.; Zou, S.; Bettinger, T.; Steffan, A. M.; Remy, J. S. Chitosan-based vector/DNA complexes for gene delivery: biophysical characteristics and transfection ability. *Pharm. Res.* **1998,** *15* (9), 1332-1339.

100. Wong, K.; Sun, G.; Zhang, X.; Dai, H.; Liu, Y.; He, C.; Leong, K. W. PEI-g-chitosan, a novel gene delivery system with transfection efficiency comparable to polyethylenimine in vitro and after liver administration in vivo. *Bioconjug. Chem.* **2006,** *17* (1), 152-158.

101. Jiang, X.; Dai, H.; Leong, K. W.; Goh, S. H.; Mao, H. Q.; Yang, Y. Y. Chitosan-g-PEG/DNA complexes deliver gene to the rat liver via intrabiliary and intraportal infusions. *J. Gene Med.* **2006.**

102. Simsek-Ege, F. A.; Bond, G. M.; Stringer, J. Polyelectrolye complex formation between alginate and chitosan as a function of pH. *Journal of Applied Polymer Science* **2003,** *88* (2), 346-351.

103. Danielsen, S.; Maurstad, G.; Stokke, B. T. DNA-polycation complexation and polyplex stability in the presence of competing polyanions. *Biopolymers* **2005,** *77* (2), 86-97.

104. Mi, F.-L.; Sung, H.-W.; Shyu, S.-S. Drug release from chitosan-alginate complex beads reinforced by a naturally occurring cross-linking agent. *Carbohydrate Polymers* **2002,** *48*, 61-72.

105. Fundueanu, G.; Nastruzzi, C.; Carpov, A.; Desbrieres, J.; Rinaudo, M. Physico-chemical characterization of Ca-alginate microparticles produced with different methods. *Biomaterials* **1999,** *20* (15), 1427-1435.

106. Yan, X. L.; Khor, E.; Lim, L. Y. Chitosan-alginate films prepared with chitosans of different molecular weights. *J. Biomed. Mater. Res.* **2001,** *58* (4), 358-365.

107. Quong, D.; Yeo, J. N.; Neufeld, R. J. Stability of chitosan and poly-L-lysine membranes coating DNA-alginate beads when exposed to hydrolytic enzymes. *J. Microencapsul.* **1999,** *16* (1), 73-82.

108. Sezer, A. D.; Akbuga, J. Release characteristics of chitosan treated alginate beads: II. Sustained release of a low molecular drug from chitosan treated alginate beads. *J. Microencapsul.* **1999,** *16* (6), 687-696.

109. Gonzalez-Rodriguez, M. L.; Holgado, M. A.; Sanchez-Lafuente, C.; Rabasco, A. M.; Fini, A. Alginate/chitosan particulate systems for sodium diclofenac release. *Int. J. Pharm.* **2002,** *232* (1-2), 225-234.

110. Gaserod, O.; Smidsrod, O.; Skjak-Braek, G. Microcapsules of alginate-chitosan--I. A quantitative study of the interaction between alginate and chitosan. *Biomaterials* **1998,** *19* (20), 1815-1825.

111. Gaserod, O.; Sannes, A.; Skjak-Braek, G. Microcapsules of alginate-chitosan. II. A study of capsule stability and permeability. *Biomaterials* **1999,** *20* (8), 773-783.

112. Huguet, M. L.; Dellacherie, E. Calcium Alginate Beads Coated with Chitosan: Effect of the Structure of Encapsulated Materials on Their Release. Process Biochemistry 31[8], 745-751. 1996.

113. Shu, X. Z.; Zhu, K. J. The release behavior of brilliant blue from calcium-alginate gel beads coated by chitosan: the preparation method effect. *Eur. J. Pharm. Biopharm.* **2002,** *53* (2), 193-201.

114. Berkland, C.; Kim, K.; Pack, D. W. Fabrication of PLG microspheres with precisely controlled and monodisperse size distributions. *J. Controlled Release* **2001,** *73* (1), 59-74.

115. Dyer, A. M.; Hinchcliffe, M.; Watts, P.; Castile, J.; Jabbal-Gill, I.; Nankervis, R.; Smith, A.; Illum, L. Nasal delivery of insulin using novel chitosan based formulations: a comparative study in two animal models between simple chitosan formulations and chitosan nanoparticles. *Pharm. Res.* **2002,** *19* (7), 998-1008.

116. Murakami, H.; Kobayashi, M.; Takeuchi, H.; Kawashima, Y. Preparation of poly(DL-lactide-co-glycolide) nanoparticles by modified spontaneous emulsification solvent diffusion method. *Int. J. Pharm.* **1999,** *187* (2), 143-152.

117. Katz, J. Developments in Medical Polymers for Biomaterials Applications. *Medical Device & Diagnostic Industry* **2001**.

118. Akinc, A.; Anderson, D. G.; Lynn, D. M.; Langer, R. Synthesis of poly(beta-amino ester)s optimized for highly effective gene delivery. *Bioconjug. Chem.* **2003,** *14* (5), 979-988.

119. Lechardeur, D.; Lukacs, G. L. Intracellular barriers to non-viral gene transfer. *Curr. Gene Ther.* **2002,** *2* (2), 183-194.

120. Douglas, K. L.; Tabrizian, M.; Piccirillo, C. A. Cell-Line Dependent Internalization Pathways and Intracellular Trafficking Determine Transfection Efficiency of Nanoparticle Vectors. *Submitted manuscript* **2006**.

121. de, S. D.; Petriz, J.; Avinyo, A.; Larriba, S.; Nunes, V.; Casals, T.; Estivill, X.; Aran, J. M. Non-viral vector-mediated uptake, distribution, and stability of chimeraplasts in human airway epithelial cells. *J. Gene Med.* **2002,** *4* (3), 308-322.

122. Gao, S.; Chen, J.; Dong, L.; Ding, Z.; Yang, Y. H.; Zhang, J. Targeting delivery of oligonucleotide and plasmid DNA to hepatocyte via galactosylated chitosan vector. *Eur. J. Pharm. Biopharm.* **2005,** *60* (3), 327-334.

123. Feng, M.; Lee, D.; Li, P. Intracellular uptake and release of poly(ethyleneimine)-co-poly(methyl methacrylate) nanoparticle/pDNA complexes for gene delivery. *Int. J. Pharm.* **2006,** *311* (1-2), 209-214.

124. Huang, M.; Fong, C. W.; Khor, E.; Lim, L. Y. Transfection efficiency of chitosan vectors: effect of polymer molecular weight and degree of deacetylation. *J. Control Release* **2005,** *106* (3), 391-406.

125. Kaul, G.; Amiji, M. Cellular interactions and in vitro DNA transfection studies with poly(ethylene glycol)-modified gelatin nanoparticles. *J. Pharm. Sci.* **2005,** *94* (1), 184-198.

126. Hashimoto, M.; Morimoto, M.; Saimoto, H.; Shigemasa, Y.; Sato, T. Lactosylated chitosan for DNA delivery into hepatocytes: the effect of lactosylation on the physicochemical properties and intracellular trafficking of pDNA/chitosan complexes. *Bioconjug. Chem.* **2006,** *17* (2), 309-316.

127. Akbuga, J.; Ozbas-Turan, S.; Erdogan, N. Plasmid-DNA loaded chitosan microspheres for in vitro IL-2 expression. *Eur. J. Pharm. Biopharm.* **2004,** *58* (3), 501-507.

128. Dastan, T.; Turan, K. In vitro characterization and delivery of chitosan-DNA microparticles into mammalian cells. *J. Pharm. Pharm. Sci.* **2004,** *7* (2), 205-214.

129. Itaka, K.; Harada, A.; Yamasaki, Y.; Nakamura, K.; Kawaguchi, H.; Kataoka, K. In situ single cell observation by fluorescence resonance energy transfer reveals fast intra-cytoplasmic delivery and easy release of plasmid DNA complexed with linear polyethylenimine. *J. Gene Med.* **2004,** *6* (1), 76-84.

130. Goncalves, C.; Mennesson, E.; Fuchs, R.; Gorvel, J. P.; Midoux, P.; Pichon, C. Macropinocytosis of polyplexes and recycling of plasmid via the clathrin-dependent pathway impair the transfection efficiency of human hepatocarcinoma cells. *Mol. Ther.* **2004,** *10* (2), 373-385.

131. Rejman, J.; Oberle, V.; Zuhorn, I. S.; Hoekstra, D. Size-dependent internalization of particles via the pathways of clathrin- and caveolae-mediated endocytosis. *Biochem. J.* **2004,** *377* (Pt 1), 159-169.

132. Rejman, J.; Bragonzi, A.; Conese, M. Role of clathrin- and caveolae-mediated endocytosis in gene transfer mediated by lipo- and polyplexes. *Mol. Ther.* **2005,** *12* (3), 468-474.

133. Godbey, W. T.; Wu, K. K.; Mikos, A. G. Tracking the intracellular path of poly(ethylenimine)/DNA complexes for gene delivery. *Proc. Natl. Acad. Sci. U. S. A* **1999,** *96* (9), 5177-5181.

134. Li, Y.; Ogris, M.; Wagner, E.; Pelisek, J.; Ruffer, M. Nanoparticles bearing polyethyleneglycol-coupled transferrin as gene carriers: preparation and in vitro evaluation. *Int. J. Pharm.* **2003,** *259* (1-2), 93-101.

135. Banerjee, T.; Mitra, S.; Kumar, S. A.; Kumar, S. R.; Maitra, A. Preparation, characterization and biodistribution of ultrafine chitosan nanoparticles. *Int. J. Pharm.* **2002,** *243* (1-2), 93-105.

136. Woodle, M. C.; Matthay, K. K.; Newman, M. S.; Hidayat, J. E.; Collins, L. R.; Redemann, C.; Martin, F. J.; Papahadjopoulos, D. Versatility in lipid compositions showing prolonged circulation with sterically stabilized liposomes. *Biochim. Biophys. Acta* **1992,** *1105* (2), 193-200.

137. Kaul, G.; Amiji, M. Long-circulating poly(ethylene glycol)-modified gelatin nanoparticles for intracellular delivery. *Pharm. Res.* **2002,** *19* (7), 1061-1067.

138. De, S.; Robinson, D. Polymer relationships during preparation of chitosan-alginate and poly-l-lysine-alginate nanospheres. *J. Controlled Release* **2003,** *89* (1), 101-112.

139. Aynie, I.; Vauthier, C.; Chacun, H.; Fattal, E.; Couvreur, P. Spongelike alginate nanoparticles as a new potential system for the delivery of antisense oligonucleotides. *Antisense Nucleic Acid Drug Dev.* **1999,** *9* (3), 301-312.

140. Quong, D.; Neufeld, R. J. DNA protection from extracapsular nucleases, within chitosan- or poly-L-lysine-coated alginate beads. *Biotechnol. Bioeng.* **1998,** *60* (1), 124-134.

141. Dumitriu, S.; Magny, P.; Montane, D.; Vidal, P. F.; Chornet, E. Polyionic hydrogels obtained by complexation between xanthan and chitosan: their properties as supports for enzyme immobilization. *Journal of Bioactive and Compatible Polymers* **1994,** *9*, 184-209.

142. Dornish, M.; Kaplan, D.; Skaugrud, O. Standards and guidelines for biopolymers in tissue-engineered medical products: ASTM alginate and chitosan standard guides. American Society for Testing and Materials. *Annals New York Academy of Sciences* **2001,** *944*, 388-397.

143. Tinsley-Bown, A. M.; Fretwell, R.; Dowsett, A. B.; Davis, S. L.; Farrar, G. H. Formulation of poly(D,L-lactic-co-glycolic acid) microparticles for rapid plasmid DNA delivery. *J. Control Release* **2000,** *66* (2-3), 229-241.

144. Douglas, K. L.; Tabrizian, M. Effect of experimental parameters on the formation of alginate-chitosan nanoparticles and evaluation of their potential application as DNA carrier. *J. Biomater. Sci. Polymer Edn* **2005,** *16*, 43-56.

145. Danielsen, S.; Strand, S.; de Lange, D. C.; Stokke, B. T. Glycosaminoglycan destabilization of DNA-chitosan polyplexes for gene delivery depends on chitosan chain length and GAG properties. *Biochim. Biophys. Acta* **2005,** *1721* (1-3), 44-54.

146. Cornelis, S.; Vandenbranden, M.; Ruysschaert, J. M.; Elouahabi, A. Role of intracellular cationic liposome-DNA complex dissociation in transfection mediated by cationic lipids. *DNA Cell Biol.* **2002,** *21* (2), 91-97.

147. Boeckle, S.; von, G. K.; van der, P. S.; Culmsee, C.; Wagner, E.; Ogris, M. Purification of polyethylenimine polyplexes highlights the role of free polycations in gene transfer. *J. Gene Med.* **2004,** *6* (10), 1102-1111.

148. Heerklotz, H.; Tsamaloukas, A.; Kita-Tokarczyk, K.; Strunz, P.; Gutberlet, T. Structural, volumetric, and thermodynamic characterization of a micellar sphere-to-rod transition. *J. Am. Chem. Soc.* **2004,** *126* (50), 16544-16552.

149. Nakai, T.; Kanamori, T.; Sando, S.; Aoyama, Y. Remarkably size-regulated cell invasion by artificial viruses. Saccharide-dependent self-aggregation of glycoviruses and its consequences in glycoviral gene delivery. *J. Am. Chem. Soc.* **2003,** *125* (28), 8465-8475.

150. Kursa, M.; Walker, G. F.; Roessler, V.; Ogris, M.; Roedl, W.; Kircheis, R.; Wagner, E. Novel shielded transferrin-polyethylene glycol-polyethylenimine/DNA complexes for systemic tumor-targeted gene transfer. *Bioconjug. Chem.* **2003,** *14* (1), 222-231.

151. Mi, F. L.; Liang, H. F.; Wu, Y. C.; Lin, Y. S.; Yang, T. F.; Sung, H. W. pH-sensitive behavior of two-component hydrogels composed of N,O-carboxymethyl chitosan and alginate. *J. Biomater. Sci. Polym. Ed* **2005,** *16* (11), 1333-1345.

152. Brazeau, G. A.; Attia, S.; Poxon, S.; Hughes, J. A. In vitro myotoxicity of selected cationic macromolecules used in non-viral gene delivery. *Pharm. Res.* **1998,** *15* (5), 680-684.

153. Koping-Hoggard, M.; Mel'nikova, Y. S.; Varum, K. M.; Lindman, B.; Artursson, P. Relationship between the physical shape and the efficiency of oligomeric chitosan as a gene delivery system in vitro and in vivo. *J. Gene Med.* **2003,** *5* (2), 130-141.

154. Hinrichs, W. L.; Schuurmans-Nieuwenbroek, N. M.; van de, W. P.; Hennink, W. E. Thermosensitive polymers as carriers for DNA delivery. *J. Control Release* **1999,** *60* (2-3), 249-259.

155. Borges, O.; Borchard, G.; Verhoef, J. C.; de, S. A.; Junginger, H. E. Preparation of coated nanoparticles for a new mucosal vaccine delivery system. *Int. J. Pharm.* **2005,** *299* (1-2), 155-166.

156. Akinc, A.; Lynn, D. M.; Anderson, D. G.; Langer, R. Parallel synthesis and biophysical characterization of a degradable polymer library for gene delivery. *J. Am. Chem. Soc.* **2003,** *125* (18), 5316-5323.

157. Godbey, W. T.; Barry, M. A.; Saggau, P.; Wu, K. K.; Mikos, A. G. Poly(ethylenimine)-mediated transfection: a new paradigm for gene delivery. *J. Biomed. Mater. Res.* **2000,** *51* (3), 321-328.

158. Bivas-Benita, M.; Oudshoorn, M.; Romeijn, S.; van, M. K.; Koerten, H.; van der, M. H.; Lambert, G.; Ottenhoff, T.; Benita, S.; Junginger, H.; Borchard, G. Cationic submicron emulsions for pulmonary DNA immunization. *J. Control Release* **2004,** *100* (1), 145-155.

159. Cartier, R.; Reszka, R. Utilization of synthetic peptides containing nuclear localization signals for nonviral gene transfer systems. *Gene Ther.* **2002,** *9* (3), 157-167.

160. Mishra, S.; Webster, P.; Davis, M. E. PEGylation significantly affects cellular uptake and intracellular trafficking of non-viral gene delivery particles. *Eur. J. Cell Biol.* **2004,** *83* (3), 97-111.

161. Schuhmacher, M.; Hillion, F. Ultrafine Feature Analysis using Secondary Ion Emission. 2001.

162. Bolton, A. E.; Hunter, W. M. The labelling of proteins to high specific radioactivities by conjugation to a 125I-containing acylating agent. *Biochem. J.* **1973,** *133* (3), 529-539.

163. Richardson, S. C.; Kolbe, H. V.; Duncan, R. Potential of low molecular mass chitosan as a DNA delivery system: biocompatibility, body distribution and ability to complex and protect DNA. *Int. J. Pharm.* **1999,** *178* (2), 231-243.

164. Galli, M. C.; Kraft, M. L.; Weber, P. K.; Hutcheon, I. D.; Boxer, S. G. Supported membrane composition analysis by secondary ion mass spectrometry with high lateral resolution. *Biophys. J.* **2005,** *88* (4), 2965-2975.

165. Guerquin-Kern, J. L.; Hillion, F.; Madelmont, J. C.; Labarre, P.; Papon, J.; Croisy, A. Ultra-structural cell distribution of the melanoma marker iodobenzamide: improved potentiality of SIMS imaging in life sciences. *Biomed. Eng Online.* **2004,** *3*, 10.

166. Quintana, C.; Bellefqih, S.; Laval, J. Y.; Guerquin-Kern, J. L.; Wu, T. D.; Avila, J.; Ferrer, I.; Arranz, R.; Patino, C. Study of the localization of iron, ferritin, and hemosiderin in Alzheimer's disease hippocampus by analytical microscopy at the subcellular level. *J. Struct. Biol.* **2006,** *153* (1), 42-54.

167. Danielsen, S.; Varum, K. M.; Stokke, B. T. Structural analysis of chitosan mediated DNA condensation by AFM: influence of chitosan molecular parameters. *Biomacromolecules.* **2004,** *5* (3), 928-936.

168. Huang, M.; Ma, Z.; Khor, E.; Lim, L. Y. Uptake of FITC-chitosan nanoparticles by A549 cells. *Pharm. Res.* **2002,** *19* (10), 1488-1494.

169. Manunta, M.; Tan, P. H.; Sagoo, P.; Kashefi, K.; George, A. J. Gene delivery by dendrimers operates via a cholesterol dependent pathway. *Nucleic Acids Res.* **2004,** *32* (9), 2730-2739.

170. Akita, H.; Ito, R.; Khalil, I. A.; Futaki, S.; Harashima, H. Quantitative three-dimensional analysis of the intracellular trafficking of plasmid DNA transfected by a nonviral gene delivery system using confocal laser scanning microscopy. *Mol. Ther.* **2004,** *9* (3), 443-451.

171. Huang, M.; Khor, E.; Lim, L. Y. Uptake and cytotoxicity of chitosan molecules and nanoparticles: effects of molecular weight and degree of deacetylation. *Pharm. Res.* **2004,** *21* (2), 344-353.

172. Douglas, K. L.; Piccirillo, C.; Tabrizian, M. Effects of Alginate Inclusion on the Vector Properties of Chitosan-Based Nanoparticles. *Submitted manuscript* **2006.**

173. Han, Y.; Zhao, L.; Yu, Z.; Feng, J.; Yu, Q. Role of mannose receptor in oligochitosan-mediated stimulation of macrophage function. *Int. Immunopharmacol.* **2005,** *5* (10), 1533-1542.

174. Su, Y.; Bakker, T.; Harris, J.; Tsang, C.; Brown, G. D.; Wormald, M. R.; Gordon, S.; Dwek, R. A.; Rudd, P. M.; Martinez-Pomares, L. Glycosylation influences the lectin activities of the macrophage mannose receptor. *J. Biol. Chem.* **2005,** *280* (38), 32811-32820.

175. Mo, Y.; Lim, L. Y. Mechanistic study of the uptake of wheat germ agglutinin-conjugated PLGA nanoparticles by A549 cells. *J. Pharm. Sci.* **2004,** *93* (1), 20-28.

176. Qaddoumi, M. G.; Gukasyan, H. J.; Davda, J.; Labhasetwar, V.; Kim, K. J.; Lee, V. H. Clathrin and caveolin-1 expression in primary pigmented rabbit conjunctival epithelial cells: role in PLGA nanoparticle endocytosis. *Mol. Vis.* **2003,** *9*, 559-568.

177. Ogris, M.; Carlisle, R. C.; Bettinger, T.; Seymour, L. W. Melittin enables efficient vesicular escape and enhanced nuclear access of nonviral gene delivery vectors. *J. Biol. Chem.* **2001,** *276* (50), 47550-47555.

178. Kamiya, H.; Tsuchiya, H.; Yamazaki, J.; Harashima, H. Intracellular trafficking and transgene expression of viral and non-viral gene vectors. *Adv. Drug Deliv. Rev.* **2001,** *52* (3), 153-164.

179. Ye, S.; Wang, C.; Liu, X.; Tong, Z. Multilayer nanocapsules of polysaccharide chitosan and alginate through layer-by-layer assembly directly on PS nanoparticles for release. *J. Biomater. Sci. Polym. Ed* **2005,** *16* (7), 909-923.

180. Pandey, R.; Ahmad, Z.; Sharma, S.; Khuller, G. K. Nano-encapsulation of azole antifungals: potential applications to improve oral drug delivery. *Int. J. Pharm.* **2005,** *301* (1-2), 268-276.

181. Ogris, M.; Walker, G.; Blessing, T.; Kircheis, R.; Wolschek, M.; Wagner, E. Tumor-targeted gene therapy: strategies for the preparation of ligand-polyethylene glycol-polyethylenimine/DNA complexes. *J. Control Release* **2003,** *91* (1-2), 173-181.

182. Cristiano, R. J. Targeted, non-viral gene delivery for cancer gene therapy. *Front Biosci.* **1998,** *3*, D1161-D1170.

183. Dizhe, E. B.; Akifiev, B. N.; Missul, B. V.; Orlov, S. V.; Kidgotko, O. V.; Sukonina, V. E.; Denisenko, A. D.; Perevozchikov, A. P. Receptor-mediated transfer of DNA--galactosylated poly-L-lysine complexes into mammalian cells in vitro and in vivo. *Biochemistry (Mosc.)* **2001,** *66* (1), 55-61.

184. Tan, P. H.; Manunta, M.; Ardjomand, N.; Xue, S. A.; Larkin, D. F.; Haskard, D. O.; Taylor, K. M.; George, A. J. Antibody targeted gene transfer to endothelium. *J. Gene Med.* **2003,** *5* (4), 311-323.

185. Shi, N.; Boado, R. J.; Pardridge, W. M. Receptor-mediated gene targeting to tissues in vivo following intravenous administration of pegylated immunoliposomes. *Pharm. Res.* **2001,** *18* (8), 1091-1095.

186. Merdan, T.; Callahan, J.; Petersen, H.; Kunath, K.; Bakowsky, U.; Kopeckova, P.; Kissel, T.; Kopecek, J. Pegylated polyethylenimine-fab' antibody fragment conjugates for targeted gene delivery to human ovarian carcinoma cells. *Bioconjug. Chem.* **2003,** *14* (5), 989-996.

187. Schneider, H.; Harbottle, R. P.; Yokosaki, Y.; Kunde, J.; Sheppard, D.; Coutelle, C. A novel peptide, PLAEIDGIELTY, for the targeting of alpha9beta1-integrins. *FEBS Lett.* **1998,** *429* (3), 269-273.

188. Jost, P. J.; Harbottle, R. P.; Knight, A.; Miller, A. D.; Coutelle, C.; Schneider, H. A novel peptide, THALWHT, for the targeting of human airway epithelia. *FEBS Lett.* **2001,** *489* (2-3), 263-269.

189. Li, J. M.; Collins, L.; Zhang, X.; Gustafsson, K.; Fabre, J. W. Efficient gene delivery to vascular smooth muscle cells using a nontoxic, synthetic peptide vector system targeted to membrane integrins: a first step toward the gene therapy of chronic rejection. *Transplantation* **2000,** *70* (11), 1616-1624.

190. Luo, D.; Saltzman, W. M. Enhancement of transfection by physical concentration of DNA at the cell surface. *Nat. Biotechnol.* **2000,** *18* (8), 893-895.

Appendix A
Conventions in Non-Viral Vector Characterisation

11.1 Size Measurements (DLS)

Due to the importance of particle size in delivery systems, as outlined in Chapter 4, measurement of particle sizes is fundamental to characterisation of the system. The most common method used for measurement of particles is called dynamic light scattering (DLS). Analysis by DLS, alternatively called photon correlation spectroscopy (PCS) or quasi-elastic light scattering (QELS), is based on the principle of Brownian motion. In solution, all particles demonstrate random motion as a result of collisions with solvent molecules. In DLS, laser light is directed at the sample and scattered by the particles to a photon detector. As the particles move the intensity of the scattered light fluctuates due to alternating constructive and destructive interference in the scattered light.

The Stokes-Einstein equation defines an inversely proportional relationship between the random motion of a particle due to Brownian motion and its size. Therefore, smaller particles move faster than larger ones. The fluctuations in the intensity of the scattered light are also related to particle size, and can be used to calculate their size. In practice the measurement occurs over a period of time during which a correlation function is generated, which plots the relative change in signal intensity over time. It is from the correlation function that particle size is calculated.

Generally, these measurements yield particle size distributions based on the intensity of light scattered by them. One disadvantage of this measurement technique is that larger particles are often over-represented in size distributions of disperse populations, owing to their ability to scatter more light than smaller particles. For relatively mono-disperse systems, this is not an issue. A further consideration in the interpretation of DLS measurements is that the method measures the hydrodynamic diameter of the particle, which includes the associated solvent layer.

Most particle size measurements generate values for the average diameter of the particles, as well as a polydispersity index (PI). The polydispersity index is

a measure of the distribution of particle sizes within the population. This value ranges from 0 to 1; with values above 0.7 being indicative of populations with a wide range of sizes and lower values being indicative of mono-disperse samples; this value does not generally fall below 0.05.

Alternatives to DLS measurements include imaging techniques, including transmission electron microscopy. The problem with techniques such as these is that particles are not measured in their native state, so that artefacts due to preparation processes may affect measured particle size. Furthermore, the nature of imaging techniques makes it difficult to ascertain the particle distribution of a population.

11.2 N:P Ratio

Most cationic delivery systems derive their charge from the presence of amino groups (NH_3^+), leading to the nomenclature *N* to describe their charge. It is important to note that *N* refers to the relative total number of amino groups present in the system, not only those present at the surface of the vector. Each nucleotide comprising DNA is composed of a nitrogenous based coupled to a sugar unit and a phosphate group ($H_2PO_4^-$). The total relative charge owing to the negatively charged phosphate groups is described by *P*. The ratio of the amino groups in the carrier to the phosphate groups in DNA is reported as the N:P ratio.

(Note: In the article published in the *Journal of Biomaterials Science – Polymer edition*, the relative amounts of carrier to DNA were reported as P:N ratios.)

11.2.1 N:P Ratio of Alginate-Chitosan Nanoparticles

The calculations of N:P ratios for alginate-chitosan nanoparticles were based on the assumption that alginate and chitosan would interact in a stoichiometric fashion, so that the alginate carboxylate groups would neutralise an equivalent number of chitosan amino groups. Although the results of studies reported in Chapter 7 contest this assumption, this practice was maintained throughout the project. Calculation of the number of chitosan amino groups also

required consideration of the degree of deacetylation of the polymer (85%, as indicated by the supplier).

11.3 Charge Measurements (Zeta Potential)

Nearly all particles reveal a surface charge when in solution, through ionisation of surface groups or adsorption of ions. The charge that develops at the surface of the particles is called the zeta potential. Zeta potential (ζ) is determined by measuring the movement of particles subjected to an electric field. When an electric field is applied, charged particles move through the solution; this movement is detected as a Doppler shift in the frequency of laser light scattered by particles. The direction of motion provides the nature of their charge (cationic or anionic), while the velocity allows the value of their charge to be calculated. It is important to realise that changes to solution conditions, including pH, ionic strength, and the presence of additional molecules or reagents, can affect the surface charge of the particles and alter the measured zeta potential.

11.4 Agarose Gel Electrophoresis

By far the most popular technique used to assess the interaction between vectors and DNA, agarose gel electrophoresis assays are reported in almost all publications related to gene delivery systems. The principle behind this assay is the movement of charged particles through a porous agarose gel when subjected to an electric field. While DNA is capable of migrating through the gel towards the cathode, vector-DNA complexes are generally incapable of migrating.

Electrophoresis assays are generally performed by preparing complexes with varying N:P ratios and loading them in the starting wells of the gel (total volume ~15 μL). The gel, which is immersed in a bath, is subjected to an electric field for a period of time, during which DNA migrates. The absence of any DNA migration is indicative of complete complexation by the vector.

This assay is also used to assess the integrity of DNA following complexation and release from vectors. Although the process of release

intracellularly is currently a matter of debate (see Chapter 6), enzymatic digestion of the carrier can be executed to release the DNA. In these assays, the form and position of the migrating DNA relative to control samples is important. Plasmid DNA generally exists in three forms: linear, coiled and super-coiled. Linear DNA generally migrates the slowest, and hence its bands are closest to the starting wells. Coiled DNA migrates faster, and super-coiled DNA migrates the fastest. Linear DNA is believed to be less effective for transfection purposes while coiled and super-coiled are thought to be equal in their transfection capabilities.

The ability of complexation with a vector to protect DNA from enzymatic digestion is also usually assessed using gel electrophoresis. Generally, complexes are exposed to DNases which are then deactivated prior to release of DNA from the vector. Degraded DNA is indicated by the presence of smears in the lane, or occasionally by a complete absence of fluorescence. This characterisation is particularly important, since the inability of a vector to protect DNA from enzymatic digestion will result in the delivery of inactive DNA to cells.

11.5 Ethidium Bromide Intercalation

Ethidium bromide (EtBr) is a small, planar molecule that intercalates between the base pairs of double-stranded DNA to produce a fluorescent signal. The strength of the fluorescence is directly related to the interaction between EtBr and DNA. Association between DNA and cationic carriers causes the DNA to compact, preventing access to EtBr. Therefore, efficient complexation of DNA results in reduced fluorescence since EtBr is unable to intercalate with DNA. Ethidium bromide exclusion assays are based on the principle that fluorescence of a solution of EtBr and DNA will be reduced gradually with the addition of carriers able to effectively complex DNA. The change in fluorescence as a function of the N:P ratio of the system is indicative of the strength of interaction between the vector and DNA.

11.6 MTT Assay

The MTT assay is a colorimetric assay that provides a relative measurement of the viability of treated versus untreated cells. Following exposure to the conditions being assessed, MTT (3-(4,5-Dimethylthiazol-2-yl)-2,5-diphenyltetrazolium bromide), a yellow solution, is added to the cells. The cells are incubated in this solution for 4 h, during which time mitochondrial enzymes reduce the chemical to insoluble purple formazan crystals. Since cell viability is directly related to the activity of mitochondria, this measurement, which requires the action of mitochondrial reductase enzymes, offers a direct measurement of viable cells. Following the initial incubation, cells are lysed and the formazan crystals are solubilised prior to spectrophotometric measurement (570 nm). Viability is generally reported relative to untreated control cells.

11.7 Evaluation of Transfection

There are a number of ways to evaluate transfection, depending on the transgene used. The most common methods, flow cytometry and confocal microscopy, rely on the production of a fluorescent protein for detection of transfection. Other methods, mainly enzymatic in nature, are used to assess the production of non-fluorescent proteins.

11.7.1 Flow Cytometry

Flow cytometry is an analysis method that can be used to assess cellular binding and internalisation of non-viral vectors, as well as transfection. Each method requires a fluorescent signal, so that it can only be used for vectors conjugated to a fluorophore or detection of expression of a transgene encoding for a fluorescent protein. The work presented in this thesis made use of fluorescein-labelled chitosan for the investigation of the interaction between nanoparticle complexes and cells. Detection of green fluorescent protein was used to assess transfection. Interpretation of data collected by flow cytometry can allow quantification of the fraction of the population exhibiting fluorescence, as well as the relative fluorescence intensity of the population.

In flow cytometry analysis, a sample of cells in suspension is flowed through a narrow channel. Within this channel, the cells pass individually through a laser beam, scattering the light. The relation between the amount of forward scattered and side scattered light can be used to evaluate the viability of the cells. Generally, only data from the viable cells in a population are considered for analysis. In flow cytometry terms, the collected results are *gated* on the viable fraction.

Simultaneous to the detection of scattered light, fluorescence emitted from the cell is detected. Up to four different wavelengths can be detected concurrently, though the analyses presented in this thesis only required the detection of fluorescein fluorescence ($\lambda_{excitation}$ 488 nm, $\lambda_{emission}$ 520 nm). Since all cells demonstrate a certain level of auto-fluorescence, analysis of untreated cells is always required as a control.

11.7.2 Confocal Microscopy

In many ways, confocal microscopy is a complementary technique to flow cytometry. As the name implies, confocal microscopy relies on the visual analysis of samples, and resembles standard microscopes. However, this technique makes use of lasers to illuminate the sample, causing fluorophores to emit fluorescence. Whereas epifluorescent microscopes allow the imaging of fluorescence within a sample, confocal microscopy improves upon this by using pinholes to reject all light except that emitted from a specific plane. This provides the ability to visualise images of a single focal plane of the sample, improving the clarity of the images. Furthermore, it provides the ability to distinctly identify the location of fluorescence relative to cell morphology. Whereas flow cytometry analyses can confirm the presence of fluorophore-labelled complexes within a cell, confocal microscopy can determine their presence within the nucleus or other sub-cellular compartments. As with flow cytometry, multiple fluorophores can be detected in the same sample, but this occurs sequentially rather than concurrently.

Confocal microscopy was used in this project to monitor the intracellular trafficking of alginate-chitosan nanoparticle complexes. For these assays,

fluorescein-labelled chitosan was used in the preparation of nanoparticles. Additional labelling of the nucleus was achieved using DAPI, which stains nucleic acids blue, and LysoTracker Red, which fluoresces in the acidic environment of lysosomes.

11.7.3 Other Methods

The expression of enzymatic proteins is most often quantified through enzymatic assays that produce a measurable signal. For example, quantification of β-galactosidase is accomplished through a colorimetric assay that measures the yellow product formed through the enzymatic activity on a colourless substrate. Similarly, luciferase production is measured through the luminescence produced by its activity on luciferin (the same reaction that produces light in fireflies). Although these methods are particularly sensitive, they are not able to provide a measure of the fraction of cells transfected.

Appendix B
Experimental Methods for Supplementary Information

12.1 DNA Complexation (Section 5.7.1)

The ability of alginate-chitosan nanoparticles to complex DNA as a function of the preparative conditions was evaluated by their ability to prevent plasmid migration during gel electrophoresis. Alginate-chitosan nanoparticles were prepared at the ratios of 1:1.5 and 1.5:1, as described in section 5.3.1. These were then characterised for size using dynamic laser light scattering, and charge using zeta potential measurements. Various volumes of nanoparticle suspensions (1-7.5 μL as prepared) were mixed with 0.25 μg plasmid DNA (pEGFP-N1, 1 mg/mL) to yield N:P ratios between 1:7 and 1:1 and incubated at room temperature for 30 min. Mixtures were loaded onto a 0.8% agarose gel, run at 100 V for 50 min, and photographed using a gel imaging station.

12.2 Cellular Interactions (Section 5.7.2)

The effect of the ratio of alginate:chitosan on the ability of the nanoparticles to bind to and penetrate cells was investigated using flow cytometry analysis. Alginate-chitosan nanoparticles were prepared using fluorescein-labelled chitosan (Carbomer) at the ratios of 1:1.5 and 1.5:1. One day prior to treatment, COS7 cells were seeded in complete medium (DMEM with 10% FBS) at $2x10^5$ cells/well in 12-well plates. For treatment, the medium was removed and replaced with 500 μL serum-free medium containing 85 μL fluorescein-labelled nanoparticles. At specified intervals (15 min, 30 min, 1 h, 2 h, 4 h, 6 h and 24 h), the medium was removed, cells were washed with cold PBS and detached with cold EDTA (0.6 mM in PBS). Cells were removed to tubes, centrifuged and resuspended in PBS, then analysed using flow cytometry (FACSCalibur). Ten thousand events were measured for each sample; appropriate controls and gates were used for analysis.

12.3 Preparation of Alginate-Chitosan Nanoparticles (Section 5.7.3)

Low viscosity sodium alginate (M_W 12-80 kDa, Sigma) was prepared by dissolving in MilliQ water. Chitosan (M_W 10kDa, ~90% deacetylated, Carbomer Inc.) was first dissolved in 1.0 M HCl and volume adjusted using MilliQ water. The pH of all three solutions was adjusted to 5.6-5.8 and filtered (0.22μm) prior to use. Nanoparticles are prepared by mixing 0.005% (w/v) sodium alginate (5950 μL) and 1% (w/v) chitosan (50 μL) to give a final weight ratio of 1:1.5 alginate:chitosan and stirred for 1 h at room temperature. All particles are characterised for size and size distribution by low-angle dynamic laser light scattering (DLS) (HPPS, Malvern Instruments). The surface charge of the particles was determined through zeta potential measurements (ZetaPlus, Brookhaven Instruments). Unless otherwise noted, nanoparticle suspensions were used directly. Filtration of nanoparticle suspensions is possible with poly(ether sulfone) filters (0.22 μm), leading to nanoparticles with a mean diameter of 109 ± 2 nm, but reduced concentration. Preparation of polymer solutions and nanoparticles under sterile conditions precluded the need to filter nanoparticle suspensions for cell studies.

12.4 Further Characterisation of Nanoparticle-DNA Complexes (Section 6.7)

The effect of DNA complexation on the size and charge of nanoparticle complexes was investigated using DLS and zeta potential analysis. Oligonucleotides (ON) from herring sperm (Sigma) were used for these experiments since the quantities required were prohibitive for the use of plasmids. Complexes were prepared using two methods. In Protocol 1, ON (2 mg/mL) were added under stirring to alginate-chitosan nanoparticles immediately following their formation and allowed to stir for an additional 30 min. In Protocol 2, ONs were first mixed with chitosan for 30 min, followed by the addition of alginate and further stirring (30 min) for the resulting formation of nanoparticles.

Appendix C
NanoSIMS

The following description of NanoSIMS instrumentation and improvements over traditional SIMS surface analysis is adapted from a manuscript written by K.L Douglas and A. Sénéchal.

13.1 NanoSIMS Instrumentation

A schematic representation of the NanoSIMS 50 (Cameca, France) is indicated in Figure 13.1. The primary ion beam employs a stream of either O^- or Cs^+ ions to bombard the sample surface. The smallest respective spot sizes, indicating absolute resolution, are 150 nm and 50 nm respectively. This model simultaneously measures the emission of five specific atomic or ionic species through the positioning of variably mounted detectors in the mass spectrometer.

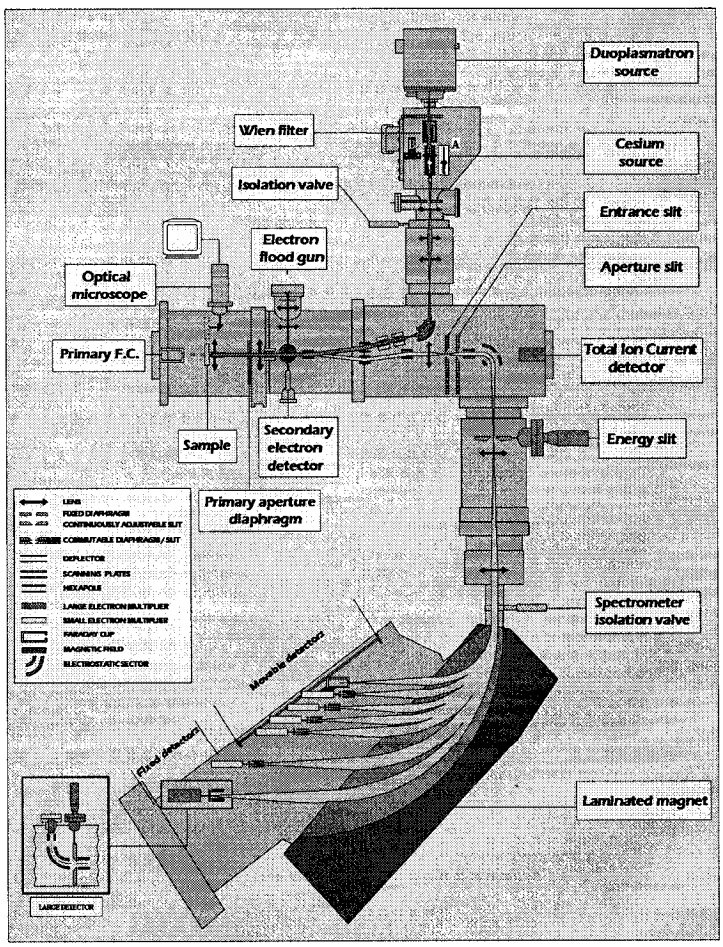

Figure 13.1. Schematic representation of the Cameca NanoSIMS 50. (Reproduced with permission granted by Cameca, France.)

13.2 NanoSIMS Theory

The intensity of sputtered secondary ions for a given species "i", or the strength of the measured signal, is defined by Equation 13.1[161]. As the intensity is directly proportional to the area being analysed, sputter area S, reducing the area being analysed reduces the secondary ion signal intensity. By improving the ionisation efficiency and probe density of the primary bombardment beam, NanoSIMS improves the ion yield by two to three orders of magnitude, thereby allowing a sufficient signal to noise ratio to be maintained during the analysis of smaller surface regions.

$$\mathbf{I_i = T \cdot Y_i \cdot d_b \cdot S \cdot S_y \cdot [i]} \qquad [13.1]$$

T: overall transmission (collection optics, mass spectrometer, and detector efficiency)
Y_i: species ion yield (number of emitted ions/number of sputtered atoms)
d_b: primary beam density
S: sputter area
S_y: sputter yield (number of sputtered atoms/number of primary ions)
[i]: fraction of species "i" in the sample surface

13.2.1 Ionisation Efficiency

The ionisation probability depends on the chemical state of the sample surface during the sputtering process, which is determined by the matrix composition itself, the implantation of primary ions, the bombardment induced diffusion and the surface reaction with the vacuum gas phase. Bombardment with reactive primary ions can increase ion yields by changing surface chemistry. New instruments use oxygen or cesium primary ions, which has been shown to enhance the yield by 2 or 3 orders of magnitude[161].

13.2.2 Primary Ion Probe Density

Probe density depends on source characteristics and the aberrations caused by the probe forming system (lens). In conventional SIMS instruments, the working distance of the probe-forming lens is fairly long (several centimetres) due to the presence of the secondary ion extraction system in front and near the sample surface. The newer NanoSIMS instruments make use of the same optical

system to co-axially focus the primary ion probe and secondary ions[161]. In the co-axially arranged system, there is a much shorter working distance of the probe-forming lens (~0.3mm). This minimises aberrations, leading to a smaller probe diameter. This arrangement has the added advantage of primary beam irradiation normal to the sample surface. This reduces any shadow effects that may arise from non-flat surfaces and a non-normal angle of incidence.

13.2.3 Secondary Ion Collection

In SIMS technique, secondary ions are separated according to their mass prior to detection. This is necessary to ensure identification and accurate quantisation of the secondary ions. Often, it is desirable to analyse samples to acquire information about multiple species. In conventional SIMS instruments, this detection is done sequentially.

Choice of the mass spectrometer of any SIMS instrument must consider the following: it must have high mass resolution capabilities since both atomic ions and molecular ions of similar mass may be sputtered from a sample; and spatial resolution and analysis time are inversely proportional to the number of analysed species using sequential detection mode[161].

In order to avoid the restrictions imposed by the sequential detection of different species, a preferred mode is parallel detection (the detection of multiple species simultaneously). There are two spectrometers that offer high mass resolution and parallel detection: time of flight (TOF) mass spectrometer and the Mattauch-Herzog double focusing mass spectrometer.

The TOF mass spectrometer allows unlimited detection of ions over a large mass range. However, the sputter rate is greatly reduced when using this system since the primary ion beam must be pulsed. For these reasons, the TOF system is more suitable when only a monolayer or sub-monolayer is being analysed, and if unknown contaminants are being investigated.

The Mattauch-Herzog double focusing mass spectrometer does not require pulsing of the primary beam, leading to good sputter rates and decreased acquisition times. It allows parallel detection of several species, but the species

must be known beforehand. For most samples, this system would be the best choice. NanoSIMS instruments make use of a Mattauch-Herzog double focusing mass spectrometer that offers high mass resolution and parallel detection of up to 5 species. This system maximises the resolution and detection of the secondary ions while minimising acquisition time.

Appendix D
Article Reprints & Copyright Waivers

Molecular Therapy: Submission confirmation

Dear Dr. Tabrizian,

Molecular Therapy has received the article entitled "CELL-LINE DEPENDENT INTERNALIZATION PATHWAYS AND INTRACELLULAR TRAFFICKING DETERMINE TRANSFECTION EFFICIENCY OF NANOPARTICLE VECTORS" on May 24, 2006. You will receive another email informing you of the manuscript number assigned to your paper shortly. Please use this number whenever you correspond with the editorial office.

This manuscript will be processed with the understanding that it:
is original
has been written by the stated authors
has not been published elsewhere
is not currently being considered for publication by any other journal
will not be submitted for such review while under review by this journal
submission for publication must have been approved by all of the authors and by the institution where the work was carried out.

IMPORTANT NOTICE

Beginning in January 2007, Molecular Therapy will be published by Nature Publishing Group (NPG). The submission and review processes at the journal will remain unchanged. However, over the late summer months production of accepted articles will begin to move to NPG.

We are pleased to announce the discontinuation of the submission fee in conjunction with the move to NPG.

Please also be aware that Molecular Therapy will no longer be accessible through Elsevier's ScienceDirect platform. To ensure continued access to the journal, be sure to request an institutional subscription through your institute's librarian.

ASGT members will continue to benefit from print and online access to the journal. ASGT members will also benefit from reduced page charges beginning in 2007! Please contact info@asgt.org for further details.

Thank you for your support of Molecular Therapy, the official journal of the American Society for Gene Therapy.

Journal of Controlled Release: Submission confirmation

Ms. Ref. No.: JCR-D-06-00326
Title: EFFECTS OF ALGINATE INCLUSION ON THE VECTOR PROPERTIES OF CHITOSAN-BASED NANOPARTICLES Journal of Controlled Release

Dear Dr Tabrizian,

Your submission entitled "EFFECTS OF ALGINATE INCLUSION ON THE VECTOR PROPERTIES OF CHITOSAN-BASED NANOPARTICLES" has been assigned the following manuscript number: JCR-D-06-00326.

Thank you for submitting your work to the Journal of Controlled Release.

Kind regards,

The Editors
Journal of Controlled Release

Journal of Biomaterials Science, Polymer Edition: Permission to include manuscript in thesis

Dear Mrs. Douglas,

We grant you non-exclusive world rights in the English language free of charge provided full credit acknowledgement will be given to Brill Academic Publishers.

The proper credit line is:
Full credit acknowledgement will be given to VSP Publishers, an imprint of Brill Academic Publishers:
((c) VSP Publishers, an imprint of Brill Academic Publishers, Leiden, The Netherlands 20..)

With best regard,

Sabine Steenbeek
Publishing Assistant STM
Brill Academic Publishers

J. Biomater. Sci. Polymer Edn, Vol. 16, No. 1, pp. 43–56 (2005)

Also available online - www.vsppub.com

Effect of experimental parameters on the formation of alginate–chitosan nanoparticles and evaluation of their potential application as DNA carrier

KIMBERLY L. DOUGLAS and MARYAM TABRIZIAN*

Department of Biomedical Engineering, McGill University, 3775 University Street, Montreal, Québec, Canada H3A 2B4

Received 20 January 2004; accepted 28 April 2004

Abstract—This study introduces a new procedure to prepare alginate–chitosan nanoparticles and examines several experimental parameters in relation to their formation and characteristics. Using DLS and TEM analysis, nanoparticle formation was shown to be predominantly affected by the ratio of alginate to chitosan, the molecular weight of the biopolymers and the solution pH. We report a method that results in spherical particles with mean diameters ranging from 323 nm to 1.6 μm, depending on the preparation conditions. The smallest particles were formed using lower molecular weight polymers with pH between 5.0 and 5.6 and having an alginate/chitosan weight ratio of 1 : 1.5. We have shown that DNA can be loaded with 60% association efficiency. Our system demonstrates suitable size, loading and release characteristics for application in drug- and gene-delivery systems.

Key words: Alginate; chitosan; nanoparticle; DNA carrier; controlled release.

INTRODUCTION

The main principles in drug and gene delivery therapies are to design systems that maintain the structure and activity of biomolecules, are non-immunogenic, release the therapeutic agent predictably over time and degrade to metabolites that are either absorbed or excreted [1]. Recently, the development of delivery systems has focused on the creation of non-viral vectors for gene therapy applications. Within this field, there are three main types of systems: those prepared with synthetic polymers, natural compounds and lipids [2]. Each type of system has its own characteristics with regard to circulation time, degradation, loading capabilities and release profiles.

*To whom correspondence should be addressed. Tel.: (1-514) 398-8129.
E-mail: maryam.tabrizian@mcgill.ca

The use of polysaccharides and specifically natural biopolymers, has commanded particular interest due to their desirable biocompatible, biodegradable, hydrophilic and protective properties [3, 4]. The interaction between biodegradable cationic and anionic biopolymers leads to the formation of polyionic hydrogels, which have demonstrated favourable characteristics for drug entrapment and delivery [5]. Chitosan and alginate are two biopolymers that have received much attention and been extensively studied for such use. Entrapment in biopolymers of therapeutic agents, including peptides, proteins and polynucleotides, has been shown to maintain their structure and activity and to protect them from enzymatic degradation [6, 7]. Additionally, many of these polymers, hydrogels in particular, are naturally hydrophilic, which is advantageous since this property is thought to contribute to longer circulation times *in vivo* and allows encapsulation of water-soluble biomolecules.

Chitosan is a natural cationic polysaccharide obtained by the N-deacetylation of chitin, a product found in the shells of crustaceans. Its use as a gene carrier has been studied by several groups due to its ability to bind DNA and protect it from degradation [8–13]. To this end, chitosan–DNA (Chi-DNA) nanoparticles have been prepared using a variety of methods, including ionic gelation or complexation, cross-linking, preparation using reverse micellar systems and chemical modification leading to self-assembly [8, 9, 14]. However, all studies with Chi-DNA nanoparticles have demonstrated significantly lower transfection efficiencies than is attainable with commercial formulations [8, 9, 12, 13]. Thorough studies of the system have shown that Chi-DNA nanoparticles are stable to challenge in salt and serum (but are pH sensitive), protect the nucleic acid from degradation by serum nucleases and are effectively taken up by cells [8, 11, 15]; the reason for inefficient transfection is, therefore, not well understood.

The incorporation of secondary polymers has been one approach used to improve the characteristics of liposome and/or polycation non-viral systems [16, 17]. There are numerous chitosan–polyanion complexes that have been investigated as delivery systems for drugs, proteins, DNA and other oligonucleotides, with encouraging results [5, 18–22]. Among the chitosan–polyanion complexes investigated, the combination of chitosan and alginate is considered to be among the most interesting for delivery systems [23].

Alginate is an anionic polysaccharide consisting of linear copolymers of α-L-guluronate and β-D-mannuronate residues. Alginates are hemocompatible, have not been found to accumulate in any major organs and show evidence of *in vivo* degradation [24]. In the presence of calcium ions, ionic interactions between the divalent calcium ions and the guluronic acid residues cause alginates to form gels. The properties of calcium–alginate gel beads make them one of the most widely used carriers for controlled release systems [25]. Coating of these beads with other polymers, including chitosan, has been shown to improve their stability during storage and in biological fluids.

Alginate–chitosan polyionic complexes form through ionic gelation *via* interactions between the carboxyl groups of alginate and the amine groups of chitosan.

The complex protects the encapsulant, has biocompatible and biodegradable characteristics, and limits the release of encapsulated materials more effectively than either alginate or chitosan alone [26]. A further advantage of this delivery system is its non-toxicity, which permits repeat administration of therapeutic agents. Alginate–chitosan (Alg-Chi) microspheres, or beads, have been widely studied for the encapsulation of drugs, oligonucleotides, proteins and cells, with promising results [23, 27–31]. Despite the attractive properties of this system, its development and application in the submicron scale has scarcely been studied. Recently, De and Robinson have reported the only preparation of Alg-Chi nanoparticles [32].

Due to the numerous desirable characteristics and demonstrated success of the Alg-Chi system, we decided to explore its development and use in the submicron scale and evaluate its potential use as a gene carrier. Through the formation of a stable polyionic system, we hoped to avoid the sensitivity to pH that is observed with Chi-DNA complexes. As well, by avoiding the use of cross-linking agents or chemically modified polymers, we aimed to develop a system that would demonstrate the biocompatibility and non-toxicity of the native polymers. Addressing the issue raised by McLaughlin *et al.* [11], who proposed that poor transfection by Chi-DNA nanoparticles may result from a limited release in the cell due to the high affinity of chitosan for DNA, we hypothesized that the incorporation of negatively charged alginate in the system would reduce the strength of interaction between the DNA and the particles, facilitating its release and increasing transfection. Prior to thorough analysis of their applicability as gene carriers, we sought first to develop and optimize the particles.

In this paper we introduce a new method to prepare Alg-Chi nanoparticles based on the formation of a polyionic complex between the two biopolymers. The influence of various experimental parameters on the formation of nanoparticles, including the ratio of the biopolymers, solution pH, addition of calcium chloride and stirring time, has been investigated. The size of the nanoparticles was determined using dynamic laser light scattering (DLS) and transmission electron microscopy (TEM) imaging, while nanoparticle composition was assessed by ATR–FT-IR. Spectroscopic methods were used to monitor the ability of the Alg-Chi nanoparticles to load and release DNA as a preliminary assessment of their suitability as gene carriers.

MATERIALS AND METHODS

Preparation of nanoparticles

Sodium alginate extracted from *Macrocystis pyrifera* was purchased from Sigma Chemical in three different molecular masses: high viscosity (HV), 120–190 kDa; medium viscosity (MV), 80–120 kDa; and low viscosity (LV), 12–80 kDa. Calcium chloride was purchased from Aldrich. Chitosan, 85% deacetylated, having molecular masses of 1000 kDa (HMW) and 50 kDa (LMW), was obtained from

Vanson HaloSource. Other chemicals were reagent grade. All chemicals were used as received without further purification or modification.

Both the sodium alginate and calcium chloride solutions were prepared by dissolving the chemicals in distilled water. The pH of the sodium alginate solution was adjusted using hydrochloric acid. The chitosan solution was prepared using a previously published method, adjusting the amount of chitosan used to yield the desired concentration [4]. Briefly, a known amount of chitosan was dissolved in a solution of 1.0 M HCl, volume adjusted using distilled water and pH modified to between 5.0 and 5.7 using NaOH.

The method used to prepare the nanoparticles is a two-step method adapted from Rajaonarivony's method of preparing alginate–poly-L-lysine nanoparticles [24]. The first step in the nanoparticle preparation is the formation of a calcium–alginate pre-gel. This was obtained by adding a calcium chloride solution (18 mM) to an alginate solution (0.063%, w/v) while stirring (Fisher Scientific Isotemp hotplate stirrer, 700 rpm). Various concentrations of chitosan solutions were then added with continuous stirring.

The effect of individual experimental parameters on the preparation of the nanoparticles was assessed while all other variables were kept constant. The concentration of the chitosan solution was varied between 0.06% and 1.5% (w/v) to obtain different ratios of alginate to chitosan (w/w) in the final solution. Solutions of high molecular weight (HMW) and low molecular weight (LMW) chitosan were combined with solutions of low (LV), medium (MV) and high viscosity (HV) sodium alginate. The pH of the sodium alginate and chitosan solutions was adjusted using sodium hydroxide or hydrochloric acid. The amount of calcium chloride added during the calcium–alginate pre-gel formation was also varied. Lastly, the final solutions were allowed to stir for 0.5, 1, 2, 5, 12 and 24 h.

Prior to analysis, all samples were centrifuged at $1100 \times g$ for 30 min to remove any large aggregates. Centrifugation under these conditions allowed aggregates to pellet, leaving nanoparticles suspended in the supernatant. Initially, particle suspensions were purified by means of dialysis using a Spectra/Por CE Float-A-Lyzer (Spectrum) with a molecular mass cut-off of 300 kDa to remove free polymer from the solution. It was found that dialysis did not change the results of DLS, TEM or zeta potential particle characterization.

Nanoparticle analysis

Morphological analysis of the nanoparticles was performed using TEM (Jeol 2000FX). Samples of nanoparticle suspensions (5 μl) were dropped onto Formvar-coated copper grids. After drying, samples were stained using phosphotungstic acid (2%, w/v). DigitalMicrograph software (Gaetan v3.4) was used to perform image capture and analysis, including sizing. Particle composition was assessed using a Perkin Elmer Spectrum One FT-IR fitted with a Universal ATR Sample Analyzer on samples that were frozen at −20°C and subsequently lyophilized (ThermoSavant ModulyoD) prior to analysis. Zeta potential analysis was performed using a

ZetaPlus (Brookhaven Instruments). The size and distribution of the particles were assessed by dynamic light scattering (DLS) using a low-angle laser light-scattering device (Malvern Instruments HPPS).

DNA loading and release study

Preliminary tests were carried out in order to assess the feasibility of using the Alg-Chi nanoparticles as gene carriers. Deoxyribonucleic acid from herring sperm (Sigma), which consists of oligonucleotides, was used for these preliminary studies. The amount of DNA introduced to the system was varied and is reported as stoichiometric ratios of DNA phosphate groups (P) to chitosan amine groups (N); the P/N ratios investigated for this study include 1 : 50, 1 : 25, 1 : 10 and 1 : 5.

Two methods, based on research examining oligonucleotide loading of alginate–poly-L-lysine nanoparticles [33], were used to load DNA in the nanoparticles. The first method (DNA+NP) consisted of mixing a certain amount of DNA (2 mg/ml) with pre-formed Alg-Chi nanoparticles (ratio 1 : 1.5, w/w). The second method (DNA+Chi) involved the preparation of nanoparticles using chitosan that had been allowed to complex with DNA. The DNA–Chitosan (DNA-Chi) complex solutions were prepared by adding the appropriate amount of DNA solution (2 mg/ml) to the chitosan solution and allowing them to mix for 24 h. Nanoparticles were then prepared as above, with the addition of the DNA-Chi in place of the usual addition of chitosan. The DNA-loaded nanoparticles were characterized through DLS sizing and zeta potential analysis, as described for the unloaded nanoparticles.

For quantitative determination of DNA loading, samples were ultra-centrifuged for 1 h at 220 000 × *g* (Beckman TL-100 Ultracentrifuge) to pellet the nanoparticles and associated DNA. Unadsorbed DNA remaining in the supernatant was quantified using a spectrophotometer at 260 nm (μQuant, Bio-Tek Instruments). Suitable controls were used for all analyses. The amount of DNA associated with the nanoparticles was calculated as the difference between the initial amount of DNA added to the suspensions and the amount measured in the supernatant. The following equations were used to determine association efficiency (AE) and mass adsorption (MA):

$$\mathrm{AE}(\%) = \frac{\mathrm{DNA_{total}} - \mathrm{DNA_{super}}}{\mathrm{DNA_{total}}} \tag{1}$$

$$\mathrm{MA} = \frac{\mathrm{DNA_{total}} - \mathrm{DNA_{super}}}{\mathrm{Mass_{np}}} \tag{2}$$

where $\mathrm{DNA_{total}}$ is the initial amount of DNA added, $\mathrm{DNA_{super}}$ is the amount measured in the supernatant following centrifugation and $\mathrm{Mass_{np}}$ is the mass of nanoparticles.

Following analysis of DNA-loading, nanoparticles prepared using P/N ratios of 1 : 25 and 1 : 10 were resuspended in phosphate-buffered saline (PBS) and stored at

room temperature for periods of 2, 4, 8, 12, 24 and 48 h. Samples were then ultracentrifuged as above and the supernatant was analyzed spectrophotometrically to determine DNA release.

Statistical analysis

For all results, triplicate readings were obtained for a minimum of three separate samples. Values reported are the mean ± standard error of the mean, unless otherwise noted. Statistical analysis was accomplished using a two-sided Student's *t*-test for two samples assuming unequal variance.

RESULTS AND DISCUSSION

Identification of nanoparticle constituents

Nanoparticles analyzed using FT-IR demonstrate absorption bands characteristic of both alginate and chitosan in addition to peaks indicative of their interaction (Fig. 1). The peak at 1520 cm^{-1} in both the chitosan and nanoparticle spectra is due to unreacted $-NH_2$ groups of chitosan. Similarly, peaks at 800 cm^{-1} and 1260 cm^{-1}, seen in the alginate and nanoparticle spectra, represent unreacted $-COOH$ groups of alginate. The peak seen at 1420 cm^{-1} in the nanoparticle spectrum has been attributed to the ionic interaction between the these two reactive groups [34]. This

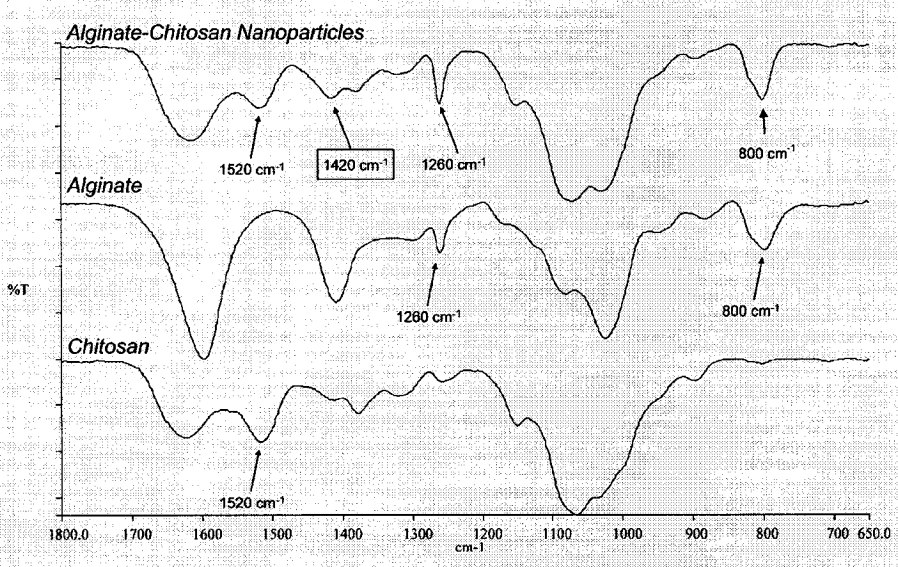

Figure 1. FT-IR spectra of alginate–chitosan nanoparticles compared to chitosan and alginate, demonstrating characteristic absorption bands of each. The peak at 1420 cm^{-1} has been attributed to the interaction between chitosan $-NH_3^+$ and alginate $-COO^-$ groups.

served to confirm that the spontaneous interaction between alginate and chitosan leads to the formation of nanoparticles.

Nanoparticle size

Effect of alginate to chitosan ratio and polymer molecular weight. Nanoparticles were prepared with HV alginate and HMW chitosan and with LV alginate and LMW chitosan at seven different Alg/Chi ratios. The resulting mean particle sizes as determined by DLS are shown in Fig. 2. The same trend can be observed for both molecular weight combinations, with the smallest sizes obtained when the Alg/Chi ratio is in the range between 1 : 1.5 and 1.5 : 1. These results confirm that smaller particles result when the availability of the functional groups are in stoichiometric proportion. Increasing the relative amount of alginate or chitosan causes an increase in DLS measured particle size up to 1.6 μm for the ratios tested. Larger sizes for these particles are attributable to the presence of larger single particles and to aggregate formation, as confirmed by TEM analysis. The trend of sizes related to Alg/Chi ratio is observed regardless of the polymer molecular weights used, though the difference is more pronounced when using HMW polymers.

Also evident in Fig. 2 is the effect of polymer molecular weight on particle size. Generally, use of the LMW polymers resulted in smaller particles for most ratios of Alg/Chi. We further studied this effect by preparing and assessing nanoparticles

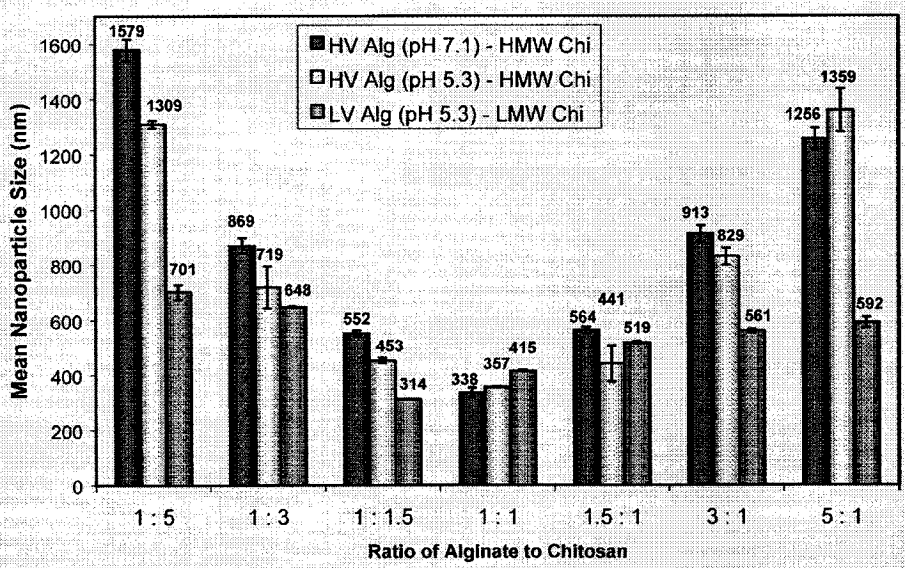

Figure 2. Effect of the ratio of alginate to chitosan on particle size ($n \geq 9$). For all samples the calcium/alginate ratio was kept constant at 0.22 and the pH of the chitosan solution was kept constant at 5.5. The first two series illustrate the effect of alginate pH on particle size; the last two series show the effect of molecular weight on particle size.

using Alg/Chi ratios of 1.5 : 1, 1 : 1 and 1 : 1.5 for all possible combinations of the different molecular weight polymers (HMW Chi with HV, MV and LV Alg; LMW Chi with HV, MV and LV Alg). Results from these permutations indicate that chitosan molecular weight has a greater influence on particle size than alginate molecular weight; generally particles prepared with LMW Chi are smaller than those prepared with HMW Chi (data not shown). Furthermore, formulations using LV alginate and LMW chitosan solutions result in the formation of fewer aggregates. This may stem from the ability of LMW chitosan to diffuse more readily in the alginate gel matrix to form smaller, more homogeneous particles. Conversely, HMW polymers may bind to the surface of such matrices, forming an outer membrane and increasing particle size [35].

Recently, De and Robinson reported the development of chitosan–alginate nanoparticles [32]. Investigating Alg/Chi ratios between 30 : 1 and 7 : 1, they found that the smallest nanoparticles resulted from a Alg/Chi ratio of 30 : 1, yielding particles with a diameter of 506 ± 26 nm. As they decreased the Alg/Chi ratio, they found that nanoparticle size increased with aggregation occurring when ratios less than 7 : 1 were used. These results contrast our DLS and TEM results, which show that increasing either the alginate or chitosan in proportion to the other increases nanoparticle size. We did notice that the large sizes observed for particles prepared with ratios of 1 : 5 or 5 : 1 result partially from the presence of aggregates, in accord with observations by De and Robinson. Potential causes for this discrepancy are pH differences, which we found to affect particle formation and size and the possibility that different driving forces control the spontaneous formation of nanoparticles as the ratio of Alg/Chi increases beyond a critical range.

Effect of pH, calcium chloride and stirring time. In order to assess the effect of pH on nanoparticle formation, particles were prepared using an alginate solution of pH 7.1 at all Alg/Chi ratios. Comparison with particles prepared using an alginate solution of pH 5.3 demonstrate generally smaller particle sizes when combined with HMW chitosan (pH 5.5) (Fig. 2). Much of the chitosan, which is poorly water-soluble and, thus, prepared under acidic conditions, likely precipitates upon addition to an alginate solution with pH 7.1, so that less chitosan is available for particle formation. As well, since the pK_a of chitosan is known to be 6.5 [8], addition to an alginate solution at pH 7.1 would result in the majority of amine groups being unprotonated and, therefore, unable to participate in ionic interactions. The few protonated groups available for interaction would result in weaker electrostatic interactions with the alginate gel, leading to larger particle sizes. Using an alginate solution with a slightly lower pH resolves these problems by allowing a stronger interaction between chitosan and alginate, leading to the formation of more compact nanoparticles. Other groups investigating chitosan for the preparation of nanoparticles, microparticles and polyionic systems report working within the same pH range (5.0–6.3) [4, 5, 36].

Additional pH studies in the more acidic range reveal that using acidified alginate (pH 2.2) or chitosan (pH 0.3) results in increased particle sizes, up to 200 nm larger (Table 1). Smaller Alg-Chi nanoparticles are obtained when both the sodium alginate and chitosan solutions have a pH in the range of 5.1 to 5.7. Within this range the carboxyl group of the alginate is ionized and the amine group of the chitosan is protonated, a necessity for optimum interaction in the polyionic complex formation. Similar observations have been reported in the formation of other polyionic complexes containing chitosan [36].

In addition to the impact of pH on particle size, other groups investigating Alg-Chi beads or microspheres suggest that the presence of calcium ions is important to maintain the alginate gel network during the reaction with chitosan [23]. In adjusting the ratio of calcium to alginate (Ca^{2+}/Alg) from 0.00 to 0.87, it was observed that an absence of calcium ions results in marginally larger particles with a wider distribution than those produced with the 'standard' ratio of 0.22 (Table 1). Similarly, those prepared with a ratio of 0.43 have somewhat larger diameters. However, all particles display similar stability, demonstrated by consistent DLS measurements after several weeks of storage, indicating that aggregation does not occur.

It is known that gel formation between the calcium ions and the guluronate (G) residues in the alginate is a direct function of the length of homopolymer G blocks, with more homopolymer G blocks leading to greater cross-linking and a stronger gel. The alginate derived from *Macrocystis pyrifera* used in this study typically has a ratio of mannuronate to guluronate residues of approx. 1.5, with less than 20% consisting of homopolymer G blocks [37]. Given this low concentration, the first step of pre-gel formation likely does not result in a strong or well-defined gel with these materials, indicating that the addition of calcium is not essential to nanoparticle formation. We found that ratios ranging from 0.00 to 0.87 do not greatly affect nanoparticle formation or size (Table 1). In contrast, De and Robinson concluded that it was necessary to have a Ca^{2+}/Alg ratio <0.2 for nanoparticle formation to occur, with microparticles forming at higher ratios [32].

Table 1.
Effect of calcium/alginate ratio and solution pH on nanoparticle size (Alg/Chi 1 : 1.5)

Alg pH (LV)	Chi pH (LMW)	Ca^{2+}/Alg ratio	Size (nm)	Polydispersity index
5.3	5.5	0.00	403 ± 1*	0.31 ± 0.01
5.3	5.5	0.22	314 ± 1	0.22 ± 0.01
5.3	5.5	0.43	400 ± 62	0.23 ± 0.06
5.3	5.5	0.87	344 ± 9*	0.20 ± 0.01
2.2	5.5	0.22	428 ± 4*	0.35 ± 0.01
5.3	5.5	0.22	314 ± 1	0.22 ± 0.01
7.1	5.5	0.22	528 ± 6*	0.34 ± 0.01
5.3	0.3	0.22	547 ± 24*	0.21 ± 0.04

The second row of each data set represents the 'standard' condition. Values are reported as mean ± SEM ($n \geqslant 9$). * indicates significance at $P < 0.05$ compared to standard nanoparticles.

This incongruity may arise from different methods of analysis; De and Robinson used nephelometry to assess the interaction between calcium and alginate, whereas we evaluated the effect of calcium addition to alginate on nanoparticle formation and found that although particle size is affected by the Ca^{2+}/Alg ratio, higher ratios and complete omission do not prevent the formation of nanoparticles.

Lastly, the stirring time of the final solution was also found to have no effect on particle size. Solutions that were allowed to stir for just 30 min or as long as 24 h contained nanoparticles whose mean sizes differed by no more than 20 nm (data not shown). This result suggests that nanoparticle formation is rapid and that reorganization of the polymers is not occurring over time. Consistent particle size measurements following room temperature storage periods up to one month confirm particle stability.

Particle analysis

Electron microscopy analysis confirmed the presence of nanoparticles and provided morphological information. With the TEM, particles were seen to be spherical and distinct (Fig. 3). Nanoparticles were considerably smaller when viewed with TEM than when measured by DLS. TEM images show particle sizes between 50 nm and 150 nm, depending on the experimental parameters used to prepare them, whereas DLS sizing indicates that the smallest population has an average diameter of at least 300 nm. This apparent discrepancy can be explained by the dehydration of

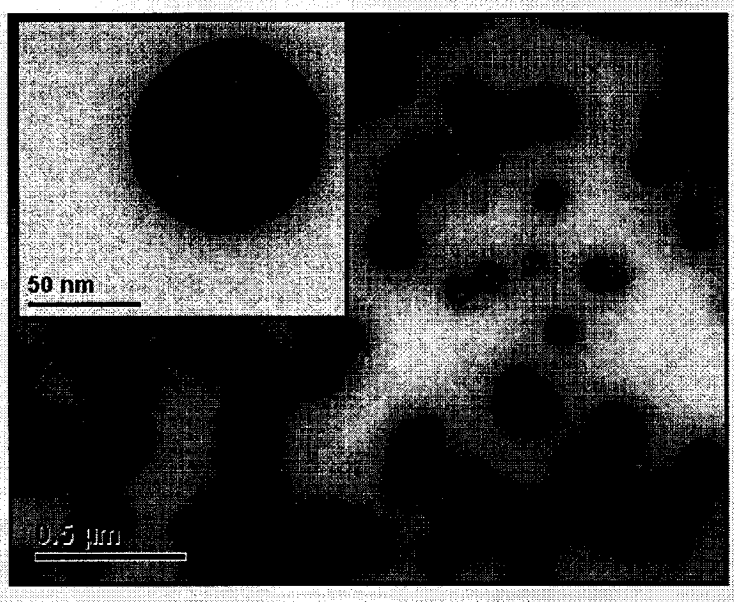

Figure 3. TEM micrograph (bar = 0.5 μm) illustrating typical particle morphology and distribution. Nanoparticles were prepared with a 1 : 1.5 ratio of LV alginate (pH 5.3) to LMW chitosan (pH 5.5) using the standard calcium/alginate ratio of 0.22. Inset: detail of one nanoparticle (bar = 50 nm).

the hydrogel particles during sample preparation for TEM imaging. Additionally, DLS measures the apparent size of a particle, including hydrodynamic layers that form around hydrophilic particles such as those composed of Alg-Chi, leading to an overestimation of particle size [38]. Our attempt to verify particle size in solution by AFM imaging in fluid was unsuccessful, since the nanoparticles were displaced by the approaching tip.

DNA loading and release study

A preliminary feasibility study analyzing the potential application of Alg/Chi nanoparticles as gene carriers was conducted by evaluating the ability of the nanoparticles to load DNA and assessing the particle characteristics once loaded. We evaluated two methods of DNA loading analogous to a study involving alginate–poly-L-lysine (Alg-PLL) nanoparticles, where it was hypothesized that oligonucleotides (ON) are shuttled into particles more rapidly when introduced with a polycation [33].

We found that DNA association in the Alg-Chi nanoparticles is affected by the method of introduction: with method 1 (DNA+NP), DNA association reaches a peak after two days, whereas for method 2 (DNA+Chi), adsorption was an average of 20% lower over the first two days of storage but continued to increase or remain steady beyond the first two days (data not shown). Generally, adsorption was higher when DNA associated with preformed nanoparticles, rather than being introduced as Chi-DNA complexes (Table 2). An adsorption efficiency of 60% (±14%) was achieved using a P/N ratio of 1 : 25, resulting in a mass adsorption of 27 ± 6 μg DNA/mg nanoparticle. The highest mass adsorption, 89 ± 5 μg DNA/mg nanoparticle, was observed with a P/N ratio of 1 : 5, using method 1. However, this system resulted in the formation of aggregates, rendering it ineffective for gene carrier applications. Comparing the results of DNA loading using both methods, we found that complexing DNA with chitosan prior to nanoparticle formation results in slower adsorption kinetics; it is evident that pre-complexing DNA with chitosan does not improve DNA loading of the nanoparticles. The discrepancy between the improvement in ON loading of Alg-PLL by pre-complexing ON with the polycation may be due to the considerably shorter chain lengths used (PLL 3.9–7.9 kDa *vs.* Chi 50 kDa) [33].

Additional characterization of the DNA-loaded nanoparticles included DLS sizing and zeta potential analysis (Table 2). With the exception of the particles prepared using the DNA+Chi method and a P/N ratio of 1 : 5, particles were significantly larger than their unloaded counterparts. Incorporation of DNA and the ensuing molecular reorganization likely causes the size increase.

Results of the zeta potential analysis are perhaps more informative. Unloaded nanoparticles have a zeta potential of 27 ± 1 mV, which was not seen to change significantly with the adsorption of up to 27 μg DNA/mg nanoparticle when prepared using method 1 (Table 2). This suggests that method 1 actually leads to DNA absorption, since surface adsorption would be expected to result in a change in

Table 2.
Influence of loading method and P/N ratio on efficiency of DNA incorporation and particle characteristics

DNA loading method	P/N ratio	Size (nm)	Adsorption efficiency (%)	Mass adsorption (μg DNA/mg NP)	ζ potential (mV)
DNA+NP	1:50	$499 \pm 3^*$	42 ± 9	10 ± 2	26 ± 1
(Method 1)	1:25	$549 \pm 2^*$	60 ± 14	27 ± 6	24 ± 2
	1:10	aggregates	54 ± 4	62 ± 4	$15 \pm 2^*$
	1:5	aggregates	39 ± 2	89 ± 5	$10 \pm 2^*$
DNA+Chi–NP	1:50	$419 \pm 6^*$	40 ± 5	9 ± 1	$17 \pm 2^*$
(Method 2)	1:25	$407 \pm 2^*$	45 ± 4	20 ± 2	$22 \pm 1^*$
	1:10	$377 \pm 3^*$	48 ± 8	57 ± 5	$16 \pm 4^*$
	1:5	$299 \pm 1^*$	26 ± 3	60 ± 7	$16 \pm 4^*$

All complexes were prepared based on the standard conditions (1:1.5 ratio of LV Alg (pH 5.3) and LMW Chi (pH 5.5) with Ca^{2+}/Alg ratio of 0.22). Values are reported as mean $\pm$ SEM ($n \geqslant 9$).
* Indicates significance at $P < 0.05$ compared to blank nanoparticles.

zeta potential. The introduction of increasing amounts of DNA to the system results in surface adsorption and a corresponding reduction of the zeta potential below the threshold necessary to prevent to particle aggregation.

In contrast, method 2 resulted in DNA-nanoparticle complexes with significantly lower zeta potentials than unloaded nanoparticles, regardless of the amount of DNA incorporated, suggesting that molecular reorganization required for particle formation is different under these conditions. Interestingly, particles prepared using this method with P/N ratios of 1:10 and 1:5 exhibited approximately equal mass adsorption and surface charges, suggesting that 60 μg DNA/mg nanoparticles may represent the upper limit of DNA incorporation for particles of this type which do not aggregate. Most significantly, zeta potential analysis indicates that DNA-loaded Alg-Chi particles retain a positive charge without aggregation, which is important for transfection purposes since it allows particles to interact with negatively-charged cell membranes [39].

A preliminary test to evaluate DNA release from the nanoparticles was performed by re-suspending two formulations of pelleted particles in PBS for 48 h. Results indicate that 6% and 3.5% of the adsorbed DNA is released from the P/N 1:10 and 1:25 formulations, respectively. Many groups working with biopolymeric nanoparticles report similar initial release rates, depending on the polymer [40–42]. The possibility of gene release, in combination with the noted loading characteristics, may be advantageous for gene therapy applications.

CONCLUSIONS

A method to prepare alginate–chitosan nanoparticles was developed and optimized to yield small, relatively monodisperse and uniform particles. The alginate/chitosan

ratio in the preparation was found to affect nanoparticle formation, as did polymer molecular weight and pH. The smallest nanoparticles have a mean diameter of 314 nm, as measured by DLS, and are prepared using low viscosity alginate and low molecular weight chitosan in a ratio of 1 : 1.5. Nanoparticle formation is improved when the pH of both the sodium alginate and the chitosan solutions are between 5.1 and 5.7.

The alginate/chitosan ratio in the preparation was found to affect particle size to a greater degree than any other parameter. Particle sizes were lowest in the range that permitted stoichiometric interaction between the functional groups of both polymers and increased to 5-times the minimum size at the ratio extremes. The molecular weight of chitosan was found to be more important in determining particle formation and resulting size than alginate molecular weight, which reinforces the hypothesized mechanism of particle formation.

DNA loading of the nanoparticles was found to occur with high efficiency; maximum adsorption efficiency was 60%, while maximum mass loading was 60 μg DNA/mg nanoparticles. Adsorption of DNA in formed nanoparticles occurred more rapidly than when a DNA–chitosan complex was used in the preparation of the particles, although the association was less stable. The high encapsulation of DNA from alginate–chitosan nanoparticles is encouraging for application in the field of gene therapy. Studies are in progress to evaluate cell–nanoparticle interactions and transfection ability.

Acknowledgements

The authors wish to thank our funding sources: the Natural Sciences and Engineering Research Council of Canada (NSERC) and the Quebec Ministère de la Recherche de la Science et de la Technologie (MRST) for making this research possible. We also wish to thank Dr. S. K. Sears and J. Mui for assistance with TEM analysis, Dr. S. Prakash and Dr. J. Bergeron for access to centrifugation equipment and Shawn Carrigan and Dr. Christelle Catuogno for advice and assistance.

REFERENCES

1. T. P. Richardson, W. L. Murphy and D. J. Mooney, *Crit. Rev. Eukaryot. Gene Expr.* **11**, 47 (2001).
2. D. Quintanar-Guerrero, E. Allemann, H. Fessi and E. Doelker, *Drug Dev. Ind. Pharm.* **24**, 113 (1998).
3. J. M. Barichello, M. Morishita, K. Takayama and T. Nagai, *Drug Dev. Ind. Pharm.* **25**, 471 (1999).
4. F. Chellat, M. Tabrizian, S. Dumitriu, E. Chornet, P. Magny, C. H. Rivard and L. Yahia, *J. Biomed. Mater. Res.* **51**, 107 (2000).
5. F. Chellat, M. Tabrizian, S. Dumitriu, E. Chornet, C. H. Rivard and L. Yahia, *J. Biomed. Mater. Res.* **53**, 592 (2000).
6. T. Madan, N. Munshi, T. K. De, A. Maitra, P. U. Sarma and S. S. Aggarwal, *Int. J. Pharm.* **159**, 135 (1997).
7. J. Davda and V. Labhasetwar, *Int. J. Pharm.* **233**, 51 (2002).

8. H. Q. Mao, K. Roy, L. Troung, K. A. Janes, K. Y. Lin, Y. Wang, J. T. August and K. W. Leong, *J. Control. Rel.* **70**, 399 (2001).
9. X. W. Li, D. K. Lee, A. S. Chan and H. O. Alpar, *Biochim. Biophys. Acta* **1630**, 7 (2003).
10. T. Sato, T. Ishii and Y. Okahata, *Biomaterials* **22**, 2075 (2001).
11. Z. Cui and R. J. Mumper, *J. Control. Rel.* **75**, 409 (2001).
12. K. Corsi, F. Chellat, L. Yahia and J. C. Fernandes, *Biomaterials* **24**, 1255 (2003).
13. S. Mansouri, P. Lavigne, K. Corsi, M. Benderdour, E. Beaumont and J. C. Fernandes, *Eur. J. Pharm. Biopharm.* **57**, 1 (2004).
14. T. Banerjee, S. Mitra, S. A. Kumar, S. R. Kumar and A. Maitra, *Int. J. Pharm.* **243**, 93 (2002).
15. Z. Ma and L. Y. Lim, *Pharm. Res.* **20**, 1812 (2003).
16. M. C. Woodle, K. K. Matthay, M. S. Newman, J. E. Hidayat, L. R. Collins, C. Redemann, F. J. Martin and D. Papahadjopoulos, *Biochim. Biophys. Acta* **1105**, 193 (1992).
17. G. Kaul and M. Amiji, *Pharm. Res.* **19**, 1061 (2002).
18. K. W. Leong, H. Q. Mao, L. Truong, K. Roy, S. M. Walsh and J. T. August, *J. Control. Rel.* **53**, 183 (1998).
19. K. A. Janes, M. P. Fresneau, A. Marazuela, A. Fabra and M. J. Alonso, *J. Control. Rel.* **73**, 255 (2001).
20. Y. Yin, M. Xu, X. Chen and K. Yao, *Chin. Sci. Bull.* **41**, 1266 (1996).
21. K. Y. Lee, I. C. Kwon, Y. H. Kim, W. H. Jo and S. Y. Jeong, *J. Control. Rel.* **51**, 213 (1998).
22. G. Borchard, *Adv. Drug Deliv. Rev.* **52**, 145 (2001).
23. F.-L. Mi, H.-W. Sung and S.-S. Shyu, *Carbohydr. Polym.* **48**, 61 (2002).
24. M. Rajaonarivony, C. Vauthier, G. Couarraze, F. Puisieux and P. Couvreur, *J. Pharm. Sci.* **82**, 912 (1993).
25. G. Fundueanu, C. Nastruzzi, A. Carpov, J. Desbrieres and M. Rinaudo, *Biomaterials* **20**, 1427 (1999).
26. X. L. Yan, E. Khor and L. Y. Lim, *J. Biomed. Mater. Res.* **58**, 358 (2001).
27. G. Coppi, V. Iannuccelli, E. Leo, M. T. Bernabei and R. Cameroni, *J. Microencapsul.* **19**, 37 (2002).
28. M. L. Gonzalez-Rodriguez, M. A. Holgado, C. Sanchez-Lafuente, A. M. Rabasco and A. Fini, *Int. J. Pharm.* **232**, 225 (2002).
29. S. Takka and F. Acarturk, *J. Microencapsul.* **16**, 275 (1999).
30. M. L. Huguet and E. Dellacherie, *Process. Biochem.* **31**, 745 (1996).
31. O. Skaugrud, *Spec. Publ. Roy. Soc. Chem.* **161**, 96 (1995).
32. S. De and D. Robinson, *J. Control. Rel.* **89**, 101 (2003).
33. I. Aynie, C. Vauthier, H. Chacun, E. Fattal and P. Couvreur, *Antisense Nucleic Acid Drug Dev.* **9**, 301 (1999).
34. F. A. Simsek-Ege, G. M. Bond and J. Stringer, *J. Appl. Polym. Sci.* **88**, 346 (2003).
35. D. Quong and R. J. Neufeld, *Biotechnol. Bioeng.* **60**, 124 (1998).
36. S. Dumitriu, P. Magny, D. Montane, P. F. Vidal and E. Chornet, *J. Bioact. Compat. Polym.* **9**, 184 (1994).
37. M. Dornish, D. Kaplan and O. Skaugrud, *Ann. N.Y. Acad. Sci.* **944**, 388 (2001).
38. S. Prabha, W. Z. Zhou, J. Panyam and V. Labhasetwar, *Int. J. Pharm.* **244**, 105 (2002).
39. P. Erbacher, S. Zou, T. Bettinger, A. M. Steffan and J. S. Remy, *Pharm. Res.* **15**, 1332 (1998).
40. H. Cohen, R. J. Levy, J. Gao, I. Fishbein, V. Kousaev, S. Sosnowski, S. Slomkowski and G. Golomb, *Gene Ther.* **7**, 1896 (2000).
41. A. M. Tinsley-Bown, R. Fretwell, A. B. Dowsett, S. L. Davis and G. H. Farrar, *J. Control. Rel.* **66**, 229 (2000).
42. L. Truong, J. T. August and K. W. Leong, *Hum. Gene Ther.* **9**, 1709 (1998).

Appendix E
Research Compliance Certificates

McGill University

APPLICATION TO USE BIOHAZARDOUS MATERIALS*

Projects involving potentially biohazardous materials should not be commenced without approval from the Environmental Safety Office. Submit applications before 1) starting new projects, 2) renewing existing projects, or 3) changing the nature of the biohazardous materials within existing projects.

1. PRINCIPAL INVESTIGATOR: Maryam Tabrizian PHONE: 8129
DEPARTMENT: Biomedical Engineering Rm 313 FAX: 7461
ADDRESS: Lyman Duff Building E-MAIL: maryam.tabrizian@mcgill.ca

PROJECT TITLE:in vitro biocompatibility study of new biomaterials

2. EMERGENCY: Person(s) designated to handle emergencies
Name: Lina Vuch Phone No: work: 398-7398 home:
Name: Pina Sorrini Phone No: work: 398-6736 home:

3. FUNDING SOURCE OR AGENCY (specify): FQRNT, CIHR, NSERC
Grant No.: FQRNT, CIHR, NSERC Beginning date: 2002, 2004, 2001 End date: May 2007, 2005, 2005

4. Indicate if this is
☒ Renewal: procedures previously approved without alterations.
Approval End Date: FQRNT, NSERC (2007, 2005)
☒ New funding source: project previously reviewed and approved under an application to another agency.
Agency: CIHR Approval End Date: 03/05/2005
☐ New project: project not previously reviewed.
☐ Approved project: change in biohazardous materials or procedures.
☐ Work/project involving biohazardous materials in teaching/diagnostics.

CERTIFICATION STATEMENT: The Environmental Safety Office approves the experimental procedures proposed and certifies with the applicant that the experiment will be in accordance with the principles outlined in Health Canada's "Laboratory Biosafety Guidelines" and in the "McGill Laboratory Biosafety Manual".

Containment Level (select one): ☐ 1 ☒ 2 ☐ 2 with additional precautions ☐ 3

Principal Investigator or course director: SIGNATURE date: 08/07/2004 (day/month/year)

Approved by: Environmental Safety Office: SIGNATURE date: 19/07/04 (day/month/year)

Expiry: 31/05/07 (day/month/year)

*as defined in the "McGill Laboratory Biosafety Manual"

5. RESEARCH PERSONNEL: (attach additional sheets if preferred)

Name	Department	Job Title/Classification	Trained in the safe use of biological safety cabinets within the last 3 years? If yes, indicate training date.
Lucie Marcotte	BMED	Research associate	No
Jean-Philippe St-Pierre	BMED	Master student	No
Cyrille Fleury	BMED	Master student	No
Linc Mongeon	BMED	Technician	No
Kim Douglas	BMED	PhD student	No
Shahabeddin Faghihi	BMED	PhD student	No

6. Briefly describe:

i) the biohazardous material involved (e.g. bacteria, viruses, human tissues, toxins of biological origin) & designated biosafety risk group

bacteria, cell lines (mammalian)
↳ E. coli (non-pathogenic)

ii) the procedures involving biohazards

cell and bacterial culture

iii) the protocol for decontaminating spills

as requested by McGill - ethanol, detergent, bleach disinfection

7. Does the protocol present conditions (e.g. handling of large volumes or high concentrations of pathogens) that could increase the hazards?

no

5. RESEARCH PERSONNEL (continued)			
Name	Department	Job Title / Classification	Trained in the safe use of biological safety cabinets within the last 3 years? If yes, indicate training date.
Shawn Carrigan	BMED	PhD student	۲۰۱۵
Dariusz Dziong	BMED	Master student	۲۰۱۵
Mylène Gravel	BMED	Master student	۲۰۱۵
Manuela Mandu	BMED	PhD student	۲۰۱۵
Cathy Tkaczyk	BMED	PhD student	۲۰۱۵
Anna Hillberg	BMED	Post doctoral fellow	۲۰۱۵

8. Do the specific procedures to be employed involving genetically engineered organisms have a history of safe use?

~~no~~ N/A

9. What precautions will be taken to reduce production of infectious droplets and aerosols?

~~n/a~~ Manipulation of cultures will be carried out in a BSC

10. Will the biohazardous materials in this project expose members of the research team to any risks that might require special training, vaccination or other protective measures? If yes, please explain.

no

11. Will this project produce combined hazardous waste – i.e. radioactive biohazardous waste, biohazardous animal carcasses contaminated with toxic chemicals, etc.? If yes, please explain how disposal will be handled.

no

12. List the biological safety cabinets to be used.

Building	Room No.	Manufacturer	Model No.	Serial No.	Date Certified
Lyman Duff	323	microzone	BK-2-4	801-4534	14/05/04

Appendix F
Curriculum Vitae

Publications

KL Douglas, C Piccirillo, M Tabrizian, *Cell-Line Dependent Internalization Pathways and Intracellular Trafficking Determine Transfection Efficiency of Nanoparticle Vectors,* **Molecular Therapy**, manuscript submitted.

KL Douglas, C Piccirillo, M Tabrizian, *Effects of Alginate Inclusion on the Vector Properties of Chitosan-Based Nanoparticles,* **Journal of Controlled Release**, under revision.

KL Douglas, M Tabrizian, *Effect of Experimental Parameters on the Formation of Alginate-Chitosan Nanoparticles and Evaluation of their Potential Application as DNA Carriers,* **Journal of Biomaterials Science – Polymer Edition**: 2005, 16(1): 43-56.

KL Douglas*, SD Carrigan*, M Tabrizian, *Nanomaterials: Perspectives and Possibilities in Nanomedicine*, **CRC Handbook of Biomedical Engineering**, 3rd ed., CRC Press, 2006. * *equal contribution*

Communications

KL Douglas, C Piccirillo, M Tabrizian, *Making the Link Between Internalization, Intracellular Trafficking and Transfection with Non-Viral Vectors*, **25th Annual Meeting of the Canadian Biomaterials Society**, Calgary Canada, May 26-28, 2006.

KL Douglas, T-D Wu, J-L Guerquin-Kern, A Croisy, C Piccirillo, M Tabrizian, *Tracking Endocytosed Alginate-Chitosan Nanoparticles using Combined NanoSIMS and Electron Microscopy*, **24th Annual Meeting of the Canadian Biomaterials Society**, Waterloo Canada May 26-28, 2005.

KL Douglas, C Piccirillo, M Tabrizian, *Development of Alginate-Chitosan Nanoparticles for Non-Viral Cell Transfection*, **Entretien Jacques Cartier**, Montreal Canada, October 2004.

KL Douglas, M Taheri, C Piccirillo, M Tabrizian, *Novel Alginate Chitosan Nanoparticles as Efficient Non-Viral Gene Carriers*, **7th World Biomaterials Congress**, Sydney Australia, May 17-21, 2004.

KL Douglas, M Tabrizian, *The analysis of novel alginate-chitosan nanoparticles for application as gene or drug carriers,* **23rd Annual Meeting of the Canadian Biomaterials Society**, Montreal Canada, May 29-31, 2003.

KL Douglas, M Tabrizian, *The Development of Novel Alginate-Chitosan Nanoparticles*, **29th Annual Meeting of the Society for Biomaterials**, Reno USA, April 30-May3, 2003.

KL Douglas, M Tabrizian, *Investigation of the Effect of Experimental Parameters on Alginate-Chitosan Nanoparticles for Application as Non-Viral Vectors*, **Controlled Release Society Winter Symposia and 11th International Symposium & Exposition on Recent Advances in Drug Delivery Systems**, Salt Lake City USA, March 3-6, 2003.

Awards and Scholarships

- Canada Graduate Scholarship, Natural Sciences & Engineering Research Council of Canada (NSERC). 2004-2006
- Post-Graduate Scholarship (PGS), Natural Sciences & Engineering Research Council of Canada (NSERC). 2002-2004
- Greville Smith McGill Major Fellowship (declined). 2006
- Eileen Peters McGill Major Fellowship (declined). 2003
- Canadian Biomaterials Society student presentation award. 2005 and 2006
- Canadian Biomaterials Society travel award. 2004 and 2006
- McGill Alumni travel award
- Merit Award for highest academic standing upon graduation, Society of Chemical Industry. 1999
- Teaching Assistant Award for Excellence (University of Waterloo). 1999
- Silver Medal Award for highest academic standing in 3rd year Chemistry, Canadian Society for Chemistry. 1998
- Canada Scholarship in Science and Engineering. 1994 – 1999
- University of Waterloo Dean's Honour Roll. 1994 – 1999
- Certificate of French Immersion. 1994

Education

McGill University, Montreal, QC **2001-2006**
Ph.D. candidate in Biomedical Engineering

University of Waterloo, Waterloo ON **1995-1999**
Honours B.Sc., Applied Chemistry, Co-op program

Queen's University, Kingston ON **1997-1999**
B.Ed., Intermediate/Senior Science

Employment

Science Teacher	Immaculata High School, Ottawa ON	1999-2001
International Teacher	Colegio Panamericano, Colombia, SA	1998
Teaching Assistant	University of Waterloo, Waterloo, ON	1998-1999
GLP Unit Member	GLP Monitoring Unit, Environment Canada	1996